



# **DESIGN METHODS FOR LOW VOLUME ROADS**

**Lélio Antônio Teixeira Brito**

Thesis submitted to the University of Nottingham  
for the degree of Doctor of Philosophy

March 2011

***'Live as if you were to die tomorrow. Learn as if you were to live forever'***

Mohandas (Mahatma) Karamchand Gandhi - 1869-1948

## ABSTRACT

This thesis is concerned with producing a simple method to design low volume roads (LVR) by means of a rationale which accounts for permanent deformation development in granular layers. Rutting is regarded as the main distress mode in unsealed and thinly sealed pavements. Hence, it is desirable that it be analytically approached rather than empirically, as in most design methods. The overall aim of this PhD thesis was to look into the behaviour of in-service roads and from a newly developed process, to advance, in a systematic manner, the elements required to produce a simple mechanistic design procedure. The study took as its basis an assessment of the proximity of the stress distribution in the pavement to the material's failure envelope.

After a literature review on unbound granular materials mechanical behaviour and on low volume roads pavement design methods, Chapters 4 and 5 discuss full scale trials carried out in Scotland on typical forest roads. The overall goal of the trials carried out within the Roads Under Timber Transport project was to establish the effect of weather and seasonal effects on the rutting of forest roads and to improve their performance while enabling the roads to be economically constructed and maintained. It appears that most of the rutting occurring in the sites surveyed came shortly after their construction/resurfacing, leading to the assumption that workmanship may be a highly important variable. Lack of compaction of the layer could be one of the likely reasons for the high initial rutting rates. Establishing the effect of weather on rutting further to the existing knowledge was, however, difficult to achieve; this was mainly due to the difficulties faced in monitoring traffic conditions. A newly developed method was needed to quantify permanent deformation development due to wandering traffic on a non-level pavement; this was achieved by the use of wheel path areas, and seemed to be a way forward in the analysis of rutting in unsealed roads.

Accelerated pavement trials are reported that aimed to evaluate the performance of aggregate under soaked conditions and the relative pavement deformation caused by different timber haulage vehicles. A road segment simulating a standard forest road section was constructed in a purpose-built facility located at the Ringour Quarry facility. Ten different trials were carried out combining three different aggregate materials and five types of vehicles. Tyre fitment, axle configuration and tyre pressure were assessed and demonstrated to play an important role on the study of rutting development. Conclusions drawn from the results suggest that management of the tyre inflation pressure and axle overload may be one of the most economic means of managing pavement deterioration in the forest road network.

A mechanistic analysis of a variety of unsealed pavements was carried out in Chapter 6; and the newly proposed methodology is described in Chapter 7. With changing loading conditions – e.g. as a consequence of the introduction of Tyre Pressure Control Systems and super single tyres – more detailed analyses are required, so that their effect can be analytically assessed. Then an analytical method is introduced for evaluating the stress-strain condition in thinly surfaced or unsurfaced pavements as typically used in LVR structures. It aims to improve the understanding of the effect of tyre pressure and contact area in regard to permanent deformation. To achieve this, several scenarios were modelled using Kenlayer software varying aggregate material, thickness, stiffness, tyre pressure & arrangement. The results usually show a fairly well defined locus of maximum stresses. By comparing this stress envelope with failure envelope, conclusions could be established about the more damaging effect of super singles over twin tyres and, likewise, the greater damage inflicted by high tyre pressures compared to that incurred by lower tyre pressures.

Finally, the framework of the proposed method contributes to LVR pavement design procedures mainly due to its simplicity. It still treats the pavement analytically, permitting a more fundamental description of the behaviour of granular layers than in simple linear elastic analysis, but by simplifying the elasto-plastic analysis for routine use it thereby reduces demands of material characterization and computational skills, thus increasing its utility in practical application.



**To Ângela**

## TABLE OF CONTENTS

<b>1. INTRODUCTION .....</b>	<b>1</b>
1.1. Background .....	1
1.2. Introduction to the project.....	3
1.3. Objectives of the research.....	4
1.4. Scope .....	4
<b>2. UNBOUND GRANULAR MATERIAL AND ROAD LAYERS.....</b>	<b>6</b>
2.1. Stress conditions .....	8
2.1.1. Stress invariants .....	10
2.1.2. In-pavement stresses .....	11
2.2. Deformability .....	13
2.2.1. Factors affecting resilient behaviour.....	15
2.3. Modelling deformability.....	16
2.3.1. Resilient models.....	16
2.3.2. Elasto-plastic models.....	20
2.3.3. Drucker-Prager yield criteria .....	23
2.4. Permanent deformation in Unbound Granular Layers .....	24
2.4.1. Rutting mechanisms .....	24
2.4.2. Factors affecting permanent deformation in UGM.....	26
2.4.3. Permanent deformation models.....	27
2.5. The Shakedown approach .....	32
2.6. Performance tests .....	34
2.6.1. The repeated load triaxial test .....	35
2.6.2. Wheel tracking test .....	37
2.6.3. K-Mould test.....	38
2.6.4. The hollow cylinder test .....	40
2.6.5. Simpler in-situ testing equipment.....	41
2.7. Key Findings.....	42
<b>3. LOW VOLUME ROADS DESIGN AND OPERATION .....</b>	<b>44</b>
3.1. Empirical approaches.....	46
3.2. Austroads pavement design guide .....	48
3.2.1. New Zealand supplement to the Australian PDG .....	52
3.3. AASHTO Guide Design .....	53
3.3.1. US Mechanistic-Empirical Pavement Design Guide.....	54
3.4. Forest roads design.....	58
3.4.1. The Forestry Civil Engineering design recommendations .....	59

3.5.	PERMANENT DEFORMATION SUPPORTING TOOLS FOR LVR .....	61
3.5.1.	<i>Low ground pressure vehicles</i> .....	62
3.5.2.	<i>Tyre pressure control system vehicles</i> .....	63
3.5.3.	<i>Percostation Technique</i> .....	65
3.6.	Super single tyres versus twin tyres .....	67
3.7.	Key Findings .....	68
<b>4.</b>	<b>FULL SCALE TRIALS IN SCOTLAND.....</b>	<b>70</b>
4.1.	An Overview of the RUTT Project .....	70
4.2.	Monitoring of the Trial Sections.....	72
4.2.1.	<i>Inspection and selection of sites</i> .....	72
4.2.2.	<i>Traffic counters</i> .....	74
4.2.3.	<i>Weather stations</i> .....	77
4.2.4.	<i>Permanent deformation monitoring</i> .....	79
4.2.5.	<i>Reference sections</i> .....	85
4.3.	The Accelerated Pavement Trials .....	88
4.3.1.	<i>Section Construction</i> .....	89
4.3.2.	<i>Vehicles</i> .....	93
4.3.3.	<i>Instrumentation</i> .....	98
4.4.	Description of the Materials Used .....	101
4.4.1.	<i>Monitoring Sites</i> .....	101
4.4.2.	<i>Reference Sections</i> .....	102
4.4.3.	<i>Accelerated Pavement Trials</i> .....	103
4.4.4.	<i>Laboratory Tests</i> .....	105
4.5.	Dielectric Properties Monitoring .....	106
4.6.	COMPUTING Rutting in Forest Roads .....	111
4.7.	Key findings .....	118
<b>5.</b>	<b>FULL SCALE TRIALS RESULTS .....</b>	<b>121</b>
5.1.	Monitoring Trial Sections .....	121
5.1.1.	<i>Weather data</i> .....	121
5.1.2.	<i>Traffic data</i> .....	122
5.1.3.	<i>Permanent deformation data</i> .....	124
5.1.3.1.	Monitoring Sections.....	126
5.1.3.2.	Reference Sections.....	129
5.1.4.	<i>Pavement exhumation findings</i> .....	129
5.1.5.	<i>Laboratory tests results</i> .....	132
5.1.5.1.	Grading .....	132
5.1.5.2.	Density and water absorption.....	132
5.1.5.3.	Ten Percent Fines .....	133
5.1.5.4.	California Bearing Ratio .....	135

5.1.5.5. Liquid Limit, Plastic Limit & Plasticity Index.....	137
5.1.6. Statistical analysis.....	138
5.2. Accelerated Pavement Trials .....	145
5.2.1. Test procedure.....	145
5.2.2. Permanent deformation data .....	149
5.2.3. Water added .....	155
5.2.4. Instrumentation – $\epsilon$ mu coils .....	157
5.3. Key findings .....	161
<b>6. MECHANISTIC ANALYSIS .....</b>	<b>165</b>
6.1. Introduction .....	165
6.2. Analysis performed.....	166
6.3. Methodology .....	170
6.4. Parameter Inputs .....	175
6.4.1. Loading arrangements .....	175
6.4.2. Materials .....	176
6.5. Validation of the analysis.....	179
6.6. Results.....	185
6.7. Key findings .....	190
<b>7. METHODOLOGY PROPOSAL AND VALIDATION .....</b>	<b>192</b>
7.1. Introduction.....	192
7.2. Pavement stress locus .....	193
7.3. Thickness Design .....	196
7.4. Subgrade Verification .....	198
7.5. Methodology rationale .....	200
7.6. Method limitations .....	204
7.7. Validation.....	205
<b>8. CONCLUSIONS .....</b>	<b>206</b>
8.1. Summary of main conclusions .....	206
8.1.1. Unbound granular materials and road layers - Chapter 2 .....	206
8.1.2. Low Volume Road design and operation - Chapter 3.....	206
8.1.3. Full Scale Trials in Scotland - Chapters 4 & 5.....	207
8.1.4. Mechanistic Analysis - Chapter 6 .....	208
8.1.5. Methodology Proposal and Validation - Chapter 7.....	209
8.2. Recommendations for Future Work .....	209
<b>REFERENCES .....</b>	<b>211</b>
<b>APPENDIXES .....</b>	<b>223</b>

## LIST OF FIGURES

Figure 2.1 – Schematic profile of (a) high-volume road & (b) low-volume road pavement.....	6
Figure 2.2 – Stress components acting on an element [Lekarp 1997].....	8
Figure 2.3 – Stress conditions under a wheel load pass [Shaw 1980].....	8
Figure 2.4 – Stresses on a pavement: (a) principal stresses – rotate; (b) no rotation – shear stress reversal [Brown 1996].....	9
Figure 2.5 – Variation of vertical and horizontal stress in granular layer of pavements with various thicknesses of asphalt [Dawson <i>et al.</i> 2007].....	10
Figure 2.6 – Stress level data for the Australian pavements analysed by Mundy [2002] .....	12
Figure 2.7 – Stress level boundaries for Australia and LCPC analysed pavements .....	12
Figure 2.8 – Stress-strain behaviour of UGMs [Werkmeister 2003].....	13
Figure 2.9 – Stress-strain behaviour of UGMs under cyclic loading in a triaxial repeated loading test [after El Abd <i>et al.</i> 2004] .....	14
Figure 2.10 – Yield surfaces from elasto-plastic models - Mohr Coulomb & Drucker-Prager .....	21
Figure 2.11 – Schematic illustrations of the kinematic hardening in terms of stress-strain response [Khogali & Mohamed 2004] .....	21
Figure 2.12 – Yield surface of the model of Chazallon, and hardening mechanism [after El Abd <i>et al.</i> 2004].....	22
Figure 2.13 – Drucker-Prager yield condition in 2D p-q stress space .....	23
Figure 2.14 – Rutting mechanisms: Mode 0, 1 and 2 respectively [Dawson & Kolisoja 2004].....	25
Figure 2.15 – Shakedown range behaviours for permanent strain versus cumulative loading - typical responses. ....	32
Figure 2.16 – Shakedown range boundaries A, B & C in terms of stress condition (p x q) [Arnold 2004].....	34
Figure 2.17 – Repeated load triaxial test equipment at the University of Nottingham.....	35
Figure 2.18 – Wheel tracking test equipment at the University of Oulu – Finland.....	38
Figure 2.19 – K-mould test apparatus [after Semmelink & de Beer 1995].....	39
Figure 2.20 - Springbox (L) sample in the mould & (R) sample set up in the apparatus.....	39
Figure 2.21 – Schematics of a hollow cylinder test apparatus [after Thom & Dawson 1993].....	40
Figure 3.1 – Flexible pavement design system for granular pavements with thin bituminous surfacing [Austroads 1992] .....	50
Figure 3.2 – Design for granular pavements (80% confidence) Source: ARRB Transport Research (1998, Figure 13.8.2.C). [Austroads 2009].....	52
Figure 3.3 – Typical Forest Road Cross Section - Forestry Commission DMRB .....	59
Figure 3.4 – Low ground pressure vehicle and its axle configuration .....	62
Figure 3.5 – TPCS Installed on a timber lorry in Scotland .....	63
Figure 3.6 – Load and inflation pressure effects on tyre contact area [after Granlund <i>et al.</i> 1999]..	64
Figure 3.7 – (a) Schematic diagram of a Percostation Installation [Saarenketo & Aho 2005] (b) Percostation's Probe (c) Percostation System.....	66
Figure 3.8 – Permanent axial strains of specimens as a function of the dielectric value of the specimen's top surface (measured in TST) [Saarenketo <i>et al.</i> 1998] .....	66
Figure 3.9 – Development of heavy goods vehicles in regard to axle and tyre configuration [Addis 2000].....	68
Figure 4.1 – RUTT Project's flow chart .....	71
Figure 4.2 – Maps of sites on the RUTT Project in Scotland .....	74
Figure 4.3 – Minuteman EVR and Junior Traffic counters .....	75
Figure 4.4 – Simplified weather station and shuttle reader for data-logger download.....	77
Figure 4.5 – Weather data obtained in RUTT Project for Till Hill Main Block at Eskdalemuir .....	78

Figure 4.6 – Weather data for Eskdalemuir/Scotland from January, 2001 to April, 2007 [source: MetOffice 2007] .....	78
Figure 4.7 – Monthly monitoring of rutting at Till Hill Main Block .....	81
Figure 4.8 – Profile reading example at Till Hill monitoring Section one. ....	82
Figure 4.9 – Repeatability test with laser measuring device for profiling of the cross sections .....	82
Figure 4.10 – Portable aluminium beam for rut profiling - at the calibration base. ....	83
Figure 4.11 - Detail of the two sided beam with 0.1m spaced readings & recording procedure .....	84
Figure 4.12 – (a) Reference section construction at Castle O'er. (b) Layer thickness monitoring during construction .....	87
Figure 4.13 – Ringour Testing Facility before construction of the test section with major dimensions indicated and sections chainage.....	88
Figure 4.14 – Barrier at both ends of the walls to contain water .....	90
Figure 4.15 – (a) Levelling of the floor (b) Compaction works at the top of the base layer .....	91
Figure 4.16 – Ringour Testing Facility – view of the test section before and after construction of the test pavement .....	91
Figure 4.17 – Mini-FWD Test Equipment.....	92
Figure 4.18 – (a) Water tank 10m above ground level (b) Pond for water supply .....	92
Figure 4.19 – Water sprinkling system during trial .....	93
Figure 4.20 – Tyre and axle arrangements for the vehicles used in the trial.....	94
Figure 4.21 – Tyre arrangements for articulated truck (dimensions in cm) .....	94
Figure 4.22 – Tyre arrangements for fixed wheelbase “Multi-Lift” truck (dimensions in cm) .....	95
Figure 4.23 – FC Foden “Multi-Lift” truck trafficking a Ringour trial.....	96
Figure 4.24 – “Low ground pressure” vehicle trailer with tyres equally spaced across pavement on stub-axles .....	96
Figure 4.25 – Loaded test vehicle equipped with TPCS .....	97
Figure 4.26 – Installation of a coil in Trial 10 .....	99
Figure 4.27 – εmu Coils’ layout at Trial 9 & 10 .....	99
Figure 4.28 – Levelling of the coils aided by a “spirit level” .....	100
Figure 4.29 – Installation of the coils in the test section.....	100
Figure 4.30 – εmu coils calibration curve.....	100
Figure 4.31 – εmu coils’ layout at Trial 11.....	101
Figure 4.32 – Grading envelope according to “Swedish Specification” [FEG 2000] .....	102
Figure 4.33 – Grading envelope for surfacing material in the reference sections .....	102
Figure 4.34 – Materials grading for the Ringour test section .....	104
Figure 4.35 – (a) Schematic diagram of a Percostation Installation [Saarenketo 2006] (b) Percostation Probe (c) Percostation System .....	107
Figure 4.36 – Permanent axial strains of specimens as a function of the dielectric value of the specimen’s top surface (measured in TST) [Saarenketo 2001] .....	107
Figure 4.37 – Percostation installation at Till Hill Main Block entrance – off B709 Eskdalemuir/Scotland .....	109
Figure 4.38 – Public and Forest Road structure layout and Percostation probes arrangement .....	109
Figure 4.39 – Examples of Percostation readings, soon after installation, for the public road B709 – Eskdalemuir .....	110
Figure 4.40 – Rut depth and Vertical Surface Deformation (VSD) measurements systematic [Arnold 2004].....	112
Figure 4.41 – Measuring rut-depth of pavement surfaces using a straight edge according to ASTM E1703-05 [2005] .....	113
Figure 4.42 – Determining maximum rut depth in an asphalt pavement according to AASHTO PP38-00 [2000].....	114
Figure 4.43 – Comparison among three different methods to determine rut depth plotted on the December 2006 profile of the Risk Site. ....	114
Figure 4.44 – Examples of tyre sitting on the wheel paths.....	115

Figure 4.45 – Difference in the sitting on the rut according to the tyre width .....	115
Figure 4.46 – Monthly readings for monitoring Section 1 at Risk site .....	116
Figure 4.47 – Area measurement of the right wheel path (RWP) for two different months at Risk Site .....	117
Figure 4.48 – Polynomial fit equation for calculation – Risk, July 2007 .....	117
Figure 5.1 – Rainfall summary for the south-western monitoring sites .....	121
Figure 5.2 – Rainfall summary for the south eastern monitoring sites .....	122
Figure 5.3 – Average rainfall in the monitoring sites in South Scotland .....	122
Figure 5.4 – Total Traffic (ESALs) per monitoring site .....	123
Figure 5.5 – Cross sections reading after data check ready for analysis - Culreoch Site .....	124
Figure 5.6 – VSD and Rut Depth for each of the monitored sections and its average value - Culreoch site .....	125
Figure 5.7 – Rut area for the monitored sections - Culreoch site .....	125
Figure 5.8 – Rutting at the monitored full scale trials - monitoring sites .....	127
Figure 5.9 – Permanent deformation results for the reference sections .....	128
Figure 5.10 – Trial Pits at Kilburn Hill at Castle O'er and Brochloch at Carsphairn Forests .....	129
Figure 5.11 – Grading envelopes for surfacing layers on six monitoring sites .....	132
Figure 5.12 – TFV Loading Machine & Displacement results for Kilburn Hill Material .....	134
Figure 5.13 – Example of aggregate before and after TFV Test for Kilburn Hill material .....	134
Figure 5.14 – Preparation and compaction of CBR samples & CBR Loading Apparatus .....	135
Figure 5.15 – CBR Results versus moisture .....	137
Figure 5.16 – (a) Penetrometer for Liquid Limit determination & (b) Plastic Limit Test .....	138
Figure 5.17– Predicted versus observed values for Model 1 (90 observations minus 13 outliers) .....	141
Figure 5.18 – Predicted versus observed values for Model 2 (194 observations minus 9 outliers) .....	141
Figure 5.19 – Impact of input variation on permanent deformation according to Model 1 .....	144
Figure 5.20 – Impact of input variation on permanent deformation according to Model 2 .....	144
Figure 5.21 – Soaked surface during trial .....	145
Figure 5.22 – Example of pictures taken in the wheel paths at the end of each round of passes .....	146
Figure 5.23 – FWD Results - summary of deduced stiffness values .....	149
Figure 5.24 – Rutting rates observed according to number of ESALs .....	150
Figure 5.25 – Rutting observed in trials at Ringour .....	151
Figure 5.26 – Depth of water applied and achieved .....	155
Figure 5.27 – Permanent deformation measured from instrumentation reading at Trial 9 .....	157
Figure 5.28 – Permanent deformation measured from instrumentation reading at Trial 10 .....	157
Figure 5.29– $\epsilon$ mu coil reading at Trials 9 & 10 .....	159
Figure 5.30 – Rut depth versus VSD measurement in Trial 10 .....	159
Figure 5.31 – $\epsilon$ mu coil result for Trial 11 .....	160
Figure 5.32 – Cross section reading using profiling beam at Trial 11 .....	161
Figure 6.1 – Parameters considered for the analysis carried out .....	166
Figure 6.2 – Experiment matrix – total of 180 analyses .....	168
Figure 6.3 – Granular layer thickness evaluated varying as a function of load arrangement and tyre pressure .....	168
Figure 6.4 – Mohr Coulomb cohesion intercept .....	169
Figure 6.5 – Example of Kenlayer output file with input parameters - NIG1 - Problem 1 .....	172
Figure 6.6 – Typical plot of computed stresses in the pavement .....	174
Figure 6.7 – Equivalent, circular loaded wheel areas .....	175
Figure 6.8 – Resilient Modulus curves for Arnold's materials [2004] .....	177
Figure 6.9 – Shakedown range boundaries for Arnold's materials [2004] .....	178
Figure 6.10 – Structure used for the non-linearity effect comparison between Kenlayer and Fenlap .....	182
Figure 6.11 – Kenlayer sensitivity measurement to variation in material self weight values .....	184
Figure 6.12 – Set of results obtained for all five problems run for NIG1 .....	186

Figure 6.13 – Resulting stress loci example compared to Australia and France loci according to Mundy [2002] .....	187
Figure 6.14 – Example of two p,q plots. $S_{\text{yield surface-failure}}$ represents the Drucker Prager yield surface. ....	188
Figure 6.15 – S results for the experiment matrix. (from top to bottom: failure, $S_{SS}$ & $S_{DT}$ surfaces) .....	189
Figure 7.1 – Stress envelopes for NIG7, NIG8 & NIG9 - Problems 1 connected by a 6th order polynomial line of regression .....	194
Figure 7.2 – Comparison of the S values resulting from a manual and a computational measurement using a polynomial line of regression .....	195
Figure 7.3 – Loci of stress concentration - compiled result for the NIG .....	196
Figure 7.4 – Design charts for the determinations of the S parameters in the aggregate layer .....	197
Figure 7.5 – Vertical stress at the top of the subgrade as a function of loading and aggregate in Dual Tyre loading arrangements.....	199
Figure 7.6 – Vertical stress at the top of the subgrade as a function of loading and aggregate in Single Tyre loading arrangements.....	200
Figure 7.7 – Flow chart for Stage 1 design .....	202
Figure 7.8 – Flow chart for Stage 2 design .....	203



## LIST OF TABLES

Table 2.1 – Factors affecting resilient behaviour .....	16
Table 2.2 – Mathematical models for Triaxial Resilient Modulus .....	18
Table 2.3 – Factors affecting permanent strain response.....	27
Table 2.4 – Models proposed to predict permanent strain [after Lekarp 1997, Arnold 2004].....	29
Table 3.1 – Example of flexible pavement design catalogue for LVR proposed by the US M-E Design Guide [NCHRP 1-37A Part 4 - Chapter 1 2004] .....	57
Table 3.2 – Indication of the pavement total thickness as a function of subgrade CBR according to the FCE Handbook .....	60
Table 3.3 – Typical pre-sets available in a TPCS car (Tireboss System) .....	64
Table 4.1 – Moisture content in Reference Sections during construction .....	87
Table 4.2 – Overlay thickness in Reference Sections.....	87
Table 4.3 – Summary of vehicles used to load Ringour trial pavements .....	97
Table 4.4 – Vehicles' Equivalent Standard Axle Load calculation according to 4 <sup>th</sup> Power Law.....	97
Table 4.5 – Loading and Moisture Condition Matrix of Ringour Trials .....	104
Table 4.6 – Collected samples origin for laboratory tests with traffic for the project period .....	105
Table 4.7 – Percostations' probes depths and identification.....	110
Table 5.1 – Traffic estimated from timber tonnage figures in ESALs .....	123
Table 5.2 - Permanent deformation results for the monitored sites classified in order of increasing rutting rates.....	128
Table 5.3 – CBR and layer's thicknesses derived from DCP results .....	130
Table 5.4 – Summary of Trial Pits.....	131
Table 5.5 – Density and water absorption results.....	133
Table 5.6 – Ten Percent Fines Results.....	135
Table 5.7 – CBR Results .....	136
Table 5.8 – Liquid Limit, Plastic Limit & Plasticity Index results .....	138
Table 5.9 – Statistical results for Model 1 .....	142
Table 5.10 – Statistical results for Model 2 .....	142
Table 5.11 - Models 1 & 2 constants and details .....	143
Table 5.12 – Thicknesses and CBR value deduced from DCP testing .....	148
Table 5.13 – Ringour trials summary chart .....	152
Table 5.14 – Moisture contents of trial pavements .....	156
Table 5.15 – Comparison between $\epsilon_{mu}$ coils and profiling beam for Trials 9 & 10.....	159
Table 6.1 – P&Q Values as obtained equated from the principal stresses output .....	173
Table 6.2 – P/Q Ratio calculated in RAD (Red cells - ratio>1.249 ; blue cells - ratio <0).....	173
Table 6.3 – Values considered for p x q plot after filtering .....	174
Table 6.4 – Materials tested in the Repeat Load Triaxial apparatus [Arnold 2004].....	177
Table 6.5 – Properties of Materials Analysed .....	178
Table 6.6 – Comparison for Kenlayer and Elsym5 results in a linear elastic analysis.....	181
Table 6.7 – Comparison for Kenlayer and Fenlap results in a non-linear elastic analysis .....	183
Table 6.8 – Comparison between Kenlayer and Fenlap with a linear elastic and a non-linear elastic models.....	183

# 1. INTRODUCTION

## 1.1. BACKGROUND

Throughout the world, reduced time and cost of travel, as well as increased safety, are the ultimate deliverables of a well engineered road system. Researches have been focused on material technology, sustainability, traffic management and information services for highway engineering standards in order to meet the increasing demand in the sector.

In the United Kingdom, the hierarchy of roads is categorized according to their function and capacities. The basic classification consists in six broad groups: Motorway, primary A-roads, non-primary A-roads, B roads, C roads and unclassified roads. Whilst the first three groups are responsible for providing the primary routes for longer distance journeys and freight transport among major urban centres, the three last ones provide access to less populated areas and rather shorter journeys.

Although the focus of mass infrastructure investment is toward high volume roads, special attention must be drawn to the low volume roads (LVRs). These are usually part of the second group – B, C or unclassified roads, in regard to the UK hierarchy. With the ever-increasing size and number of heavy trucks using LVRs, it is an escalating challenge to construct and maintain these pavement structures in an economic manner using inexpensive materials and techniques.

Although traffic volumes on these roads remain relatively low compared with the inter-city highways, severely limiting the ability of the road owner/maintainer to obtain a significant income from tolls or taxation, vehicle loads are usually necessitating a reasonably high performance ability. LVRs provide the primary links to the highway transportation system. They provide links from homes and farms to markets, raw materials from forests and mines to mills. They provide public access to essential health, education, civic, and outdoor recreational facilities. The LVR link between raw materials and markets is critical to economies locally and nationally in all countries around the world [Coghlan 1999].

For all these reasons, it is important to invest in research that increases our ability to sustain and improve such roads in an economic manner. Such pavements, sealed and unsealed, generally comprise a great length of road networks throughout the world, especially in developing countries, hence requiring attention. Thin or low volume

---

pavements represent in the United Kingdom 95% of the road network [British Road Federation 1999].

It must be highlighted that the techniques involved in designing LVRs are consistently different from those used in the other branches of highway engineering. Based on the widely-supported idea that traditional highway engineering standards are not appropriate for LVRs [Coghlan 1999, Visser & Hall 2003, El Abd *et al.* 2004] and that most current pavement design guides for roads constructed largely or entirely of unbound layers [TRL 1993, HMSO 1994, Austroads 1995] specify aggregate assessment for unbound pavements according to tradition, more appropriate design methods are required.

Hall and Bettis [2000] highlight that the use of standard methods for designing low volume roads may result in structures of substantial, and perhaps unwarranted, sections, resulting in fewer miles of low-volume roads pavements constructed, having, therefore, unwanted effect in local economies.

A methodology to design this specific type of pavement structures should be accurate enough so that the main cause of distress in low volume roads – permanent deformation or rutting [Arnold 2004, Dawson *et al.* 2005] – can be avoided and the level of serviceability sustained. For this reason, one of the key parameters to be carefully studied whilst analyzing a LVR design method is its competence in predicting the layers' permanent deformation development.

Most current pavement design guides [TRL 1993, HMSO 1994, Austroads 1995] assume that the permanent deformation is restricted to the subgrade soil foundation, neglecting the contribution of the unbound granular material (UGM) from the base layers in the total rutting. Nevertheless, studies in real scale have shown that UGM play an important role in the rutting process [Little 1992, Arnold 2004, Dawson *et al.* 2005] and needs, therefore, to be integrated into pavement design/assessment guides.

Over recent years, some researches have aimed at understanding unbound granular material behaviour, its properties and performance in regard to permanent deformation. Several studies, as discussed in chapter 2, have accomplished great advances in the topic, despite the difficulties involved in the study of such complex material.

Nonetheless, few of them have managed to go further in approaching the topic from a design perspective, and none have yet managed to produce a successful mechanistic-based approach, certainly due to the high complexity involved. This thesis aimed at the examination of the available methods and latest studies in this subject, attempting to marshal a mechanistic-empirical approach to the design of low volume roads, eventually making proposals to improve their accuracy.

---

Considering the limited resources readily available for low volume roads owners, the new design processes for roads, maintenance and rehabilitation need to be rather straight forward. Hence, the work carried out attempted to assemble a design procedure which encapsulated the mechanical behaviour of the granular material into a simple procedure that accounts for subgrade strength, loading type and permanent deformation of the aggregate layer, analysing the interaction of these in an easily interactive manner.

## **1.2. INTRODUCTION TO THE PROJECT**

This research is the result of a three years project carried at the University of Nottingham, supported by the Programme Alþan - the European Union Programme of High Level Scholarships for Latin America -, the Nottingham Transportation Engineering Centre - NTEC and the RUTT Project which was a partnership between the Forestry Civil Engineering/Scotland and the University of Nottingham.

The work developed consisted of an initial phase on which most of the effort was dedicated to set the RUTT project up and running, choosing representative sites of typical behaviour forest roads in southern Scotland and establishing procedures for data collection. In addition, during the project, accelerated pavement trials at full scale were carried out to validate the results obtained and for further understanding of the granular material behaviour. The project ran during the first two years of this research, monitored 21 sites in Southern Scotland and accomplished 11 full scale trials. In a later stage, materials were tested in the laboratories of the University of Nottingham.

From an understanding of the mechanical behaviour and usual types of distress in low volume roads, a mechanical assessment of a variety of conditions were carried out in the light of the usual parameters typically featured in such roads. The analysis, along with the results obtained in the earlier stages, enabled a procedure to be assembled which aids the design of granular layers for pavements subject to low volume traffic.

Considering that the main distress mechanism of granular layers is the development of permanent deformation that accumulates to an incremental collapse, the method proposes to look at rationale of this mechanism by assessing the proximity of the stress distribution in the pavement to its failure envelope. The higher the reliability expected to the road, the further the stress condition in the granular layer ought to be kept away from its failure envelope. The stress distribution is then proposed to be encapsulated into a simple stress parameter which is compared to the material strength. For pavement design, different pavement structures and materials are evaluated until this parameter is limited to an acceptable level, preventing the granular layer from rutting.

---

This procedure used along with other design criteria, i.e. the assessment of other permanent deformation mechanisms, such as subgrade failure, results in a simple design method delivered in this research. Use of data available in the literature from other collaborators and from the RUTT project allowed the procedure to be validated for in-service roads.

### **1.3. OBJECTIVES OF THE RESEARCH**

The overall aim of this PhD thesis is to look into the behaviour of in-service roads and from a newly developed process, to advance, in a systematic manner, the elements required to produce a simple mechanistic design procedure.

The goals that drove the author in the research are:

- To review models for predicting permanent deformation in LVR structures.
- To provide a simplified version for routine implementation by users that is applicable for both new LVR pavement design and rehabilitation design.
- To validate this from available performance data (some of which were collected by the author).

Specific goals attempted in the thesis are:

- Contribute to a better understanding of the elasto-plastic characteristics of the constituent unbound granular material.
- Select and/or suggest appropriate model(s) of non-linear stress/strain behaviour of soils and aggregates, verifying which resistance parameters in unbound materials better model the incremental repeated load strain phenomenon.
- Examine and calibrate prediction models for failure criteria validating the results obtained in-situ (R.U.T.T project) and other available data.
- To marshal the design approach into a design/assessment guide.

### **1.4. SCOPE**

In order to accomplish the objectives set for this research, the following topics are discussed in the next chapters: a literature review of unbound granular materials, road layers and permanent deformation behaviour in Chapter 2; low volume roads design and operation in Chapter 3; full scale trials in Scotland in Chapters 4 and 5; the mechanistic

---

analysis carried out in Chapter 6; and the methodology proposal and validation in Chapter 7.

The understanding about the behaviour of unbound granular material used as pavement layers for typical low volume roads structures is reviewed in Chapter 2. The principal mechanism of deformability - resilience and plasticity of these materials are approached as well as the Shakedown concept. A review of the performance tests used to measure deformability parameters is also briefly described. In Chapter 3, the types of existing design methods for LVR structures are compiled and a further discussion provided on how these roads operate so as to enable a more comprehensive analysis of the available monitoring tools and typical loading types.

Chapter 4 brings the trials carried out in Scotland during the RUTT project. A full description of the research carried out is presented and the monitoring trial sections and accelerated trials are described. The Chapter also covers the methodology for the monitoring trial section and materials employed. The results obtained are detailed and discussed in Chapter 5.

Chapter 6 includes the mechanistic analysis on which is based the new proposed methodology in Chapter 7. The description of the analysis with the structure used and the materials inputs are detailed in the former chapter whereas the proposed methodology and its validation is in the latter.

Chapter 8 provides conclusions and suggestions for future work.

---

## 2. UNBOUND GRANULAR MATERIAL AND ROAD LAYERS

Pavements in low volume roads have very similar road structures to those in other sectors of highway engineering, except for the bound layers which usually have high costs for the hydraulic or asphalt binder. Hence, the granular layers are traditionally the most competent layers and have the function to spread the load over a weaker subgrade.

There are various issues concerning LVR engineering: Coghlan [1999], Visser & Hall [2003] and El abd *et al.* [2004] confirm that traditional highway engineering standards may not be appropriate and that little data concerning LVR performance, cost, use, etc. is available. Most pavement design methods are based on linear elastic calculations; such methods give good results for rigid pavements, with bituminous or cement treated base and subbase layers.

However, for low traffic pavements with unbound granular layers they are considerably less satisfactory because of the stress dependency of this material's behaviour and because of its variability due to source and climatic variations (Figure 2.1). Furthermore, traditional high-volume highway engineering planning and standards often incorporate high implied levels of service that are not appropriate for LVRs and that, when used, result in unnecessarily expensive solutions, rendering as impracticable some projects that could, otherwise, have been accomplished.

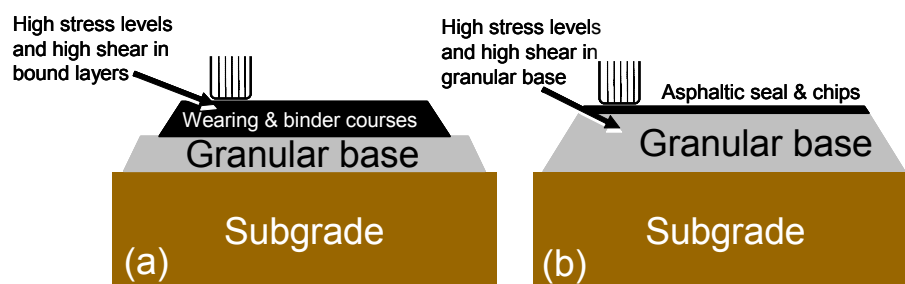


Figure 2.1 – Schematic profile of (a) high-volume road & (b) low-volume road pavement

UGM materials (and subgrade soils) exhibit two main deformation modes when subject to cyclic loading: resilient deformation (which may be elastic or inelastic – that is, hysteretic – in nature), which can be responsible for fatigue cracking of the upper, bonded layers, and permanent (plastic) deformation, responsible for rutting in the wheel paths. The permanent deformation is a consequence of the small contribution caused by each cycle

– wheel pass. Although the resilient deformation (recoverable) is almost invariably greater than the plastic deformation (non-recoverable) caused by one cycle, after many cycles the plastic component often becomes significant and may lead to an eventual failure of the pavement due to excessive rutting.

The resilient deformation suffered by the granular material due to a wheel pass is not harmful to the pavement structure, although it may interfere in operational costs, e.g. by causing higher fuel consumption due to energy dissipated in deflecting the layer [Douglas & Valsangkar 1992]. The plastic deformation, however, may lead to the failure of the structure if it keeps building up with each loading cycle. It is the rationale of a pavement design guide to account for that and to steer the designer towards a solution that will prevent it from happening. The design method must be able to determine if the traffic for the designed life will cause a total accumulation of plastic deformation that falls within the maximum operational level of rutting, guaranteeing serviceability of the road throughout its entire life, or, whether it will be necessary to establish maintenance interventions to make this achievable.

Despite the importance of rutting of UGMs, especially in low traffic pavements, there is no well-established method to study the permanent deformation of UGMs in the laboratory, and to predict their rutting in the pavements. According to [El Abd *et al.* 2004], in the absence of a satisfactory method to predict rut depth, the design of pavements with unbound granular material layers remains, in most design methods, very empirical. Due to these oversimplified methods, it is not possible, today, to take full advantage of the real performance of UGM. There is a strong need to improve this situation, and to develop and introduce into current practice:

- Appropriate mechanical performance tests to determine the resistance to permanent deformation of unbound granular material;
- More appropriate models to predict their permanent deformation in pavements.

Performance tests in UGM are approached in Section 2.6, as well as models to predict permanent deformation in Section 2.4.3. Nonetheless, these concepts are approached only as an understanding for the rationale of the problem in study. The design procedure for low volume roads design proposed in Chapter 7 approaches in a simplified manner both of these concepts, in order to be able to be readily available for LVR owners.

---



## 2.1. STRESS CONDITIONS

The passage of a wheel load over a pavement produces stresses and strains in all underlying layers. The normal stresses at a point within a soil mass are generally a function of the orientation of the plane chosen to define such stresses, while the strains are a function of these stresses.

The stresses acting on a given element in a material can be defined by its normal and shear stress components, as illustrated in Figure 2.2. It can be proved that, for any general state of stress through any point in a body, three mutually perpendicular planes exist on which no shear stresses act. The resulting stresses on these planes are thus represented by a set of three normal stresses, called  $\sigma_1$ ,  $\sigma_2$  &  $\sigma_3$ . The principal stresses ( $\sigma_1$ ,  $\sigma_2$  &  $\sigma_3$ ) are physical invariants that are independent of the choice of the co-ordinate system (X,Y,Z).

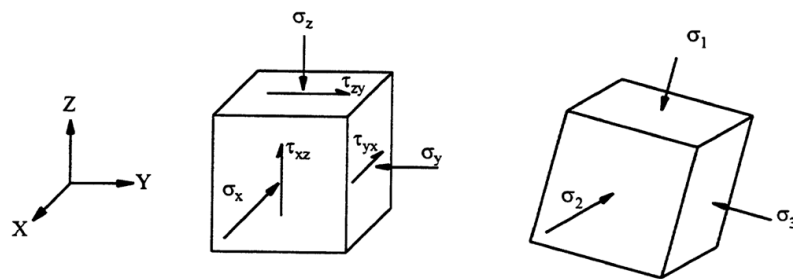


Figure 2.2 – Stress components acting on an element [Lekarp 1997]

The stresses produced by the passage of a wheel load in a given element inside a pavement within the plane of the wheel track can be graphically represented as in Figure 2.3. When the load moves, the vertical stress  $\sigma_v$  and the horizontal stress  $\sigma_h$  present a relatively sinusoidal variation, and are maximum when the centre of the load is directly above the element being analysed. Figure 2.4 shows the associated pattern of principal stresses illustrating the rotation of principal planes which takes place.

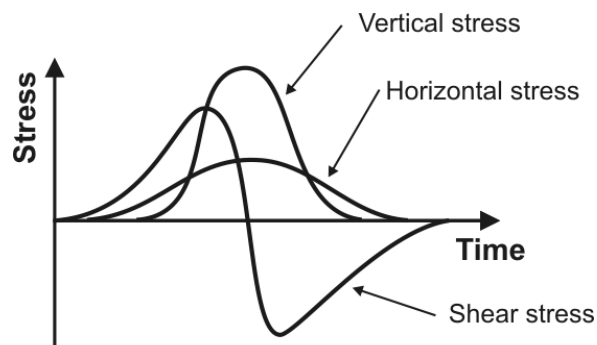


Figure 2.3 – Stress conditions under a wheel load pass [Shaw 1980]

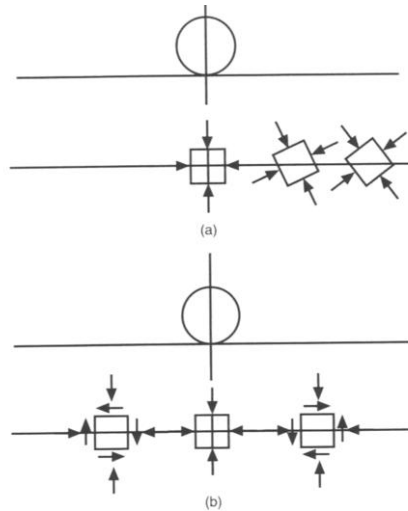


Figure 2.4 – Stresses on a pavement: (a) principal stresses – rotate; (b) no rotation – shear stress reversal [Brown 1996]

The stress states shown above can only be reproduced with considerable difficulty by a laboratory test, such as a Hollow Cylinder Apparatus, described further in section 2.6.4. As one approach to the study of materials behaviour is the selection of equipment which reproduces the field situation, several types of tests have been developed to test unbound granular material under both static and dynamic conditions.

A LVR structure can be simply constituted of local subsoil, as a foundation to the road structure, with one or more overlays of UGM. Alternatively, a bituminous surfacing can be used to increase the capacity and/or road quality. If only UGM is used in the pavement, then the vertical and horizontal stresses are positive (compression), since UGM do not carry tensile stresses. Only with thicknesses greater than a certain limit of bituminous material, or other bonded mixture, can negative stresses (tension) appear.

Dawson [2007] stress the principle involved in load distribution in LVR structures: in the case of LVR pavement layouts containing bituminous surfacing, the surfacing needs to be greater than a threshold thickness, around 40mm, in order to achieve effective load spreading and significantly reduce stress on the lower aggregate base layers. In the analyses shown in the study, the maximum vertical stress  $\sigma_{v_{max}}$  to which the base layer is submitted is nearly the same as for a 1mm (minimum thickness necessary for the computer program used by the authors to analyse the stresses), 10mm or 20mm layer of bituminous standard asphalt mix used on top of the base layer. With a thickness of 40mm, the  $\sigma_{v_{max}}$  reduces by approximately 40%, while for 200mm, the  $\sigma_{v_{max}}$  reduces by approximately 65%. Therefore, it appears that there is little effective bending stiffness until the layer is much more than 20mm thick. Figure 2.5 pictures the vertical and horizontal stress distribution within a pavement structure of various asphalt thicknesses.

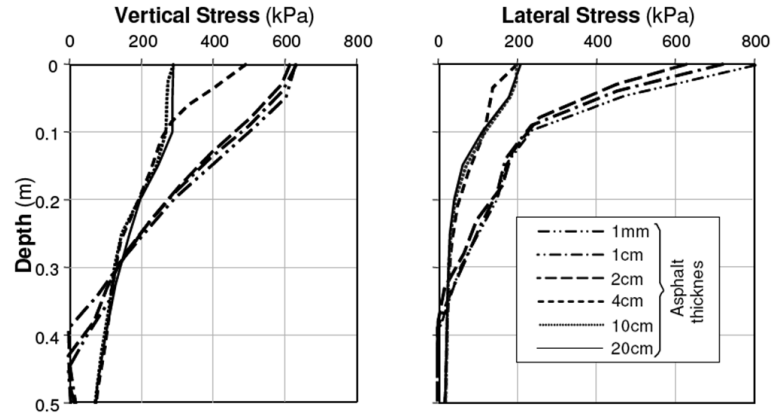


Figure 2.5 – Variation of vertical and horizontal stress in granular layer of pavements with various thicknesses of asphalt [Dawson *et al.* 2007]

Mundy [2002] studied a wide range of pavements that have been modelled in order to derive a stress locus which encompassed all stress combinations expected within the UGMs of any loaded pavement configuration. From this information, he derived a new set of stress conditions that can be applied to the RLT test to determine moduli for design purposes. On applying the new stress sequence to testing a material, it was found that the variation in resilient modulus for repeated testing was 4% or less for the basecourse stress sequence.

### 2.1.1. Stress invariants

At every point in a stressed body there are at least three planes, called principal planes. The three stresses normal to these principal planes are called principal stresses ( $\sigma_1$ ,  $\sigma_2$ ,  $\sigma_3$ ). The magnitude and direction of each of these stresses is called stress tensor. However, the stress tensor itself is a physical quantity and, hence, is independent of the coordinate system chosen to represent it. There are certain invariants associated with every tensor which are also independent of the coordinate system.

In order to simplify the stress-strain analysis, the applied stresses can be divided into volumetric and shear components. As a result, the general stress state in a three dimensional system can be given by the following functions:

$$p = \frac{1}{3}(\sigma_1 + \sigma_2 + \sigma_3) \quad \text{Equation 1}$$

$$\tau_{oct} = \frac{1}{3}\sqrt{(\sigma_1 - \sigma_2)^2 + (\sigma_2 - \sigma_3)^2 + (\sigma_3 - \sigma_1)^2} \quad \text{Equation 2}$$

Where:  $p$  = mean normal stress

$\tau_{oct}$  = octahedral shear stress

Both  $p$  and  $\tau_{oct}$  are stress invariants. Despite the different stress invariants used, it is common in soil mechanics, particular in triaxial conditions, to describe the shear stress invariant as deviator stress or principal stress difference,  $q$ , where:

$$q = \tau_{oct} \frac{3}{\sqrt{2}} \quad \text{or} \quad q = \sigma_1 - \sigma_3 \quad \text{Equation 3}$$

Likewise, in a triaxial condition,  $\sigma_2$  becomes equivalent to  $\sigma_3$  and  $p$  can, therefore, be simplified to:

$$p = \frac{1}{3}(\sigma_1 + 2\sigma_3) \quad \text{Equation 4}$$

Another widely used stress invariant, mainly for resilient deformation modelling is theta ( $\theta$ ), known as bulk stress; this is equal to the sum of all principal stresses or simply  $3p$ .

### 2.1.2. In-pavement stresses

Mundy [2002] examined the use of a wide range of unbound granular materials in various pavements. The research studied analytical design methods for unsealed or thinly sealed pavements largely constituted of unbound granular layers.

He conducted a theoretical study to determine the stress regimes experienced by UGM in a variety of different flexible pavement types, namely the Australian and the French. The pavement type analysed to determine the stress, and subsequent stress loci boundaries considered bituminous surfacing thickness ranging from 0mm (spray seal) to 100mm, quality of the aggregate material ranging from high to marginal in quality, non linear elastic modelling of material modulus with stress ( $k-\theta$ ),  $E_v/E_h$  between 1.0 to 2.0 and pavement foundation with stiffness of 30MPa, 50MPa and 100MPa.

The French study considered similar conditions with bituminous surfacing thickness from 40mm or 60mm to 120mm, subgrade stiffness of 50MPa and unknown  $E_v/E_h$  ratio. A typical plot of the results obtained in the study for a select range of pavements commonly constructed in Australia is presented in Figure 2.6. Similarly, Figure 2.7 shows the stress level envelopes for the Australian and French structures analysed.

Both plots enabled Mundy [2002] to establish testing stress paths to concentrate within the stress boundaries defined; as the pavement stress distribution to the structured ana-

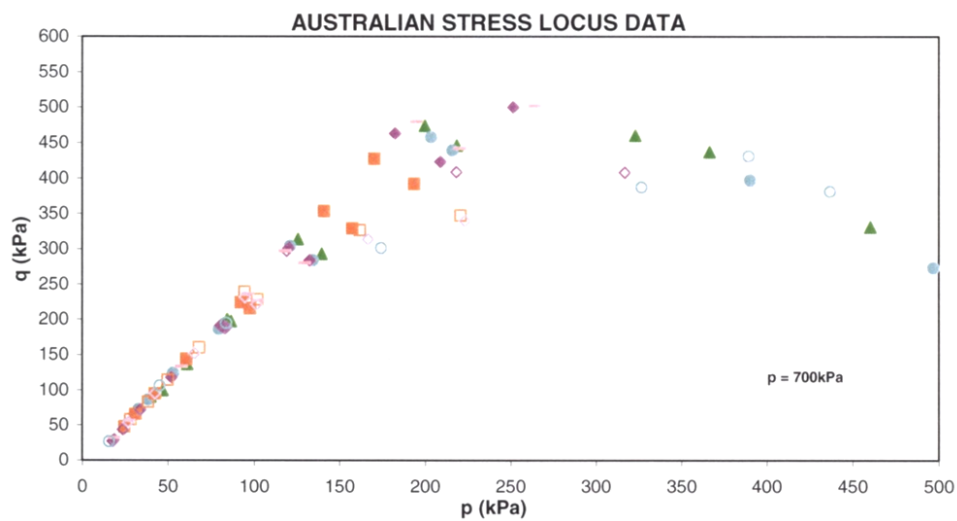


Figure 2.6 – Stress level data for the Australian pavements analysed by Mundy [2002]

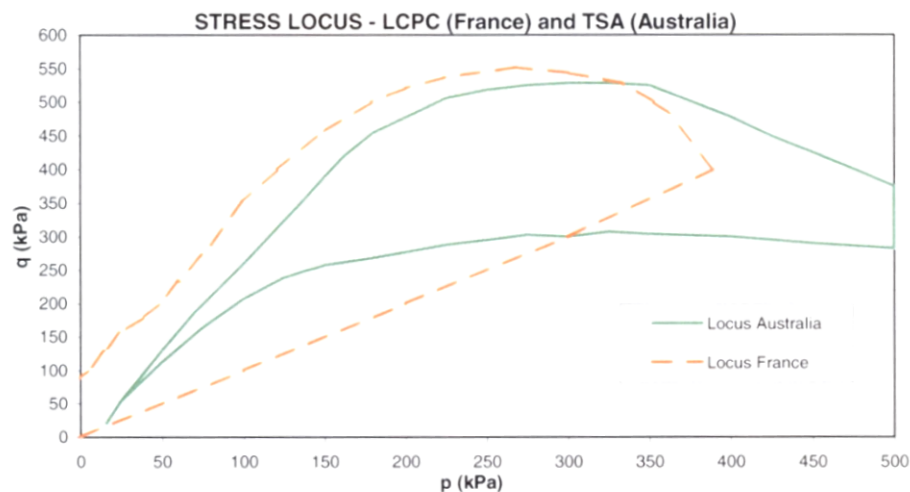


Figure 2.7 – Stress level boundaries for Australia and LCPC analysed pavements

lysed were found to lie within the locus boundaries shown in Figure 2.7. The Australian locus extends to higher levels of  $p$  due to the very thin bituminous spray seal pavement analysed as opposed to the French pavements which has a rather more even distribution to the higher stiffness layer on top, resulting in lower  $p$  results.

The French locus extends to higher levels of  $q$ , for a given level of  $p$ , than the Australian locus. One factor causing this result is that no correction for lateral stress was undertaken in the French study, hence,  $q$  values are higher and  $p$  values are slightly lower [Mundy 2002]. In addition, he managed to derive shear zones in  $q$ - $p$  spaces to reflect material's quality in the same study.

## 2.2. DEFORMABILITY

UGM are different from soils in their physical characteristics and also in their response to applied cyclic load. Hence, its deformability must be approached accordingly. An UGM is an assembly of a large number of individual particles with different shapes and sizes. These materials carry only a very small amount of tensile strain [Wenzel 1998].

There are two main deformability modes of interest in unbound granular material: under monotonic loading and under cyclic loading. Typically, the behaviour under cyclic loading is of major interest for pavement engineering. The deformability under static loading provides complementary knowledge for use with a classical soil mechanics framework, which is widely used for the assessment of UGM behaviour.

The deformation resistance of an UGM depends on the applied stress, which is a function of the loading condition (vehicle speed, weight, axle layout, tyre characteristics) and the pavement structure. The behaviour shown in Figure 2.8 is typical for UGMs; as the vertical stress increases, the material's resistance to further deformation diminishes.

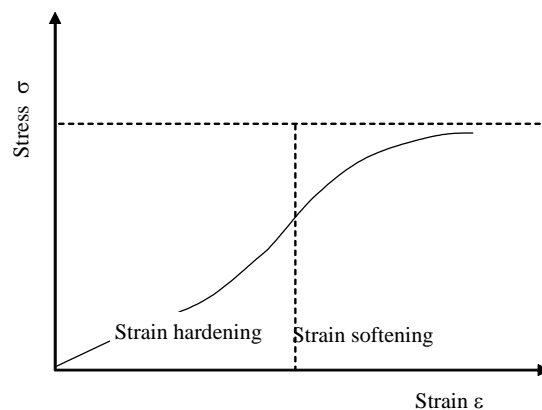


Figure 2.8 – Stress-strain behaviour of UGMs [Werkmeister 2003]

At low levels of stress, the stiffness of the material increases with rising magnitudes of load (strain hardening). The compacted UGM becomes even more closely packed and harder to move, as its components (particles) are forced into new, interlocked positions. As the stress increases further (near to failure) the stiffness of the material decreases (strain softening). Eventually, the material fails.

The typical behaviour of an UGM under cyclic loading in a repeated load triaxial test is presented in Figure 2.9. During the first cycles, the permanent strains increase rapidly, and the elastic strains, more appropriately referred as resilient strains for pavement purposes, decrease; after this initial phase, the permanent strains tend to stabilize, or continue at a slower rate– the response of the material becomes, then, essentially elastic.

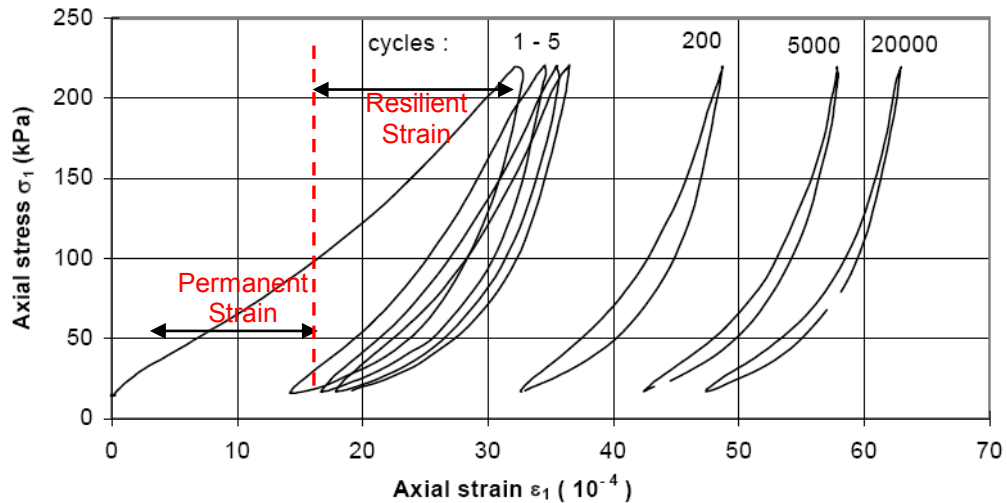


Figure 2.9 – Stress-strain behaviour of UGMs under cyclic loading in a triaxial repeated loading test [after El Abd *et al.* 2004]

This “stable” behaviour is generally obtained after several thousand loading cycles. It should be noticed that the elastic part of the response is strongly non-linear, i.e. stress-dependent. The approach generally used to study this complex behaviour consists in studying and modelling separately the resilient behaviour and the plastic behaviour [El Abd *et al.* 2004].

As seen in Figure 2.9, the stress-strain relationship for UGM is non-linear. The area of one cycle in stress-strain space (the hysteresis loop) corresponds to the work consumed per volume element. The greatest part of this work is transformed into heat energy. It partly causes a change of the material properties, which eventually leads to damage. Only a small part of this work will be accumulated [Werkmeister 2003].

In practical terms for this research, it is important that the pavement stress condition is within the domain of the resilient deformation or that the permanent deformation is controlled. It becomes evident the importance to have the ability to model these two behaviours separately and its interaction from the design perspective. The permanent deformation development in LVR in form of ruts is the main distress mode of these pavements, and broadly a consequence of the deformability in the pavement layers. Considering that granular layers are typically the competent layers in low volume roads structures, modelling their deformability enables to mechanistically approach their design.

### 2.2.1. Factors affecting resilient behaviour

In general, the resilient behaviour of granular materials can be affected by many factors, such as: stress level, confining stress mode, stress rotation, method of compaction, density, water content, anisotropy, stress history, freeze-thaw cycles.

The seasonal variation in granular materials has a notorious effect on their resilient properties. This happens mostly due to the variation in the moisture, which not only varies due to its content, but also in freezing temperatures which greatly enhances material stiffness. Conversely, during a thawing season, stiffness may drop severely causing the material to be very little resilient and to develop great permanent deformation.

Unlikely factors affecting permanent deformation (Section 2.4.2), elastic properties may not be as affected by the number of cycles. The cyclic loading may have a strong effect on the compaction level and, therefore, in the density of the material what can, eventually, lead to a change in the resilient behaviour. Nevertheless, the change in resilience of granular materials due to the number of cycles can be translated as a function of the variation in stress history, density or other material property.

A number of studies has been undertaken to assess the influence of various factors on resilient stiffness of unbound materials. Lekarp *et al.* [2000] summarised the factors that affect the resilient stiffness of granular materials in a state of the art review. In all, seven factors were identified and a semi quantitative assessment was undertaken. The testing was generally undertaken using repeated load triaxial (RLT) apparatus.

It is important to note that the overall assessment of these factors is complicated by the variability of materials tested; potential variability of equipment and research procedure [Chen *et al.* 1994, Dawson *et al.* 1994], location and type of on-sample measuring devices [Mohammad *et al.* 1994]. The factors controlled during sample preparation and conditioning are summarised in Table 2.1.

---



Table 2.1 – Factors affecting resilient behaviour

Factor	Response
Stress	General agreement among several researchers [including Uzan 1985, Sweere 1990] that the most significant influence on resilient properties of granular materials measured in a RLT is stress level.
Density	No simple and direct correlation between resilient modulus and density. Thom [1988], Khogali and Zeghal [2000] concluded that density does not significantly affect the resilient response of UGM. Lekarp <i>et al.</i> [2000] suggest that the resilient stiffness generally increases with increasing density. Hoff <i>et al.</i> [2004] states the dependency of density on the level of compaction & methodology adopted during sample preparation.
Effect of grading, fines content, and maximum grain size	Studies highlight the influence of grading on resilient modulus, including dependence on overall grading and nominal aggregate size [including Thom 1988]. In addition, the influence of grading is shown to be a function of the contrast between fines and aggregate [Tian <i>et al.</i> 1998].
Effect of water content (during sample preparation and testing)	Rada & Witzak [1981] and Khogali & Zeghal [2000] indicate this to be the second most significant variable (after stress). Excess pore water pressures have been shown to decrease element modulus [Raad <i>et al.</i> 1992], while other researches indicate reductions due to the lubrication of particle to particle contacts [Thom & Brown 1987].
Effect of aggregate type and particle shape	Hardness and resistance to crushing appeared to show little significance to resilient stiffness. However, Thom [1988] noted a correlation between friction (related to the particle to particle contact) and elastic modulus.
Effect of stress history and number of load cycles	Testing in a RLT showed that the load history of an unbound granular material does not significantly affect its resilient stiffness [Brown & Hyde 1975].
Effect of load duration, frequency, and load sequence	Research in this area appears to be in general agreement that load duration and frequency appear to have very little or no impact on resilient stiffness values [Lekarp <i>et al.</i> 2000].

## 2.3. MODELLING DEFORMABILITY

### 2.3.1. Resilient models

In the traditional theories of elasticity, the elastic properties of a material can be defined by its modulus of elasticity ( $E$ ) and Poisson's Ratio ( $\nu$ ) which are material constants. A similar approach has been widely used when dealing with granular materials, but the modulus of elasticity is replaced with the resilient modulus ( $MR$ ) to indicate the non-linearity, that is the stress-dependence and the inelastic nature of the behaviour. The method of calculating resilient parameters is the same as would apply to an isotropic, linear-elastic material under uniaxial stress conditions [Lekarp *et al.* 2000].

When cyclic confining pressure is applied, the generalized Hooke's Law is employed for 3-dimensional stress-strain relationships of an isotropic, linear-elastic material. The resilient modulus and Poisson's ratio are then derived from:

$$M_r = \frac{\Delta(\sigma_1 - \sigma_3)\Delta(\sigma_1 + 2\sigma_3)}{\varepsilon_{1,r}\Delta(\sigma_1 + \sigma_3) - 2\varepsilon_{3,r}\Delta\sigma_3} \quad \text{Equation 5}$$

$$\nu = \frac{\Delta\sigma_1\varepsilon_{3,r} - \Delta\sigma_3\varepsilon_{1,r}}{2\Delta\sigma_3\varepsilon_{3,r} - \varepsilon_{1,r}\Delta(\sigma_1 + \sigma_3)} \quad \text{Equation 6}$$

Where:  $\sigma_1$  = major principal stress

$\sigma_3$  = minor principal stress

$\varepsilon_{1,r}$  = recoverable axial strain

$\varepsilon_{3,r}$  = recoverable horizontal strain

Several researches have outlined mathematical models to describe the resilient modulus as function of the stress state. Some of the models found in the literature are given in Table 2.2.

Dunlap [1963] and Monismith *et al.* [1967], in the 60's, indicated that the resilient modulus increases with confining pressure and is sensibly unaffected by the magnitude of repeated deviator stress, provided the deviator stress does not cause excessive plastic deformation. They, therefore, proposed an expression solely based on the effect of confining stress as given by Equation 7.

The k- $\theta$  model (Equation 8) originally proposed by Biarez [1962], and afterwards by Seed *et al.* [1967], Brown & Pell [1967] and Hicks [1970] is a well known and widespread approach to describe the resilient behaviour. The simplicity of this model has made it extensively accepted for analysis of stress dependency of material stiffness. However, the disadvantage of this model is that it assumes a constant Poisson's ratio and the effects of stress on resilient modulus are accounted for only the sum of the principal stresses. Some authors have reported the limitation of this model [Sweere 1990, Kolisoja 1994].

Table 2.2 – Mathematical models for Triaxial Resilient Modulus

Expression	Eqn.	Reference	Expression	Eqn.	Reference
$M_r = k_1 \sigma_3^{k_2} \quad M_R = K_1 \left( \frac{\sigma_3^{k_2}}{p_o} \right)$	(7)	Dunlap [1963] Monismith <i>et al.</i> [1967]	$M_r = \frac{\theta}{q} (A + Bq)$	"CCP" (15)	Nataatmadja & Parkin [1989]
$M_r = k_1 \theta^{k_2} \quad M_r = k_1 \left( \frac{\theta}{p_o} \right)^{k_2}$	(8)	Seed <i>et al.</i> [1967]	$M_r = \frac{\theta}{\sigma_1} (C + Dq)$	"VCP" (16)	
$M_r = k_2 + k_3 (k_1 - \sigma_d) \quad k_1 \geq \sigma_d$ $M_r = k_2 + k_4 (\sigma_d - k_1) \quad k_1 < \sigma_d$	(9)	Thompson & Robnett [1979] Raad & Figueroa [1980]	$M_r = N_1 q^{N_2} \sigma_3^{N_3}$	(17)	Pezo [1993]
$M_r = k_1 p_o \left( \frac{\theta}{p_o} \right)^{k_2} \left( \frac{q}{p_o} \right)^{k_3}$	(10)	Uzan [1985]	$M_r = A \left( \frac{p_m}{p_u} \right)^B \left( \frac{p_u}{\delta_p} \right)^C$	(18)	Karasahin [1993]
$M_r = k_1 p_o \left( \frac{\theta}{p_o} \right)^{k_2} \left( \frac{\tau_{oct}}{p_o} \right)^{k_3}$	(11)		$M_r = A (\eta_{\max} - \eta) p_o \left( \frac{\theta}{p_o} \right)^{0.5}$	(19)	Kolisoja [1997]
$M_r = k_1 \left( \frac{J_2}{\tau_{oct}} \right)^{k_2}$	(12)	Johnson <i>et al.</i> [1986]	$M_r = B (\eta_{\max} - \eta) p_o \left( \frac{\theta}{p_o} \right)^{0.7} \left( \frac{q}{p_o} \right)^{-0.2}$	(20)	
$M_r = k_1 \left( \frac{p}{q} \right)^{k_2}$	(13)	Tam & Brown [1988]	$M_r = k_1 p_o \left( \frac{\theta}{p_o} \right)^{k_2} \left( \frac{\tau_{oct}}{p_o} + 1 \right)^{k_3}$	(21)	NCHRP 1-37A - Part 2 [2004]
$M_r = k_1 \frac{\theta^{k_2}}{10^{A1}}$	(14)	Elliot & Lourdesnatham [1989]	$M_r = k_1 p_o \left( \frac{\theta - 3k_6}{p_o} \right)^{k_2} \left( \frac{\tau_{oct}}{p_o} + k_7 \right)^{k_3}$	(22)	NCHRP 1-28A [2004]
$M_r$ = Resilient Modulus $\sigma_1, \sigma_2, \sigma_3$ = principal stresses $\sigma_d = q$ = deviator stress = $\sigma_1 - \sigma_3$ $p$ = mean normal stress = $(\sigma_1 + \sigma_2 + \sigma_3)/3$ $\tau_{oct}$ = octahedral shear stress = $(2^{0.5}/3)q$	$J_2$ = first stress invariant = $\sigma_1 \sigma_2 + \sigma_2 \sigma_3 + \sigma_3 \sigma_1$ $\theta$ = bulk stress = $3p$ $\delta_p = p_{\max} - p_{\min}$ $p_u$ = unit pressure (1kPa)	$p_o$ = atmospheric pressure (100kPa) $\eta$ = material porosity $\eta_{\max}$ = maximum porosity $N_1, N_2 = (10-A), (1-k_1)$ , and $(-k_2)$ , respectively, in $\text{Log}(\epsilon_1, r) = A + k_1 \text{Log} \sigma_1 + k_2 \text{Log} \sigma_2$	$\epsilon_1, r$ = resilient axial strain $k_1, k_2, k_3, k_6, k_7$ m, A - J = model parameters $A1 = \text{mR}^3$ R = strength/stress		

Other researchers found necessary to include other parameters in order to enhance the capability of the models for other materials and/or to increase the accuracy of the existing available models. Detailed discussions are available elsewhere [Lekarp *et al.* 2000, Yau & Von Quintus 2002, Andrei *et al.* 2004, Project NCHRP 1-28A 2004].

Yau and Von Quintus [2002], in the FHWA-RD-02-051, tested the granular materials of several pavement sections participating in the Long Term Pavement Performance Program – LTPP<sup>1</sup> – in the United States of America, for triaxial resilient modulus. They found out the constitutive Equation 17, in Table 2.2, to be an excellent fit to the MR test results included in the LTPP database. Specifically, almost 92% of the LTPP MR test results have response characteristics that can be accurately simulated by such model. Equation 21 is the equation selected for use in the development of the 2002 Design Guide – Project NCHRP 1-37(A) [AASHTO 2004].

Equation 22 combines both the stiffening effect of bulk stress (the term under the  $k_2$  exponent) and the softening effect of shear stress (the term under the  $k_3$  exponent). Through appropriate choices of the material parameters  $k_1$ - $k_7$ , one can recover the familiar two-parameter bulk stress model for granular materials and its companion two parameter shear stress model for cohesive soils, the Uzan-Witczak “universal” model [Witczak & Uzan 1988], and the  $k_1$ - $k_6$  model from the Strategic Highway Research Program’s (SHRP) flexible pavement performance models [Lytton *et al.* 1993].

Although some of the models may be simply based on curve fitting, others are more laborious; their capability to better describe the behaviour is what was sought by their authors. Despite the behaviour of soils and granular materials being known to be elasto-plastic, such elastic models are still widely used, due to the complexity of elasto-plastic models as discussed later.

The European project COURAGE [1999] largely studied the modelling of the resilient behaviour of unbound granular materials. In the project, a review of available resilient behaviour models was performed and several, widely used, models were evaluated by comparison with triaxial test results on different unbound granular materials.

The aim of the results of the RLT tests, obtained at a variety of stress conditions and density/moisture states, was to be able to describe aggregate performance in a manner suitable for inclusion in analytical pavement design procedures. This was achieved using

---

<sup>1</sup> The LTPP (Long-Term Pavement Performance Program) is a research program of 20 years that began in 1987. The program monitors in-service pavements, covering more than 2400 experimental sections of bituminous pavements and Portland concrete pavements in the USA and Canada. It is managed by the FHWA (Federal Highway Administration) and is part of the SHRP (Strategic Highway Research Program).

---

non-linear constitutive relationships for the material's resilient stress-strain behaviour in order that their parameters could be used in structural pavement analysis computer code to iteratively reach a stress-strain solution.

It was concluded that the non-linear elastic model proposed by Boyce [1980], and modified by Hornych *et al.* [1998] to take into account anisotropy, describes well the resilient behaviour of UGMs.

Tutumluer *et al.* [1998] and Kim *et al.* [2004], among others, discussed the determination of anisotropic resilient moduli in granular materials. Preliminary results of the former authors obtained from four aggregates tested using the Illinois FastCell (UI-FC) indicated definite directional dependency (anisotropy) of aggregate moduli. The resilient moduli computed in the vertical and radial directions varied significantly with the applied stress states.

As much as the anisotropy is an important behaviour in unbound granular materials and should be accounted for while modelling these materials, it is a rather complex concept for the scope of this research. The anisotropy is the property which establishes the direction dependency of the material behaviour.

### **2.3.2. Elasto-plastic models**

As granular materials behave partly in an elastic manner and partly in a plastic manner, both linear and non-linear elastic models are, inevitably, limited in scope as the plastic portion is neglected. For this reason, as in the field of soil mechanics, elasto-plastic models that simulate accurately the monotonic and cyclic behaviour of soil and granular materials were developed. These are considered the most complex and accurate models used in soil mechanics nowadays, although their practical use is still restricted due to the high complexity and extensive requirements of material characterization.

Few authors have developed specific elasto-plastic models for pavement applications. Recent developments in this field have been proposed by Bonaquist and Witczak [1997], Hicher *et al.* [1999], Chazallon [2000] and Werkmeister [2003].

The primary purposes of the models are to define the yield surface, after which the elastic domain is no longer valid and from there, permanent deformations start to develop. Mohr-Coulomb and Drucker-Prager criteria are commonly used for modelling plasticity in granular materials [Chen 1994]. The basic difference in the Drucker-Prager model is its sensibility to the hydrostatic stress component, assuming a conical shape yield surface as opposed to the Mohr-Coulomb criterion which translates the yield surface as a cube (Figure 2.10). The Drucker-Prager criterion is further discussed in Section 2.3.3.

---

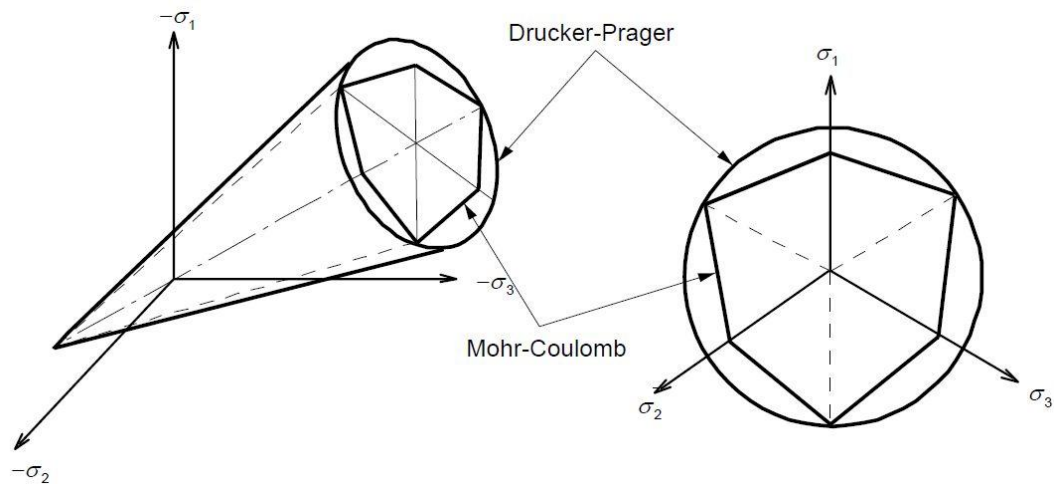


Figure 2.10 – Yield surfaces from elasto-plastic models - Mohr Coulomb & Drucker-Prager

A limitation of these models is that they were developed from monotonic loading cases and as such, they may not realistically model the lower load levels of fast cyclic loading that a pavement experiences [Steven 2005].

Hardening can also be added to elasto-plastic models. Hardening is where the failure surface/yield line moves resulting in an increase in strength that occurs after a defined amount of permanent strain. Hardening can occur many times provided there is a relationship between the yield surface and permanent strain. Khogali & Mohamed [2004] illustrate in their work the change in the resilient behaviour after many cycles, indicating a hardening effect translated in the tangential modulus of the material (Figure 2.11). As the elastic behaviour changes, so does the yield surface which tends to get further for a harder material.

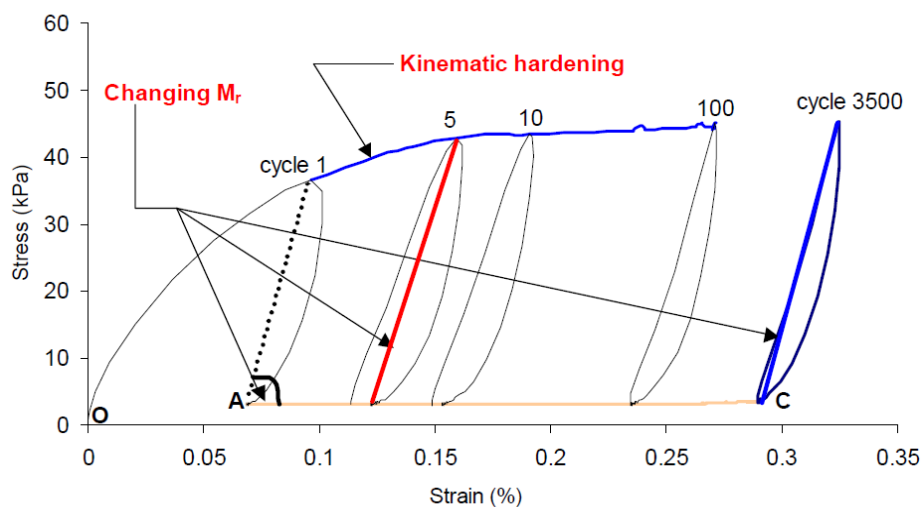


Figure 2.11 – Schematic illustrations of the kinematic hardening in terms of stress-strain response [Khogali & Mohamed 2004]

A more complex model, as the one developed by Chazallon [2000] and Chazallon *et al.* [2002] is based on the work of Hujeux [1985], according to El Abd *et al.* [2004]. It is an elasto-plastic cyclic mode with kinematic hardening, applicable to large numbers of load cycles. The model uses the yield function and plastic potential of the non-associated Hujeux [1985] model. The formulation used is a one mechanism model used for the monotonic loading of sands based on the critical state concept. The model was first presented in Chanzallon [2000], and some modifications have been added since.

Figure 2.12 shows an example of the yield surface of the model developed by Chanzallon [2000], after El Abd *et al.* [2004]. It is possible to visualize the development of the yield surface during a cyclic load excursion between points A and B in the  $(p, q)$  stress space. During the first loading from A to B, the origin of the surface is at point O, and the size of the surface grows during loading (isotropic hardening). When unloading starts, from point B, the origin of the surface moves to point  $O_2$ . The position of the surface continues to change, during unloading and subsequent reloading (isotropic and kinematic hardening).

Werkmeister [2003] studied the plastic component of UGM behaviour in order to formulate an appropriate mathematical model supported by data from experimental investigations to be implemented in the existing Elastic Dresden Model. This was achieved through the study of the Shakedown theory, which establishes the limit on which a critical stress level separates a stable condition, from the permanent deformation development point of view, from an unstable condition in a pavement. According to the “shakedown” concept, this is termed the “shakedown limit”. This concept is later discussed in this Chapter.

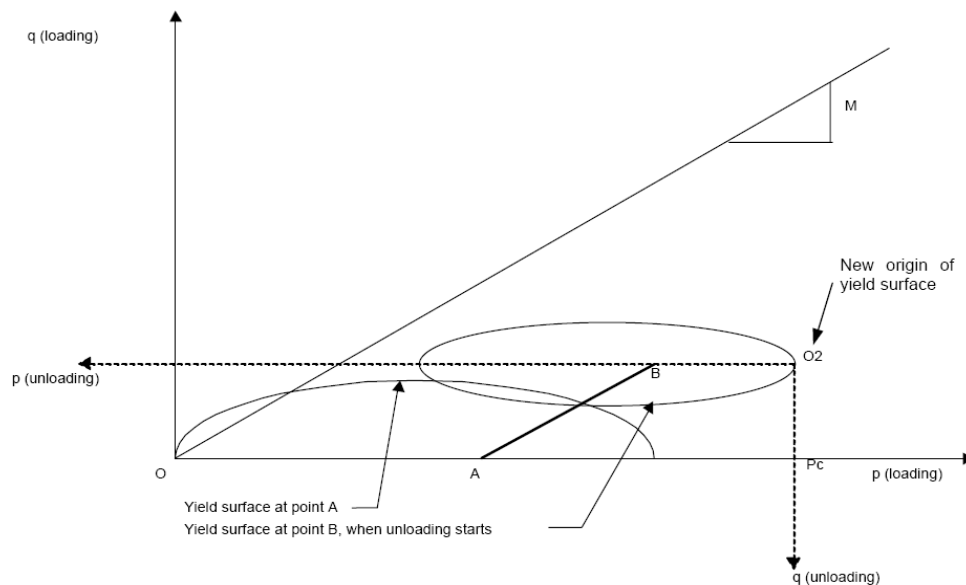


Figure 2.12 – Yield surface of the model of Chazallon, and hardening mechanism [after El Abd *et al.* 2004]

### 2.3.3. Drucker-Prager yield criteria

Elastoplastic models have two parts, an elastic and a plastic or yield phase. The material response is elastic up to a failure stress limit, after which if the stress continues to increase, undergoing plastic (permanent) straining. Drucker-Prager proposed in 1952 a model which extended the Von Mises yield criterion to include the hydrostatic component of the stress tensor. This model is a linear elastic and isotropic criterion for modelling the plastic phase up to a yield surface after which the elastic domain is no longer valid.

Drucker-Prager yield surface -  $F_s$  - can be defined in terms of mean normal stress ( $p$ ) and principal stress difference ( $q$ ) as per Equation 23.

$$F_s = q - p \cdot \tan\beta - d = 0$$

Equation 23

Where:  $\beta$  = the angle of the yield surface in  $p$ - $q$  stress space (Figure 2.13)

$d$  = the  $q$ -intercept of the yield surface in  $p$ - $q$  stress space (Figure 2.13)

If the experimental data is not readily available, the yield line can be obtained from Mohr-Coulomb friction angle,  $\phi$ , and cohesion,  $c$ . From relationships between  $p$ - $q$  stresses and principal stresses the Mohr-Coulomb failure line can be plotted in  $p$ - $q$  space to represent a Drucker-Prager failure criterion. It can be shown that the angle of the failure line in  $p$ - $q$  stress space,  $\beta$ , is defined by Equation 24 and the  $q$ -intercept,  $d$  is determined using Equation 25 for triaxial test conditions (i.e.  $\sigma_2 = \sigma_3$ ).

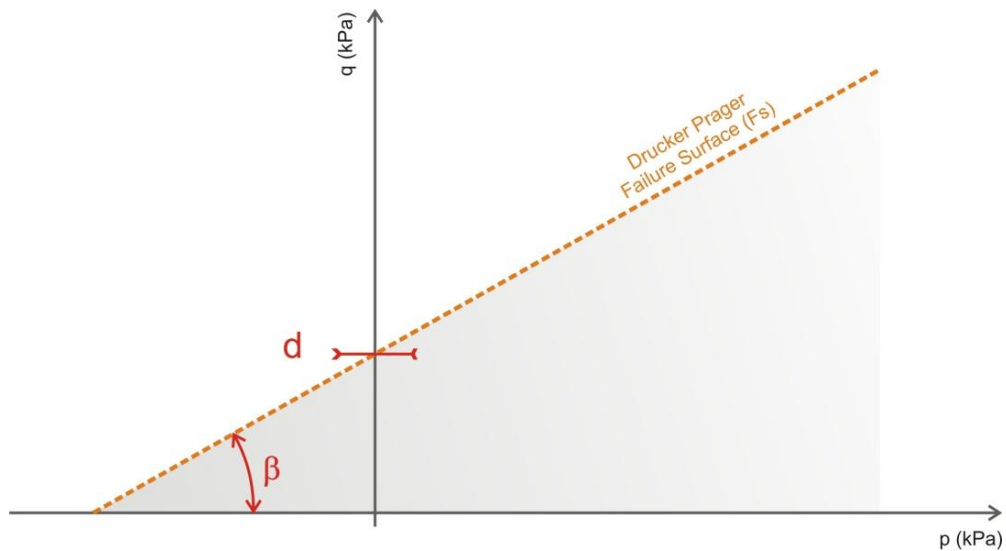


Figure 2.13 – Drucker-Prager yield condition in 2D  $p$ - $q$  stress space



$$\tan \beta = \frac{6 \sin \phi}{3 - \sin \phi} \quad \text{Equation 24}$$

$$d = \frac{6c \cos \phi}{3 - \sin \phi} \quad \text{Equation 25}$$

## 2.4. PERMANENT DEFORMATION IN UNBOUND GRANULAR LAYERS

Flexible pavement design methods have, as one of their primary goals, the aim of limiting permanent deformation in a pavement structure. Therefore, it is important to have a good understanding of the rutting mechanism in a road structure, its initiation process and development modes, specifically in granular layers, as they can contribute up to 70% of surface rutting as indicated by accelerated pavement tests [Ceratti *et al.* 2000, Arnold 2004, Núñez *et al.* 2008].

The loading imposed on flexible pavement structures generates resilient, or elastic, deformation ( $\epsilon_r$ ) and permanent, or plastic, deformation ( $\epsilon_p$ ), as pictured in Figure 2.9. Although the permanent deformation during one cycle of loading is normally just a fraction of the total deformation produced by each load repetition, the gradual accumulation of a large number of these small plastic deformation increments could lead to an eventual failure of the pavement due to excessive rutting [Lekarp & Dawson 1998].

Thom and Brown [1989] found that ranking materials in terms of their stiffness was not the same as ranking materials in terms of their resistance to deformation. A material with the lowest stiffness did not have the lowest resistance to deformation, highlighting the importance of advances in the research of permanent deformation in pavements from an elasto-plastic approach.

### 2.4.1. Rutting mechanisms

According to Dawson & Kolisoja [2004], rutting can occur due to a number of reasons. Fundamentally there are four contributory mechanisms, which can be labelled as Modes 0, 1, 2 and 3, for convenience.

- Mode 0 – Compaction of granular layers alone – A self-stabilizing mode or rutting usually occurs due to under-compaction of the granular layer prior to trafficking. In limited amounts, this mode of rutting may be beneficial for the pavement, provided that it stiffens the layer, resulting in a better load distribution. Ideally, there would be no deformation at the subgrade surface.

- Mode 1 – Shear deformation of granular layers – Usually occurs in weaker granular materials. It appears as a dilative heave adjacent to the wheel track. This rutting is largely a consequence of inadequate granular material shear strength in the aggregate close to the pavement surface. Ideally, there would be no deformation at the subgrade surface.
- Mode 2 – Shear deformation within the subgrade with the granular layer following the subgrade – when aggregate quality is better, then the pavement as a whole may rut. Ideally, this can be viewed as the subgrade deforming with the granular layer(s) deflecting bodily on it (i.e. without any thinning). This is the least desirable of modes 0, 1 and 2 as it is not readily correctible.
- Mode 3 – Particle Damage (e.g. attrition or abrasion, perhaps by studded tyres) can be a contributor to the same surface manifestation as seen in Mode 0 rutting, though, of course, the mechanism is very different.

A schematic representation of the modes mentioned above is presented in Figure 2.14. The same authors also describe rutting due to a combination of the above mechanisms.

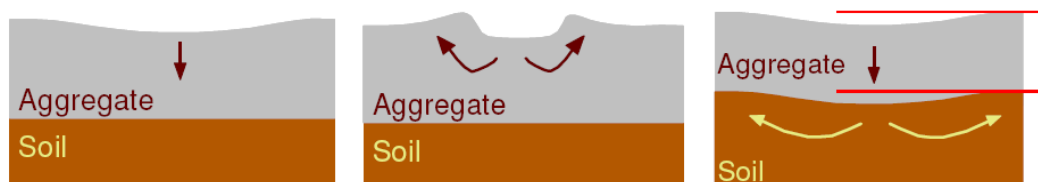


Figure 2.14 – Rutting mechanisms: Mode 0, 1 and 2 respectively [Dawson & Kolisoja 2004]

Mode 0 is typically a self-stopping occurrence once adequate compaction has taken place and Mode 3 is usually addressed by particle strength requirements. Mode 1 failure is the core topic of this research which is tackled with the proposed methodology in Chapter 7. Mode 2 is also approached by verifying the allowable stress condition at the top of the subgrade.

Typically, ruts in roads are the result of a combined effect of the named modes. It is expected that Mode 1 will be more evident with canalised trafficking (e.g. forest roads) where wheel wander is not available. Conversely, Mode 2 is expected to be more evident under wandering traffic with Mode 0 more likely to make a contribution in this case as the "kneading action" of a wandering tyre - more effective in achieving compaction [Dawson & Kolisoja 2004]

### 2.4.2. Factors affecting permanent deformation in UGM

Lekarp [1997], Werkmeister [2003] and Arnold [2004] point out the many factors affecting permanent deformation response of granular materials: stress level; confining pressure mode; principal stress rotation; number of load application; moisture content; stress history; density; grading, fines content and physical properties of aggregate particles.

Arnold [2004] highlights that stress level has the most significant effect on permanent strain, followed by the number of load applications. Werkmeister [2003] states that, in comparison to other influencing factors, grading is of less importance for both the resilient and permanent deformation behaviour, although a relatively balanced grading, within specification of road authorities, is prerequisite for a good performance.

The effect of principal stress rotation, schematically explained earlier (Figure 2.4), on permanent strain behaviour of granular materials under repeated loading, is not yet fully understood. This is possibly due to the fact that the repeated load triaxial testing (RLT), the most common means of reproducing traffic conditions in laboratory, fails to provide the continuous change in direction of principal stresses. The literature available indicates that the stress reorientation in UGM during trafficking results in larger permanent deformation strains than those predicted by RLT. The hollow cylinder apparatus, described later, is a nearer approximation of the real condition. However, due to its complexity of operation and few studies on the subject, the apparatus does not yet provide fully understating of the stress rotation on permanent deformation behaviour.

The key factors that affect permanent deformation in a UGM and their likely response are summarized in Table 2.3.

Barksdale [1972] studied the accumulation of permanent deformation in regard to fines content and aggregate type. Allen [1973] compared plastic strain development under repetitive loading in samples of crushed limestone and gravel. Thom and Brown [1988] investigated the behaviour of a crushed limestone at different gradings and densities. Janoo and Bayer II [2001] studied the effect of aggregate angularity on base course performance.

Korkiala-Tanttu [2008] described that besides the materials factors, there are others that influence permanent deformation in granular materials, namely: number of load repetitions, geometry of the structure (layer thickness, the inclination of the side, slope, the distance of the side slope), initial state of the pavement layers (e.g. anisotropy), temperature and moisture conditions, loading factors (maximum load, loading rate, loading history, rotation of the principal axis, lateral wander, tyre pressure, wheel type) and periodical behaviour (seasonal changes) including the changes in saturation degree.

---

Table 2.3 – Factors affecting permanent strain response

Factor	Response
Stress Level [after Morgan 1966]	At constant " $\sigma_3$ ", the accumulated $\epsilon_{pa}$ is directly proportional to the " $\sigma_d$ ". Conversely, the accumulated $\epsilon_{pa}$ is inversely proportional to " $\sigma_3$ " at constant " $\sigma_d$ ".
Confining pressure mode [after Sweere 1990]	In repeated load triaxial test conditions, the mode of confining pressure, constant or variable, affect the magnitude of $\epsilon_{pa}$ .
Principal stress rotation [after Lekarp 1997]	Stress reorientation in granular materials during trafficking result in larger $\epsilon_{pa}$ than those predicted by simple cyclic testings.
Number of load application [after Lekarp 1997]	Increasing load cycles will always increase $\epsilon_{pa}$ . For low applied stresses, stable $\epsilon_{pa}$ behaviour can be achieved. Shakedown theory can help determining such stress level.
Moisture content [after Thom & Brown 1987]	A rise in water content will cause an increase in permanent deformation.
Stress history [after Brown & Hyde 1975]	$\epsilon_{pa}$ resulting from a successive increase in the stress level is considerably smaller than the $\epsilon_{pa}$ that occurs when the highest stress is applied as a single pulse.
Density [after Barksdale 1972]	Increased density results in lower $\epsilon_{pa}$ .
Grain Shape [after Allen 1973]	Angular material undergoes smaller $\epsilon_{pa}$ .
Fines Content [after Barksdale 1972]	Increasing fines content generally increases $\epsilon_{pa}$ . As fines hold water more readily, the effect may be due more to water than grain size. Added fines content also increase relative density which reduces $\epsilon_{pa}$ . (see Grading effect below)
Surface Roughness [after Thom & Brown 1988]	Macro level surface roughness probably correlates better with the ability of the material to resist to $\epsilon_{pa}$ .
Grading [after Werkmeister 2003]	If the grading is changed such a way that relative density increases, then resistance to $\epsilon_{pa}$ will rise.

$\epsilon_{pa}$  = permanent axial strain;  $\sigma_3$  = confining stress;  $\sigma_d$ =deviator stress

### 2.4.3. Permanent deformation models

The modelling of permanent deformation in unbound granular materials has been approached by several researchers in several different ways, viz:

- a. Correlations between static and dynamic loading – Lentz and Baladi [1981]

- b. Correlations between resilient and plastic behaviour – Veverka [1979]
- c. Permanent deformation moduli – Jouve *et al.* [1987]
- d. Modelling of permanent strain and number of cycles – Barksdale [1972], Sweere [1990], Wolf & Visser [1994], Poute *et al.* [1988, 1996]
- e. Modelling of permanent strain and stresses – Lashine *et al.* [1971], Barksdale [1972], Pappin [1979], Nishi *et al.* [1994], Poute *et al.* [1996], Lekarp & Dawson [1998]
- f. Shakedown theory – Sharp [1983], Werkmeister *et al.* [2001]

The modelling of permanent deformation in unbound granular material allows the modelling of the long-term behaviour of pavement structures. It is essential for this analysis to take into account the gradual accumulation of permanent strain with number of load applications and the important role played by stresses. Hence, the main objective of research into long-term behaviour should be to establish a constitutive relationship which predicts the amount of permanent strain at any number of cycles at a given stress level.

This has been sought by many of the approaches mentioned. Their aim is to predict the magnitude of permanent strain from known loads and stress conditions. Although some of them have managed to describe certain materials in specific situations, others have succeeded to broaden their capabilities. None of them, however, have yet fully managed to describe unbound material behaviour in regard to permanent deformation as a function of the various aspects discussed in the previous Section.

A detailed discussion for aspects “a” to “e” is found elsewhere [Lekarp 1997]. Item “f” has been briefly discussed in Section 2.3.2 and further discussion is found in Werkmeister *et al.* [2001], Werkmeister [2003] and Arnold [2004].

For convenience, Table 2.4 provides a summary of some of the models described above.

---

Table 2.4 – Models proposed to predict permanent strain [after Lekarp 1997, Arnold 2004]

Expression	Equation	Reference	Parameters
$\varepsilon_{1,p} = a\varepsilon_r N^b$	26	Veverka [1979]	$\varepsilon_{1,p}$ = accumulated permanent strain after $N$ load repetitions
$K_p(N) = \frac{p}{\varepsilon_{v,p}(N)}, G_p(N) = \frac{q}{3\varepsilon_{s,p}(N)}$	27	Jouve <i>et al.</i> [1987]	$\varepsilon_{1,p}^*$ = additional permanent axial strain after first 100 cycles
$G_p = \frac{A_2\sqrt{N}}{\sqrt{N} + D_2}, \frac{G_p}{K_p} = \frac{A_3\sqrt{N}}{\sqrt{N} + D_3}$	28		$\varepsilon_{1,p}(N_{ref})$ = accumulated permanent axial strain after a given number of cycles $N_{ref}$ , $N_{ref} > 100$ $\varepsilon_{v,p}$ = permanent volumetric strain for $N > 100$ $\varepsilon_{s,p}$ = permanent shear strain for $N > 100$
$\frac{\varepsilon_{1,p}}{N} = A_1 N^{-b}$	29	Khedr [1985]	$\varepsilon_N$ = permanent strain for load cycle $N$
$\varepsilon_{1,p} = a + b \log(N)$	30	Barksdale [1972]	$\varepsilon_i$ = permanent strain for the first load cycle
$\varepsilon_{1,p} = aN^b$	31	Sweere [1990]	$\varepsilon_r$ = resilient strain
$\varepsilon_{1,p} = (cN + a)(1 - e^{-bN})$	32	Wolff & Visser [1994]	$K_p$ = bulk modulus with respect to permanent deformation
$\varepsilon_{1,p}^* = \frac{A_4\sqrt{N}}{\sqrt{N} + D_4}$	33	Paute <i>et al.</i> [1988]	$G_p$ = shear modulus with respect to permanent deformation
$\varepsilon_{1,p}^* = A \left( 1 - \left( \frac{N}{100} \right)^{-B} \right)$	34	Paute <i>et al.</i> [1996]	$q$ = deviator stress $p$ = mean normal stress $q^0$ = modified deviator stress = $\sqrt{2/3} \cdot q$
$\varepsilon_{1,p} = \sum \varepsilon_N = \sum \frac{1}{N^h} \varepsilon_i$	35	Bonaquist & Witczak [1997]	$p^0$ = modified mean normal stress = $\sqrt{3} \cdot p$
$\varepsilon_{1,p} = \frac{q/a\sigma_3^b}{1 - \left[ \frac{(R_f q)/2(C \cos \phi + \sigma_3 \sin \phi)}{(1 - \sin \phi)} \right]}$	36	Barksdale [1972]	$p^*$ = stress parameter defined by intersection of the static failure line and the $p$ -axis $p_0$ = reference stress
$\varepsilon_{1,p} = \varepsilon_{0.955} \ln \left( 1 - \frac{q}{S} \right)^{-0.15} + \left\{ \frac{a(q/S)}{1 - b(q/S)} \right\} \ln(N)$	37	Lentz and Baladi [1981]	$L$ = stress path length $\sigma_3$ = confining pressure $N$ = number of load applications

$\varepsilon_{1,p} = 0.9 \frac{q}{\sigma_3}$	38	Lashine <i>et al.</i> [1971]	S	= static strength
$\varepsilon_{s,p} = \left( \text{fn } N \right) L \left( \frac{q^0}{p^0} \right)_{\max}^{2.8}$	39	Pappin [1979]	$\varepsilon_{0.95S}$	= static strain at 95 percent of static strength
$A = \frac{\frac{q}{(p+p^*)}}{b \left( m - \frac{q}{(p+p^*)} \right)}$	40	Paute <i>et al.</i> [1996]	C	= apparent cohesion
$\frac{\varepsilon_{1,p}(N_{ref})}{(L/p_0)} = a \left( \frac{q}{p} \right)_{\max}^b$	41	Lekarp and Dawson [1998]	$\phi$	= angle of internal friction
$\varepsilon_p(N) = A \left( 1 - \left( \frac{N}{100} \right)^{-B} \right) \times \left( \frac{1}{p_a} \right)^r \times \left( \frac{q}{p} \right)^s$	42	Akou <i>et al.</i> [1999]	fnN	= shape factor
$PD = dN + \frac{cN}{\left[ 1 + \left( \frac{cN}{a} \right)^b \right]^{1/b}}$	43	Theyse [2002]	$R_f$	= ratio of measured strength to ultimate hyperbolic strength
$PD = dN + a(1 - e^{-bN})$	44		h	= repeated load hardening parameter, a function of stress to strength ratio
$PD = te^{aN} - ue^{-bN} - t + u$	45		$A_1$	= a material and stress-strain parameter given (function of stress ratio and resilient modulus)
$\log N = -13.43 + 0.29RD - 0.07St + 0.07PS - 0.02SR$	46		A2-A4, D2-D4	= parameters which are functions of stress ratio q/p
$SR = \frac{\sigma_1^a - \sigma_3}{\sigma_3 \left( \tan^2 \left( 45^\circ + \frac{\phi}{2} \right) - 1 \right) + 2C \tan \left( 45^\circ + \frac{\phi}{2} \right)}$	47		m	= slope of the static failure line
			a, b, c, d	= regression parameters (A is also the limit value for maximum permanent axial strain)
			A, B, t, u	= permanent deformation (mm)
			$\sigma_1^a$	= applied major principal stress
			SR	= shear stress ratio (a theoretical maximum value of 1 indicates the applied stress is at the limit of materials shear strength defined by C and $\phi$ )
			RD	= Relative Density (%) in relation to solid density
			St	= degree of saturation (%)
			PS	= Plastic Strain (%)

Korkiala-Tanttu [2008] developed a relatively simple material model for unbound materials, which is analytical and uses a nonlinear elasto-plastic concept. Equation 48 and Equation 49 describe the model proposed:

$$\varepsilon_p = C \cdot N^b \cdot \frac{R}{1 - R} \quad \text{Equation 48}$$

$$a = C \cdot \frac{R}{1 - R} \quad \text{Equation 49}$$

Where:  $\varepsilon_p$  = permanent vertical strain

$R$  = deviatoric stress ration ( $q/q_f$ )

$a$  = permanent shear strain component

$b$  = shear ratio parameter depending on the material and

$C$  = material parameter depending on the compaction and saturation degree

The method was tested against results obtained from the Mohr-Coulomb failure criteria and Hardening Soil model from the Plaxis® software. According to the author the calculation approaches underestimate the permanent strains for the high load levels and overestimate it for the lower load levels. The later studies of the same author, however, [Korkiala-Tanttu 2009] have shown that the calculation method performed well with Accelerated Pavement Tests (APT) in contrast to the first computations with the theoretical models. The APT results from Denmark and Sweden structures resulted in errors ranging from +7% to -17% when compared to the results predicted using the Plaxis® Hardening Soil.

Several pavement performance prediction models have been proposed over the years. Many of these models are developed for application in a particular region or country under specific traffic and climatic conditions. Therefore, most of the times, they cannot be easily applied for different conditions than those tested [Saba *et al.* 2006].

Yet the methods above are well consolidated and representative models, the Shakedown approach, described next, was the base rationale used in the method proposed in this work. This was mainly due to the fact that the permanent deformation from a simple perspective can be considered to be stress dependent. Hence, by positioning the stress condition in the granular layer within certain boundaries - shakedown ranges - the rutting mechanisms can be more easily understood and, therefore, handled.



## 2.5. THE SHAKEDOWN APPROACH

The essence of a shakedown analysis is to determine the critical shakedown load for a given pavement. Pavements operating above the critical shakedown load are predicted to exhibit increased accumulation of permanent plastic strains under long term repeated loading conditions that eventually lead to incremental collapse (e.g. rutting). Those pavements operating at load levels below this critical shakedown load may exhibit some distress, but should settle down and reach an equilibrium, state in which no further plastic mechanical deterioration occurs [Werkmeister *et al.* 2001].

The shakedown approach is not specifically an elasto-plastic model, as it is designed to establish the limits on which a granular layer may operate, and not to model strains. It can provide designers with a range of stress-strain limits at which the pavement is desired to operate.

From a design perspective a critical shakedown stress value in terms of that due to a wheel load is not practical as the wheel loading cannot be changed. Further, deriving critical shakedown stress from lower and upper bound theorems and utilising friction angle and cohesion from monotonic shear failure tests is both difficult and questionable [Arnold 2004].

For design purposes, this implies that the maximum load level which is associated with a resilient response must be known and then not exceeded, if the onset of permanent deformation is to be prevented. Possible behaviour can be categorized as either Range A, B or C [Dawson & Wellner 1999], illustrated in Figure 2.15.

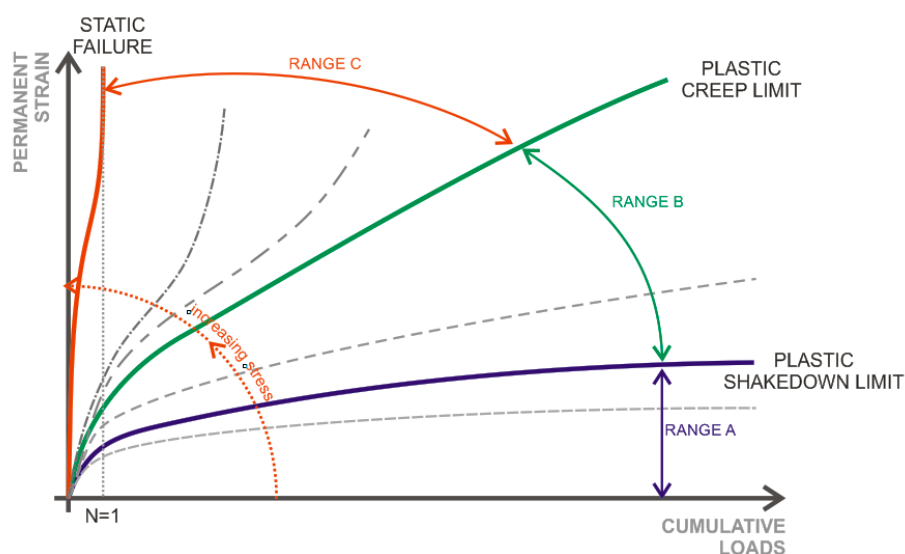


Figure 2.15 – Shakedown range behaviours for permanent strain versus cumulative loading - typical responses.

- Range A – is the non-plastic range and for this condition to occur the response shows high strain rates per load cycle for a finite number of load applications during the initial compaction period. After the compaction period the permanent strain rate per load cycle decreases until the response becomes entirely resilient and no further permanent strain occurs. This range occurs at low stress levels and Werkmeister *et al.* [2001] suggest that the cover to UGMs in pavements conventionally surfaced by asphalt concrete should be designed to ensure that the stress levels in the UGM will result in a Range A response to loading.
- Range B – is the plastic creep range. Initially behaviour is like Range A during the compaction period. After this time the permanent strain rate (permanent strain per load cycle) is either decreasing, constant or slightly increasing. For the duration of the RLT test the permanent strain is acceptable yet the response does not become entirely resilient. However, it is possible that if the RLT test number of load cycles were increased to perhaps 2 million load cycles the result could either be Range A or Range C (incremental collapse).
- Range C – is the incremental collapse range where initially a compaction period may be observed and, after this time, the permanent strain rate increases or remains constant (but at a rather high magnitude of plastic strain per cycle) with increasing load cycles.

If the unbound granular layers behave in a manner corresponding to Range A, the pavement will “shake down”. After post-compaction deformations, no further permanent strains develop and the material subsequently responds elastically. Thus Range A is permitted in a pavement, provided that the accumulated strain before the development of fully resilient behaviour is sufficiently small. The material in Range B does not “shake down”, rather it will achieve failure at a very high number of load repetitions. In that case the resilient strains are no longer constant and will increase slowly (decrease of stiffness). Range C behaviour - incremental collapse or failure - should not be allowed to occur in a pavement. The shakedown analysis of repeated load triaxial test results can be used for ranking materials as a performance specification method to determine the resistance against rutting of UGMs. Of course the shakedown limits of the UGL are also strongly dependent on seasonal effects (mainly moisture content). The moisture content has been identified as the factor having the largest influence on the mechanical properties of UGM [Werkmeister *et al.* 2001].

As the deformations of granular material are highly stress dependent, the recent development of models have extensively been based on the shakedown concept. Arnold [2004] presents the shakedown boundaries for two materials (later referenced in Chapter

6) - a better performance material (NI Good) and a worse performance material (NI Poor). Figure 2.16 illustrates the range boundaries in terms of stress condition.

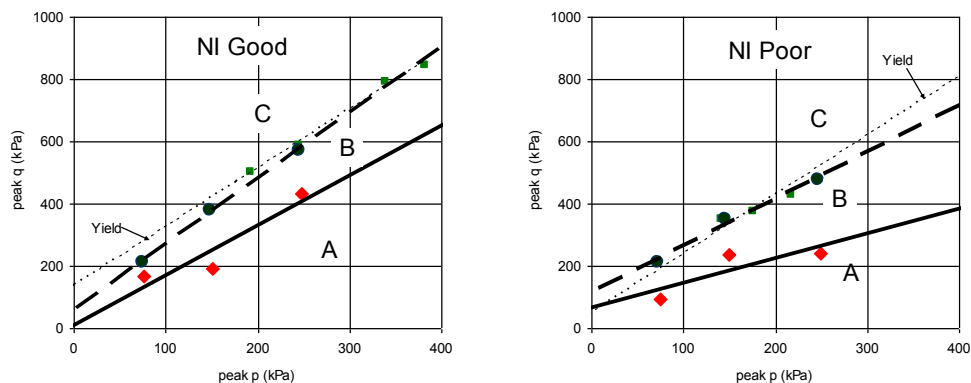


Figure 2.16 – Shakedown range boundaries A, B & C in terms of stress condition ( $p \times q$ )  
[Arnold 2004]

It becomes evident that the poorer material approaches failure condition faster, especially at lower stress conditions. In addition, the poorer material features a more restrict Range A, reaching the plastic creep limit faster, in special for higher stress conditions.

## 2.6. PERFORMANCE TESTS

There are several existing tests, and a wide range of complex procedures, to verify the performance of unbound granular materials. At the most practical, *in situ* testing could provide the most representative characterization of the materials, but controlling loading and measuring the response is not an easy task.

Several *in situ* testing devices have been developed over the years. Results from static loading tests, such as California Bearing Ration and Static Plate Bearing Test, are used to predict material behaviour under dynamic loading condition. Devices such as Clegg Hammer, Falling Weight Deflectometer (FWD), and Dynamic Plate Bearing Test employ dynamic loads which are closer to the actual traffic loading situations. The most realistic approach, however, involves those devices that are able to reproduce the repeated stresses caused by the moving wheel load, using an accelerated time scale. Full-scale pavement test facilities such as the South African Heavy Vehicle Simulator (HVS), the Australian Accelerated Facility (ALF) and the Brazilian Full Scale Test Facility have been effectively used for this purpose [Sharp 2004].

By its nature, laboratory testing enables the control of many factors which affect the behaviour of the tested material. For unbound materials, the cyclic load triaxial test is currently the main test used to study stress-strain behaviour under different conditions of

grading, moisture content, and density. Wheel tracking tests, the K-Mould test and hollow cylinder apparatus are among other lab tests used to assist in the performance prediction of unbound material [Semmelink & de Beer 1995, Richardon 1999, El Abd *et al.* 2004].

### 2.6.1. The repeated load triaxial test

The repeated load triaxial test (RLT) approximates the stress condition in a real pavement structure by applying a cyclic deviator stress component ( $\sigma_d$ ) – vertically –, and a cyclic or static confining stress component ( $\sigma_3$ ) – horizontally –, in a cylindrical specimen. Although both deviator and confining stress are cycled, the RLT is limited in that only principal stresses can be directly applied to a test specimen and because of the axisymmetric arrangement two of these must necessarily be equal. Furthermore, during the passage of a wheel load, the principal stresses within the pavement rotate due to shear stress reversal, whereas in a triaxial apparatus they, at best, can only rotate, instantly, by  $90^\circ$ .

The triaxial test has several advantages. It is relatively inexpensive compared to field tests and it is less time consuming. In addition, stresses can be applied to a specimen as pulses that simulate those applied to an element in an actual pavement. It can test both soils and granular materials and the stress paths are controllable. Apart from the determination of the resilient modulus (MR) of the materials under several stress states, it is also possible to measure the Poisson's Ratio if radial displacement measurement is available in the test. Figure 2.17 shows a picture of the repeated load triaxial test equipment at the University of Nottingham.



Figure 2.17 – Repeated load triaxial test equipment at the University of Nottingham

The equipments available allow triaxial testing with use of constant confining pressure (CCP) or variable confining pressure (VCP). The VCP triaxial tests are a closer simulation of actual field conditions than the CCP tests, since in the road structure the acting confining stress is of cyclic nature. Brown and Hyde [1975] showed that VCP and CCP tests yield the same MR-values, provided the confining stress,  $\sigma_3$ , in the CCP test, is equal to the mean value of  $\sigma_3$  in the VCP test. The authors also showed that the values obtained for Poisson's Ratio in the CCP tests differ considerably from those obtained in the VCP tests. Allen and Thompson [1974] compared the test results for MR obtained from both CCP and VCP and reported higher values of resilient modulus computed from the CCP test data. They also showed that the CCP tests resulted in larger lateral deformations.

The RLT can be used to study both the resilient properties and the plastic properties of soils and granular material. The materials can be tested in representative conditions of density and water content and in drained and undrained conditions. There are several equipments already assembled allowing different specimen sizes to be tested, which enables the testing of finer materials in smaller specimens and coarser materials in larger apparatuses. Most repeated load triaxial testing facilities currently available have specimen diameters of 300mm, 150mm or less, although some as large as 500mm in diameter have been constructed [Lekarp & Isacsson 2000]. In conclusion to the investigation of the effect of specimen height to diameter ratios in triaxial testing results, Taylor [1971] proposed that if the height of the specimen is about twice its diameter, the significance of size effect on the measurements would be negligible. This premise has been widely accepted and used in the vast majority of triaxial equipments.

It is generally accepted in the geotechnical community that the size of the specimen must be significantly larger than the maximum particle size of the granular material to be tested; typically, values of 10 are accepted for the ratio "specimen diameter / maximum aggregate size". Lekarp and Isacsson [2000], based on an investigation of previous works, suggested that the specimen diameter should be 5 times bigger than the maximum particle size. Sweere [1990] suggested that a ratio of 7 should be considered ideal. Theyse [2000] affirms that if the same relation is lower than 4, the material strength will be over-estimated.

For RLT tests with constant confining stress, the resilient modulus is defined as the ratio of the peak axial repeated deviator stress to the peak recoverable axial strain of the specimen, as expressed below:

$$M_r = \frac{\Delta(\sigma_1 - \sigma_3)}{\varepsilon_1} \quad \text{Equation 50}$$

Where:  $M_r$  = resilient modulus

$\sigma_1$  = major principal or axial stress

$\sigma_3$  = minor principal or confining stress

$\varepsilon_1$  = major principal or axial resilient strain

$\Delta$  = means “change in”

Mundy [2002] extensively studied the stress levels that should be used during the triaxial tests. Given that granular materials are stress-dependent, materials must be assessed at stress conditions representative of those *in-situ*, under applied design traffic loadings. This is particularly important given that resilient modulus and permanent strain rate are very sensitive to the applied stress conditions experienced by a material element (i.e., stress-dependent).

The repeated load triaxial test is not only used for studies on the resilient behaviour of granular materials, but also for their permanent deformation behaviour. It constitutes the prime performance test for unbound materials used nowadays. This capability will be further discussed in a future version of this document.

### 2.6.2. Wheel tracking test

Among the laboratory tests used for the study of unbound granular material behaviour, the wheel tracking test can be considered suitable equipment for the simulation of the complex stress state imposed on a road structure by traffic loading, something that is difficult to achieve in other laboratory tests. The rotating nature of the principal stresses, referred to in Section 2.1, due to the approach and departure of the loading, is well simulated in this test, and this can be of great importance when setting out to determine permanent deformation.

Testing of UGM requires large sized wheel tracking devices, which allow testing of a layer of granular material of realistic thickness (typically 20 to 30cm). A device of this type has been developed by Belt *et al.* [1997], at the University of Oulu – Finland. This equipment (Figure 2.18) was designed to test a complete pavement structure, consisting of a bituminous wearing course, a granular layer and the sub-grade. The structure is built in a rigid steel container, of 1200 x 900 x 600 mm (length x width x height). The maximum load applied by the wheel is 25 kN, and the loading speed is 5 km/h.



Figure 2.18 – Wheel tracking test equipment at the University of Oulu – Finland

In the European research project [COURAGE 1999], the large wheel track from the University of Oulu was used to compare permanent deformation behaviour of different unbound granular materials, and has led to the same ranking of materials, in terms of resistance to permanent deformation, as in the cyclic load triaxial test. Further conclusions drawn from the testing were that a very thinly surfaced unbound granular pavement would experience at least 73 to 95% of the total layer permanent deformation in the upper half of the base course layer and the resilient strains would be between 1.5 and 2.5 times greater than in the lower half due to the higher stress states near the surface.

### 2.6.3. K-Mould test

Developed in South Africa to study the behaviour of UGM under cyclic loading, the K-Mould test has similar principle to that of the RLT. Its difference concerns on the system used to apply the confining stress: instead of using a fluid to confine the material inside a triaxial chamber, a steel mould confines the material via elastic springs. The springs push the cell wall against the cylindrical specimen with the effect that the lateral restraint increases as the granular specimen is being loaded vertically and the specimen attempts to expand laterally.

The apparatus, described in detailed in Semmelink & de Beer [1995] and shown in Figure 2.19, allows the determination of parameters like elastic modulus, Poisson's ratio, cohesion and friction angle, all from a single test specimen.



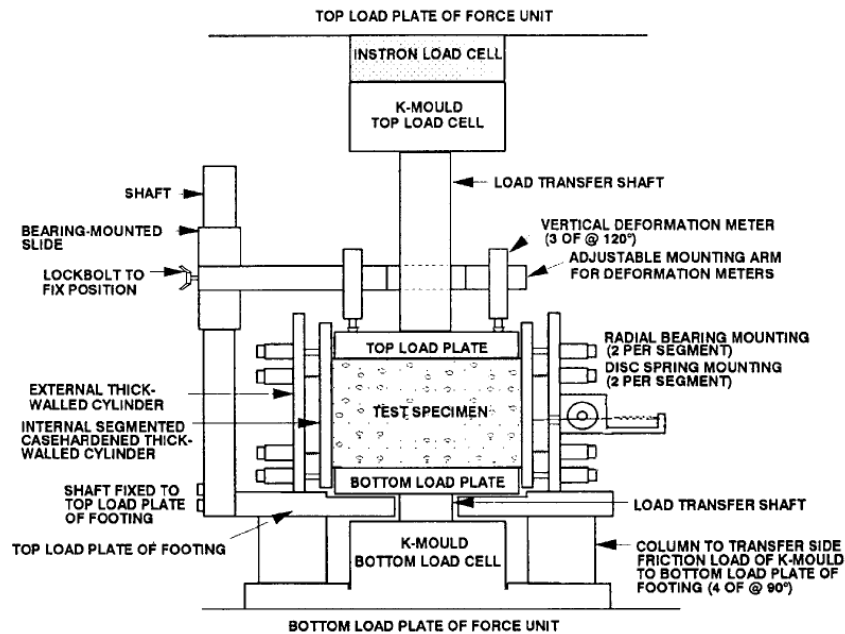


Figure 2.19 – K-mould test apparatus [after Semmelink & de Beer 1995]

A major advantage over the RLT is that the specimen can be prepared in the apparatus, so complex specimen preparation is largely avoided.

An equipment developed in the UK [Edwards *et al.* 2004], known as the Spring-box, provides a similar testing method as the K-Mould with some simplifications and advantages. Compatible with the Nottingham Asphalt Tester (NAT) apparatus, the Spring-box uses a cubic sample of 170mm edge and is capable of accommodating aggregate size up to 40mm. While K-mould uses a cylindrical specimen with wall divided into 8 segments and spring-loaded, the Spring-box uses spring-loaded walls, but only in one direction. The apparatus has the advantages of combining simpler routine tests than K-mould or RLT tests and is capable of adjusting, for example, moisture state like the CBR (California Bearing Ratio) test [Thom *et al.* 2005] but having the ability to deliver more realistic loading conditions and fundamental parameters at lower cost.

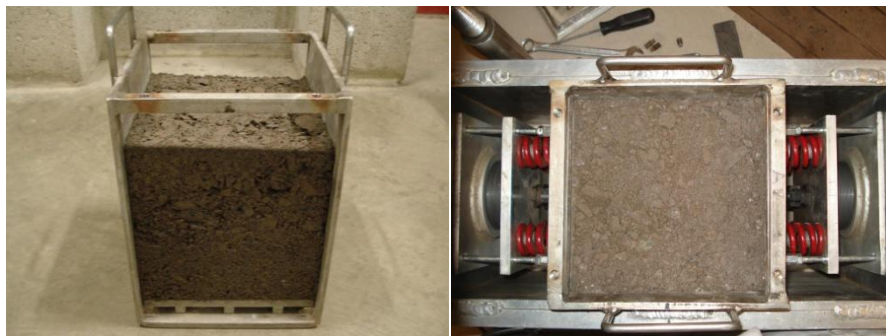


Figure 2.20 - Springbox (L) sample in the mould & (R) sample set up in the apparatus



A similar apparatus was also developed in Illinois known as the Fastcell [Seyhan & Tutumluer 1999] for the characterization of unbound granular material. The Fastcell has been widely used by those researchers to study the anisotropy of granular material.

#### 2.6.4. The hollow cylinder test

In the study of the permanent deformation behaviour of granular material, the repeated load hollow cylinder test apparatus (HCA), shown schematically in Figure 2.21, appears to be a promising device, according to Chan [1990]. It is capable of applying reversing shear stresses to the test specimen meaning that realistic *in-situ* stress conditions caused by a moving wheel loading can be simulated. Furthermore, the study of material anisotropy, principal stress rotation effects and the influence of different intermediate principal stresses are all made possible using the HCA.

In the HCA, a repeated torsion can be applied to a hollow thin-walled cylinder. If the hollow cylinder is at the same time subjected to an axial and a lateral stress over both the inner and outer cylinder faces, then the stress conditions imposed on an element of material will realistically simulate the stress conditions experienced by a pavement in service. However, the major limitation of the apparatus is that it can only accommodate scaled down material samples and the effects of using scaled down samples are not always known. Neither can the apparatus cycle cell pressures easily, and is not possible to cycle all stresses independently.

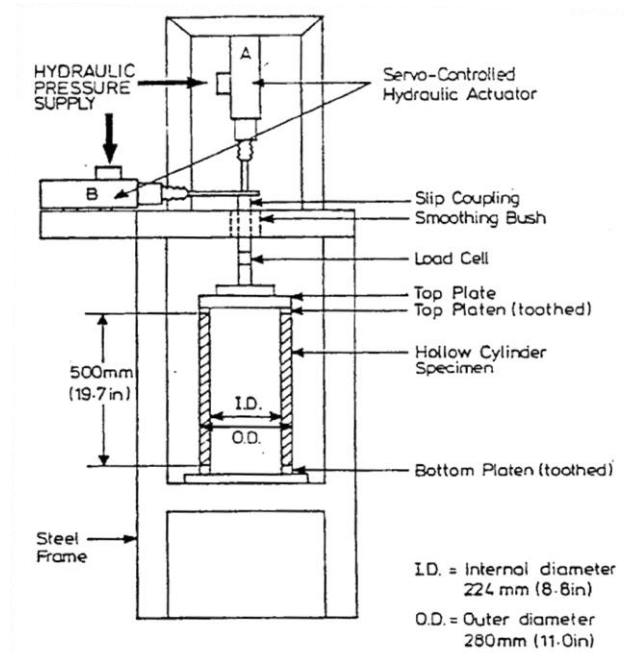


Figure 2.21 – Schematics of a hollow cylinder test apparatus [after Thom & Dawson 1993]

Chan [1990] has studied the effect of stress rotation on permanent deformation of unbound granular materials using a HCA. He found that, for the same stress levels, principal stress rotation leads to a significant increase of permanent deformations, whereas resilient behaviour is practically unaffected by stress rotation.

### 2.6.5. Simpler in-situ testing equipment

For the purpose of this research, it is important to mention several other simple tools to assess *in-situ* pavement performance. Although laboratory tests provide the most accurate method to determine aggregate properties they may not be readily available. In addition, their costs are typically high for LVR engineering and its interpretation sometimes not pragmatic.

The California bearing ratio (CBR) is a penetration test for evaluation of the mechanical strength of road subgrades and basecourses. The test is performed by measuring the pressure required to penetrate a soil sample with a plunger of standard area. The measured pressure is then divided by the pressure required to achieve an equal penetration on a standard crushed rock material. It is used worldwide and several studies have already produced materials database and correlations to other tests, although the validity of these correlations are restrict and their use must be careful.

The Dynamic Cone Penetrometer (DCP) was developed in 1959 by George F. Sowers. The DCP, as it is used nowadays, uses an 8.0 kg hammer dropping through a height of 575mm that strikes the anvil to cause penetration of 20mm diameter cone (60° vertex angle). The DCP is already standardised by ASTM D6951 [2009].

The blows required to drive the embedded cone to a certain depth have been correlated by others to N values derived from the Standard Penetration Test (SPT) and, more commonly, to CBR of the material. Likewise, the variance in the penetration rate aids the detection of sublayers thickness in the pavement.

Piouslin and Done [2005] describe the use of the software UK DCP developed by TRL as a tool to analysis and design of low volume roads. Several other works used DCP as means to correlate to CBR [Harison 1987, Gabr *et al.* 2001, Abu-Farsakh *et al.* 2005, Visser 2007]. The UK DCP version 3.0 uses the correlation in Equation 51 to correlate penetration in mm/blow with CBR values.

$$\text{Log}_{10}(\text{CBR}) = 2.48 - 1.057 \text{ Log}_{10}(\text{pen rate [mm/blow]})$$

Equation 51

Another rather simple equipment, yet not as inexpensive as the DCP, are the portable deflectometers. With similar principal of a full scale Falling Weight Deflectometer (FWD), the portable deflectometers test the material for its stiffness by dropping a hammer from a similar height to a DCP, but measures the near surface deflection by the use of either accelerometers or geophones. With the impact load measured by a load cell and the deflection measured in the near surface, it becomes possible to backanalyse the deformation stiffness of the layer.

Even simpler is the 'Clegg Hammer' comparing a dropped weight equipped with an accelerometer.

The important characteristic that must be highlighted is their ability to signal the mechanical behaviour of the material from a simple manner. Enough is to take both of these equipments (DCP and portable deflectometers) on site to have a broad assessment of the tested material competence. Both of these tools are used in the field full scale trials carried in Scotland in this research, described later in Chapters 4 and 5.

## 2.7. KEY FINDINGS

The literature review covered in this chapter aimed to look at the behaviour of granular materials and road layers from a low volume road design perspective. Emphasis was given to the stress conditions in LVR structures as well as types of deformability in granular layers and its modelling. The key findings for the review brought in this chapter can be summarized below:

- Most methods currently used for LVR design neglect permanent deformation in the granular layers and design the pavement layers as means to protect the subgrade from permanent deformation.
  - Surfacing needs to be greater than around 40mm in sealed pavements in order to achieve effective load spreading and significantly reduce stress on the lower aggregate base layers [Dawson *et al.* 2007]. Hence, thinly surfaced or unsurfaced LVR structures concentrate vertical and horizontal stress in the granular layer.
  - The stress level analysis in Australian and French pavements [Mundy 2002] suggests the existence of a stress loci to a combination of road structure and pavement materials. This existence of these loci also reflects the material quality and is a good indication to be used in design methods.
  - Permanent deformation development in LVR occurs in form of ruts. They are the main distress modes of these pavements, and broadly a consequence of the deformability
-

in the pavement layers. As the granular layers are typically the competent layers in these structures, modelling the deformability is vital for the concept of a mechanistic design approach.

- The modelling of the elastic behaviour in granular materials is well developed. Nonetheless, the elasto-plastic models are, at present, an important subject of study and very complex to be easily incorporated in simple design procedures.
- The rutting mechanisms can be divided into three modes, namely: Mode 0, Mode 1 and Mode 2. The first being a self-stopping occurrence once adequate compaction has taken place. Mode 2 usually occurs with better quality aggregate and can be usually tackled by designing a road structure to spread the stress to an admissible vertical stress at the top of the subgrade. Mode 1, however, is the main subject approached in the next Chapters, where design criteria must account for the permanent deformation development in granular layers.
- Several factors affect the behaviour of permanent deformation in UGM. Broadly, aggregate quality and stress conditions account, to some extent, for the granular layer behaviour.
- The shakedown theory applied to granular layers has demonstrated to be a useful tool and shall be considered in the analysis as a reference to a simple design procedure. Its capability to guide the permanent behaviour of UGM as a function of the stress level into three simple stages is ideal. Range A doesn't represent a problem as far as permanent deformation is concerned, while Range C needs to be avoided and Range B needs to be handled for the desired road conditions - rutting level.
- In regard to performance tests, the simple in-situ tools represent the best potential for use as a material assessor for LVR owners. However, Repeated Load Triaxial tests are fundamental for the determination of elasto-plastic properties whereas other tools as the K-Mould, Fastcell or the Spring-box may represent rather simpler tools for similar laboratory assessment.

It must be highlighted that although this research attempted to cover a wide literature review, it is yet restrict to some extent to the available knowledge used the research described in the further chapters. Hence, research studies in some other countries, such as the South African Pavement Design Guide, were only consulted as a reference but not detailed described.

---

### 3. LOW VOLUME ROADS DESIGN AND OPERATION

Rutting is the main distress mode in unsealed and thinly sealed pavements. Hence, it is desirable that it be analytically approached rather than empirically, as in most design methods. It is only by understanding each material's behaviour that engineers will be able to anticipate the reliability of a given structure, subjected to certain traffic and environmental conditions. If only empirical assessment tools are employed, then different conditions than those which provided performance benchmarks, could be never reliably accounted for. Better use of available materials cannot be planned, either.

Some design methods advocate that rutting only occurs within the subgrade provided that the unbound granular materials (UGM) comply with materials specification. Hence, by limiting the vertical elastic strain at the top of the subgrade, it would be possible to assure a new pavement structure against rutting. This assumes minimally two things:

- a) Recipe-based specification of UGM, which typically includes criteria for aggregate strength, durability, cleanliness, grading and angularity, would provide some guarantee of sufficient resistance to rutting.
- b) The elastic properties of the subgrade material would have a direct relationship with these implied plastic properties.

Both of these conditions have very weak validity for granular and soil materials, if any. Such over-simplified methods for pavement design make it impossible to take full advantages of alternative materials and often provide a low reliability procedure.

Newer studies of plasticity in unbound granular materials for pavements such as Boyce [1980], Lekarp [1997], Werkmeister [2003], Arnold [2004], Korkiala-Tanttu [2008], among others, have greatly advanced the topic. Most of these permanent deformation models available are based on laboratory triaxial tests, what can be at times expensive tests for LVR projects.

The aim of a pavement design guide (PDG) is to select the most economic pavement structure – material, layer thickness, construction process – which provides a satisfactory level of service for the anticipated traffic. Input variables for a pavement design guide should comprise the following:

---

- 
- Design traffic
  - Subgrade & pavement materials
  - Environment
  - Construction & maintenance
  - Methods, capabilities & options
  - Road geometry
  - Equipment availability
  - Social concern
  - Sustainability

In order to perform the assessment of a proposed pavement structure, distress prediction models must be present so that the life-cycle can be evaluated and economical appraisals accomplished, granting the road owner tools to enable him/her to make the choice of investment.

When designing a pavement overlay, or regravelling in case of unsurfaced roads, additional information must be available about the existing pavement condition. Determining if the pavement needs additional strength to provide satisfactory service during the design period is a key aspect.

Consequently, it is incontestable that, from the pavement engineering point of view, knowing the material properties and using adequate models of deterioration prediction forms the basis of a successful pavement design guide. It is by means of predicting the behaviour of the pavement when exposed to the anticipated traffic that it is possible to propose an adequate solution. As discussed in Section 2.4.3, modelling of the unbound granular material in regard to permanent deformation will help provide pavement design guides with more appropriate assessment tools for designing LVR structures.

Nonetheless, most current pavement design and evaluation guides for roads constructed largely or entirely of unbound layers, or for pavement foundations so constructed [TRL 1993, HMSO 1994, Austroads 1995], specify aggregate assessment for unbound pavements according to tradition - by an examination of particles for strength, durability, cleanliness, grading and angularity. The rationale for this is the experience that premature failure of road layers made from these materials is then uncommon.

---

Many design procedures further simplify matters by also designing the aggregate thickness on the basis of experience. For example, many design methods draw on the work of Hammit and others [Webster & Watkins 1977, Webster & Alford 1978, Hammit 1970 cited in Little 1992] in which different thicknesses of a particular aggregate were placed over clays of varying strength (as characterised by CBR) and subjected to lorry trafficking. Using this information requires the tacit assumption that any local granular material (which meets or exceeds a given set of aggregate particle quality checks) performs in the same manner as that used by Hammit [1970]. Clearly, this is highly unlikely. Material, climate, compaction and mixtures may all differ widely and the degree at which particles exceed the stated requirements is not taken into account. In fact, design is only as successful as it is because of the many implicit, and some explicit, safety margins incorporated into the design procedures.

Even when semi-analytical design is employed [e.g. Shell 1985, AASHTO 1992], the pavement's design and evaluation has been based upon the elastic performance of the compacted aggregate. With the introduction of the new AASHTO guide [2004], advanced models are available for aggregates within a designing procedure, but they are considered in the context of thickly sealed pavements where the stresses are relatively small and failure unlikely; not to mention the complexity involved in gathering the required data which is somewhat disproportional to the resources available for LVR engineering.

Thus, specifications for unbound materials and subgrade soils for LVRs continue to be stated either by physical form or, in advanced cases, in terms of an assessment of the resilient modulus [AASHTO 1986, StandardsAustralia 1995, CEN 2004]. Where such an advanced assessment of the elastic parameters is used, the thickness of an unbound layer (or residual life of the layer) is estimated using design criteria based on elastic fatigue. Both traditional and elastic approaches fail to explicitly recognise the inelastic and plastic behaviour.

### **3.1. EMPIRICAL APPROACHES**

The most common referenced parameter in pavement design procedures to assess road foundations is the CBR. The CBR was developed by The California State Highways Department and is, in essence, a simple penetration test developed to evaluate the strength of road subgrades. It consists of causing a plunger of standard area to penetrate a soil sample at a standard rate; the load required to cause the penetration is plotted against the measured penetration, and the result expressed as a percentage of a value to be expected for a high quality aggregate layer. It is currently standardized in Europe as EN 12236:2006 [BS 2006].

---

The stronger the subgrade (the higher the CBR reading), the less thick it is necessary to design and construct the road pavement, this gives a considerable cost saving. Conversely, if CBR testing indicates that the subgrade is weak (a low CBR reading – typically, less than 3%), we must construct a suitable thicker road pavement to spread the wheel load over a greater area of the weak subgrade in order that the weak subgrade material is not deformed due to overstressing (either monotonically or incrementally), causing the road pavement to fail.

The CBR, in spite of its limited accuracy, still remains a generally accepted method of determining subgrade strength in some countries; and as such this information, along with information on traffic flows and traffic growth, is used to design road pavements.

Hammit in 1970 [cited in Little 1992], based on the earlier work of Ahlvin [1959] and on the analysis of 59 pavement test sections undertaken in his work, proposed a model to determine the thickness of unsurfaced pavements as a function of CBR and the number of axle passes necessary to generate a rut depth of 75mm – which was considered the failure criteria. Equation 41 expresses the model Hammit proposed in his work.

$$h = (0.0236 \log N_{75} + 0.0161) \sqrt{\frac{P}{CBR}} - 17.8A \quad \text{Equation 52}$$

Where:  $h$  = aggregate layer thickness (m)

$N_{75}$  = number of axle passes to produce a rut depth of 0.075m

$P$  = single wheel load (kN)

$CBR$  = California Bearing Ratio (%)

$A$  = wheel-pavement contact area in (m<sup>2</sup>)

Giroud & Noiray [1981] advanced on the work of Hammit and based on the developments made by Webster & Watkins [1977] and Webster & Alford [1978] proposed a new relationship for designing unpaved roads – Equation 53. The main advantage of the approach proposed by Giroud & Noiray [1981] is that the new pavement thickness is a function of rut depth chosen by the designer as the failure criteria.

$$h = \frac{0.19(\log N_r - 2.34(r - 0.075))}{CBR^{0.63}} \quad \text{Equation 53}$$

Where:  $r$  = design maximum rut depth (mm)

$N_r$  = number of standard axles to produce a rut depth  $r$  in mm

The Transport and Road Research Laboratory (TRRL) method for design of flexible pavements [Powell *et al.* 1984] is based on the performance of experimental roads



interpreted in the light of structural theory. The method consists, initially, in determining the need of a capping layer over the subgrade – used to improve the bearing capacity of the road foundation for construction traffic – and its thickness, in this case, as a function of the CBR of the subgrade. For CBR greater than 5% no capping layer is necessary; for CBR between 2% and 5%, the capping layer must be 350mm thick; for CBR below 2%, a thickness of 600mm is prescribed. The sub-base, base and surfacing thicknesses are determined with the use of design charts based on previous experimental research.

In methods where an analytical analysis is proposed, the UGMs are generally considered as linear elastic materials. The value of their elastic moduli are often determined on the basis of empirical rules, and the design criterion used for these materials is generally a criterion limiting maximum vertical elastic strain  $\varepsilon_z^e$  at the top of the unbound layers and/or at the top of the subgrade, of the form in Equation 54 [Veverka 1979].

$$\varepsilon_z^e \leq A.N^{-b} \quad \text{Equation 54}$$

Where: N = number of load applications

A, b = model parameters

As underlined by Sweere [1989], although empirical pavement design procedures have the main advantage of being based on vast experience with the performance of existing roads, and, therefore, by definition, thoroughly validated, the empirical methods indeed only operate within the limits of the experience on which they are based. Extrapolation of their applicability may be quite hazardous. A change in the traffic, weather, material quality, construction standards, etc, can easily change the expected behaviour and invalidate the design assumptions.

### 3.2. AUSTROADS PAVEMENT DESIGN GUIDE

The Austroads Pavement Design Guide (PDG) [1992], first published in 1987, constituted until 2004 the key reference in Australia for road pavement design, when the new Austroads Pavement Design Guide [2004] was delivered. It was one of the first guides to incorporate mechanistic analysis to flexible pavements designing and, hence, an important reference to studies on this theme.

One of the main elements the Austroads PDG deliberates is the design of new flexible pavements consisting on unbound granular materials thinly sealed. Because the performance of unsurfaced pavements can be considered heavily dependent on local materials, local environmental conditions and maintenance policies, the PDG considers that an approach to that should not be within its scope.

---

The procedure suggests initially the evaluation of the subgrade strength. This can be considered the most important factor in determining pavement design thickness, composition and performance in this guide. The measures of subgrade support contemplated are: CBR, elastic parameters and modulus of subgrade reaction (k). The two first ones are of interest to flexible pavement design, and the first and third to rigid pavements.

To those cases on which more detailed characterization of materials is not viable, standard values are suggested. Correlations between CBR and vertical elastic modulus is also offered following the well known expression “Modulus (MPa) = 10 x CBR”<sup>2</sup>. Dynamic and static cone penetration tests are also empirically correlated to CBR as an alternative method of subgrade evaluation. With the CBR determined for the subgrade, the “basic pavement thickness” is then established, aided by a proposed chart.

The design of the new flexible pavement proceeds with the assessment of the traffic over the design period followed by road classification and limits for road roughness, with which a proposed pavement’s composition must be chosen from a set of layouts offered. The different sequences provided are: asphalt + granular base; asphalt + cemented material base; asphalt + granular base + cemented material; or asphalt on top of subgrade.

To choose the pavement combination, a stress-strain analysis must be carried out aided by a computational software capable of performing a mechanistic analysis. The distress criteria must then be verified. For the case of interest in this research study – thinly sealed pavements with unbound granular material base – the distress mode of relevance is permanent deformation (manifesting itself as rutting) which is controlled by limiting the maximum vertical compressive strain at the top of the subgrade.

The basic design thickness is, therefore, the thickness of UGM which limits the vertical compressive strain at the top of the subgrade to a tolerable level throughout the life of the pavement. The limiting criterion is giving by Equation 55, derived by applying the mechanistic procedure described in the PDG to the range of pavement layouts proposed.

$$N = \left( \frac{8511}{\varepsilon_v} \right)^{7.14} \quad \text{Equation 55}$$

Where:  $\varepsilon_v$  = vertical compressive resilient strain at the top of the subgrade (in microstrains) and  $N$  = allowable number of repetitions of  $\varepsilon_v$  strain.

---

<sup>2</sup> Although the correlation is offered for use by this PDG, its use is highly discouraged. As CBR is basically a benchmark test, Resilient Modulus is a material's mechanical property. As such, the correlation can not be made in principle.

---

The allowable number of repetitions must be then compared to the designed traffic; if the allowable number of repetitions is greater than designed traffic, the structure can be considered suitable. If not, the pavement structure should be modified – sequence, thickness or material quality, and the procedure run again. Figure 3.1 shows schematically the mechanistic design procedure used in the Austroads PDG for granular pavements with thin bituminous surfacing.

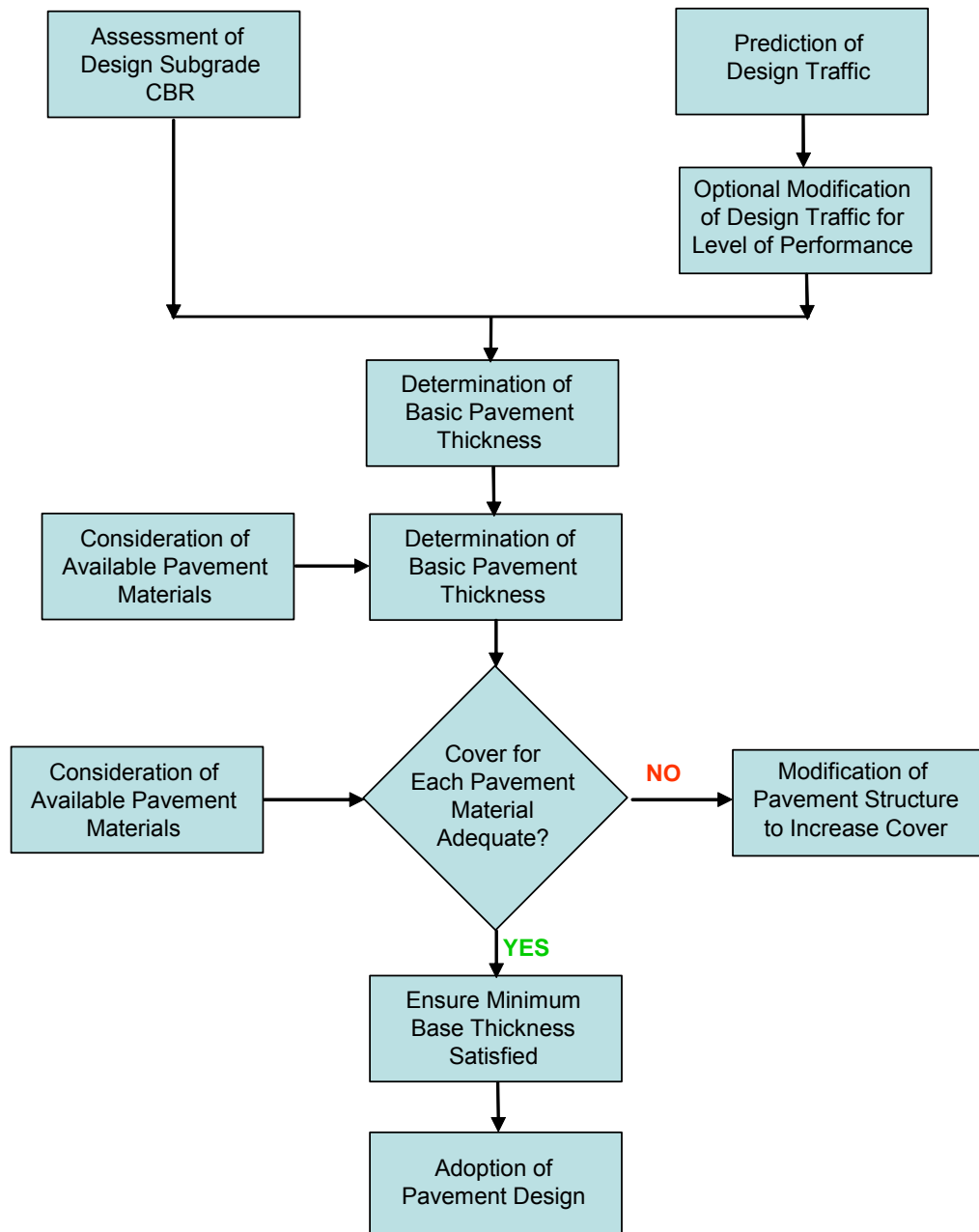


Figure 3.1 – Flexible pavement design system for granular pavements with thin bituminous surfacing [Austroads 1992]

Among the advantages presented by the guide, the consideration of granular materials as cross-anisotropic seems to be relevant. In addition, the proposed sub-layering methodology to account for stress dependence of the granular layer stiffness through a modular ratio for vertical moduli of the adjoining sub-layers, as represented by Equation 56, contributes to the quality of results expected from the guide.

$$R = \left( \frac{E_{top\_of\_base}}{E_{subgrade}} \right)^{1/n} \quad \text{Equation 56}$$

Where:  $R$  = the modular ratio for reduction of the sublayers

$E_{top\_of\_base}$  = modulus at the stress level determined at the top of the unbound base layer

$E_{subgrade}$  = modulus at the stress level determined at the top of the subgrade

$n$  = number of sub-layers in which the total thickness of UGM is divided into

Given the ratio “ $R$ ” calculated as above, the modulus of each sub-layer may subsequently be calculated by multiplying “ $R$ ” by the known modulus of the adjacent underlying layer, starting with the subgrade.

Among the limitations of the proposed methodology, the premise of modulus of elasticity of 2800MPa for the asphaltic layers adopted for the charts conception must be taken into account. Only for the full depth asphalt pavements, there is a broader range of stiffness available. The high relevance given to CBR instead of modulus of elasticity, ought to be addressed, provided that it may lead, in many cases, to unreliable assessments of the road foundation as already broadly discussed by researchers [Thom & Brown 1987, Sweere 1990].

In addition, despite permanent deformation being considered as the primary distress mode (an incontestable fact for such pavement structures) only limiting the vertical compressive strain at the top of the subgrade as the means of assuring admissible rutting levels, may lead to unreliable results.

The non-existence of maximum tolerable vertical compressive stress or strain levels for unbound granular layers and the lack of an assessment of the influence and limits for plastic behaviour on these materials also suggest limitations to the guide.

The new Guide to Pavement Technology - Part 6: Unsealed Pavements from the Austroads released in September [2009] seems to follow the same course previously presented. According to the guide, the thickness design methodologies are no different to those for sealed roads with thin bituminous surfacings [Austroads 2008].

As input parameters, the procedure requires the determination of the design traffic value, CBR of the subgrade and the design curves presented in Figure 3.2. The material shall be selected according to tradition: materials must be strong enough to support the load and reduce the stress on the subgrade without causing serious rutting of the top layer by deformation of the subgrade. Water ingress is controlled by the provision of a high crossfall (4-6%).

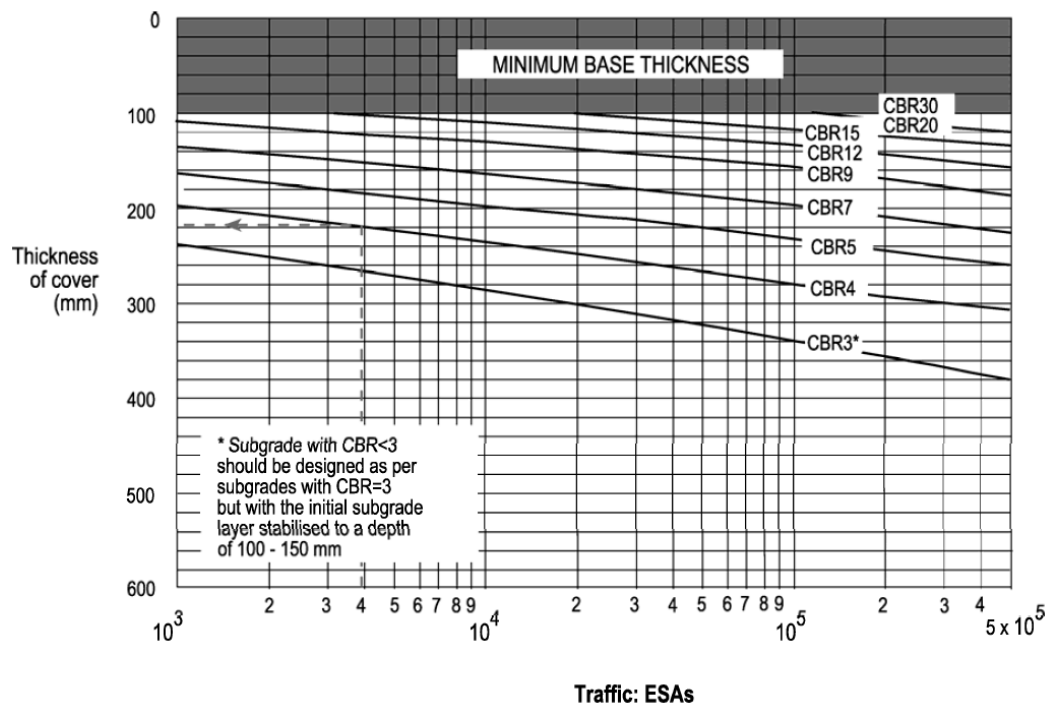


Figure 3.2 – Design for granular pavements (80% confidence) Source: ARRB Transport Research (1998, Figure 13.8.2.C). [Austroads 2009]

The thickness determined from Figure 3.2 represents a minimum structural thickness to protect the subgrade from deformation (rutting) under trafficking during its design life. The guide makes the provision of aggregate loss that should be handled with routine patrol grading for reshaping the surface.

It is noticed that a minimum base thickness is stated as 100mm and subgrades with CBR lower than 3 should be stabilized to a depth of 100-150mm.

### 3.2.1. New Zealand supplement to the Australian PDG

The New Zealand Supplement to the Australian Pavement Design Guide - APDG 2004 -, by Transit New Zealand [2007], covers some of the aspects overlooked by the APDG, in the reviewed versions. It basically forwards the design method to use of the Circly

program, as suggested by the APDG to sealed pavements. With the program, the granular material performance is accounted for by the consideration of its stiffness. Non-linearity and cross-anisotropy are also available at the software.

Notwithstanding, the Circly program will also design the pavement layers based on the principle of an admissible vertical resilient strain at the top of the subgrade what, as previously discussed, yields into the same rationale of fully elastic behaviour of the granular layer and correlation of the elastic properties of the subgrade with its elasto-plastic properties, what is somewhat undesirable.

### 3.3. AASHTO GUIDE DESIGN

The AASHTO Guide for design of pavement structures [AASHTO 1993] is principally based on the results of the AASHO Road Test, supplemented by existing design procedures in the state departments of transportation in the United States. In this guide, granular layers are mainly characterized in terms of resilient moduli, which should be determined using cyclic loading triaxial tests. However, the resilient modulus can be substituted by structural numbers if the designer counts on a great deal of experience. The 1993 AASHTO guide predicts pavement condition as a function of distresses translated into one single index, the Present Serviceability Index (PSI).

It is assumed that different materials with identical behaviour should be assigned the same structural number (SN), an empirical value calculated from the structural coefficients and thickness of the layers comprising the pavement structure. SN can be obtained from a table with subgrade CBR and design traffic as the input. A combination of surfacings, base and sub-base is selected according to Equation 57.

$$SN = \sum_{i=1} a_i D_i \quad \text{Equation 57}$$

Where:  $a_i$  = structural layer coefficient of layer  $i$ , which is a measure of the relative ability of the material to function as a structural component of the pavement, where:

$$a_2 = 0.249 (\text{Log}_{10} E_{BS}) - 0.977, \text{ base coefficient}$$

$$a_3 = 0.277 (\text{Log}_{10} E_{SB}) - 0.839, \text{ sub-base coefficient}$$

$$D_i = \text{thickness of layer } i$$

For granular base and sub-base layers,  $a_i$  is multiplied by a “drainage factor  $m_i$ ”, which depends on the drainage ability of the material or quality of drainage and on local climatic conditions or time taken to remove the water (e.g.  $m_i=1.4$  is well-drained materials in areas of low rainfall and  $m_i=0.4$  for the opposite case). This factor effectively increases or decreases the structural contribution of a granular layer.

Equivalent thicknesses were also calculated from an elastic stress analysis by picking some criterion value (e.g. vertical subgrade stress beneath the load) and maintaining it constant for various combinations of stiffness,  $E$ , and layer thicknesses.

The moduli of granular materials are given values based on either laboratory tests or according to the  $k$ - $\theta$  model (Equation 8), with  $k_1=3000$  (wet) to 8000 (dry) and  $k_2= 0.5$  to 0.7. For the subgrade, an effective resilient modulus is established which is equivalent to the mean of all the seasonal modulus values.

Hall and Bettis [2000] investigated the procedures used for low volume road pavement design guides in eleven states in the United States. The authors found that states that have developed specific design procedures, as opposed to using the procedures recommended by AASHTO, did so in an effort to “tailor” specific values or design parameters to their particular needs.

In Hall and Bettis [2000] study, an example of a consideration omitted from the AASHTO guide design for low volume roads was, particularly, the consideration of heavy traffic. According to the authors, the Oklahoma and Virginia procedures tackled this issue more properly than the AASHTO PDG, which introduced provisions for the “over loaded trucks” and a consideration of heavy vehicles greater than 5% of ADT in the design methods, respectively.

In order to compare the results obtained in the various investigated state procedures, a simple calculation for a LVR pavement structure following each procedure was contrasted with the results using the 1993 AASHTO guide design. As an overall conclusion, the authors found that the AASHTO guide leads to results less conservative than those coming from regional procedures.

The guide seems to be limited from the permanent deformation development in granular layer - subject in discussion. Hence, the limitation of the procedure remain broadly the same as the Australian Pavement Design guide, on which the vertical strain on top of the subgrade is still considered as the key parameter for the calculation of the UGL thickness.

### **3.3.1. US Mechanistic-Empirical Pavement Design Guide**

The National Cooperative Highway Research Program – NCHRP 1-37A – released in 2004 the Guide for Mechanistic-Empirical Design of New and Rehabilitated Pavement Structures [AASHTO 2004]. This guide has been widely investigated by researches as it promised to be the first real mechanistic-empirical approach for pavement design.

---

Among the innovations the guide presents, is a complex modelling of asphalt behaviour, considering several inputs for binder and mix properties and modelling several distress modes. The climate is now part of the database provided by the guide and can be considered highly relevant for the design procedures.

For asphalt, the model for permanent deformation is an enhanced version of Leahy's model [Leahy 1989], modified by Ayres [1998] and then by Kaloush [2000]. For prediction of unbound materials permanent deformation, the model is based on Tseng and Lytton's model [Tseng & Lytton 1989], which was modified by Ayres [1998] and later on by El-Basyouny and Witczak [NCHRP 2004].

According to the Appendix GG of NCHRP 1-37A [NCHRP 2004], the use of the Ayres's modified models in the calibration process resulted in several unfavourable conditions. Predictions of the rut depth were found to possess high degree of scatter and, most importantly, the amount of the rutting in the subgrade was found to be very high. With this latest development, El-Basyouny and Witczak set out to develop a final, accurate model modification that could be used in the Design Guide.

It must be highlighted that CBR correlations with resilient modulus are still used in this PDG. Appendix CC-1 of the NCHRP 1-37A [Witczak *et al.* 2004] reports the correlations of CBR values with soil index properties.

The main procedure used by the NCHRP 1-37A to perform the calculations is through the use of the software provided along with the guide M-E PDG. Appendix RR of the document provides information about the finite element procedure used for flexible pavement analysis. The routine for stress analysis behind M-E PDG consists of a 2 dimensional nonlinear finite element modelling technique, called DSC2D developed by Dr. Desai from the University of Arizona - Tucson – USA. The key features of DSC2D for the purposes of the 2002 Design Guide include:

- Axisymmetric nonlinear analysis formulation
- Stress dependent resilient modulus model for unbound pavement layers
- Full-slip, no-slip, and intermediate interface conditions between layers
- Infinite boundary elements for reducing total analysis model size

The model adopted in DSC-2D (M-E PDG) for resilient modulus of UGM is that presented in Equation 22. The proposed equation combines both the stiffening effect of bulk stress (the term under the  $k_2$  exponent) and the softening effect of shear stress (the term under the  $k_3$  exponent). Through appropriate choices of the material parameters, one can recover the familiar two-parameter bulk stress model for granular materials and its

---



companion two parameter shear stress model for cohesive soils, the Uzan-Witczak “universal” model and the k1-k6 model from the Strategic Highway Research Program’s (SHRP) flexible pavement performance models - Equation 21.

A comparison between the 1993 AASHTO Guide and the M-E PDG allows to identify the differences between the two approaches. The key conceptual differences can be summarized as follows:

- The 1993 AASHTO guide designs pavements to a single performance criterion, the present serviceability index (PSI), while the M-E PDG simultaneously considers multiple performance failure criteria (e.g., rutting, cracking, and roughness – for flexible pavements).
- The 1993 AASHTO guide directly computes the layer thicknesses. The M-E PDG is an iterative performance prediction procedure. A trial section is defined and evaluated by its predicted performance against the design criteria. If the result is not satisfactory, the section is modified and reanalyzed until an acceptable design is reached.
- The M-E PDG requires many more input parameters, especially environmental and material properties. It also employs a hierarchical concept in which one may choose different quality levels of input parameters depending upon the level of information and resources available, technical issues, and the importance of the project.
- The 1993 AASHTO guide was developed based on limited field test data from only one location (Ottawa, IL). The seasonally adjusted subgrade resilient modulus and the layer drainage coefficients are the only variables that account to some extent for environmental conditions. The M-E PDG utilizes a set of project-specific climate data (air temperature, precipitation, wind speed, relative humidity, etc.) to adjust material properties for temperature and moisture influences.
- The 1993 AASHTO guide uses the concept of ESALs to define traffic levels, while the M-E PDG adopts a more detailed load spectra concept. As pavement materials respond differently to traffic pattern, frequency and loading and traffic loading in different seasons of the year also has different effects on the response of the pavement structure, these factors can be most effectively considered using the load spectra concept.

Although these differences seem clear, their impacts on performance prediction are more obscure. The different ways that the two procedures define performance make direct comparisons difficult. The 1993 AASHTO guide predicts pavement condition as a function of distresses translated into one single index (PSI). The M-E PDG predicts directly the

---

structural distresses observed in the pavement section and the PSI concept is no longer employed.

Although flexible pavements are approached mechanistically in this PDG, there are several empirical correlations inherent to the characterization of pavement materials. However, it seems that pavements built only of aggregate layers, have an empirical load yet rather extensive. The NCHRP 1-37A presents a dedicated section of the guide to LVRs. The proposed procedure is a simplification of the M-E PDG for situations where resources or time do not permit the level of effort required. Table 3.1 illustrates an example of flexible design catalogue for LVR for a design reliability of 75%. The values in the cells represent the thickness of the HMA layer and the baser layer, respectively.

Table 3.1 – Example of flexible pavement design catalogue for LVR proposed by the US M-E Design Guide [NCHRP 1-37A Part 4 - Chapter 1 2004]

Design reliability - 75%																
Climatic Region	Chicago (freeze)						Atlanta (non-freeze)									
Frost Penetration into Subgrade and Frost Classification of Soil (for non-frost susceptible soils, use the non-freeze climate cells.)	Yes. Soils subjected to freeze-thaw weakening						No. All soils									
Stabilised subgrades or improved foundation layer	No			Yes			No				Yes					
Type of aggregate base material	Crushed stone		Pit run		Crushed stone		Pit run		Crushed stone		Pit run		Crushed stone		Pit run	
Relative quality of subgrade soil	Low traffic: 50,000 trucks/buses															
Very good	50.8	152.4	50.8	152.4	N A		N A		50.8	152.4	50.8	152.4	N A		N A	
Good	50.8	203.2	50.8	203.2	N A		N A		50.8	203.2	50.8	203.2	N A		N A	
Fair	50.8	203.2	50.8	203.2	N A		N A		50.8	203.2	50.8	203.2	N A		N A	
Poor	63.5	203.2	63.5	203.2	50.8	152.4	50.8	152.4	50.8	203.2	50.8	203.2	50.8	152.4	50.8	152.4
Very poor	88.9	203.2	88.9	203.2	50.8	152.4	50.8	152.4	50.8	203.2	76.2	203.2	50.8	152.4	50.8	152.4
Medium traffic: 250,000 trucks/buses																
Very good	63.5	152.4	76.2	152.4	N A		N A		63.5	152.4	76.2	152.4	N A		N A	
Good	63.5	203.2	76.2	203.2	N A		N A		63.5	203.2	76.2	177.8	N A		N A	
Fair	76.2	203.2	101.6	203.2	N A		N A		63.5	203.2	88.9	203.2	N A		N A	
Poor	101.6	228.6	114.3	228.6	63.5	152.4	76.2	152.4	76.2	228.6	88.9	228.6	63.5	152.4	76.2	152.4
Very poor	127.0	254.0	139.7	254.0	76.2	152.4	88.9	152.4	101.6	254.0	127.0	254.0	76.2	152.4	88.9	152.4
High traffic: 750,000 trucks/buses																
Very good	101.6	152.4	114.3	152.4	N A		N A		101.6	152.4	114.3	152.4	N A		N A	
Good	101.6	203.2	114.3	203.2	N A		N A		101.6	203.2	114.3	203.2	N A		N A	
Fair	114.3	203.2	127.0	203.2	101.6	152.4	114.3	152.4	114.3	203.2	127.0	203.2	101.6	152.4	114.3	152.4
Poor	139.7	254.0	152.4	254.0	114.3	152.4	127.0	152.4	114.3	254.0	127.0	254.0	114.3	152.4	127.0	152.4
Very poor	152.4	304.8	165.1	304.8	114.3	203.2	127.0	203.2	139.7	304.8	152.4	304.8	114.3	203.2	127.0	203.2
	HMA (mm)	Agg. (mm)														

All designs are based on the structural requirement for a design analysis of 20 years, with either a 50% or 75% level of reliability, which represents a general range for design of LVR. The maximum number of heavy vehicles over the design life in the design lane considered for LVR in this guide is limited to 750,000.

Finally, it ought to be highlighted that although the M-E PDG has been presented as a very complete and up-to-date routine for pavement design guide, incorporating various complex models to simulate the performance of road pavements, its applicability seems to lack such advances to Low Volume Roads design. To structures where little finance investments are usually available, complex material parameters, which require complex

testing procedures, may not be viable to use. Furthermore, the simplifications considered in the software to granular material modelling, yet reasonable to thick asphaltic layers, for structures constructed mostly of UGM, they can easily lead to misguidance.

The simplifications presented in Part 4 of the guide focused on Low Volume Roads, and as exemplified in Table 3.1, could also be considered rather extreme to pavements that despite the low number of vehicle passes, usually carry very high loads. The simplifications must be careful not to lead the pavement to an early failure, or, in the other extreme, be too conservative, which could prevent the project of being accomplished.

Despite the possibility to run the MEPDG program for other scenarios, Part 4 - Chapter 1 of the Guide does not present any solution for unsealed pavement; all the constructed scenarios suggest the use of HMA surfacing with thickness ranging from 64 to 165mm. The aggregate base layer ranges from 152mm to 305mm for the same cases.

### **3.4. FOREST ROADS DESIGN**

Timber harvesting and haulage, forest management and wood processing are important economic activities in several countries, utilising virgin forests which have been growing over the past century or from reforested areas.

Road maintenance in this type of roads is responsible for a great part of the costs involved in timber abstraction. Because the transport system generates a large share of forest goods' cost, it is therefore targeted by engineers. Not only does the forest road's condition affect lorries' maintenance costs, but it also influences travel time, driving comfort and accident risk, among other factors.

In order to improve the forest roads' condition and to help finding an optimum of financial resource investment with cost/effective timber haulage, forest owners, mainly from the country's government party, have been dedicating efforts in researching maintenance patterns to minimize operational cost yielding to more competitive prices.

Examples of such projects are the Roadex projects - a technical trans-national cooperation of project sequels with participants from the European Northern Periphery, namely, Greenland, Iceland, Norway, Sweden, Finland, Northern Scotland and Ireland. More closely, the Roads Under Timber Transport - RUTT project, which was part of this research and is later approached in Chapter 4.

The main concerns in this subject encompass the applicability of laboratory developed permanent deformation models to be assessed for in-situ behaviour and the calibration of

---

analytical pavement modelling from a simplified perspective. This aims to provide LVR owners with practical design tools, focused on tackling permanent deformation.

Typical forest roads engineering and operation procedures are described next.

### 3.4.1. The Forestry Civil Engineering design recommendations

The Forestry Civil Engineering - FCE - is the civil engineering arm of the Forestry Commission and responsible for roads and bridge construction and maintenance in the United Kingdom. Not only they carry out the works but also establish the design and maintenance procedures for the forest roads looked after by the Forestry Commission. Most of the private roads also tend to use the FCE recommendations as part of the engineering schemes.

The FCE compiled their specification in the Forestry Civil Engineering Handbook [Forestry Enterprise 2004], which contains most of the needed guidelines for road and bridge works as well as road planning and economic appraisal. In addition, the Design Manual for Roads and Bridges - DMRB 070403 provide the needed standard parameters, such as design speed (25 km/h), design load (44 tonnes), road running width (3.4m), etc. Figure 3.3 shows a typical forest road cross section.

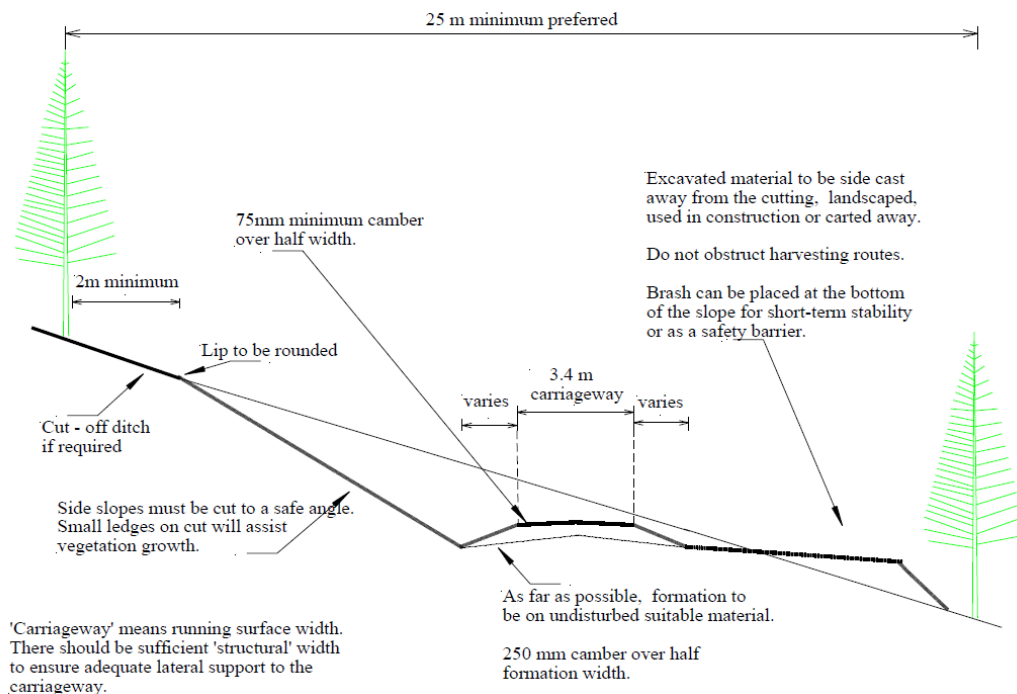


Figure 3.3 – Typical Forest Road Cross Section - Forestry Commission DMRB

Table 3.2 – Indication of the pavement total thickness as a function of subgrade CBR according to the FCE Handbook

Typical material (but see previous table)	CBR (%)	Pavement Thickness (mm)	Minimum Formation Width (mm)
Peat, silt	<2	>850 (consider excavation)	6000
Silty clay	2	700	5500
Heavy clay	3	550	5400
Sandy clay	4	475	5400
Saturated sand	7	325	5400
Fine sand	10	250	5400
Graded sandy gravel	20	150	5400
Rock	250+	Min. 100 to allow grading of surface	5400

The road design procedure covers all drainage requirements such as gradients of ditches, relief culverts, slope shapes and clearances, etc. As far as pavement design is concerned, the handbook proposes the use of a granular layer as means to protect the subgrade. As such, the assessment of the subgrade is suggested to be carried out with use of a DCP, and then correlated the material CBR. Table 3.2 indicates the pavement total thickness as a function of subgrade CBR. The handbook also indicated that the pavement thickness can often only be assessed by a site based competent judgement. It also states that material used needs to be of appropriate strength for the depth below surface while lower layers can often be constructed using low quality locally won material.

Materials are specified according to their Aggregate Impact Value (AIV) [BS 1990b] and Ten Per Cent Fines [BS 1990c]. It is said that an aggregate with AIV of less than 25 to be suitable for wearing courses, whereas an AIV value of less than 20 indicates a good material for crushing. AIV values greater than 35 are recommended to be submitted for further analysis before use.

The top 100mm of pavement must make use of a durable stone that will not readily break down under the wheel loading. It must also be suitable for grading and rolling. If heavy usage by vehicles with tracks is foreseen, the surface material should then have an AIV/SIT (Stewart Impact Test) value < 20. Grading should follow the same specification proposed by the Swedish specification as later presented in Section 4.4.

There is a specific section for roads constructed over peat. Generally, according to the peat stability and road use, the alternatives presented are: partial material excavation, pre-loading and surcharging or geotextile use. In addition, alternatives as reinforcement with inverted Stump or Latticed Brash are also available; the former uses stumps from outside the roadline which are then inverted and placed between the roadline stumps while the latter uses a lattice of brash or small trees than are put underneath the constructed embankment.

### 3.5. PERMANENT DEFORMATION SUPPORTING TOOLS FOR LVR

Several studies have aimed at ways of minimizing the effect of permanent deformation in low volume roads, having proposed and investigated various techniques. Some of the available options are:

- a. Higher quality aggregate, in terms of angularity, grading and particle strength, as this will provide a layer that cannot so easily suffer Mode 1 failure, as seen in Section 2.4.1.
- b. Use of geosynthetics to prevent loss of aggregate in the soft subgrade, keeping the effective thickness of the aggregate layer maintained through the pavement life-cycle as well helping to absorb tensile strains.
- c. Lower tyre/contact pressures through higher tyre prints or different axle configuration, reducing levels of stresses in the layer
- d. Monitoring equipment to allow the recognition of low bearing capacity seasons, e.g. spring thaw, allowing weight restrictions to be enforced.

The quality of aggregate has been targeted by many road authorities' specifications. Many design procedures specify thresholds for aggregate abrasion, crushing value, percent of fines, polished stone value, grading, flakiness, etc. These are usually defined in national standards and/or design guides.

It is presented next some available tools which represent up-to-date resources to aid the operation in forest roads. These types of roads are fundamentally constructed for timber haulage; secondarily, they may represent local access. They provide an important fraction of the total network and are responsible, among others, for preventing the depopulation of rural areas by allowing villages and small towns to minimise the high freight costs due to their distance from industrial centres.

Additionally, many areas in northern countries are rather susceptible to seasonal weather impacts that hinder or even prevent access, periodically denying these rural communities from accessing even basic food, education and health provision, and significantly reducing their ability to trade due to the unreliability of the highway link.

Hence, the higher the operation cost of LVR network, the higher is the impact in economy. The capability of using a weak road for temporary transport or, yet, maintaining operational roads during spring thawing may represent a considerable benefit.

---

### 3.5.1. Low ground pressure vehicles

As an alternative to increase the quality of pavement, a reduction in the applied contact pressure by the tyres reduces the stress and strain levels in the near surface of trafficked layers. In this scenario, the Forest Enterprise in Scotland tested a prototype vehicle with a bespoke axle configuration; the back axles are divided in two segments: each one with an equally spaced pair of tyres, totalling four distributed tyres per rear axle (Figure 3.4)

The trailer has this unique configuration of axle and wheels designed to reduce ground pressure overall and spread the weight across the carriageway, compensating for the rutting in the wheel tracks made by standard vehicles. As the axle is split in two segments with independent suspension, the difference in road surface level between the position of the outermost and the innermost tyre, which may be high in roads with severe rutting, generates a twist in the semi-axle, allowing all the tyres to maintain good contact with the pavement and, therefore, assuring a good loading spread.

It is important to notice the drawbacks of this axle configuration. There is a higher initial cost of the vehicle, a higher fuel consumption than normal axle layout – due to a higher drag caused by the higher contact area, a heavier wheel combination and difficult access for maintenance of the internal tyres.

This vehicle enables the haulage in weak roads or during wet conditions that would normally prevent the vehicle from running without causing irreversible damage. Furthermore, it may also gather access in non-paved roads on which temporary entrance may be necessary. Finally, the reduced damage in the forest roads compensates in a manner for the extra running cost; this balance may be economically assessed in order to establish an ideal pattern for its use.



Figure 3.4 – Low ground pressure vehicle and its axle configuration

### 3.5.2. Tyre pressure control system vehicles

Tyre pressure control systems (TPCS) allow the operator of a loaded vehicle to increase or decrease the inflation pressure of the vehicle's tyres in order to match road conditions whilst the vehicle is underway. With use of this technique, it is possible to reduce the contact pressure that the tyres are placing on the pavement structure. The TPCS system is of growing use in some countries in the forest business [Douglas *et al.* 2003]. The variable pressure in the tyres has a direct effect on the area in contact with the pavement, and, therefore, the contact pressure tyre-pavement.

Figure 3.5 shows a TPCS installed on a timber lorry in Scotland. The detail highlights the sidewall bulge due to heavy load and low inflation pressure. It is important to notice that the contact area increases considerably not due to the sidewall bulge but due to the increase of the length of the tyre tread print. Table 3.3 shows an array of tyre pressures pre-sets available in a lorry with TPCS fitted with a commercial system.

Figure 3.6 from Saarenketo and Aho [2005] study, adapted from Granlund *et al.* [1999], shows the load and inflation pressure effects on the tyre contact area. It is possible to see that, at a much reduced air pressure, the contact area is almost 60% higher than at a normal air pressure. The greater area leads to a less damaging stress being passed to the pavement, both vertically and as shear due to traction and braking. Thus aggregate does not deform as much, tyres do not have to climb out of so great a depression and grip is increased.

Douglas *et al.* [2003] presents a study on which the fundamentals of the TPCS, such as contact stresses, are investigated. They carried out a factorial study varying tyre load and tyre inflation pressure on laboratory conditions at full scale. A steel bed plate with T-shaped strain gauged sensors allowed the authors to investigate the stress distribution in several different configurations of load and tyre inflation.



Figure 3.5 – TPCS Installed on a timber lorry in Scotland



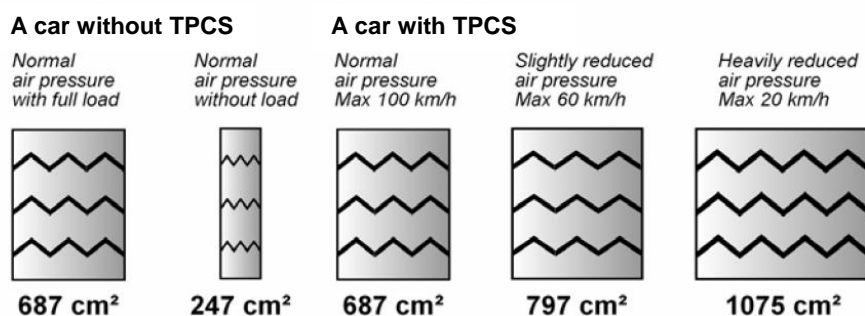


Figure 3.6 – Load and inflation pressure effects on tyre contact area [after Granlund *et al.* 1999]

Table 3.3 – Typical pre-sets available in a TPCS car (Tireboss System)

SETTING	SETTING	Drive		Trailer		Max	Max
#	DESCRIPTION	kPa	psi	kPa	psi	Mph	Time
1	Highway Empty	483	70	483	70	none	No Limit
2	Off-Highway Empty	207	30	483	70	50	No Limit
3	Push Road Loaded	276	40	448	65	10	No Limit
4	Secondary Loaded	414	60	517	75	20	No Limit
5	Main Line Loaded	552	80	689	100	50	No Limit
6	Highway Loaded	724	105	793	115	none	No Limit
7	Emergency Traction	207	30	448	65	5	5 min
8	Tractor Only-Bobtail	414	60	793	115	none	No Limit

They concluded that, although many authors point to beneficial effects of TPCS, there is sufficient justification to pursue the question of whether the use of low-inflation-pressure tyres on chip seal pavements may lead to aggregate plucking (due to high transverse shear stress for the edge rib of the tyre at low pressure), severely damaging the sealed road surface. This would be an unwelcome result, given the benefits observed in the use of TPCS on unsealed, unbound roads surfaces.

At lower pressures the same vehicle may cross a softer pavement without causing rutting or wheel spin. The technique also seems to result in much less tyre wear [Munro & MacCulloch 2007] and, perhaps, fuel use. The drawback is that the vehicle cannot travel at speed on conventional pavements without safety concerns and extra fuel use and tyre wear, so the pressure must then be increased to conventional levels. This system is credited in reducing the rutting damage in unsealed roads and also in improving ride quality for drivers.

### 3.5.3. Percostation Technique

The Percostation Technique, developed by the Estonian company Adek Ltd, measures the dielectric value and electrical conductivity of the material being tested. It is derived from an earlier equipment from the same company, called Percometer, which was first used to estimate the frost susceptibility of subgrade soils [Saarenketo 1995a] and, later, to measure the water susceptibility of base aggregates [Saarenketo 1995b, Saarenketo & Scullion 1996]. It assists in managing rutting by allowing road owners to estimate when their road materials are too wet to perform adequately.

A Percostation comprises of a Percometer capable of processing and data logging the information from up to five probes installed in an in-service structure, and can be remotely controlled. The output values obtained from the system are: Dielectric value (E), Electrical Conductivity (J) and temperature in all connected probes, plus air temperature in the Percostation cabinet.

Saarenketo *et al.* [2002] explains the principle of the equipment; in dielectric measurements, the Percometer measures the real part of the relative dielectric value. The measurement is based on the change in capacitance caused by the material at the tip of the probe, which is in contact with the ground. The contact surfaces at the tip of the probe are insulated from one to another with Teflon, forming a capacitor. The specific capacitance of the capacitor is directly dependant on the dielectric value of the surrounding material. When measuring dielectric value, the Percometer uses a measuring frequency of 40-50MHz. When measuring electrical conductivity, the Percometer uses a measuring frequency of 2kHz. Dielectric measurements with the Percostation are reliable when the conductivity of the measured material is lower than 1000mS/cm.

Figure 3.7 shows the schematic diagram of a Percostation installation, as well as a Percostation probe and system.

Saarenketo & Aho [2005] report on ideas and innovations about monitoring low volume roads. They say one of the key parameters that have been found to be effective in permanent deformation risk assessment is the dielectric value of unbound road materials. They state that the sensitivity to permanent deformation of unbound materials can be evaluated by taking samples from the base course and then conducting Tube Suction Tests (TST) on them.

---



Figure 3.7 – (a) Schematic diagram of a Percostation Installation [Saarenketo & Aho 2005] (b) Percostation's Probe (c) Percostation System

Dielectric properties of soils and aggregate materials are affected by a number of soil characteristics including soil water content, dissolved salt content, clay content and mineralogy, and soil temperature. Dawson and Kolisoja [2004] highlight that dielectric assessments (e.g. Tube suction, Percostation or Percometer methods) measure, in effect, the free water in the aggregate, although this may only be true for deionised water.

Some studies, many of which have been carried out to assess roads with freezing problems, have been searching for a relationship between dielectric behaviour of the granular layers and permanent axial deformation susceptibility in roads during freezing/thawing. The methodology used consists, basically, of TST to be carried out in the laboratory, along with repeated loading triaxial (RLT) tests from which it is possible to establish a parallel between dielectric value and permanent strain (see Figure 3.8).

Figure 3.8 shows the relationship between the dielectric value of a sample's surface and the permanent deformation measured after a freeze-thaw cycle in RLT tests at TUT-Finland [Saarenketo *et al.* 1998]. Deformation values higher than 2% were extrapolated from behaviour at a reduced number of cycles of loading.

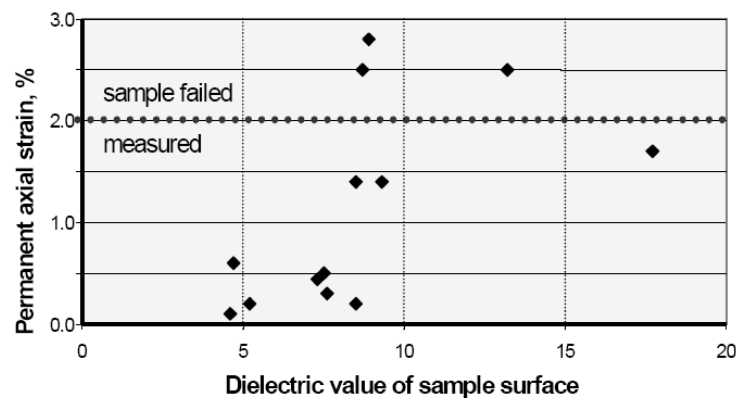


Figure 3.8 – Permanent axial strains of specimens as a function of the dielectric value of the specimen's top surface (measured in TST) [Saarenketo *et al.* 1998]

Results showed that higher plastic deformation values were measured in samples with dielectric value higher than 8 [Saarenketo *et al.* 1998]. The measured dielectric values in RLT samples (400mm) were slightly lower than corresponding values in TST samples (200mm), possibly because of the thickness of the samples used.

Dawson *et al.* [2007] recommend the use of measured dielectric values as a guideline for checking susceptibility of base materials for design purposes. The authors recommend that the tube suction measured dielectric value of the compacted aggregate to be less than 10, preferably less than 9, after drying the specimen at 40 - 50°C and then letting it absorb water from the base of the specimen until a constant mass is reached.

### **3.6. SUPER SINGLE TYRES VERSUS TWIN TYRES**

One of the issues that has motivated several studies, and the use of different types of tyre sizes at the Accelerated Pavement Trial later described in Section 4.3, was the widespread use of super single tyres on lorries used by the timber industry for transport in the UK.

The use of super single tyres in lieu of the dual tyre fitment is known to be a current trend in European countries as well as in other places across the globe [Addis 2000]. In addition, as a general trend, heavy goods vehicles regulations tend to increase allowable weights over time. Both facts together concern road authorities because the high damaging level caused in the roads, and therefore, the higher maintenance costs.

As a consequence of the ongoing researches for more economical freight transport, tyre sizes have been changing in pursuit of lower maintenance costs and, thus, the introduction of the “super-single”-sized tyres. With wider nominal section widths, these new large pneumatics (e.g. 385mm wide) are replacing two of the previous thinner tyres (e.g. 295mm wide, each), thus reducing cost to the vehicle owner. Recently “super-super-single”-sized tyres have been introduced (width = “495mm”) although these have not yet been seen on forest-operating trucks.

Figure 3.9 illustrates the development of heavy vehicle tyre & axle configurations, as suggested by the research program COST 334 [Addis 2000]. It can be noticed that the “far future” designated in 2000 with the use of lower/higher tyre inflation pressures is already a reality today with the TPCS vehicles previously mentioned in 3.5.2. However, a change that may be interesting for the near future, is the use of wider tyres on the front axle (something suggested further in this report) as a means of addressing one of the possible causes of the highest damage levels.

---

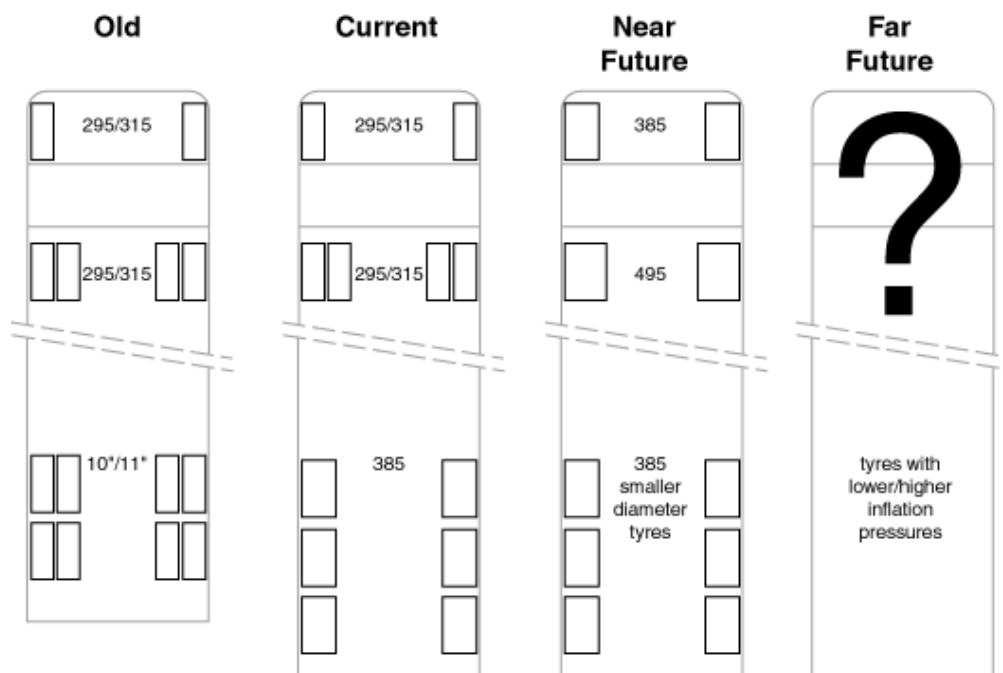


Figure 3.9 – Development of heavy goods vehicles in regard to axle and tyre configuration [Addis 2000]

The instinctive thinking that super singles establish a more severe condition to trafficked pavements need to be investigated for LVR structures, and this has motivated the investigation carried out in the accelerated pavement trials in this research. Forest Roads in Scotland are constantly used by lorries with super single tires fitted.

### 3.7. KEY FINDINGS

The focus of this chapter was to provide a review on the traditional design guides for Low Volume Roads along with an overview of typical LVR operation such as forest roads. The coming chapters will detail the work carried out in this research founded on the following key findings from this Chapter:

- The empirical methods provided the initial engineering basis for designing roads. Assessment of material's behaviour according to tradition and pavement trials provided the first designing methods. Although effective for a given scenario, empirical assessment has very limited validity and needs, therefore, to be advanced into more analytical methods.
- California Bearing Ratio still stands as the main material strength parameter for designing purposes. Correlations with DCP are available and there are several methods that reference the use of DCP as an important tool. Attention should be

given to the fact the CBR is a benchmark test; consequently, its consideration inspires limitations to the design procedures.

- There are so far two main streams in designing unsealed or thinly sealed low volume roads: from empirical correlations - which has been reduced throughout the years with advance in mechanistic concepts; and linear elastic mechanistic methods which are most of the times packed into design charts or tables that simplify the required analysis.
  - The empirical-mechanistic approaches are expanding their use, as computer programs are more readily available, some of them making use of anisotropy and non-linearity of the granular behaviour. Permanent deformation assessment remains out of scope of these approaches.
  - The available empirical-mechanistic PDG for low volume roads base their concept in protecting the subgrade from permanent deformation by varying the required base layer. This is done by limiting the calculated vertical strain on top of the subgrade - which assumes a misguided correlation between elastic with plastic behaviour.
  - Despite studies have advanced in the understanding of permanent deformation in granular layers, design guides fail to introduce in a routine basis this concept. All of the guides researched neglect the main failure mechanisms in these roads - rutting in the granular material. Some studies [Werkmeister 2003, Arnold 2004, Korkiala-Tanttu 2008] have already presented procedures for permanent deformation assessment in granular layers, although not packed into a design procedure.
  - By understanding the limitations of the available tools for designing a LVR, it is clear evident that the input parameters ought to cope with the resources at road owners disposal, some of which may be as simple as a DCP analysis; the material's assessment needs to be as straight forward as possible, ideally with strength parameters more easily obtainable - such as existing databases.
  - Alternative tools as tyre pressure and use of dielectric measurement may be somehow approached in a PDG, as they represent important tools of growing use in LVR in Europe. The available literature shows that these tools are also present in other countries as Canada and United States of America [Bradley 2002, Douglas *et al.* 2003, Saarenketo 2006].
-

## 4. FULL SCALE TRIALS IN SCOTLAND

Full scale trials provide essential data for the understanding of pavement distress mechanisms and validation of performance prediction models. The Forestry Commission/Scotland engaged in a research project to evaluate the performance of forest roads pavements as part of the Strategic Timber Transport Forum program, conceiving the Roads Under Timber Transport - RUTT - project.

The RUTT project was a partnership between Forestry Civil Engineering/Scotland and the University of Nottingham that started in September 2006 and ran until May 2008 with the overall goal of establishing the effect of weather and seasonal effects on the rutting of forest roads and improving their performance while enabling the roads to be economically constructed and maintained.

The project comprised four broad studying areas: monitoring of in-service forest road sections, accelerated pavement trials, dielectric monitoring of forest and public road sections with the Percostation technique and an economical assessment of road cost for maintenance and operation with use of the HDM-4.

The author participated in setting up the program and the research brief for the first three studies and gathering and analysing data for the first two studies as well as reporting the final outcome of the study [Brito & Dawson 2008, Brito *et al.* 2008]. The Percostation research was mainly developed by the Roadscanners Oy consulting company and is detailed in Saarenketo [2008]. The economical assessment with use of the HDM-4 tool was developed by the Roughton Group and is reported by Taylor [2008]. The Percostation technique which monitors the dielectric properties of material in pavement layers is approached in this research as basis for the project's discussion while the economical assessment is not further discussed as it is out of the scope of this research.

### 4.1. AN OVERVIEW OF THE RUTT PROJECT

The RUTT project was primarily conceived within the timber industry; hence, its broad aims embrace, especially, forest road engineering aspects, although many of the outcomes may be of use for a wider research and LVR communities. The study is mainly aimed to look at the following aspects:

---

- a. To evaluate the large differences in forest road damage according to season and to seek to determine climate *versus* usage relationships;
- b. to establish the capacity of weak (thin) forest and public roads in terms of safe numbers of loads that may pass;
- c. to investigate early collapse with traffic volumes around 50 loaded trucks a day using a purpose-built test facility;
- d. to assemble more accurate transport and road maintenance costs and then investigate how the combined costs might be evaluated;
- e. to investigate the effect of super single tyres, twin tyres and low ground pressure vehicles axle's layout on permanent deformation development.

The author of this thesis was mainly involved in looking into aspects a, c and e.

In order to accomplish this, four main groups of activities were planned:

- i. Study of in-situ pavement material condition (using the Percostation Technique) [Saarenketo 2008];
- ii. Monitoring of in-service forest roads for rutting development;
- iii. Full scale accelerated testing, to assess the key factors influencing rutting (performed at Ringour); and
- iv. An economic assessment of the maintenance of these roads using pavement management techniques [Taylor 2008].

Figure 4.1 shows a flow chart of how the listed activities interact in order to achieve the broad goal of the project: to have the most cost-effective road as possible in roads used for timber harvesting in southern Scotland.

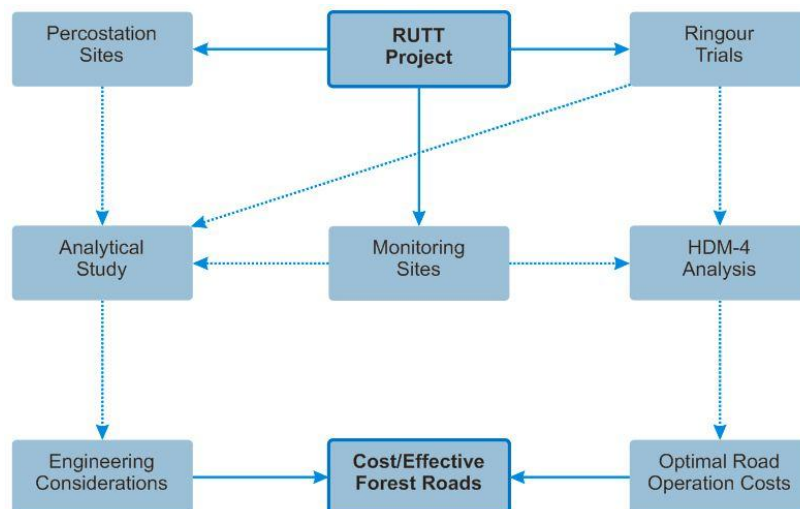


Figure 4.1 – RUTT Project's flow chart



Three principal objectives were defined for the in-forest work. These were:

- i. To monitor rutting at 21 in-forest sites, taking measurements at two or more cross sections at each site together with traffic and weather monitoring (to help address aims “a” and “d” in Section 4.1). These sites are known as the “Monitoring” sections;
- ii. to undertake more detailed studies at five sites in order to observe the behaviour of known constructions (to help address aim “a”). These sites are known as the “Reference” sections; and
- iii. to install, *in-situ*, and to monitor continuously, two sets of sensors (“Percostations”) that measure the dielectric properties of the road layers. Dielectric properties appear to relate to available moisture. One would be installed in a forest road, the other in a public road (to address aims “a” and “b”).

## **4.2. MONITORING OF THE TRIAL SECTIONS**

The aim of the monitoring sections was to obtain data representative of the variety of conditions and materials that exist in the forest roads in Southern Scotland and, also, to obtain data that is inter-relatable between sections allowing the study of weather and seasonal effects on rutting.

The same measurement routines as adopted for the monitoring sections were also adopted for the reference section, and are described below. The only difference between the monitoring sections and the reference sections was in regard to the periodicity that the survey was carried out; in periods with low traffic anticipated, the reference sections would undergo a less frequent surveying.

### **4.2.1. Inspection and selection of sites**

As a first step to be taken toward the implementation of the project, a list of 56 entrances of forest roads, which are referred as “sites”, was available for inspection. The selection of the sites aimed to provide factorial connection (the possibility of comparing readings taken in one place with those taken in another) between those selected.

From the initial list of 56 sites, 29 sites were actually surveyed, and the sites with no potential for considerable traffic over the project’s period were disregarded due to the fact that they would not meet the basic purpose of the study: to accumulate considerable permanent deformation over the monitoring interval. All these 29 sites were then inspected in regard to:

---

- Topography – classified as road on side slope, road on embankment, road in cutting, road over peat or overlay construction.
- Longitudinal gradient – evaluated in percentage by chainage.
- Watertable and drainage conditions – by visual inspection.
- Aggregate type – by visual inspection.

Details of the selected monitoring and reference sites along with their respective initial inspection record can be elsewhere [Brito & Dawson 2008]. The final selection of sites was composed by six sites located in forests managed by the private sector and the remaining fifteen sites managed by the Forestry Commission, totalling 21 monitored sites.

The primary criteria for the selection of the sites to be part of the RUTT project was the traffic forecasted by the area forestry civil engineers, followed by the importance of the forests in which they were located from a strategic point of view. In regard to the choice of the reference sections, the main reason considered for their selection was the connectivity to other forest roads as network usage should lead to higher traffic volumes on the selected link. In addition, roads that were too flat were eliminated to avoid places where potholing was likely to occur, and therefore, misleading performance monitoring in regard to rutting of the cross section.

Figure 4.2 is a map of Southern Scotland locating the sites selected for the project. Eleven sites are located in or close to the Galloway Forest in Southwest Scotland. Another seven are located in or close to the Scottish Borders Forest and other three are in the West Argyll region, North-West of Glasgow. The “Reference” sections can be considered as part of the “Monitoring” network as the same information is collected, as a minimum, from both types.

Monthly measurement of rut depths were planned for each section at two cross sections (minimum), while those with a forecast of higher traffic over the project’s period were equipped with four cross section for monitoring. The highly trafficked sites were provided, also, with traffic, rainfall and temperature monitoring using automated equipment allowing data-logging over the whole project period. The methods and equipment used for monitoring the sections are described below.

---

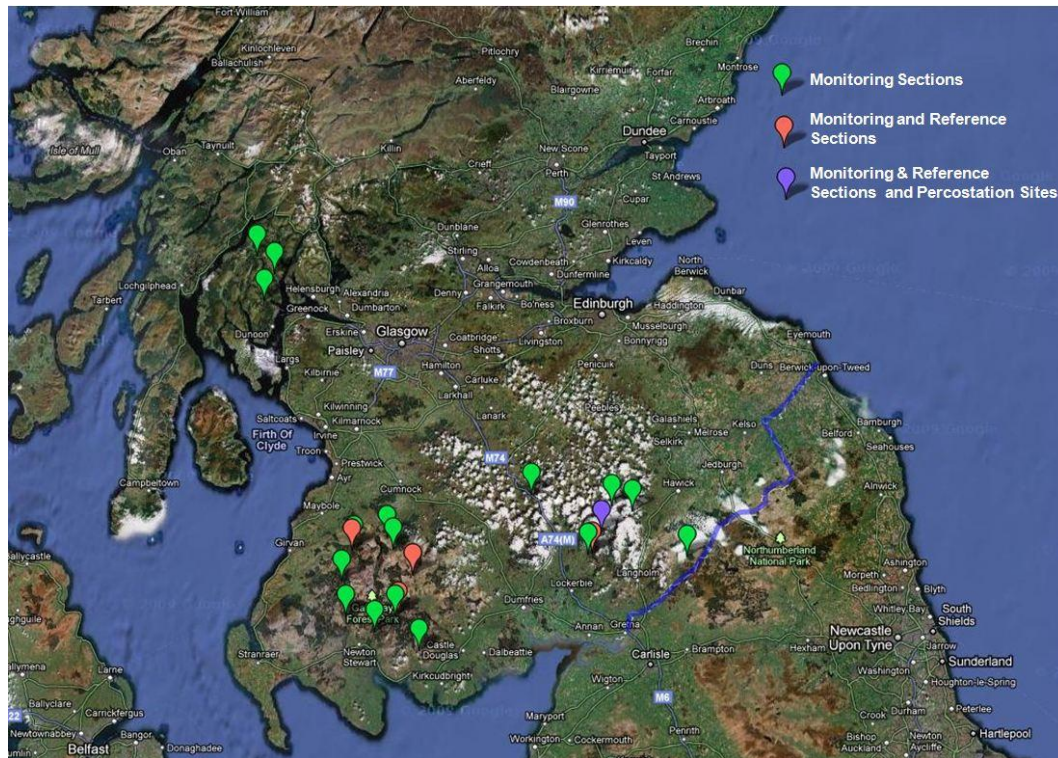


Figure 4.2 – Maps of sites on the RUTT Project in Scotland

#### 4.2.2. Traffic counters

An important input for the analysis of the permanent deformation development rate is the traffic volume on the monitored sites. Three strategies are considered for assessing that:

- Installation of traffic counters
- Estimation according to timber volume harvested
- Historical data.

Ideally, the option of a traffic counter ought to provide the most reliable measure, whereas estimating traffic from timber volume harvested yields inaccuracies due to consideration of constant gross weight vehicles. Historical data could be considered the least accurate strategy taking into account the variability of timber felling operation schemes.

Due to budgeting restrictions, only 17 traffic counters could be acquired for the project. Because many of the forest roads are used by timber lorries and small vehicles, car and vans, which for the purpose of the project are considered innocuous in causing damage to these roads, traffic counters with a classifier algorithm were considered ideal. However, only eight counters could be afforded with classifier system. The other nine were able only to count the total number of axles with no classification.

For those sites where no traffic counting was available, the traffic volume was obtained by correlating it to timber volume felled per month. Where classification was not available, it was expected to sample vehicles distribution by rotating the position of the classifying counters.

Two different models of traffic counters were suggested and acquired: the Minuteman® EVR Recorder, from Counters and Accessories – a two channel traffic recorder/classifier designed to record the flow of traffic over one or more lanes using rubber hoses/tubes; and the Junior traffic counter – a simple traffic counter designed to record the total flow of traffic over one or two lanes using a rubber tube, from the same manufacturer. The first one is able to classify vehicles according to several different protocols (e.g. FHWA U.S; EUR) aided by the VDA-Pro Software, whereas, the second (the “Junior” version) is only able to provide total flow without any classification. Figure 4.3 shows a picture of the traffic counters.



Figure 4.3 – Minuteman EVR and Junior Traffic counters

Both counters have proved to be rather ineffective for use in forest roads. After contacting the counter's manufacturers and attempting to modify the algorithm of the software, the results were still far from reasonable when compared to the timber amount harvested in the period and according to the local engineering judgment of traffic volume.

According to the manufacturer, the main problem is due to the absence of a flat surface on which the tubes should lay flushed. Hence, mostly because of the wheel paths' rutting and/or corrugation causing the tubes to be somewhat suspended in some areas, false 'hits' are recorded by the pressure sensors in the counters, giving a false reading to the software, making the classification and counting algorithms malfunction. This explanation does not explain why misreadings were still evident at sites where the sensor tubes were

fixed to a firm substrate (i.e. on the bridge decks immediately prior to the monitoring section at Eskdalemuir (Till Hill) and Gair), and an explanation of misreadings in such circumstances has not been convincingly provided.

In regard to the “Junior” counter, which provided only the total number of axle passes, a problem with the sensitivity of the trigger mechanism caused several months delay in collecting readings before an appropriate sensitivity could be arranged for all the counters. During this period, it was anticipated that the mis-triggering could be allowed at a later stage by a calibration factor applied to the actual readings obtained. In fact, this proved not to be possible, so no means of equating the axle count to number of lorries could be established.

In addition to the problems described, both counters experienced various different faults and tube punctures, making continuous reading difficult even if the outputs could be considered reliable.

In an attempt to search for an alternative, another company was later contacted, towards the end of the project. They supplied a unit credited with being able to give good results when used together with more robust type of tubes having a “D”-shaped cross-section.

The two different manufacturer counters were installed at one of the monitoring sites, Steel Road – Riccarton, to be compared and cross checked against the count made by a standard motion-detector-activated CCTV. The Minuteman counter was damaged by water that penetrated the cabinet from the rain, damaging the main board and therefore corrupting the file’s data. The camera installed was ineffective in providing clear pictures. The images were reported to be fuzzy and no clear vehicle count could be accomplished. The alternative counter was the only equipment that provided consistent data for the one month period on which all three systems were left on site. Although the reports generated by this counter seem to be of high quality and good support was obtained from the manufacturer, no independent cross-check could be carried out for the reasons just described.

Finally, because no traffic data was available at the end of the project, timber tonnages were gathered from the area operating managers. These figures were then equated into number of vehicles following the simplification that only articulated lorries with 44.2 of total gross weight were in use over the monitored roads. According to table Table 4.4 in Section 4.3 - this vehicle has an Equivalent Standard Axle Load of 4.94.

---

### 4.2.3. Weather stations

Aiming to promote the investigation of forest roads damage in regard to season and weather, simplified weather stations were acquired and installed in all twenty one monitoring sites of the project.

The station consists of a rain collector (tipping bucket system) fitted with a micro-processed event logger capable of storing 365 days of data when setup for a 30minutes resolution. The event logger is also supplied with a temperature sensor which is logged to the system at the same frequency.

The downloading of the stored data is made via shuttle reader – an optical based sensor which is capable of storing data for further downloading to an office computer. Figure 4.4 shows a picture of the tipping bucket, event logger and shuttle reader.



Figure 4.4 – Simplified weather station and shuttle reader for data-logger download

All sites have already been supplied with a simplified weather station and have had data collected since December 2006. The logged entries must be post processed aided by the HOBOWare Pro software ®, with which the statistics can be obtained at the desired resolution. Figure 4.5 shows an example of the results obtained for the Till Hill Main Block, at Eskdalemuir site, presented at a one day resolution.

Data available at Eskdalemuir Meteorological Office has been also requested for the effect of validation of this system. Furthermore, as the Eskdalemuir Forest has 4 sites in

its surrounding area participating in the RUTT Project, including the Percostation sites, extra weather data was then put available for extra analysis, such as: sunshine amount, grass minimum temperature, wind speed and directions and maximum gust – all at an hourly resolution. Figure 4.6 shows monthly temperature and rainfall records for the site from January 2001 to April 2007, obtained from the Meteorological Office UK. No further data could be obtained as the Meteorological Office UK only supply four sets of data free of charge for research studies.

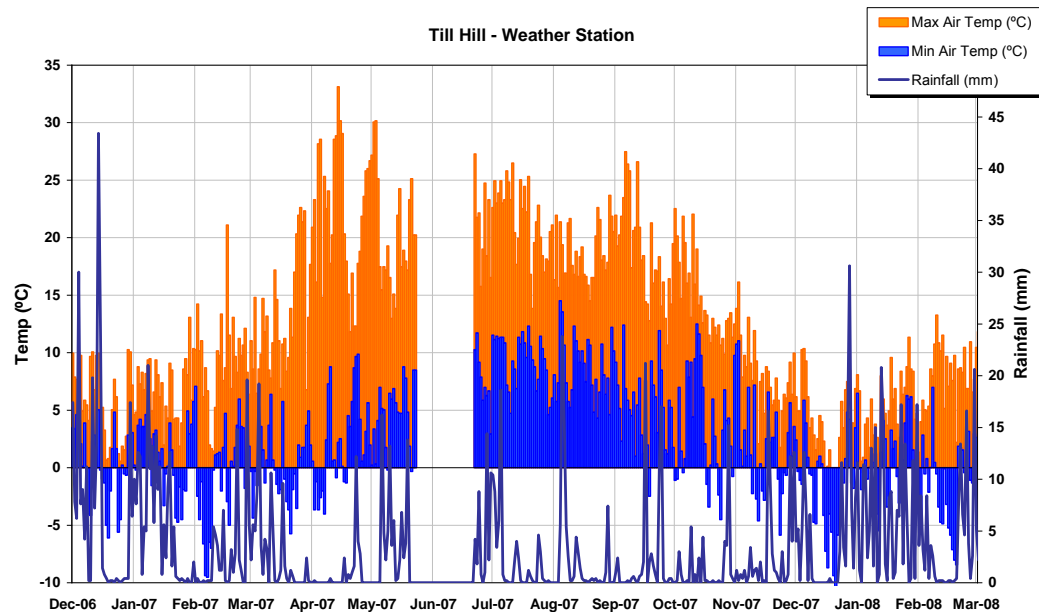


Figure 4.5 – Weather data obtained in RUTT Project for Till Hill Main Block at Eskdalemuir

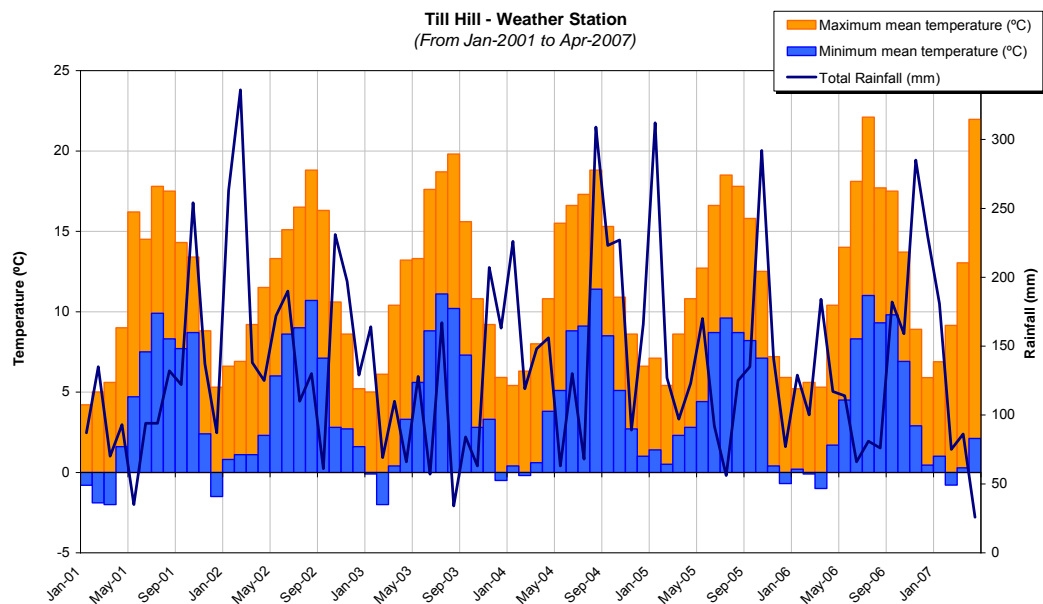


Figure 4.6 – Weather data for Eskdalemuir/Scotland from January, 2001 to April, 2007  
[source: MetOffice 2007]

By the comparison between the readings collected with the system setup and the Metoffice, a good correlation was obtained, indicating the readings could be considered appropriate for the purposes of this study.

Finally, most of the weather stations provided reliable information. There were few problems whilst downloading some of the stations and others were lost or stolen during the course of the project. The majority of the sites, however, had their temperature and rainfall monitored throughout most of the period of the project.

#### **4.2.4. Permanent deformation monitoring**

The monitoring of the permanent deformation development at all monitoring and reference sites was performed on a monthly basis. The protocol proposed for the cross section profiling includes the use of an aluminium beam conceived specifically for the RUTT project. The calculations for the rutting measurement are detailed in Section 4.6.

Each monitoring section consists of a pair of concrete blocks measuring approximately 0.60 x 0.60 x 1.00m (W x L x H). These blocks are intended to provide a fixed datum during the project although local circumstances do not always make this achievable. The concrete blocks are levelled and fitted with a steel profile to support cantilever arms which offered a backbone for the profiling beam (see Figure 4.7), which has major dimensions of 0.2 x 0.2 (quadrangular section) by 5m in length. Readings were then taken at 0.1m resolution across the carriageway.

The purpose of having two sets of measurements at each location was also to guard against situations where unrepresentative damage occurs. Additional sets were erected at Kilburn Hill and Tillhill main block where there were lengths of different construction.

Each pair of blocks provides one cross section. For those sites where 2 monitoring sections were installed, pairs were generally placed 15m apart. In those sites with 4 monitoring sections, there were two groups spaced usually 200 to 500m between the groups, and 15m within each group.

The protocol for the permanent deformation monitoring consists of:

- Use of a laser measuring device<sup>3</sup> equipped with a built-in Bluetooth transmitter, allowing connection with a handheld computer for data storage (both an HP iPaq and

---

<sup>3</sup> The measuring device used was the Leica Disto®. The precision obtained by the equipment in the type of ground used in the monitoring sections is 0.005m.

---



a Panasonic Toughbook were used). The type of equipment speeds up the collection process and guarantees error-free recording.

- The laser was positioned over each hole and the reading transmitted when stable. The readings were automatically logged onto a PlusXL spreadsheet which was later downloaded onto a PC and converted into Microsoft Excel format.
- 46 readings were taken at 0.1m spacing across the road, totalling 4.50m of cross section measurement.
- Pictures were taken of each section with a scaled straight edge to aid the determination of the cross-section's representativeness.

Figure 4.7 shows the pictures taken for the whole period of the project at Till Hill forest road entrance. They include a straight edge to aid in a visual record of the monitoring sections. The maintenance overlay carried out in April 2007 at Till Hill Main Block is visible in the pictures and noticeable in the profile graphs. Exemplar data obtained from the readings are presented in Figure 4.8.

In regard to data processing for cross section plotting, two corrections are carried out: the first concerns the misreading due to instability of the laser measuring device (occurrence is at a minor scale) and the second is a correction performed due to variation in the sitting height of the cantilever arms on the poles – performed on a regular basis. This is either deliberately caused to accommodate an overlay or to restore operational comfort, or even due to a improper sitting of the arms due to frost, water or rust inside the profile. To allow for this, a correction is calculated and offset from the readings, transferring the measuring plane to the foot of the concrete block – which is expected to provide a stable reference. The correction is based on the measured distance between the top of the cantilevered arms and the top of the concrete blocks at each side of the road.

The correction due to instability of the measuring laser device is performed as follows: if the absolute value is 0.15m different from the reading at the same point in the previous month and visually appears not to lie on the shape of the cross section, the value represents a misreading and is substituted by the average value between the previous and next point. Figure 4.9 shows the results for a repeatability test carried out in order to check consistency between the two usual operators and the operational procedure.

---



Figure 4.7 – Monthly monitoring of rutting at Till Hill Main Block

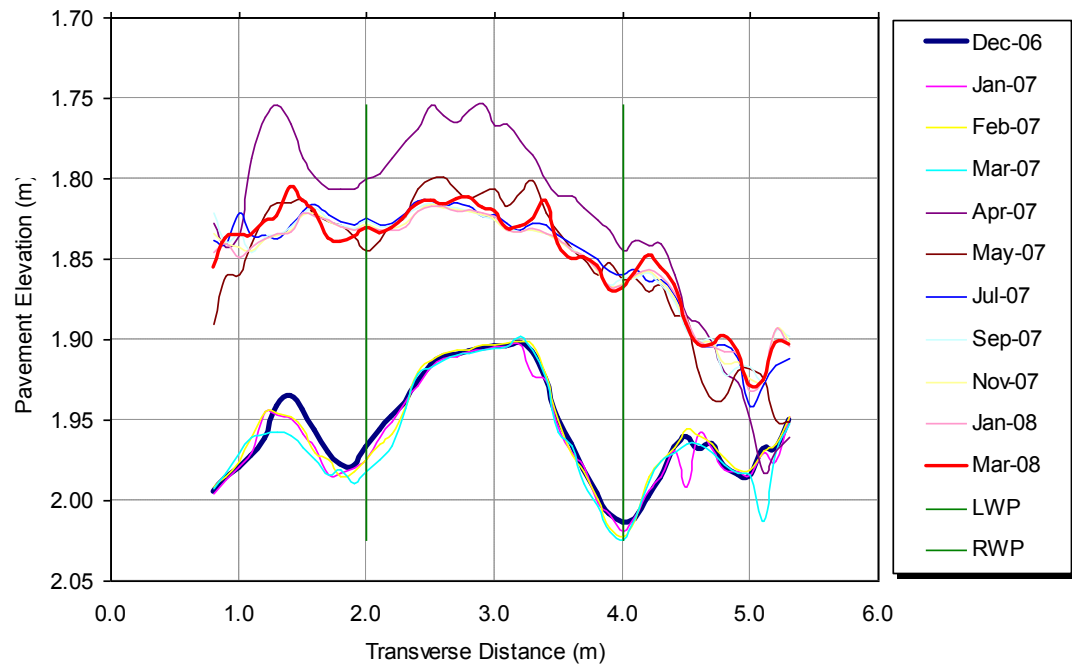


Figure 4.8 – Profile reading example at Till Hill monitoring Section one.

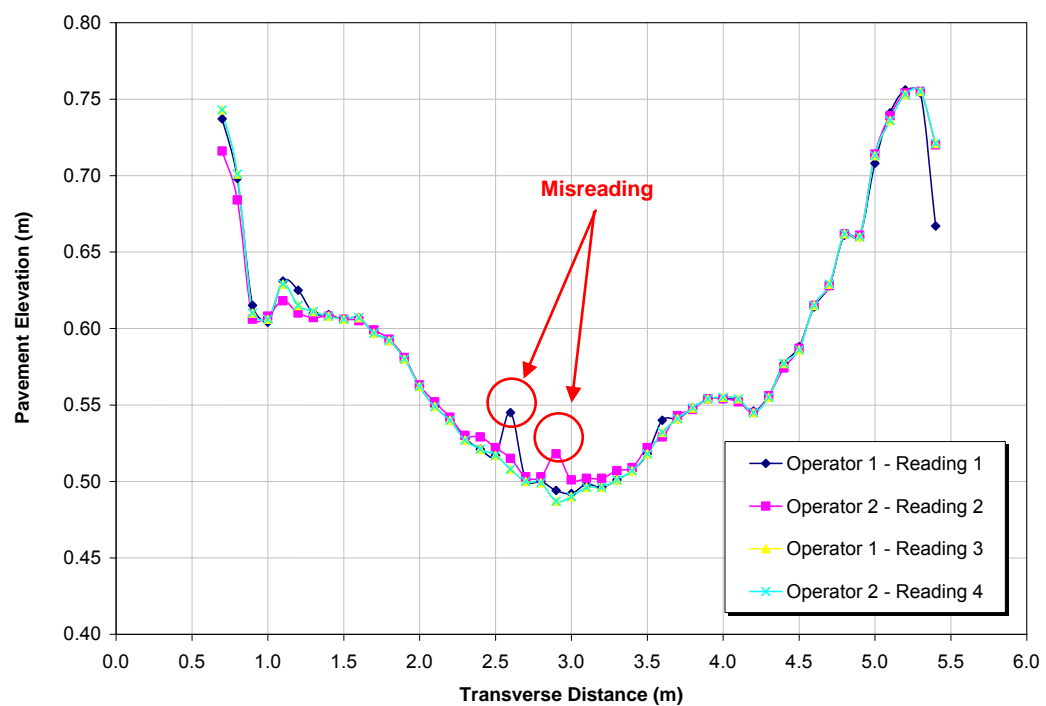


Figure 4.9 – Repeatability test with laser measuring device for profiling of the cross sections



For the permanent deformation monitoring at the Full Scale trials, a slight different protocol was used. Five monitoring stations for cross section readings were established in the trial section (T1 to T5). On each station a set of supports were levelled and fixed to support a 5.5m long aluminium beam (Figure 4.10) to allow height readings relative to a datum to be taken at 0.1m spacings across the road. Initially, profile readings were taken from three monitoring stations at the quarter and half points (T1, T3 & T5).

This was done for the first two trials when a single set of readings were measured at each station. It was realised that there was an inherent error in that the measurements were taken to an uneven surface and readings were dependant on whether the beam hit the top of a stone or passed down alongside it. It was decided to take measurements from both sides of the beam (i.e. 0.1m apart along the length of the section – see Figure 4.11) for subsequent trials so that the measurements might be averaged and the error reduced.

Usually a misreading only occurred on one side of the beam (at any particular transverse distance), so another benefit of measuring on both sides of the beam is that such a misreading becomes evident, later, during data plotting, and the parallel reading on the other side of the beam provides redundancy. Once this procedure had been adopted, the profile was subsequently measured at two stations at the third points (T2 and T4) as they seemed reasonably representative.



Figure 4.10 – Portable aluminium beam for rut profiling - at the calibration base.



Figure 4.11 - Detail of the two sided beam with 0.1m spaced readings & recording procedure

Measurements were taken of the changing surface profile of the road after 10, 20, 40, 70 and 100 passes (Figure 4.11). The distances from the aluminium beam were measured with the same instrument earlier described in this section.

It was initially suggested that, as the wheel paths developed during the test, the readings should be taken at a closer resolution. Hence, the beam was conceived with gaps for reading at each 0.1m over the 5.5m length of the beam, apart from two parts of 1m in length – offset by 0.3m from both sides of the centre – in which part the reading locations were spaced at every 0.05m.

After three trials the extra readings taken at a higher frequency in the wheel paths proved to be time consuming and of minor contribution to the data interpretation, especially in those trials with two vehicles running at the same time – the wheel paths were no longer developed in the centre of the trial sections as now 4 different paths were being trafficked. Consequently, readings were taken at a constant spacing of 0.1m across the whole section.

To analyse the rutting developed, two methods were used: rut depth and vertical surface deformation (VSD) (Figure 4.40), as discussed in Section 4.6. The rut depth considers the upward shoving at the edges of the wheel path, and is determined by placing a straight edge across the surface.

Finally, it is important to remark that for the analysis performed, many points collected by the laser device had to be manually corrected, as inconsistencies were found in the readings. Although no major adjustments were required, without them, the results were likely to suffer distortions. Corrections were done based on common sense.

#### 4.2.5. Reference sections

The reference sections have similar aims and provide similar information to, as the monitoring sections, producing a comparative benchmark for the results. In addition, they aimed to determine the influence of the surfacing layers: whether it makes a difference to pavement performance and, if so, to what extent. Furthermore, the effect of climate and drainage on the behaviour of surfaced pavements, particularly on the upper aggregate, could also be assessed.

The location of the reference sections is shown in Figure 4.2. Three sites were located in or close to the Galloway Forest in Southwest Scotland and two in or close to the Scottish Borders Forest. The sites were chosen mainly on the basis of those where most traffic was expected.

It was intended to construct each reference section with an overlay of variable thickness in order to provide several benchmarks of rutting behaviour in each section to which to compare the performance of the monitoring sections. In this way, the performance of a standard surfacing built to the same specifications at all reference sections could be compared, giving information about site and climate effects, and the performance of the monitoring sections would be comparable to this reference performance. Unfortunately it was not possible to construct to the high standard required to fully accomplish these goals.

The principal objective for the construction of the reference sections was to allow the investigation of the rutting effect on a controlled material used as overlay. Due to the fact that forest roads are usually built with material abundant in the area which is frequently not processed, that is, not been subjected to any crushing and grading control, the comparison of the performance of both monitoring and reference section enabled inferences to be drawn concerning the cost-benefit of using controlled material as a means of managing rutting development. As both sections were a few metres apart with no intersections between them, it was possible to guarantee that the traffic, weather, road foundation and maintenance records were similar.

The construction techniques were exactly the same as those used by the FCE. The new segments were laid and compacted immediately over the existing roads. Each reference section had a consistent longitudinal gradient and a 75 mm camber, meeting the FCE handbook which recommends a minimum cross slope of 4.5% falling from the crown.

The sites were equipped with three reference cross sections – positions for rutting monitoring. These cross reference sections were 30m apart requiring somewhat more than 60m of a new overlay to be put in place. By extending 10m beyond the reference

---

cross sections at both ends, improved construction quality was expected at the reference cross sections and there was distance for traffic path and dynamic patterns to become established by the time the vehicle arrives at the reference position. The reference sections had, therefore, a total length of 80m.

It was desired to control grading, compaction level and thickness. The overlay was designed to be laid as a “wedge” from 0.1m to 0.2m thick, so as to monitor its effectiveness and economy at a variety of thicknesses. The material used is later described in Section 4.4.

The construction of all five sites took place during the 2007 winter. Till Hill main block and Kilburn Hill at Castle O’er Forest were constructed in February 2007, and Linfern, Waterside and Polmaddy in March 2007. Due to low temperatures and the impossibility of concluding the work within a day at the first two sites, the overlay froze and compaction was not therefore carried out. At the other sites, compaction followed the protocol suggested by the Manual for Highways Works – Volume 1, controlling the number of passes according to the roller characteristics, which bases the FCE Surfacing Specification for Principal Forest Roads [Tyrrell 2004a].

For the construction works a grader with front loader was available. The aggregate was laid and spread without moisture control on site. In the three sites in the West region (Linfern, Polmaddy and Waterside) a 12 tonne roller with vibration was available for compaction, in the remaining two sites, as mentioned earlier, no compaction was carried out. Batter rails and a traveller technique were used to control the desired thickness of the layer. Figure 4.12 shows the works being carried at Castle O’er Forest – Kilburn Hill. Figure 4.12 shows (a) levelling of the surfacing and (b) surveying of the layer thickness during construction works.

Table 4.1 shows the results of moisture content determinations for the granular material of all five sites during their construction. Due to the “wedge” construction described above, thicknesses of 0.10m, 0.15m and 0.20m were expected to be achieved at the measuring points in each reference section thus allowing rutting behaviour to be assessed as a function of the overlay thickness. The resulting thickness of the reference sections are registered in Table 4.2. The measurements of thicknesses were calculated from the difference between the cross section measurement prior to overlay construction and the one taken at the first subsequent monitoring month, at 2m and 4m in the transverse distance. It must be noted that the differences between the desired and measured thicknesses are considerably higher than intended in some reference sections.

---



Figure 4.12 – (a) Reference section construction at Castle O'er. (b) Layer thickness monitoring during construction

Table 4.1 – Moisture content in Reference Sections during construction

Reference Site	Moisture Content
Castle O'er SR1	4.9%
Castle O'er SR3	4.7%
Till Hill Main Block SR1&2	4.8%
Till Hill Main Block SR3	5.3%
Waterside SR2	3.9%
Linfen SR2	4.2%
Polmaddy SR	5.0%

Table 4.2 – Overlay thickness in Reference Sections

	SR1		SR2		SR3	
	<i>Measured</i>	<i>Targeted</i>	<i>Measured</i>	<i>Targeted</i>	<i>Measured</i>	<i>Targeted</i>
Linfen	0.10	0.10	0.18	0.15	0.19	0.20
Polmaddy	0.13	0.10	0.20	0.15	0.23	0.20
Till Hill*	0.09	0.10	0.29	0.15	0.28	0.20
Waterside	0.20	0.20	0.24	0.15	0.11	0.10
Kilburn Hill*	0.27	0.20	0.24	0.15	0.21	0.10

\* Sites weren't compacted and measurement of thickness took place 1 month after construction



### 4.3. THE ACCELERATED PAVEMENT TRIALS

The accelerated pavement trials took place at inactive Forestry Commission Quarry known as Ringour in Bennan Forest. Ringour is located off the A762 road, 4 miles south of New Galloway and 15 miles north of Castle Douglas in south west Scotland. Most of the stone has been won from the present level and thus the quarry provides plenty of secure space to build the trial facilities.

The site was used to construct specific road sections in a more controlled fashion. A pair of concrete walls (Figure 4.13) was provided to act as a confinement of the pavement edges and to provide a datum from which to monitor rutting under controlled trafficking. The major dimensions are shown below and detailed arrangements are illustrated in Appendix A.

Previous trials results at the Risk quarry in 2002 [Tyrrell 2004b] helped to establish a procedure to study rut development to test a pavement in a single day with only 100 vehicle passes. These trials provided the basis for implementing the test procedures used in this research.

In three trials the author observed that the surface deformation reflected what usually occurs on forest roads in adverse winter conditions when most forest roads fail. These tri-

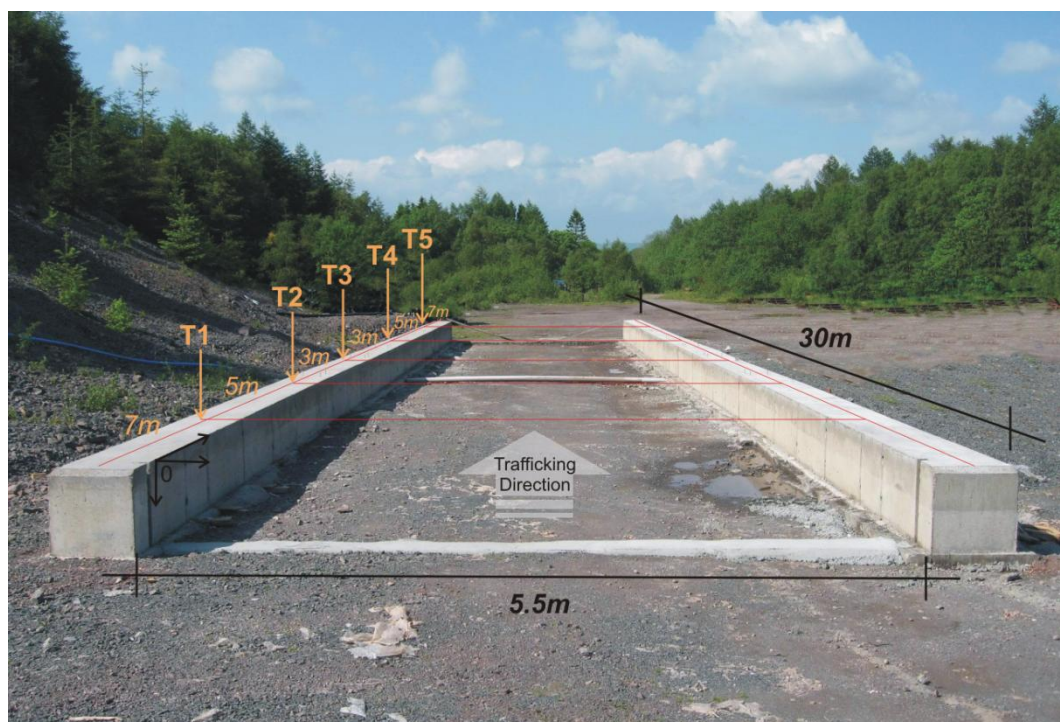


Figure 4.13 – Ringour Testing Facility before construction of the test section with major dimensions indicated and sections chainage

als were undertaken with the pavements thoroughly wetted. The results revealed that the rate of rutting became linear after an initial settlement in the surface.

It became apparent that it was very difficult to prepare the test surface to a consistent degree of compaction. Thus, to compare of the effects of different vehicles, an allowance has to be made for the compaction or strength of pavement. A solution was found during the trials at Ringour, of running two vehicles on the test road at the same time.

The purpose of the pavement trials at Ringour was to measure and study the pavement behaviour of a variety of aggregates under haulage vehicles employed in the forest industry. The academic aim of the study was to advance the understanding of the deformation process on unbound roads. In so doing, the more practical application for the forest industry is achieved by deriving comparisons between timber haulage vehicles, including low ground pressure and tyre pressure control systems recently introduced. The knowledge of pavement behaviour in relation to road aggregates quality and vehicle configuration enhances the forest manager's ability to evaluate road and vehicle options.

The trials aimed to evaluate the performance of aggregate under saturated conditions and the relative pavement deformation caused by the timber haulage vehicles. In particular, different traffic types (axle arrangements, tyre arrangements, tyre inflation pressure) were investigated. The main goal of the programme was to gather sufficient data to determine the principal controls affecting rutting and the sensitivity to changes in the value of the road material type and condition. In an endeavour to investigate the permanent deformation development mechanisms in standard forest roads, instrumentation was placed within the pavement layers to monitor the inner rutting process development throughout two trials. This information assisted in the interpretation of the observed behaviour.

#### **4.3.1. Section Construction**

The construction of the trial section took place in April and May 2007. It consisted of two retaining walls for the test section as well as watering and profile measuring systems.

The test section is 30m long and 5.5m wide contained by 600mm wide and 600mm high concrete retaining walls (Figure 4.13 & Appendix A). The section follows the quarry floor at a fall of 1 in 100. The width was chosen by taking a vehicle width of 2.4m plus two strips 1.5m wide on either side. These margins are amply wide for the lateral restraining effect of the retaining walls not to be significant, as simple mechanist analysis demonstrated nil stresses developing close by due to traffic loading.

---



Figure 4.14 – Barrier at both ends of the walls to contain water

A duct to carry a water MDPE pipe was laid across the section and cast into the bottom of the walls at the midpoint. Ducts were also cast into the walls at heights of 150mm and 450 mm. The lower ducts were to allow water to drain or be retained when plugged. The upper ducts were placed to provide for connections to instrumentation. Slots were cast into the inside of the walls near the ends to house boards to form a barrier to contain water (Figure 4.14).

The test pavement was over 600mm thick. Some 100mm down material was laid on the quarry floor to make up the level for the base (Figure 4.15a). A 300mm base of free draining Type 3 material was laid and compacted in two equal layers (Figure 4.15b). This provides a cushion and mitigates the stiffness of the hard quarry floor on the surfacing. Then two 150mm layers of Type 1 aggregate were laid and compacted over the base layers. Figure 4.16 illustrates the initial and final stages of the test section construction. The material specification is detailed in Section 4.4.3.





Figure 4.15 – (a) Levelling of the floor (b) Compaction works at the top of the base layer



Figure 4.16 – Ringour Testing Facility – view of the test section before and after construction of the test pavement

A standard compaction protocol was followed [Highways Agency 2005] in order to reduce variability in compaction levels among the various trials. The protocol suggests a vibratory roller with 3000kg per metre width of vibrating roll (FC HAMM Roller) and 5 passes whilst compacting 150mm thick layers, meeting the same requirements as the FCE [Tyrrell 2004a]. This was achieved by compacting the section in 3 strips with 5 passes each; an overlap between the strips was eventually required. In addition, the level of compaction was further monitored during construction with a Prima 100 Falling Weight Deflectometer (Figure 4.17).

Between trials, road's surface was prepared by loosening or replacing the aggregate followed by re-grading and compacting the upper layer. It was profiled flush with the top of the walls and levelled across the section, falling longitudinally.



Figure 4.17 – Mini-FWD Test Equipment

In order to promote the soaking of the road surface, a watering system was mounted on the concrete rails on both sides of the section. The watering system was fed by gravity with a tank (Figure 4.18a) positioned on top of the nearby slope above giving a minimum head of 10m. The tank was 5.0m long x 2.5m wide x 1.2m deep giving a capacity of 15,000 litres at a filling depth of approximately 1m. Water was pumped from a holding pond (Figure 4.18b) into the storage tank and then fed by gravity to the road through 150m of 50mm diameter piping leading to a sprinkler system.



Figure 4.18 – (a) Water tank 10m above ground level (b) Pond for water supply





Figure 4.19 – Water sprinkling system during trial

The sprinkler system at each side of the road consisted of two 25m long lengths of 22mm diameter copper pipe with 1mm diameter holes at 100mm centres. The system provided a flow of one litre per second and needed filling only once for each test. It provided a strong flow capable of spraying at least two thirds the way across the test surface. The spray (Figure 4.19) was controlled and adjusted by two valves on each copper pipe allowing the whole road to be evenly dowsed. The road surface could be kept fully wetted before and during testing.

#### 4.3.2. Vehicles

A variety of conventional and unconventional vehicle types were used to traffic the trial sections. Most of the vehicles were loaded to their operational limit with timber logs, apart from the Forestry Commission's Multi-Lift (ML) used throughout the trials as the reference vehicle that was loaded with concrete blocks, for consistent load reference purposes. The total gross weights and axle/tyre configuration of the vehicles employed are summarized in Figure 4.20.

The most common vehicles used were an articulated truck and trailer (Articulated DAF), the trailer being fitted with super-single tyres (see Figure 4.21), and the FC rigid body vehicle (ML) with twin tyres (see Figure 4.22). The FC vehicle is pictured in Figure 4.23.

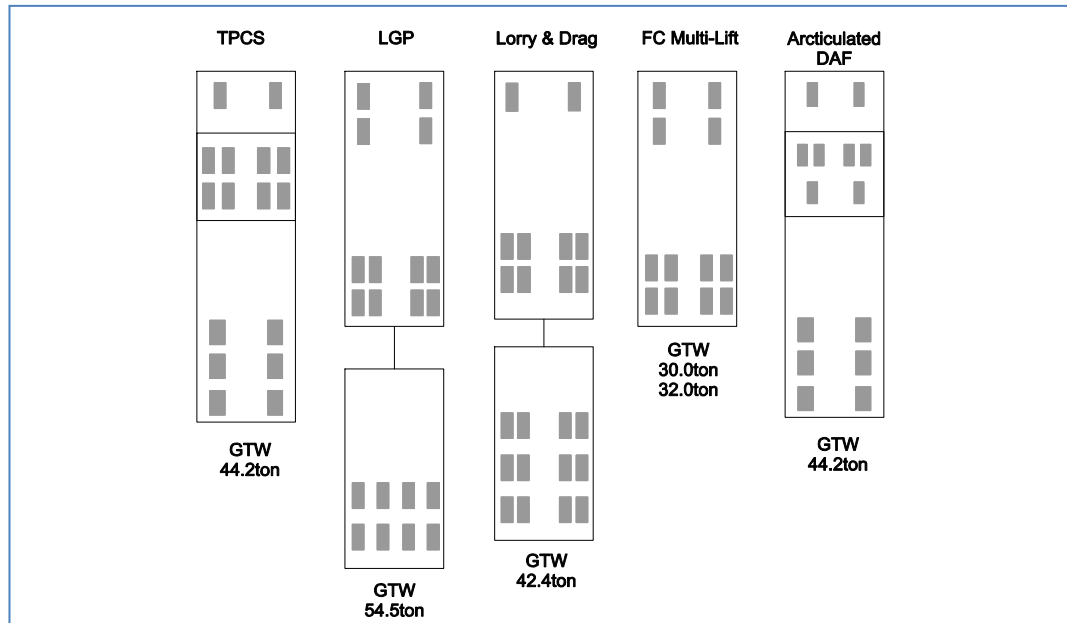


Figure 4.20 – Tyre and axle arrangements for the vehicles used in the trial

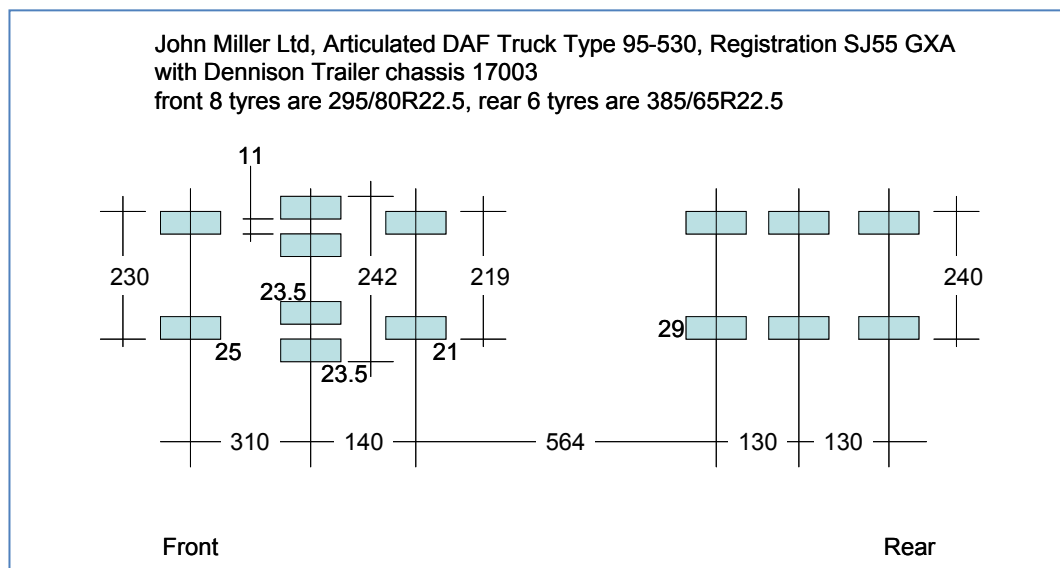


Figure 4.21 – Tyre arrangements for articulated truck (dimensions in cm)

The dimensions of all the vehicles used are given in Appendix B, together with their tyre pressures. During the investigation of performance of the pavement sections it was discovered that some of the tyres were not inflated to their correct pressures. In the later trials these were, therefore, adjusted as much as possible to their desired values.

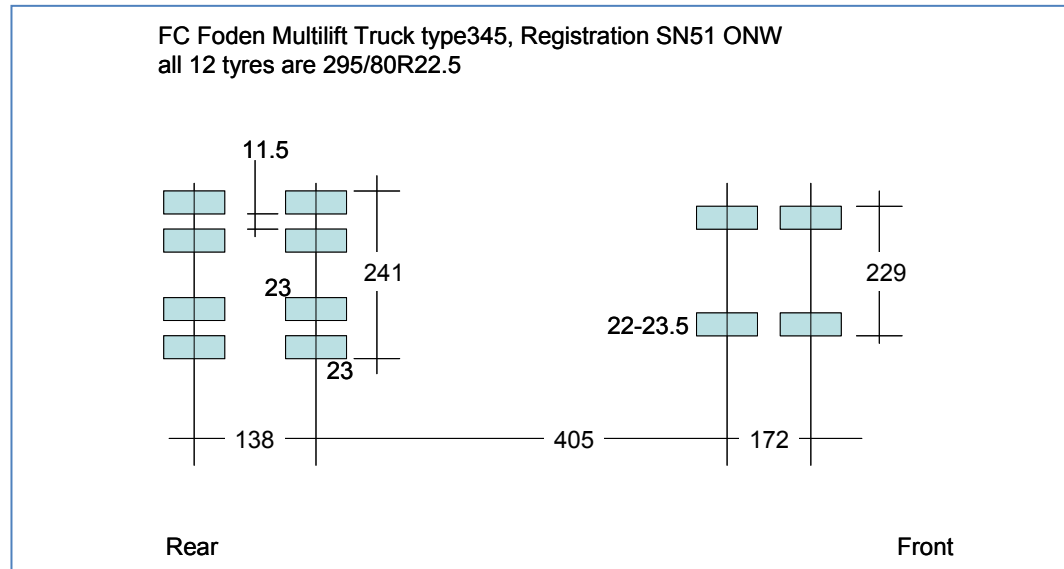


Figure 4.22 – Tyre arrangements for fixed wheelbase “Multi-Lift” truck (dimensions in cm)

Low Ground Pressure (LGP) vehicle (see Figure 4.24) was also used, as presented in Section 3.5.1. Although this vehicle has the same number of wheels as a twin-tyred lorry, the effect of load spreading caused by the use of two pairs of independently suspended semi-axes and evenly spaced tyres across the chassis allows a more even distribution of load across the pavement, even if the road is cambered.

An alternative means of applying low ground pressure is via the use of low pressure tyres. In modern implementations, these are applied using Tyre Pressure Control Systems (TPCS) from the driver’s cab, as discussed in Section 3.5.2. Figure 4.25 shows a vehicle so fitted.

Table 4.3 shows a summary of the vehicles employed during the trials. Note, especially, the use of low tyre pressure vehicles (Trials 7 & 8), a vehicle with wheels spaced equally along the axle (Trial 5) and vehicles with “super-single” tyres (single tyres nominally 385mm wide as opposed to a pair of tyres each nominally 295mm wide).

On the basis of the axle loadings of each vehicle, the equivalent damaging potential of each vehicle was estimated according to the familiar “4<sup>th</sup> Power Law” and the number of ESALs (Equivalent Standard Axle Loads) per vehicle pass was computed (see Table 4.4). Some estimates of loading were required for some vehicles in order to achieve this. The computation also relies on the assumption that damage increases with the axle loading raised to the 4<sup>th</sup> power. This “law” is known not to apply to the rutting of pavements with no bound course, but the alternative methods are no more reliable, so the 4<sup>th</sup> power computation is used on the basis that it is, at least, familiar [Dawson 2008].





Figure 4.23 – FC Foden “Multi-Lift” truck trafficking a Ringour trial



Figure 4.24 – “Low ground pressure” vehicle trailer with tyres equally spaced across pavement on stub-axes



Figure 4.25 – Loaded test vehicle equipped with TPCS

Table 4.3 – Summary of vehicles used to load Ringour trial pavements

				Vehicle 1	Vehicle 2
	Vehicles	N° of Axles	Tyre Configuration	Mean pressure	Mean pressure
Trial 1	ML	4	Twin Tyres	?	
Trial 2	ML	4	Twin Tyres	?	
Trial 3	Artic	6	Super Singles	114	
Trial 4	Lorry&Drag + ML	6/4	Twin Tyres	121	?
Trial 5	LGP	6	Twin Tyres*	74	
Trial 6	Artic + ML	6/4	Super Single/Twin Ty.	105	113
Trial 7	TPCS	6	Super Single	75	
				100	
				115	
Trial 8	ML	4	Twin Tyres	70	
		4	Twin Tyres	110	
Trial 9	Artic + ML	6/4	Super Single/Twin Ty.	100	100
Trial 10	Artic + ML	6/4	Super Single/Twin Ty.	100	100
Trial 11	ML	4	Twin Tyres	110	

\* = wheels on trailer are spaced equally across the axle, not as discrete pairs at each end  
 + = "followed by". The 2<sup>nd</sup> vehicle trafficked the same pavement but along an offset path

Table 4.4 – Vehicles' Equivalent Standard Axle Load calculation according to 4<sup>th</sup> Power Law

Vehicle	Trial	GTW (kN)	Axles load (kN)						ESAL
			Front				Rear		
FC Fodem - Multi-Lift	# 1,2,4,6,8	300400	62500	62500	87700	87700			3.63
FC Fodem - Multi-Lift	# 9 #11	319900	62500	62500	97450	97450			5.15
J.M. Artic	# 3,6,9,10	442000	60000	95000	65000	74000	74000	74000	4.94
J.M. Lorry & Drag	# 4	424000	75000	95000	95000	53000	53000	53000	5.33
LGP	# 5	545000	80000	80000	105000	105000	87500	87500	10.80
J.J. - TPCS	# 7	442000	60000	95000	65000	74000	74000	74000	4.94

One deficiency of the technique is immediately apparent. The TPCS (low tyre pressure) vehicle is computed to have the same damaging capacity as the same vehicle at higher tyre pressures because damage is assumed to be based solely on axle loading. Clearly this is erroneous as lowering tyre pressures unquestionably reduces pavement damage. However the same set of data also shows a relevant point – the so-called “Low ground pressure” vehicle causes more damage per pass than conventional vehicles. This apparent anomaly is not because the special trailer does not spread the load better than conventional vehicles (it does) but because the truck pulling the trailer imposes significant damage which is greater than the damage saved by using the novel trailer.

#### **4.3.3. Instrumentation**

For the purpose of studying the mechanism of rutting development in forest road structures, the response of the pavement during three trials at Ringour was monitored using instruments installed in the test section. The first instrumented trial, Trial 9 & 10, included five  $\epsilon$ mu strain coils (for measuring displacement) installed, and Trial 11, a total of 16 coils.

The soil strain instrumentation used at Ringour is the  $\epsilon$ mu strain coil system [Janoo *et al.* 1999] from the University of Nottingham.  $\epsilon$ mu strain coils were fabricated and calibrated at Nottingham. The  $\epsilon$ mu strain coil sensors work on the principle of inductance coupling of free-floating wire-wound disks. Sets of  $\epsilon$ mu strain coils are placed vertically above each other to enable vertical displacement to be recorded at varying depths in the pavement and subgrade material.

The placement of the  $\epsilon$ mu coils was a time consuming process as it is important to ensure the coils are in perfect vertical alignment and they are lying perfectly flat. Attention was given to installation depths, so that instruments were placed in the desired position, level and relative position to the wheel track.

For Trial 9 & 10, as the test section had been previously reconstructed, it was necessary to dig holes to place the sets of coils at the desired depths. After the placement of the coils the hole was filled and re-compacted manually. Figure 4.26 shows a coil placed at 150mm depth. Cables were overfilled with a thin layer of sand in order to avoid sharp contact with larger stones, damaging wires.

In Trials 9 & 10, two sets of coils were installed at section T4 - Figure 4.27. Each set was installed in the outer wheel path of both vehicles used in the trial. The depths used were established so as to capture the maximum deformations expected and in accordance to the equipment capability.

---





Figure 4.26 – Installation of a coil in Trial 10

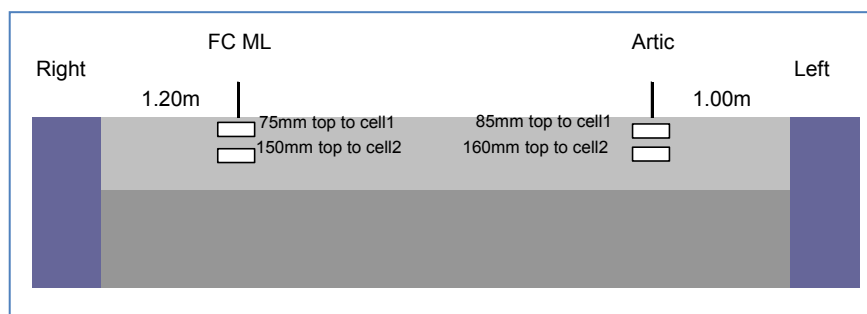


Figure 4.27 – εmu Coils' layout at Trial 9 &amp; 10

In Trial 11, the coils were placed in a different fashion. At the desired depths, the layers were prepared and compacted prior to the coils' installation. Each coil was then placed, pinpointed and levelled aided by a "spirit level" (Figure 4.28). After placing the coil, or a set of coils, wires were manually covered (Figure 4.29). With caution, machinery would then complete the level of the surface and compact the test section thoroughly.

After the trial, all coils were recovered from the test pits and calibrated in the laboratory in order to provide a correlation between voltage (the native output format read on site) and displacement units, allowing, therefore, the determination of the strains generated within the pavement during the trial. The calibration curves used are presented in Figure 4.30.

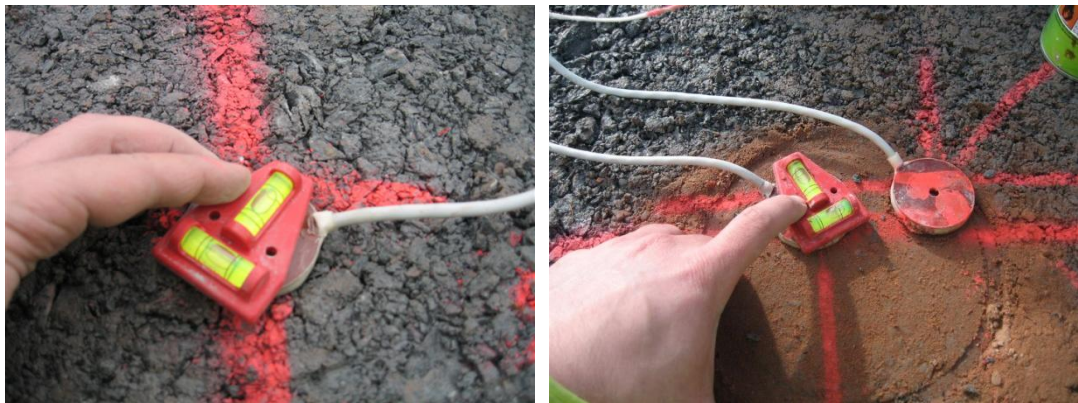
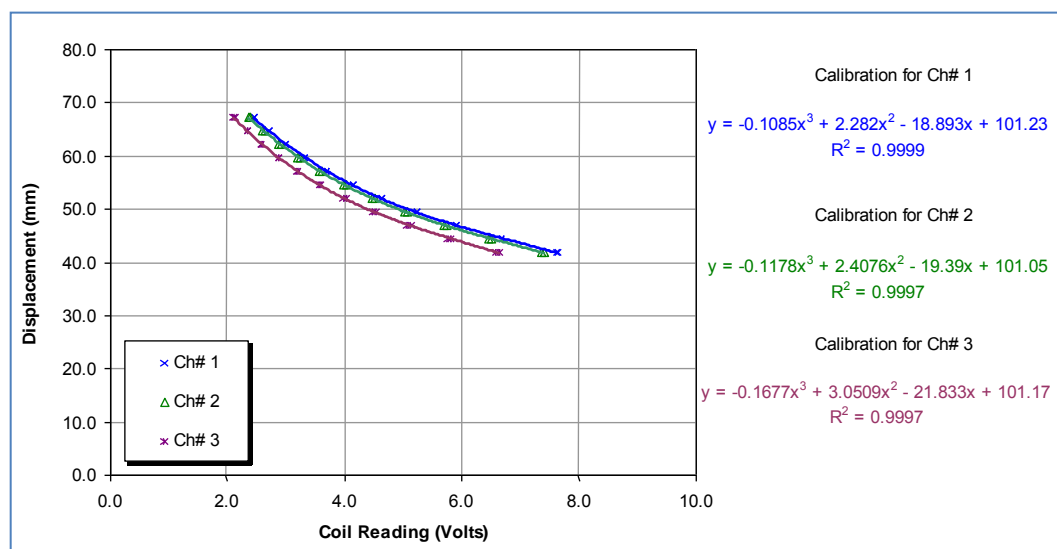


Figure 4.28 – Levelling of the coils aided by a “spirit level”



Figure 4.29 – Installation of the coils in the test section

Figure 4.30 –  $\epsilon$ mu coils calibration curve

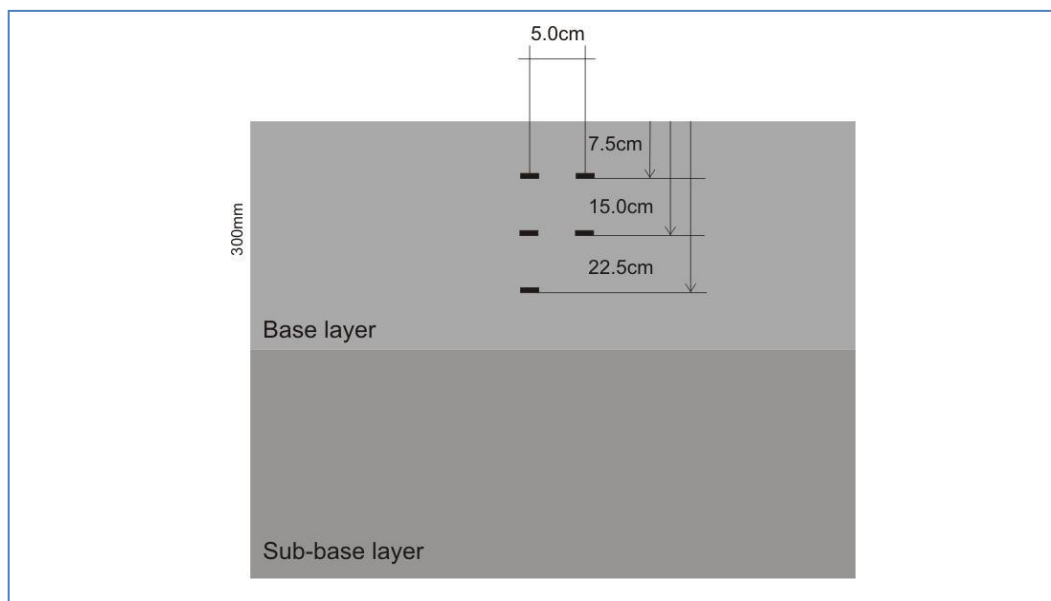


Figure 4.31 –  $\epsilon\mu$  coils' layout at Trial 11

For this last trial, coils were placed in three different locations (see Figure 4.31). One was installed at monitoring section T2 at the right hand side wheel path, and another two, at section T4, one at each wheel path. As only one vehicle was used in this Trial, all readings provided redundant information about the trial. This is particularly important, as instruments tend to stop giving a reasonable reading if moved away from their position during compaction or if wires are broken during installation procedure. Therefore, it is wise to include some redundancy, in order to ascertain that correct data has been collected.

#### 4.4. DESCRIPTION OF THE MATERIALS USED

##### 4.4.1. Monitoring Sites

The monitoring sections materials were the ones existing on site when the project started. Traditionally, the monitored forest roads were characterized by local subgrade, usually non-stabilized with an overlay of granular material from local quarries.

All sites were initially surveyed and the existing material classified, where possible, by a visual inspection carried out accompanied by a local road technician. A detailed inspection brief of all sites along with a descriptive list of the selected sections and materials description can be found elsewhere [Brito & Dawson 2008].

A more thorough characterisation of the monitoring site materials was achieved with the pavement exhumation. During the pit opening, material was sampled for laboratory test

and the Dynamic Cone Penetrometer - DCP, used to correlate with the identifiable layers' CBR. Section 5.1 summarizes the trial pits description and the CBR characterization.

The laboratory tests carried out are later described in Section 4.4.4.

#### 4.4.2. Reference Sections

The grading envelope proposed for the new aggregate used in the reference sections was the one with growing use by FCE/Scotland in their maintenance works, the so-called "Swedish Specification" [FEG 2000], adapted from one in use in Sweden. Figure 4.32 illustrates the grading envelope of the aggregate mix desired - Base course.

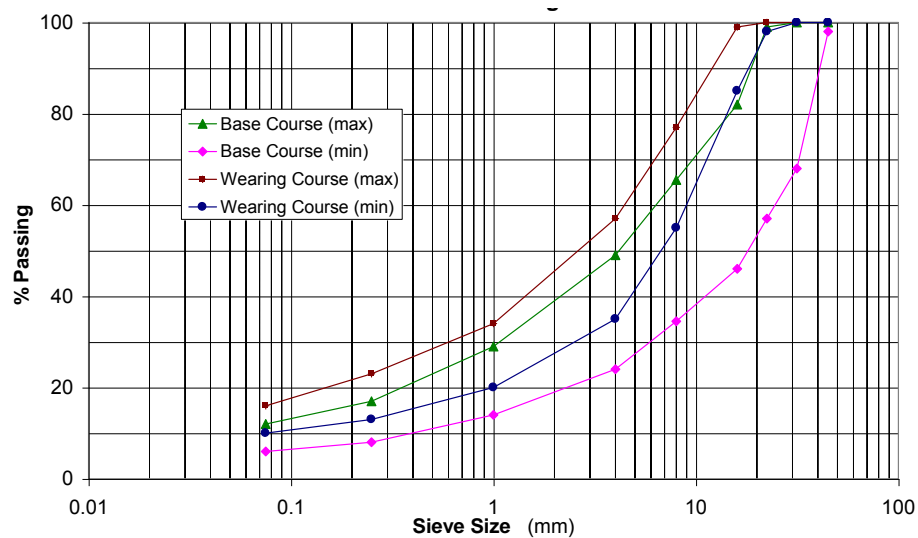


Figure 4.32 – Grading envelope according to "Swedish Specification" [FEG 2000]

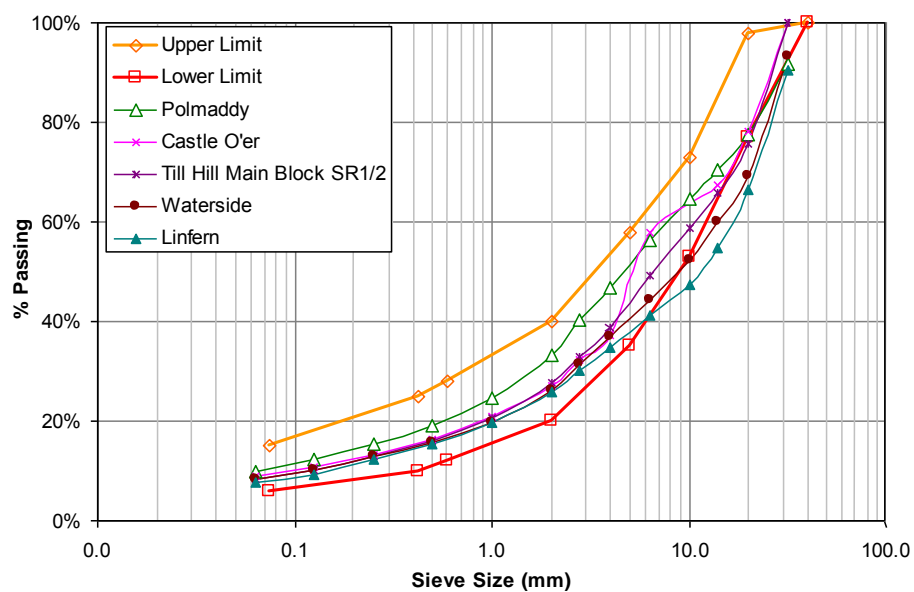


Figure 4.33 – Grading envelope for surfacing material in the reference sections

Figure 4.33 shows the desired grading envelope limits and grading results from samples collected from all five sites during the construction process. Linfern and Waterside had the coarser fractions outside the grading envelope, leading the mixture to be coarser than the specification. All other reference sites' material was inside the proposed specification. The aggregate used in the sections came from the Tarmac Quarry at Morrington.

#### **4.4.3. Accelerated Pavement Trials**

Three different aggregates were used on the test road as surfacing course throughout the eleven trials and one material was used as a base course. All the aggregates came from greywacke sources which is the region rock predominant formation in South Scotland and commonly used to build forest roads. Greywacke is an ancient rock comprising varying amounts of gritstone, siltstone and shale that are heavily folded, faulted and metamorphosed resulting in a high degree of inconsistency being found at a local scale in quarries and more widely across the region. The best quarries are located in deposits where gritstone predominate and there are fewer beds of closely laminated rocks. Gritstones, by themselves, make an excellent roadstone, but the shale inclusions weaken the aggregate considerably. The aggregates weather badly under traffic in five or so years and, as they deteriorate, the fines increasingly attract water to the detriment of pavement strength.

The granular materials used were:

- a) a Type 1 standard material for base and sub-base in road works in the United Kingdom – [Highways Agency 2007] from Morrington Quarry,
- b) a material from FC's Risk Quarry – a lower quality material that has previously demonstrated considerable rutting in previous trials [Tyrrell 2004b],
- c) a Type 1 material from the FC's Craignell Quarry,
- d) a Type 3 [Highways Agency 2007] material from Morrington Quarry.

The first three materials were used in several trials as the surfacing aggregate, whereas the last one was only used beneath the other aggregate layers to provide a cushion and mitigate the effects of the hard quarry floor on the surfacing.

The materials tested for permanent deformation evolution were tested under dry and saturated conditions. The purpose of the water is to weaken the material allowing higher levels of permanent deformation within 100 vehicle passes. The combinations of materials, material condition and trafficking arrangements is shown in Table 4.5.

---



Table 4.5 – Loading and Moisture Condition Matrix of Ringour Trials

VEHICLE TYPE \ MATERIAL	Key	Morrington Type 1		Risk Quarry Material		Craignell FC Type 1	
		Dry	Wet	Dry	Wet	Dry	Wet
FC Foden with twin tyres	ML	#1	#2 #8*		#6	#9	#10 #11
Artic DAF with super singles	Artic		#3		#6	#9	#10
Lorry & drag with super singles	L&D		#4				
LGP Vehicle	LGP		#5				
TPCS Vehicle	TPCS				#7		

# represents the chronological order of the trials

\* Trial with tyre pressures of 70psi and after 110psi

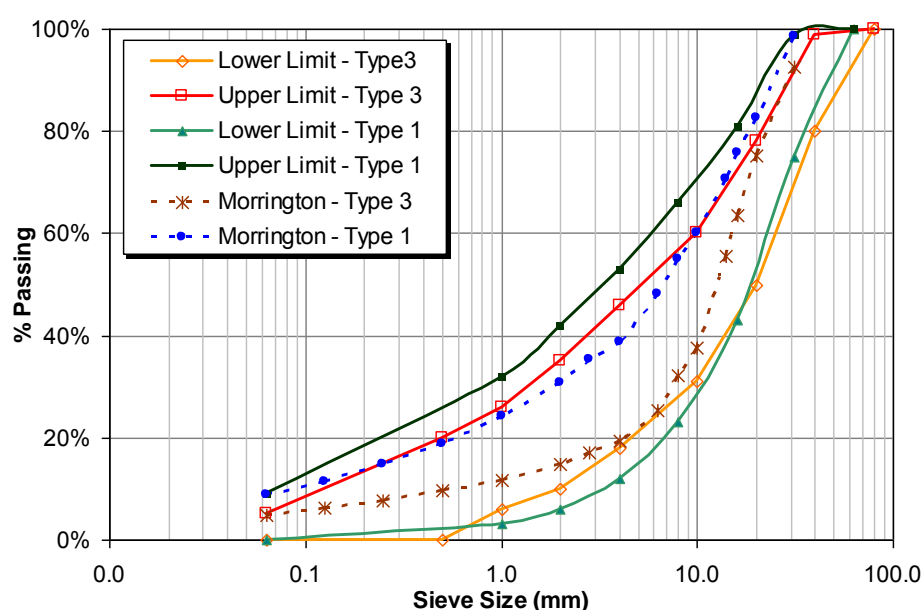


Figure 4.34 – Materials grading for the Ringour test section

Figure 4.34 shows the grading envelope for the range of Morrington Type 1 & the Type 3 materials, along with the gradings of the actual materials used at Ringour. Note that all materials are finer than the upper limit of both the “Type 1” and “Type 3” grading requirements and that the Risk material is too fine to be described as either “Type 3” or “Type 1”. The grading curve for Morrington Type 3 material has almost a bi-linear shape indicating that it is almost single-sized and, potentially, very permeable.

Dynamic Cone Penetrometer (DCP) tests were carried out to assess the material's strength. The data was analysed using the UK DCP software, from TRL, which has the capability of dividing the layers of the tested structure, using a penetration rate classification technique, and can correlate the penetration rate with California Bearing Ration (CBR) following the TRL relationship for a 60° cone (Equation 51 - Section 2.6.5).

#### 4.4.4. Laboratory Tests

Laboratory tests were carried out in order to classify material for the considered representative sites monitored during the project. It was attempted to collect material from sites on which it was possible to collect reliable data, picking sites ranging from low to high traffic and that were fairly scattered in the regions monitored. Table 4.6 show the sites which were material sampled.

All samples were collected during the pavement exhumation at the end of the project period. They were collected on site from the pits and packed for testing at the laboratories at the University of Nottingham. The tests carried out were: Grading, Density and Water Absorption, Ten Percent Fines, California Bearing Ratio, Liquid Limit and Plastic Limit and Plasticity Index.

The tests carried out follow the EN standards and the test procedure as described in detail elsewhere [Head 2006].

Table 4.6 – Collected samples origin for laboratory tests with traffic for the project period

	<b>Total Traffic (ESALs)</b>	<b>Sample Collected</b>
Craignell	509	X
Tallaminnock FD	597	
Dryfehead Complex	1107	
Till Hill (Main Block)	1458	X
Gair	2702	
Kilburn Hill	2844	X
Bidhouse	3304	
Ferter	3419	
Linfem	4223	
Brigton	4326	
Riccarton - Steel Road	4420	X
Polmaddy	5415	
Culreoch	5656	
Risk	5843	
Waterside	8890	X

#### 4.5. DIELECTRIC PROPERTIES MONITORING

The Percostation Technique, developed by the Estonian company Adek Ltd, measures the dielectric value and electrical conductivity of the material being tested. It is derived from earlier equipment from the same company, called Percometer, which was first used to estimate the frost susceptibility of subgrade soils [Saarenketo 1995a] and, later, to measure the water susceptibility of base aggregates [Saarenketo 1995b, Saarenketo & Scullion 1996]. It assists in managing rutting by allowing road owners to estimate when their road materials are too wet to perform adequately.

A Percostation comprises a Percometer capable of processing and data logging the information from up to five dielectric probes installed in an in-service structure, and can be remotely controlled. The output values obtained from the system are: Dielectric value (E), Electrical Conductivity (J) and temperature (T) in all connected probes, plus air temperature in the Percostation cabinet.

Saarenketo [2006] explains the principle of the equipment. The measurement is based on the change in capacitance at the tip of the probe, which is in contact with, and modified by, the ground. The response of the sensor tip/ground interaction to a high frequency signal comprises a magnitude and phase change element. Both can, in principle, be measured, although in the Percometer implementation, only the magnitude (the real part) of the relative dielectric value is measured.

In the Percometer / Percostation equipment, the contact surfaces at the tip of the probe are insulated from one to another with Teflon, forming a capacitor. The specific capacitance of the capacitor is directly dependant on the dielectric value of the surrounding material. When measuring dielectric value, the Percometer uses a measuring frequency of 40-50MHz. When measuring electrical conductivity, the Percometer uses a measuring frequency of 2 kHz. Dielectric measurements with the Percostation are reliable when the conductivity of the measured material is lower than 1000mS/cm.

Saarenketo [Saarenketo] reports on ideas and innovations about monitoring low volume roads. He says that one of the key parameters that have been found to be effective in permanent deformation risk assessment is the dielectric value of unbound road materials. He states that the sensitivity to permanent deformation of unbound materials can be evaluated by taking samples from the base course and then conducting Tube Suction Tests (TST) on these samples.

Figure 4.35 shows the schematic diagram of a Percostation installation, as well as a Percostation probe and system.

---



Figure 4.35 – (a) Schematic diagram of a Percostation Installation [Saarenketo 2006] (b) Percostation Probe (c) Percostation System

Dielectric properties of soils and aggregate materials are affected by a number of soil characteristics including soil water content, dissolved salt content, clay content and mineralogy, and soil temperature. Dawson and Kolisoja [2004] highlight that dielectric assessments (e.g. Tube suction or Percometer methods) measure, in effect, the free water in the aggregate, although this may only be strictly true for deionised water.

Despite the theoretical difficulties in relating dielectric properties of soils and aggregates to mechanical behaviour, several studies have shown a relationship between dielectric behaviour of the granular layers and susceptibility to permanent deformation under repeated loading (see Figure 4.36, for example). The Figure shows that low amounts of plastic deformation accumulate when a material is subjected to repeated pulse loading provided the dielectric value remains below about 8 [Saarenketo 2001].

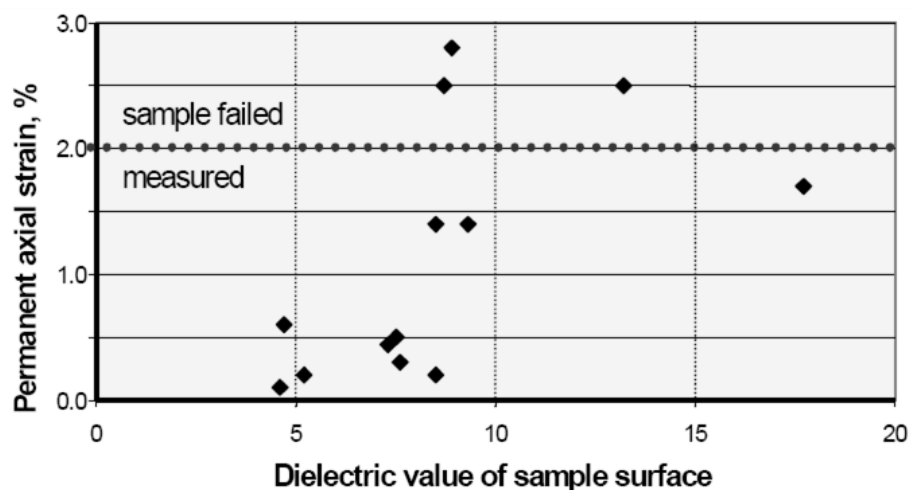


Figure 4.36 – Permanent axial strains of specimens as a function of the dielectric value of the specimen's top surface (measured in TST) [Saarenketo 2001]

The Percostation site's aims are principally to promote a better understanding of the water behaviour in the construction. To achieve this, five probes were inserted at various

depths in the pavement. The equipment has the capability of log all probes on an hourly basis and be remotely downloaded. Initially there were some equipment faults which prevented readings from being collected, but these were overcome and data has been collected remotely via a GSM link for almost a year at the time of writing for one installation and about 9 months for the other.

The sites chosen for the installation of the Percostations were:

- Till Hill – Main Block Entrance at Eskdalemuir Forest, located 4 miles away from Eskdalemuir Town, and
- The public road, the B709, 50m south of the above entrance.

By having both Percostation in proximity, data should be inter-relatable, making it viable to compare the forest road and the public road behaviour in regard to season and weather. The proximity to Eskdalemuir Weather Station and a GSM radio signal reliably available at the site, to permit remote access to the equipment, were also issues in favour of the choice. The second station, with the same specifications as the first, was located on a public road with a structure representative of those in the region.

The installation followed the procedure proposed by the Roadscanners Oy - Finland, who had already successfully installed 9 other Percostation in Europe. The steps followed can be summarized as follows:

- Excavation of a trench of, approximately, 1.2m x 1.2m (l x w) by 1.0m in depth.
- Drilling borehole to desired probe depths and horizontal position.
- Place the probes in the boreholes and re-fill trench.
- Install cabinet, solar panel and Percostation data-logger.

A period of 15 to 30 days was allowed before data collection was started, enabling the probes to establish proper contact with the surrounding material, which was somewhat disturbed by the installation procedure.

The monitoring of the Percostation started effectively in October 2006 for the public site, and January, 2007 for the forest road site (having been delayed due to technical problems with the equipment). Data access is available through modem download and should be made every 30 days. The recording of the data provides the following information: dielectric value, electrical conductivity and temperature for all five probes, plus air temperature inside the equipment cabinet, all at two hours resolution.

---

Figure 4.37 illustrates the installation sequence of the Percostation in the forest road entrance at Till Hill main block. The structural cross sections for both the public and forest roads are schematically represented in Figure 4.38, with probe depths in scale with the layers thicknesses.



Figure 4.37 – Percostation installation at Till Hill Main Block entrance – off B709 Eskdalemuir/Scotland

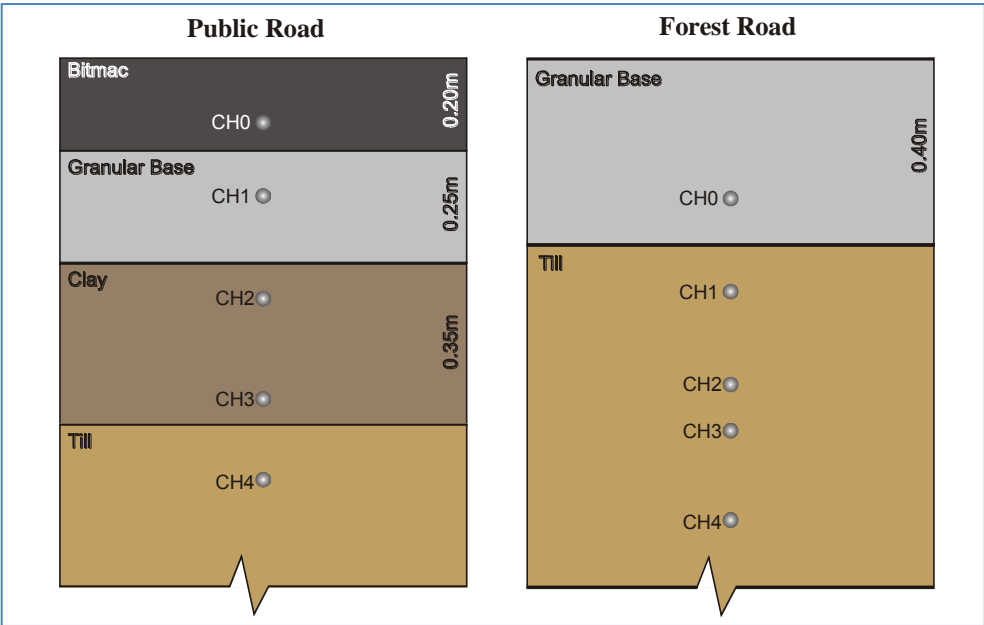


Figure 4.38 – Public and Forest Road structure layout and Percostation probes arrangement

Table 4.7 – Percostations' probes depths and identification

Channel #	Public Road		Forest Road	
	Probe N°	Depth (m)	Probe N°	Depth (m)
0	10	0.15	11	0.30
1	110	0.30	111	0.50
2	210	0.50	211	0.70
3	310	0.75	311	0.80
4	410	0.90	411	1.00

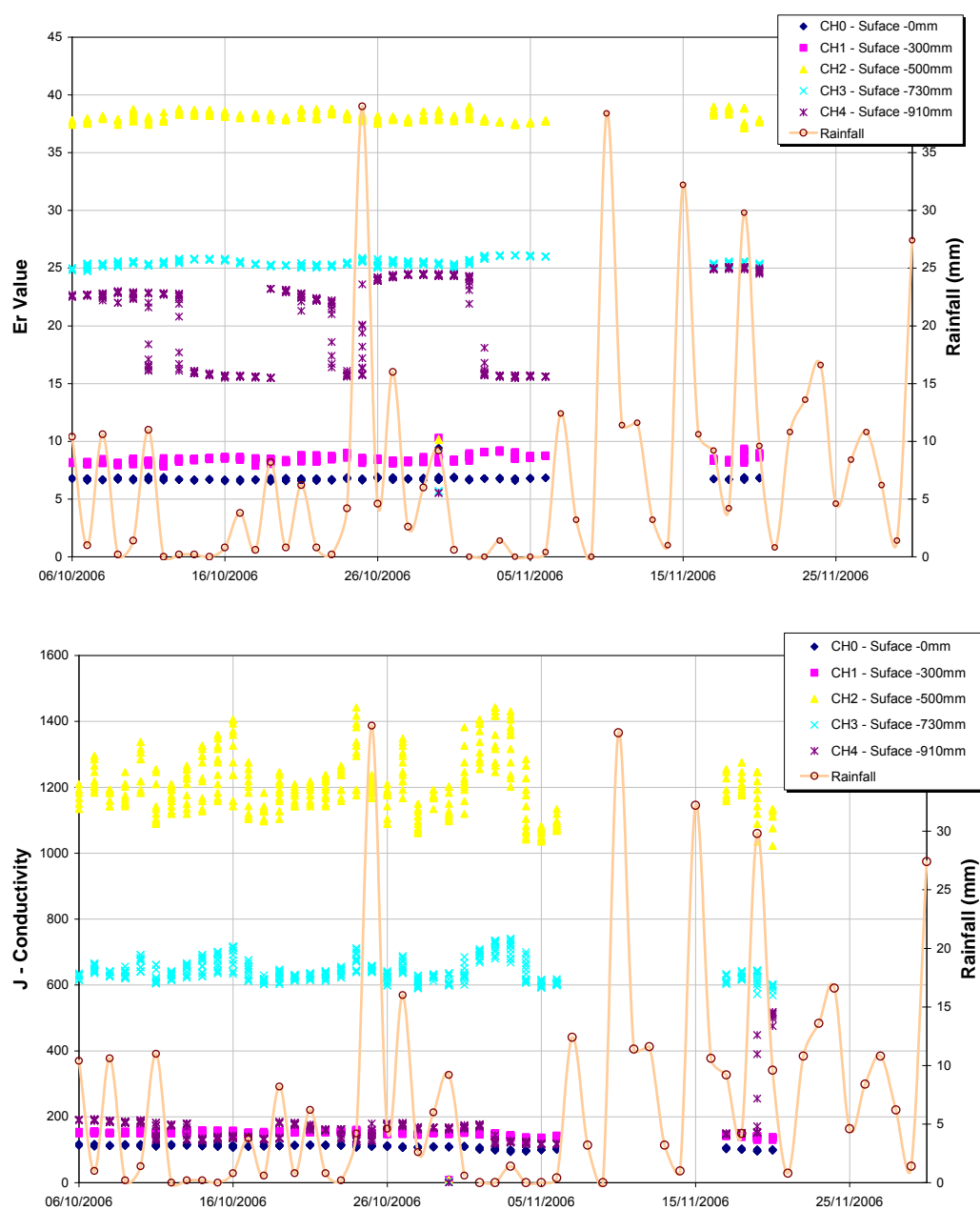


Figure 4.39 – Examples of Percostation readings, soon after installation, for the public road B709 – Eskdalemuir

Probe identification codes and depths are recorded in Table 4.7. Figure 4.39 shows examples of the Percostation's readings for Dielectric Value ( $E_r$ ) and Electric Conductivity (J) for the Public Road from 6<sup>th</sup> October 2006 to 30<sup>th</sup> November 2006. Full details and results for the whole period of the project can be found elsewhere [Saarenketo 2008].

#### 4.6. COMPUTING RUTTING IN FOREST ROADS

Several methods and algorithms for determining permanent deformation in road cross sections have already been developed by various researchers. Most of them, however, have focused on sealed roads and with little variation in the wheel path location. This is mostly due to the trafficking system in roads which usually have single direction traffic and, usually, well defined boundaries of the carriageways. Additionally, the camber in most public roads tends not to be very prominent. This lack of camber can lead to a radical change in the way a vehicle "feels" the rut, compared to the response on a well cambered, unsealed pavement as typically found in the forest environment.

The study carried out by the SHRP program in the United States, for its Long Term Pavement Performance studies, reported in Simpson [2001] as "*Characterization of Transverse Profiles*", shows some of the methods used to determine permanent deformation in roads including the use of laser 'rut-bars'. Nowadays most systems for measuring the profiles of pavements with sealed surfaces are inertial profilers with 3 or 5 lasers sensors mounted on a bar attached to the chassis of a high speed vehicle. The key findings of this study are summarized below:

- The transverse location of the laser rut-bar dramatically affects the measurements and, hence, the rut depth computation. Thus, consistent lateral placement of the survey vehicle is essential to obtain repeatable rut depth measurements using the three- or five-point rut-bar, laser-based, procedure.
- The three rut measurement systems employed (wire line<sup>4</sup>, three point laser, and five point laser) do not provide the same rut depth values. In other words, the two laser rut-bar measurement systems did not necessarily provide a measurement of the rut depth that is similar to the true total amount of rutting as measured by the wire line method.
- Although the rut depths obtained from the five-point laser rut-bar measurements are more highly correlated with the wire line rut depths, they consistently underestimate the mean wire line rut depth.

---

<sup>4</sup> described on the following pages - Figure 4.43

---



- Due to the highly variable measurement of rut depth using the three- or five-point method, consistent year-to-year measurements may be difficult to achieve.

The system used to monitor the permanent deformation in this study, a profiling beam with measurements at 0.1m, provided the data for the rut depth calculations. Several methods for determining the rut depth were assessed. Because the type of data available for the calculations were an actual profile of the cross section as opposed to 3 or 5 dip readings usually measured in rut-bars, the three- or five-point algorithms were disregarded, as they usually yield poorer interpretations. Hence, the methods considered to be employed were:

- Vertical Surface Deformation (VSD)
- Rut depth according to ASTM E1703-05 [2005]
- Rut depth according to AASHTO PP38-00 [2000]
- Wire line model

The VSD is the difference between the current cross section level and the start reference level of the pavement. The VSD is considered better for describing surface deformation than the rut depth measured with the straight edge as the latter measurements are influenced by shoving at the edges of the wheel paths [Arnold 2004]. However, rut-depth (depth to bottom of the wheel track trough from a straight line joining the peak of the shoulders of ruts) will usually be a better indicator of serviceability to the user. A comparison between the VSD and a standard rut depth measurement is presented in Figure 4.40.

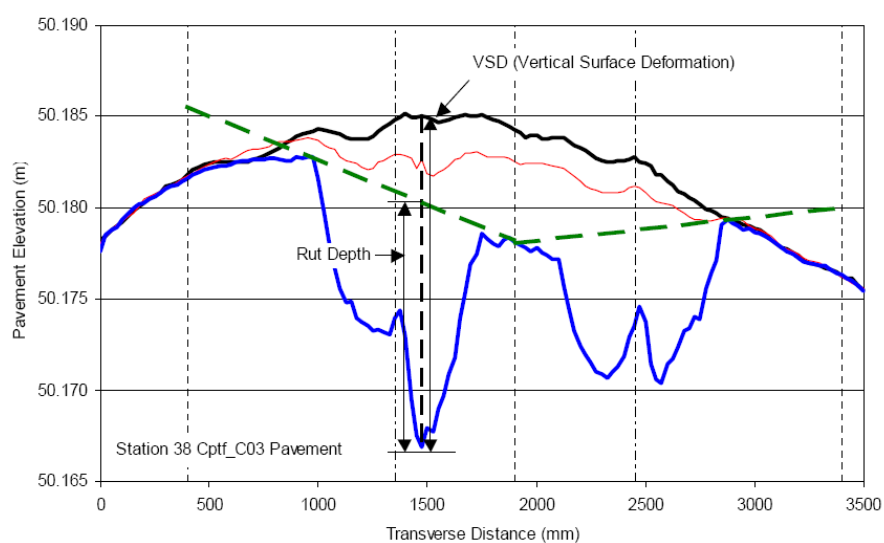


Figure 4.40 – Rut depth and Vertical Surface Deformation (VSD) measurements systematic [Arnold 2004]

Rut depth is usually determined using a straight edge across the pavement and it considers the upward shoving at the edges of the wheel path. The ASTM standard E1703-05 [2005] basically proposes that the straight edge placed in a plane perpendicular to traffic flow should provide the datum to a gauge that must measure the distance between the bottom of the straight edge and the deepest point in the wheel path in a fashion such that the gauge remains perpendicular to the straight edge. This yields a non-vertical measurement if the rut shoulders are not at the same height – a common situation where the road has a pronounced crown, camber or longitudinal gradient. Figure 4.41 illustrates the method proposed by the standard.

The so-called “wire line model” is a simplified algorithm that suggests that a straight line should connect the highest point of both road shoulders and, at the deepest point of each wheel path, the rut depth should be the vertical distance between that point and the line. The protocol proposed by the AASHTO PP38-00 [2000] suggests that the rut depth should be the difference between the lowest point in the wheel path and the mean vertical distance to the near shoulder and centre crown. Figure 4.42 illustrates the proposed method.

It must be observed that all these methods were originally proposed to measure the permanent deformation in sealed roads. They may work effectively when applied to thick layered systems with high stiffness mixtures of which the surface is usually constructed with only a small camber, but this is not the case on forest roads where the surface should be cambered with 5% falls from the crown, or with a 5% crossfall sloping inwards on steep side slopes and where longitudinal gradients are preferred to prevent the formation of potholes due to water ponding.

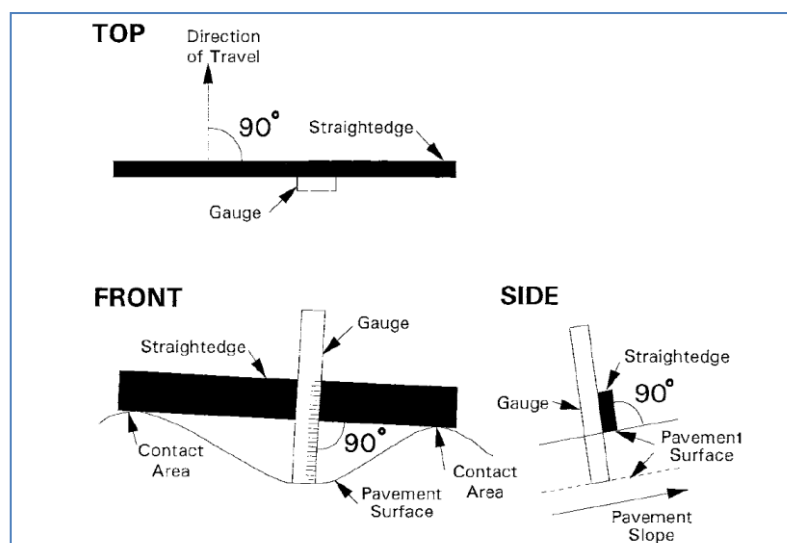


Figure 4.41 – Measuring rut-depth of pavement surfaces using a straight edge according to ASTM E1703-05 [2005]

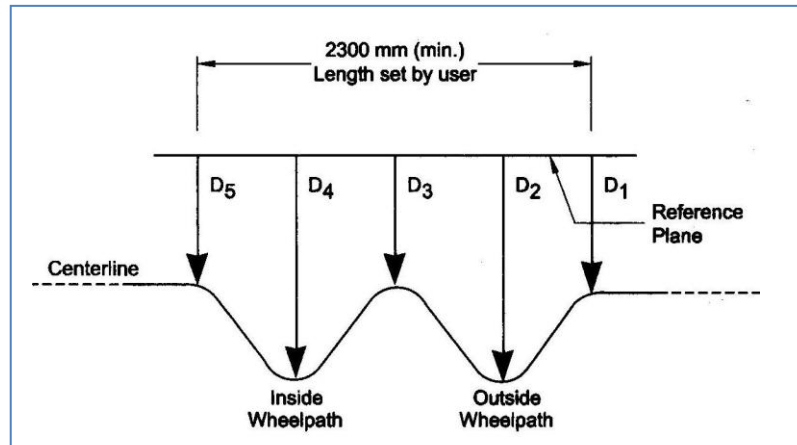


Figure 4.42 – Determining maximum rut depth in an asphalt pavement according to AASHTO PP38-00 [2000]

Figure 4.43 illustrates some of the issues that occur if the different methods are applied to a typical forest road profile. It is obvious that the wire line model (b) is the least applicable method, provided that it disregards completely the camber of the road, yielding the least rut depth of the three methods. Comparing the methodologies proposed by the ASTM E1703-05 [2005] and by the AASHTO PP38-00 [2000], it seems that the latter will provide better results, based on the fact that the former tends to vary more according to the shape of the rut. However, depending on the “sitting” of the axle on the road, the vehicles will experience the rut depth differently.

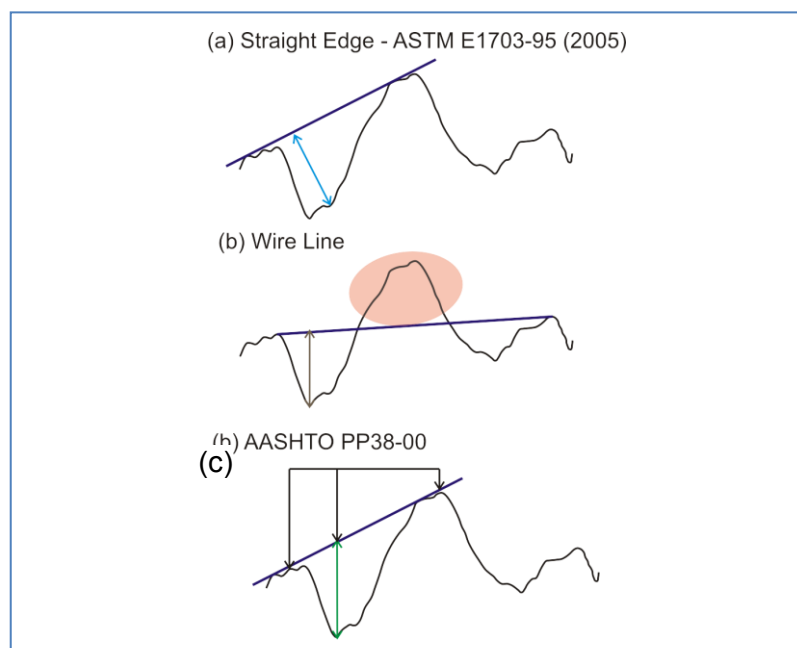


Figure 4.43 – Comparison among three different methods to determine rut depth plotted on the December 2006 profile of the Risk Site.

Figure 4.44 gives an example of a tyre sitting on an actual forest road profile; (a) shows the sitting of a standard twin-tyred axle with an un-deformed vertical scale (b) the sitting of standard twin-tyred axle with the vertical scale exaggerated and, finally (c) a low ground pressure vehicle with the vertical scale also exaggerated. Figure 4.45 shows the difference in the sitting for a super single fitted axle and a standard twin tyred axle.

Both pictures show the sensitivity of the sitting in the rut as a function of the type of tyre and axle configuration. From this analysis, it seems that the method proposed by the ASTM E1703-05 [2005] may yield results more representative of what happens in real forest roads.

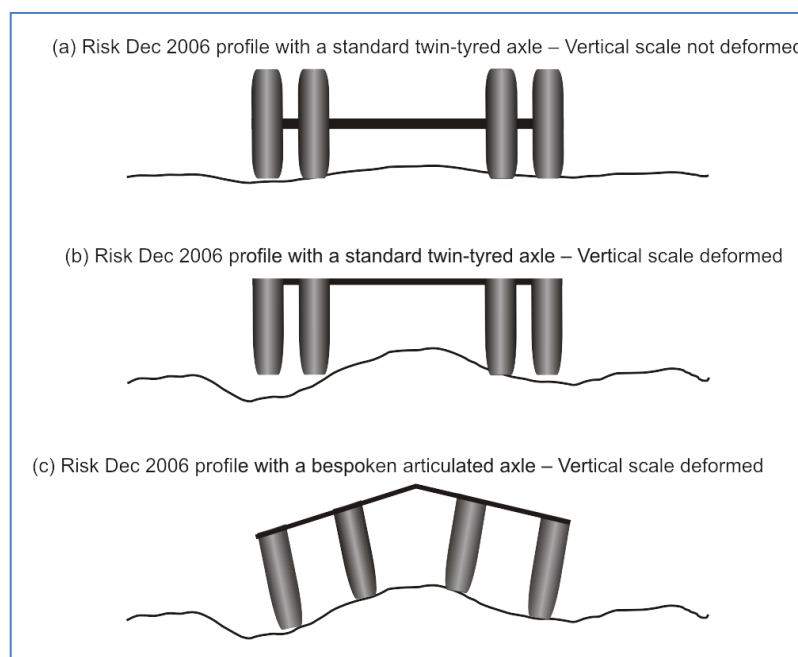


Figure 4.44 – Examples of tyre sitting on the wheel paths

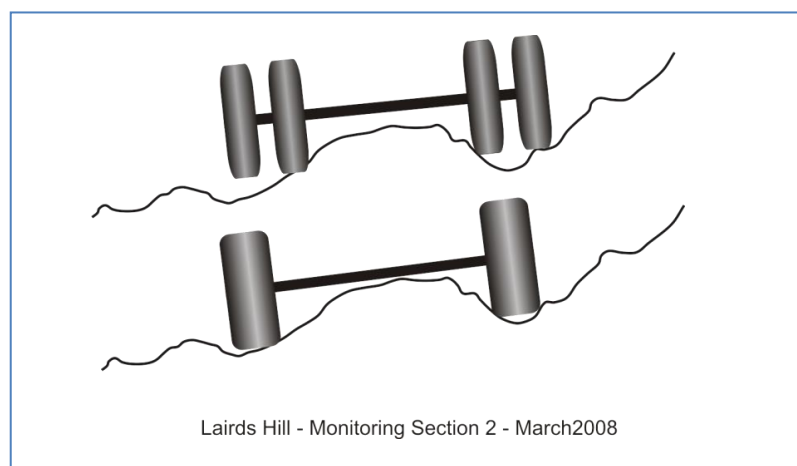


Figure 4.45 – Difference in the sitting on the rut according to the tyre width

The main problem is that all of the previously mentioned methods do not cope well with wandering traffic. The measurements depend either on the first month of monitoring to provide a datum (in the case of the VSD) or on the lowest point in the rut depth (the others discussed methods). In each case, wandering of the traffic is likely to give a false impression of rut depth development. Figure 4.46 shows a typical case encountered during the analysis of the results in the RUTT project. Not only does the lowest point in the wheel path “wander” laterally, but the shape of the rut itself also changes. In this example it is possible to notice that in the right wheel path (RWP) the rut actually reduces at some points between December 2006 and July 2007, which may be contrasted with what happens in the left wheel path, LWP. Possibly this is because of a counter-clockwise movement (shear deformation) from the LWP to the RWP caused by the higher rut in the LWP causing the vehicle to lean sideways and, hence, cause the nearside of the vehicle to have more pressure on the wheels, causing the pressure between tyre and pavement to increase at that point.

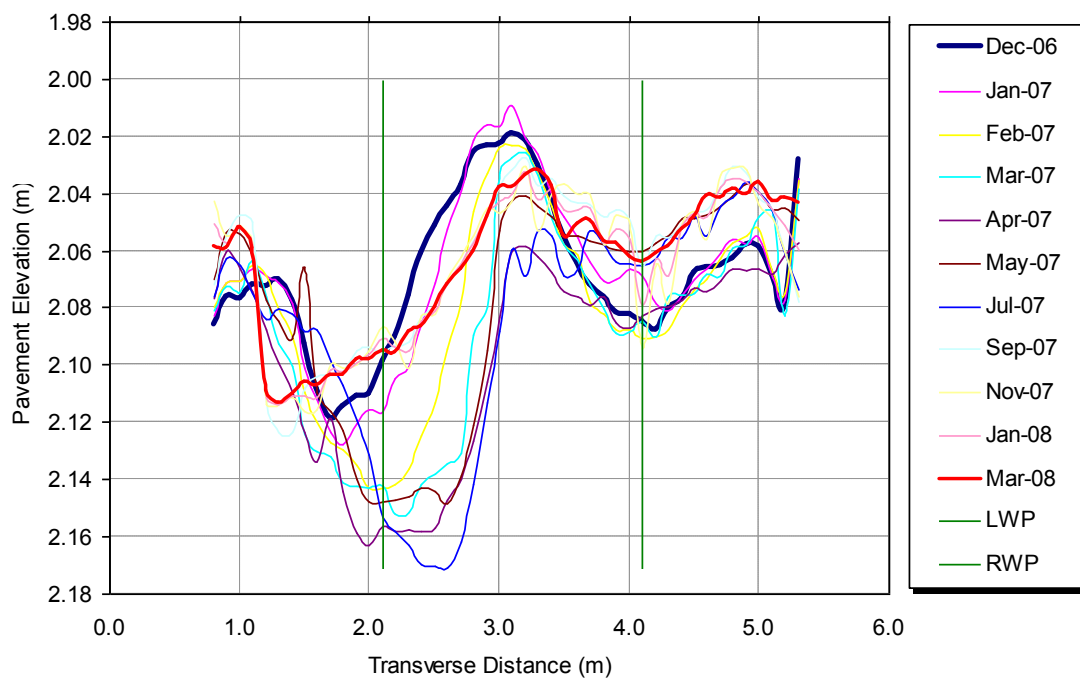


Figure 4.46 – Monthly readings for monitoring Section 1 at Risk site

For the above reasons, a new method for the analysis of the results was eventually suggested. The method relies on the calculation of the area formed between the cross section profile and a datum within each wheel path area – which, for the purposes of this project, was fixed as a zone 0.6m wide. The difference among each month’s area reading and the first month reading gives the increase (or reduction – in some cases) in area of the rut. Figure 4.47 pictures an example of the proposed methodology.

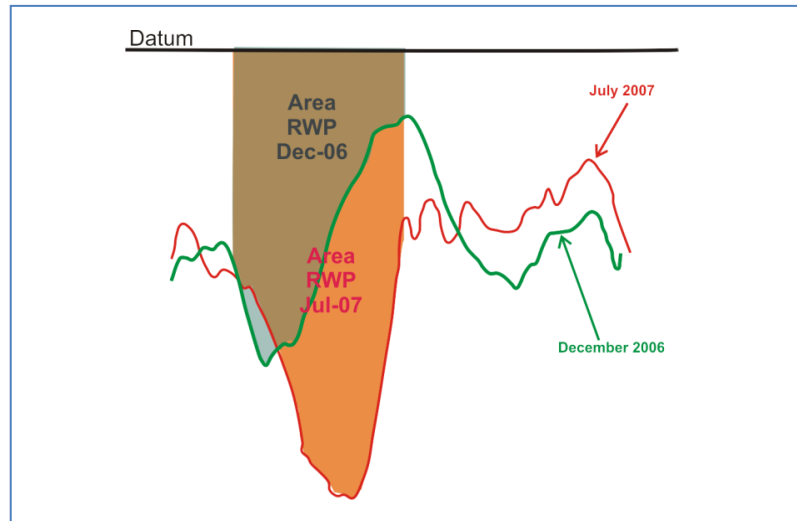


Figure 4.47 – Area measurement of the right wheel path (RWP) for two different months at Risk Site

The area was always calculated centred on the wheel path position ( $\pm 0.3\text{m}$  from the centre of the wheel track centre). This centre was surveyed at the end of the project period for all monitoring sections. In effect, this was a visual assessment of the maximum rut position on the last date on which measurements were collected.

Area was obtained by integrating symbolically a quadratic polynomial that had been fitted through the dip readings in each wheel path. This method was preferred over a numerical approximation of the area because outlier values caused by the movement of individual aggregates particles and/or inaccuracies in the measuring device are smoothed by the mathematical fit. Then, when the area is computed by the calculus technique, it does not contain major inconsistencies as a consequence of those outlier readings.

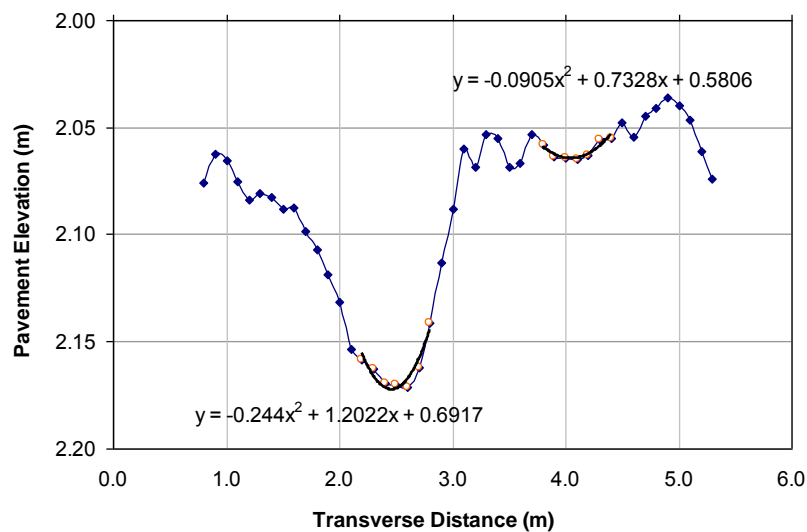


Figure 4.48 – Polynomial fit equation for calculation – Risk, July 2007

Figure 4.48 shows an example of the procedure programmed in Microsoft Excel to perform the proposed algorithm.

From the area calculated it is possible to divide the result by the wheel path width considered (i.e. by 0.6m) and arrive at some kind of “average” rut depth which effectively takes into account the shape of the rut. This value can be more intuitively interpreted and was therefore chosen as the means of presenting, in this thesis, the results of the permanent deformation at the monitoring sites.

The choice of width over which the area was calculated (0.6m) was selected on the basis of the observations of the road profiles in the project. A smaller width considered for the area calculation would not covered the wander of the traffic and could potentially have missed the maximum rut. On the other hand, a greater value would be likely to include some “dead zone” where no movement in the outer edges of the pavement occurred. This would have the effect of reducing the “average rut” reading (see previous paragraph) and would also have made a polynomial fit in the wheel path zone much more difficult. A successful polynomial fit is vital if the readings contain a fairly high amount of variance – as observed in the RUTT project sites. With this polynomial fit calculated through the rut zone, a smoothened surface provided the best reference for the area calculation, minimizing variances in the readings.

#### **4.7. KEY FINDINGS**

This chapter has described the activities performed at the RUTT project and on which the author sourced most of the data for this research. Most of the difficulty was to set up such a comprehensive study project in a short period of time as it started in September 2006 and the first readings were taken in December of the same year. Considering the distance run for data collection and extensive work to be carried out, the project was overall successful.

Due to administrative difficulties, data collection had a delayed start reducing the project time to 19 months, as opposed to 24 months initially conceived. This was a major drawback as the planning period was severely reduced. Hence, many problems that could have being addressed beforehand arose during the course of the project, delaying activities. The alternative of delaying the commencement of work on-site was not available due to the necessity to include the whole of a winter in the monitoring period.

Below some of the key findings for the work discussed in this Chapter are summarised:

---

- 
- From a total of 21 initially chosen sites, 15 sites went through for the whole project with data for traffic (correlated to timber tonnages), weather and permanent deformation, providing a large database for analysis.
  - Inspection and selection of sites could have been improved if anticipated timber tonnage for the project period had been more accurately forecasted, enabling the expensive instruments to be rationalised and, perhaps, dealt thoroughly during the project's period.
  - Traffic counters represented an unsettling problem. Not only in the roads on which a flushed install was difficult to obtain but also in even surfaces and bridge decks, the installed system worked erroneously.
  - It was evidenced that, due to large number of light vehicles using forest roads - user cars and maintenance crew vans - it is important that counters be fitted with classifying mechanisms.
  - It is recommended that, in case another project requires traffic counting on forest roads, these are to be installed on a paved area or over a bridge (although, even with this adjustment, the experience where the counter was installed on a bridge at Eskdalemuir suggests that there may still be problems). In case it has to be installed directly on an unsealed pavement, D tubes must be used, and brackets should be fitted to keep the tubes well attached along the cross the section. The manufacturer of the counter must be contacted to supply a software capable of coping with this type of readings and a trial should be carried out before installing the equipment on a permanent basis. With the limited experience obtained at the end of the study, it seems that some manufacturer's equipment is much more suitable than others.
  - Simple weather stations with tipping buckets provided reliable information and could supply important rainfall data for analysis. An important issue is the installation in open areas for unbiased results. A mechanism for pin pointing the device is also advisable, as its small size may easily put into trouble finding the device for downloading.
  - Those responsible for maintenance of the roads were not informed of the need to stop regarding, reprofiling or overlaying of the monitored sections - although signs placed on every monitoring section requested that any type of maintenance service be reported to the RUTT engineers. This led to many sites losing important information that could have enriched the study.
  - The designed beam provided a reliable tool for permanent deformation monitoring. Using the concrete blocks as benchmarks supplied later datum for correction of water
-



frost inside the cantilever arms yielding to their improper sitting. A correction scheme was established by transferring the measuring plane to the foot of the concrete block.

- The device used to measure permanent deformation needs either to be changed for some faster reading instrument (i.e. with a higher frequency acquisition rate), or more time should be allowed for the readings to be taken – which could lead to problems under severe weather. This will avoid reading mistakes and consequently provide easy-to-use data, without the need to filter errors so often.
- Difficulties were found to obtain the targeted overlay thickness in the reference section. This was partly due to the fairly limited action of the levelling mechanism used (batter rails) and enhanced to the freezing action of the winter time that caused difficulties in evenly distributing the material in form of the desired wedge. Compaction was also an issue to unavailability of equipment what represented a technical hitch for two sites.
- The early Ringour trials may have had an undesirable degree of variability in the testing components, such as moisture content throughout the trial and variability in the vehicles' tyre pressure. This has been, however, addressed in later trials.
- The option of running two vehicles at a time represented advantages in regard to extending the possibility of extra tests and the ability to make direct comparison. The downside of this procedure is that only the outer wheel paths are representative as the inner paths are somewhat overlapped. The proximity to the outer edges may have represented a slight distortion as the testing lane was initially designed to be 1m away from the centre of each wheel path, and this was sized down to around 0.5m by running two vehicles at a time in order to keep a minimum separation of the paths.

In the event that another research study in the same context is carried out in the future, it is suggested that more scattered sites with monitoring areas concentrated on less number of locations be employed. This way works can be concentrated in certain areas, providing more representative information through the use of more cross section readings, surface inventory, roughness surveying, water table, pavement foundation, maintenance works, among others. Of course, it would be necessary to be more certain than in the present study that these, more limited, number of sections were to be adequately trafficked and would not be interfered by maintenance crews. Without this control and knowledge, the more extensive, albeit less carefully studied, range of monitoring sites was a sensible choice as it allowed for loss of individual sections without the study being completely curtailed.

---

## 5. FULL SCALE TRIALS RESULTS

In this chapter, all the results concerning the full scale trials from the RUTT project are summarized.

### 5.1. MONITORING TRIAL SECTIONS

#### 5.1.1. Weather data

The data collected during the project is summarized in graphs for each site containing maximum & minimum air temperature and rainfall. For each site with a weather station graphics, as exemplified by Figure 4.5, has been produced (see Appendix C). Below, Figure 5.1 & Figure 5.2 present a quick summary of the rainfall in the two main areas of the project: south-west and south-east Scotland. West Argyle results are not included as only data from January 2007 to April 2007 of the Birdfield site was collected.

Figure 5.3 shows the average result – minus/plus one standard deviation in the error bars – for each of the two study areas in South Scotland.

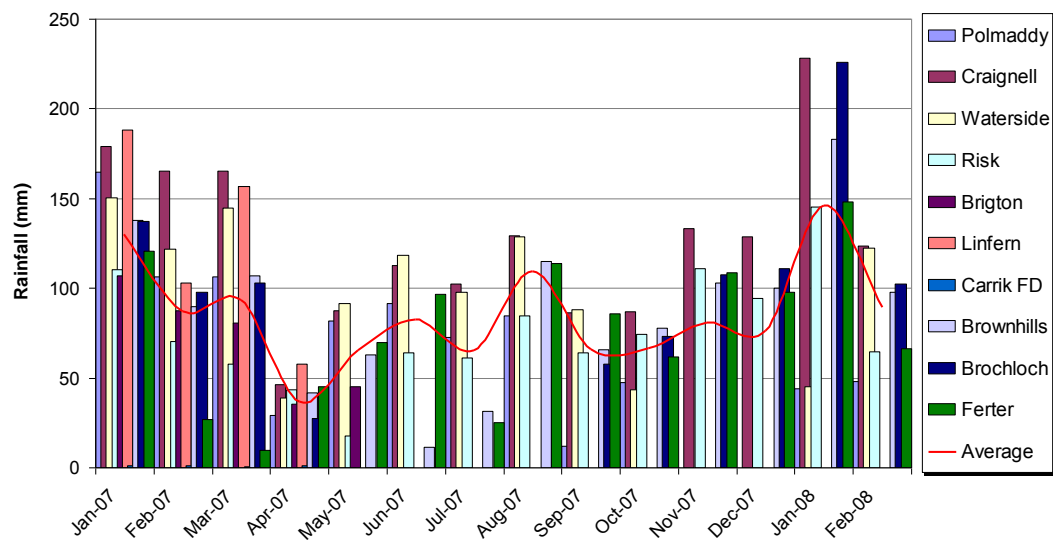


Figure 5.1 – Rainfall summary for the south-western monitoring sites

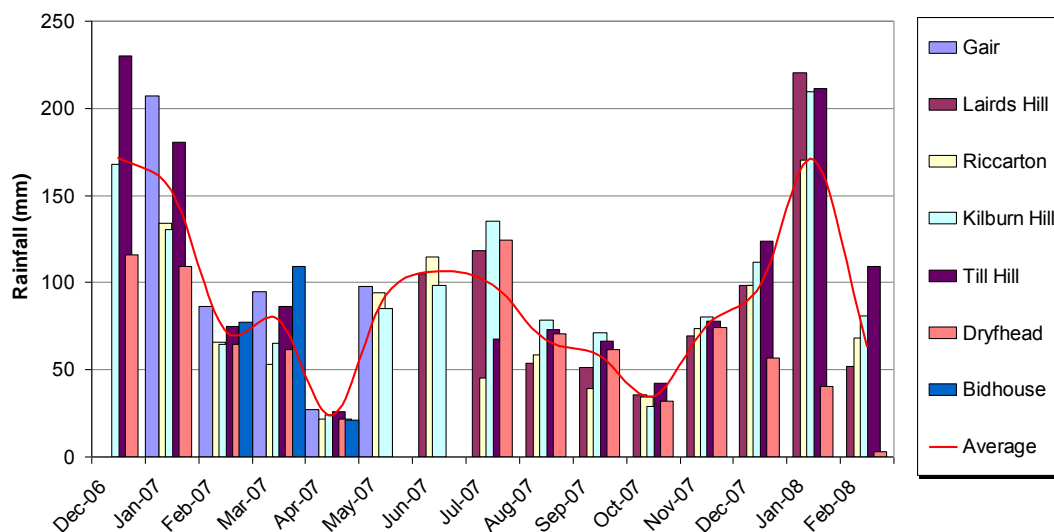


Figure 5.2 – Rainfall summary for the south eastern monitoring sites

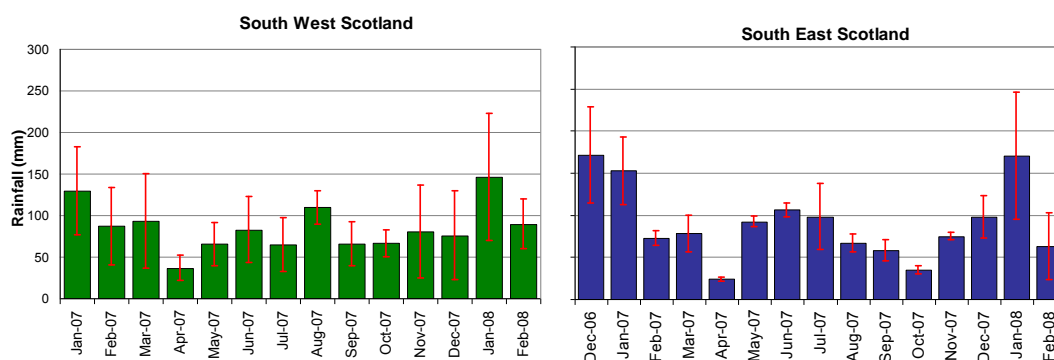


Figure 5.3 – Average rainfall in the monitoring sites in South Scotland

### 5.1.2. Traffic data

As discussed in Section 4.2.2, traffic counters failed to provide reliable data. As this was a key parameter for the analysis, traffic had to be estimated based on timber tonnages provided by the area operating managers. Timber volume was then equated to Equivalent Standard Axle Loads (ESALs), as previously discussed, based on the consideration that all traffic in the monitoring sites could be considered a standard articulated lorry of total gross weight of 44.2 tons. Table 5.1 and Figure 5.4 summarize the results considered for the analysis.

For some of the sites, timber volumes were not available. Therefore, these could not be further analysed in regard to permanent deformation developing rates.

Table 5.1 – Traffic estimated from timber tonnage figures in ESALs

	dez/06	jan/07	fev/07	mar/07	abr/07	mai/07	jun/07	ju/07	ago/07	set/07	out/07	nov/07	dez/07	jan/08	fev/08
Gair	218	511	581	311	403	303	257	114	5	0	0	0	0	0	0
Riccarton - Steel Road	0	0	0	0	0	0	0	0	290	532	476	1129	585	633	776
Kilburn Hill	0	481			926			420			763			254	
Culreoch	233	127	258	222	342	204	435	213		0	1219	698	323	623	758
Polmaddy	348	290	289	545	580	532	705	978		0	89	152	221	320	365
Craignell	85	171	85	163	5	0	0	0		0	0	0	0	0	0
Waterside	85	330	455	670	462	1057	933	1222		0	1754	654	309	623	336
Risk	303	933	437	388	527	345	285	1285		0	1222	79	28	10	0
Brigton	195	326	177	783	810	339	662	1033		0	0	0	0	0	0
Linfen	0	141	310	167	159	9	15	734		0	338	417	446	1096	390
Tallaminnock FD	0	0	0	0	0	0	0	0		0	0	0	0	150	447
Till Hill (Main Block)	0	688			654			14			0			102	
Dryfehead Complex	0	517			210			380			0			0	
Bidhouse	0	473			522			481			918			909	
Ferter	220	245	184	130	0	0	0	0	674	0	712	213	174	516	351

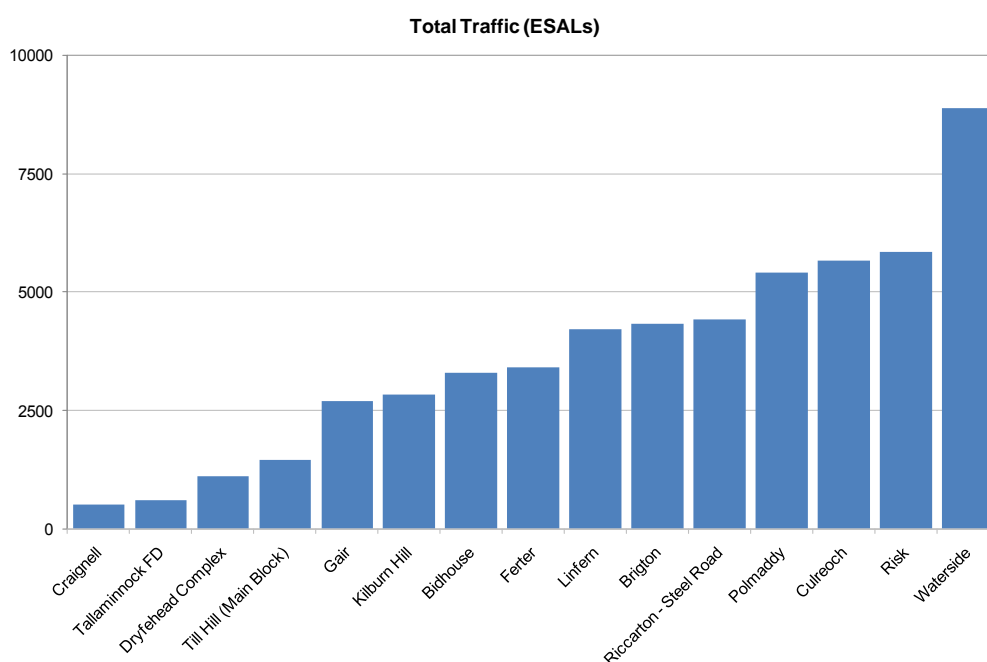


Figure 5.4 – Total Traffic (ESALs) per monitoring site

Although extracted timber volumes have been obtained, for some of the sites the data seem to be somewhat inconsistent with observed rutting on the roads. Next sections will show that, for some monitoring sites which had zero timber volumes declared (and, thus, zero trafficking deduced), there was clear evidence of rutting development, suggesting that yet timber correlation was the only available form of traffic correlation, the results may have some level of distortion.

### 5.1.3. Permanent deformation data

Most of the problems encountered during the permanent deformation data collection were worked around. Difficulties with very limited literature available yielded into a newly developed procedure. For all monitoring sites and reference sections, all collected data was firstly elaborated into a spreadsheet for data verification. The procedure described earlier in Section 4.2.4 corrected most of the anomalies verified and pictures provided an auxiliary mean of checking the results consistency. When data seems to present a flawed result, pictures for that section were browsed allowing for problems detection and correction. Common problems relied mainly in swapped sections within the same site - an error while attributing the filename could easily lead to that. Nonetheless, this was easily worked around as each section and side provided almost a unique reference - making easy the error detection while analysed in pair with the photographs.

After dip measurements were organized and checked, a correction was calculated and offset from the readings, transferring the measuring plane to the foot of the concrete block. From there the procedure detailed in Section 4.6 resulted in the permanent deformation calculation.

Figure 5.5 shows an example of the cross sections readings for the entire period of the project ready for analysis after data filtering. Note the green bars delimiting the wheel path in each section.

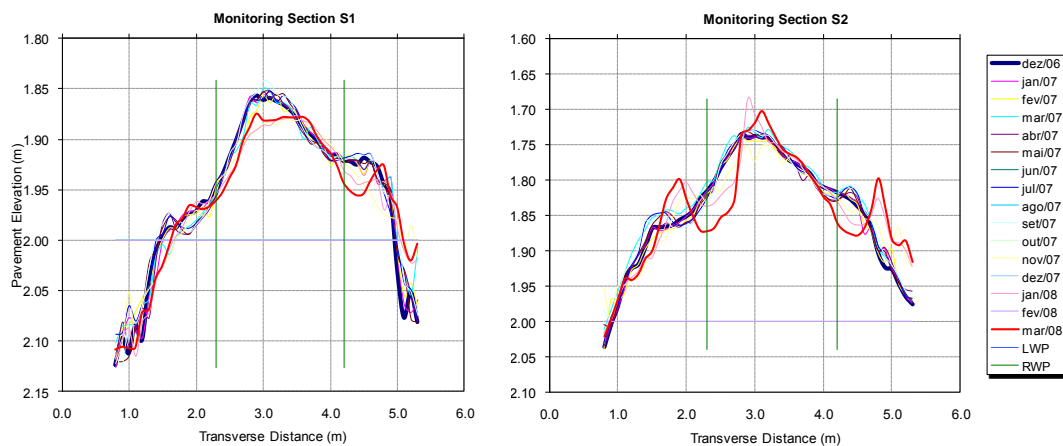


Figure 5.5 – Cross sections reading after data check ready for analysis - Culreoch Site

Figure 5.6 shows both the vertical surface deformation (VSD) and the rut depth measured for each of the monitored sections. Note that VSD features a stable reading, but shows very little sensitivity to the rutting observed in the site. From Figure 5.5 it is noticeable that the deformation occurred. The rut depth reads that more clearly than VSD despite its rather pronounced oscillation.

Figure 5.7 pictures the proposed methodology discussed previously in section 4.2.4, with the rut area plotted for each month and section. A more stable reading with a growing pattern can be observed. The value seems to propose an as stable reading as VSD yet more sensitive, and hence loyal to in-situ readings and not as oscillatory as the rut depth. Accordingly, rut area suggests coping better with wandering traffic in unsurfaced roads.

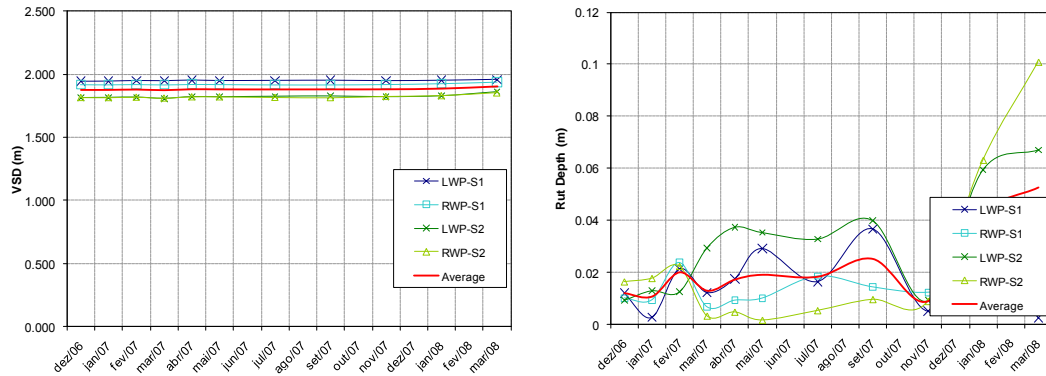


Figure 5.6 – VSD and Rut Depth for each of the monitored sections and its average value  
- Culreoch site

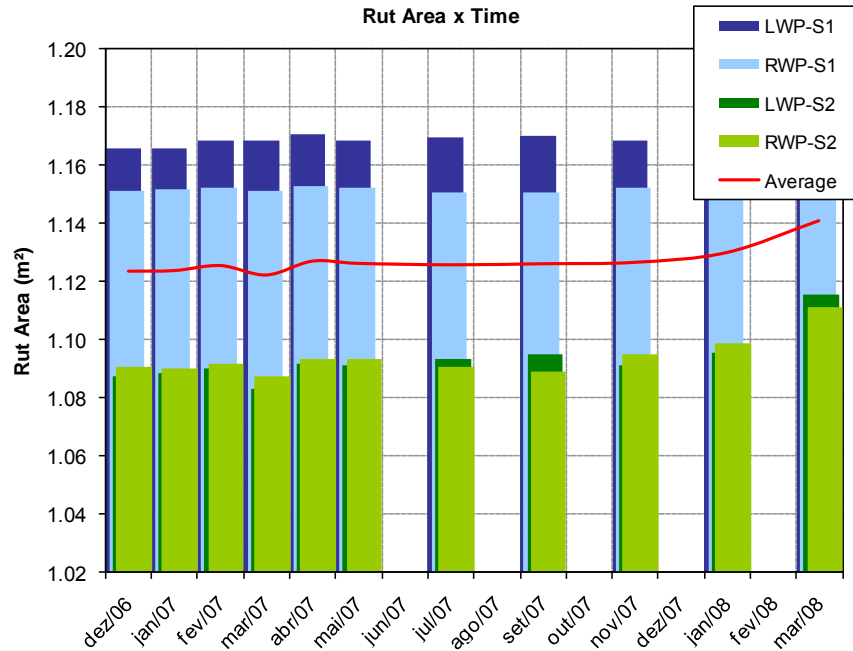


Figure 5.7 – Rut area for the monitored sections - Culreoch site

#### 5.1.3.1. Monitoring Sections

A summary of the results for the permanent deformation measured at the monitoring sites for the whole period of the project is presented in Figure 5.8. Those sites where no information was obtained for timber volume, and hence traffic, were not considered for this analysis. The procedure used to obtain the rutting evolution was:

- i. Calculate the rutting areas for both wheel paths in every cross section, as discussed in Section 4.6. Results are compiled in Appendix D in the format presented in Figure 5.5 to Figure 5.7.
- ii. Divide the calculated rutting area by the wheel path width (0.60m), in order to obtain the average rut depth.
- iii. For those months on which readings were not collected - either traffic or rutting - the previous month value was replicated.
- iv. It was then equated the difference in rutting and traffic on a monthly basis. Should the rutting value of a month be negative, this was neglected and zeroed. These inconsistencies usually happened when a type of maintenance was carried out or, for some reason, vehicles started to deviate largely the current wheel path.
- v. The monthly differential readings were then integrated throughout the project period, allowing the growing rutting behaviour to become evident.
- vi. Timber tonnage was then equated from each site into Equivalent Standard Axle Loads (ESALs).
- vii. Accumulated traffic was then compared to each month with the permanent deformation records obtained in item v.

The total permanent deformation calculated using the described procedure disregards road maintenance change in structure. As it zeroes the rutting when it encounters a negative accumulated deformation (item iv above), a new rutting development is simply stacked into the previous reading, allowing the total traffic in the period to be contrasted to rutting development within the same period. This was necessary mainly due to the lack of information of the road maintenances carried out, what led to a level of variation in the permanent deformation readings.

Figure 5.8 and Table 5.2 present the results obtained.

---

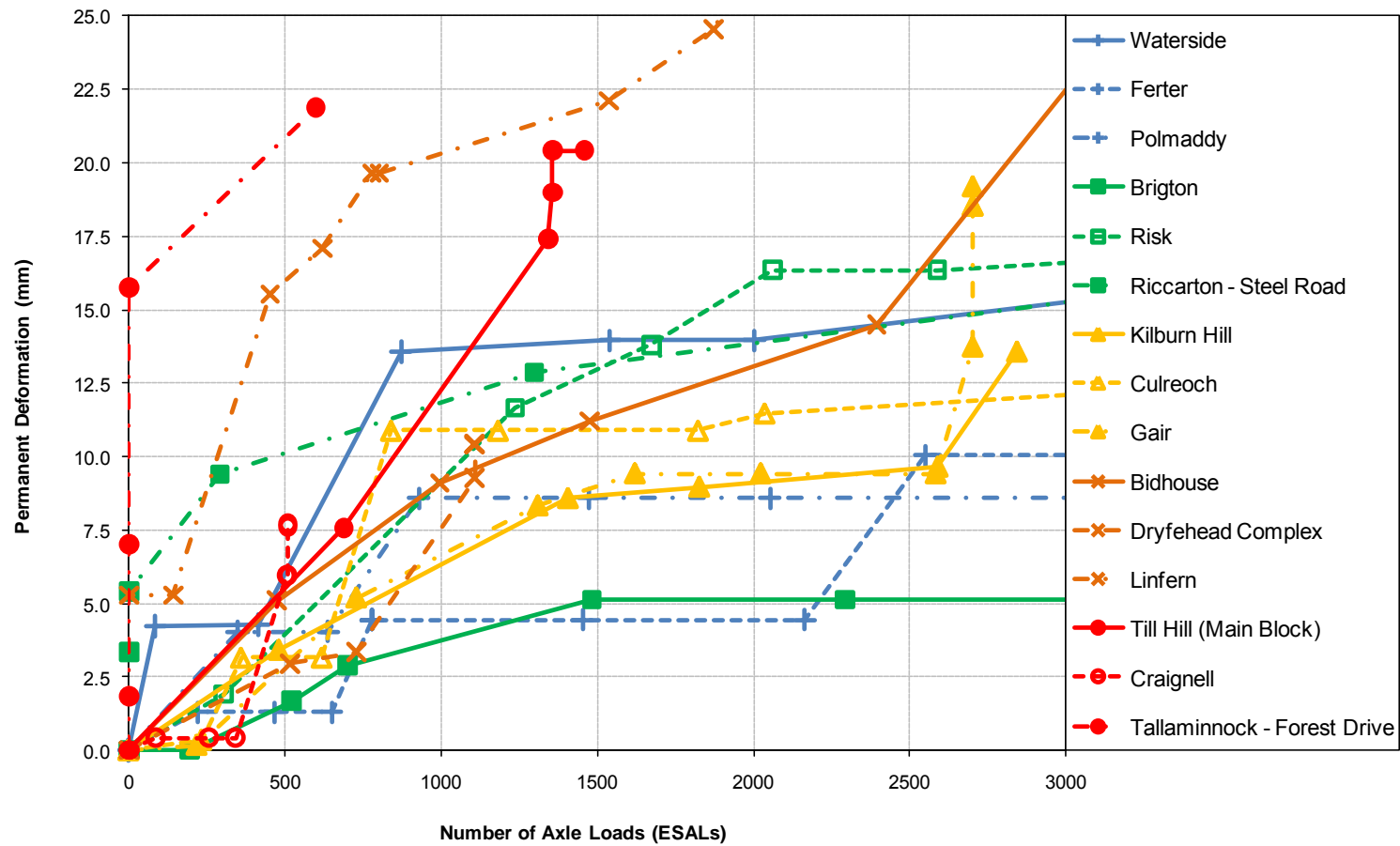


Figure 5.8 – Rutting at the monitored full scale trials - monitoring sites



Table 5.2 - Permanent deformation results for the monitored sites classified in order of increasing rutting rates

	Site name	Permanent Deformation (mm)	Total Traffic (ESALs)	Rutting rate (mm/ESALx10 <sup>3</sup> )
15	WATERSIDE	24	8890	2.7
14	FERTER	10	3419	2.9
13	POLMADDY	17	5415	3.1
12	BRIGTON	15	4326	3.4
11	RISK	20	5843	3.5
10	RICCARTON (Steel Road)	18	4420	4.0
9	KILBURN HILL	14	2844	4.9
8	CULREOCH	36	5656	6.3
7	GAIR	19	2702	7.1
6	BIDHOUSE	26	3304	8.0
5	DRYFHEAD	10	1107	9.4
4	LINFERN	43	4223	10.3
3	TILL HILL (Main Block)	20	1458	14.0
2	CRAIGNELL	8	509	15.2
1	TALLAMINNOCK (Forestr Drive)	22	597	36.6

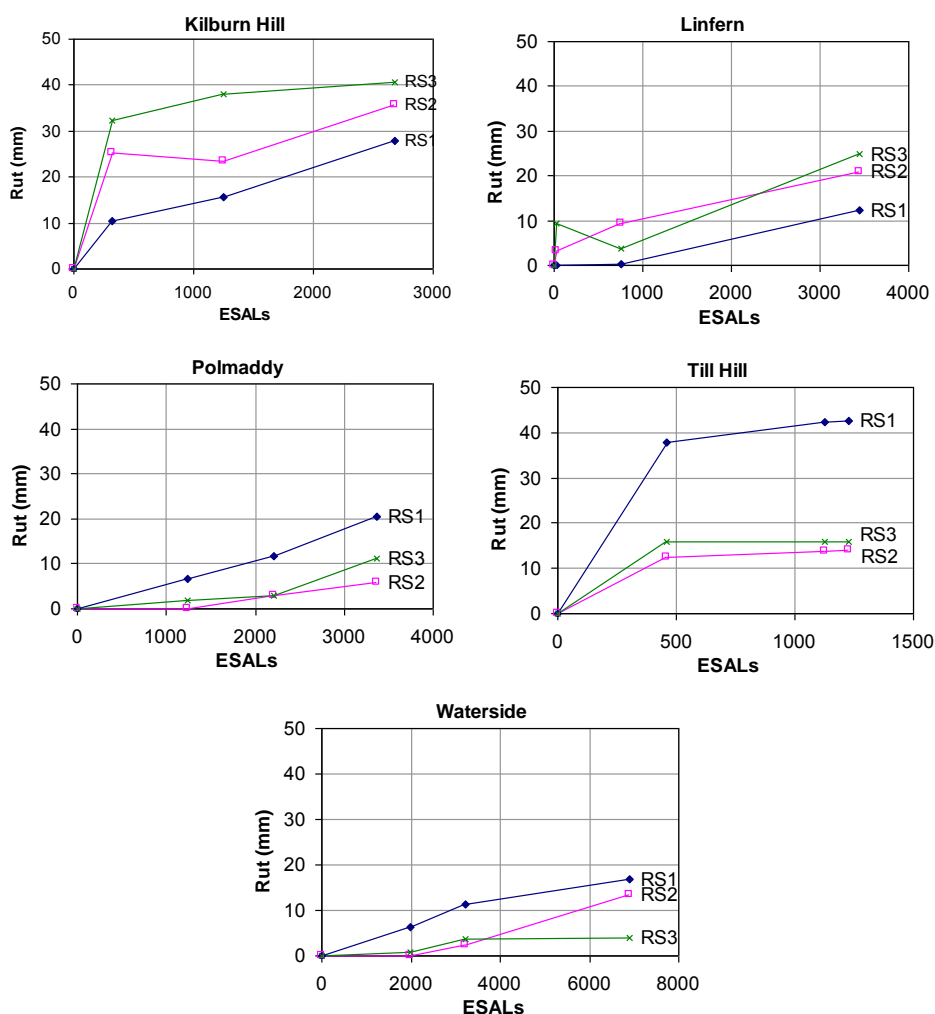


Figure 5.9 – Permanent deformation results for the reference sections

### 5.1.3.2. Reference Sections

Reference sections were analysed in regard to permanent deformation following the same protocol used for the monitoring sections described earlier. Figure 5.9 shows the summary of the results obtained for each site separately. Table 4.2 in Section 4.2.5 gives the thicknesses for each of the reference sections.

### 5.1.4. Pavement exhumation findings

Trial pits were carried out in most of the monitoring sites at the end of project for the purpose of identification of the pavement structure. In some sites, samples were collected for characterisation of the surfacing layers. Figure 5.10 illustrates an example of the pit carried out on the Brochloch site at Carsphairn Forest.



Figure 5.10 – Trial Pits at Kilburn Hill at Castle O'er and Brochloch at Carsphairn Forests

All trial pits were excavated in between each pair of monitoring cross sections, usually set 20m apart. The excavations were carried out helped by a small digger and the trench was usually opened from the edge to the middle of the carriageway. Trial pits depths varied in order to reach the top of subgrade, where excavation stopped.

The information recorded was:

- A local assessment of the material types and origins when possible,

- The thicknesses of surfacing layers and, when possible to identify, of the base layers,
- DCP readings at the base of the pit when materials and condition allowed,
- A picture of the trial pit.

Table 5.3 shows the results for CBR and layers thickness determined from DCP results. For this analysis the software UK DCP 3.1 from TRL [2006] was employed using the correlation presented by Equation 51 as discussed in Section 2.6.5.

The sites from which material was collected were: Waterside, Till Hill, Kilburn Hill, Steel Road, Risk and Craignell. The first three sites were chosen to be sites with monitoring and reference section and, hence, sites that could provide more resources for the study. The three last sites were chosen based on the judgement (data had not been analysed by the time the trial pits were carried out) that they were either with high or low permanent deformation throughout the project and would, this way, provide examples of a better and of a poorer material quality.

Table 5.4 summarizes the materials encountered during the excavations.

Notice that the trial pits were opened at the end of project - March 2008, when there was still freezing temperatures. Hence, some of the subgrades could be considered stiffer than usual.

The thickness of the bottom layer of each structure cannot be considered as final. These values are determined based on the depth on which the DCP test was stopped.

Table 5.3 – CBR and layer's thicknesses derived from DCP results

		Layer	CBR (%)	Thickness (mm)			Layer	CBR (%)	Thickness (mm)
1	Waterside	1	7	312	9	Ferter	1	8	766
		2	42	251	10	Gair	1	26	102
2	Bidhouse	1	13	348			2	12	131
							3	19	41
3	Till Hill 3/4	1	9	87	11	Kilburn Hill 1/2	1	14	177
		2	123	150			2	69	101
4	Brigton	1	154	17	12	Kilburn Hill 3/4	1	225	7
		2	269	9			2	110	21
		3	82	16			3	104	15
5	Brochloch	1	56	49	13	Lairds Hill	1	14	359
		2	11	187			2	7	149
		3	23	69	14	Linfern	1	4	345
6	Brownhills	1	26	174			2	19	201
		2	3	184	15	Polmaddy	1	50	163
7	Culreoch	1	13	349	16	Steel Road	1	9	433
		2	54	123	17	Carrick FD	1	10	481
8	Dryfhead	1	8	192					
		2	41	229					

Table 5.4 – Summary of Trial Pits

Site Name	Layer 1 (Top)	Layer 2	Layer 3 (Bottom)
KILBURNHILL 1/2	CRUSHED (BLACK ESK) ROCK Layer depth - 75mm	AS DUG GREYWACHE/TILL Layer depth -400mm	PEAT Layer depth -50mm ON MINERAL SOIL
GAIR	RED/ORANGE GREYWACHE/TILL Layer depth -400mm	RED/ORANGE GREYWACHE/TILL Layer depth -400mm	GREY/GREEN CLAY
FERTER	Crushed Rock Layer depth - 150mm	AS DUG ROCK Layer depth -180mm	TILL
DRYFEHEAD	SMALL AS DUG GREYWACHEE Layer depth - 250mm	SMALL AS DUG GREYWACHE Layer depth - 250mm	PEATY MINERAL SOIL Layer depth - 200mm
CULREOCH	Crushed Rock Layer depth - 100mm	SANDY TILL Layer depth -300mm INCREASING TO 500/600mm	PEATY MINERAL SOIL
CRAIGNELL	150mm surfacing Craignell crushed. 75mm down	150 mm - ???	
BROWNHILLS	180 - 200mm Crushed Rock	380 mm Steel Slag - very porous material	Rocky Till
BROCHLOCH	230mm - as dug local GREYWACHE	580mm rocky till	
BRIGTON	Crushed Rock 75mm down Layer depth - 130mm	ROCKY TILL Layer depth - 600mm	BEDROCK & WET
BIDHOUSE	AS DUG LOCAL GREYWACHE Layer depth - 400mm	HIGH FIBRE CONTENT PEAT Layer depth -160mm	
WATERSIDE	100mm surfacing aggregate as dug + shelly material	150mm Till	150mm Peat mineral soil
TILHILL	AS DUG GREYWACHE Layer depth - 100mm	ALLUVIAL BROWN GRAVEL Layer depth -300mm	RED GRAVEL/ STONY TILL & SILT Layer depth -200mm FREE DRAINING SUBGRADE
TALLAMINNOCH FD	RED Crushed Rock Layer depth - 150mm	CRUSHED ROCK Layer depth -100mm	AS DUG ROCK Layer depth - 300mm ON MINERAL SOIL
STEELE ROAD	AS DUG LOCAL GREYWACHE Layer depth - 250mm	ASH EX STEAM TRAINS RICCARTON JUNCTION Layer depth -250mm	ROCKY GREYWACHE TILL Layer depth - 330mm ON MINERAL SOIL (OVERFILL ROAD)
RISK	100mm surfacing - 75mm crushed run.	Leveling layer - corser than surfacing ~50mm	
POLMADDY	60mm black shale	200mm light brown till	400mm or + orange till
LINFERN	Crushed Rock Layer depth - 80mm	GRAVEL Layer depth -350mm	MINERAL SOIL Layer depth - 170mm ON PEAT
LAIRD'S HILL	AS DUG LOCAL GREYWACHE Layer depth - 400mm	RED SANDY CLAY Layer depth - 460mm	
KILBURNHILL 3/4	CRUSHED (BLACK ESK) ROCK Layer depth - 100mm	RED GREYWACHE Layer depth - 170mm	AS DUG GREYWACHE Layer depth - 400mm ON PEAT

### 5.1.5. Laboratory tests results

#### 5.1.5.1. Grading

Grading analyses for all samples collected during the pavement exhumation were carried out following the procedure established by the European Standard EN 933-1 [BS 1997]. The so-called “Swedish specification” is inserted in Figure 5.11 for comparison to the materials described in Section 4.4. This specification provides the reference to materials currently specified for forest roads maintenance, as discussed by Tyrell [2004a].

It can be readily noticed that most of the materials reclaimed are much coarser, with less fines (i.e. more single-sized), than those specified by the Swedish specification. Only the Craignell and Waterside materials approach the specified envelope, but these still have too much coarse material and not enough fines in them.

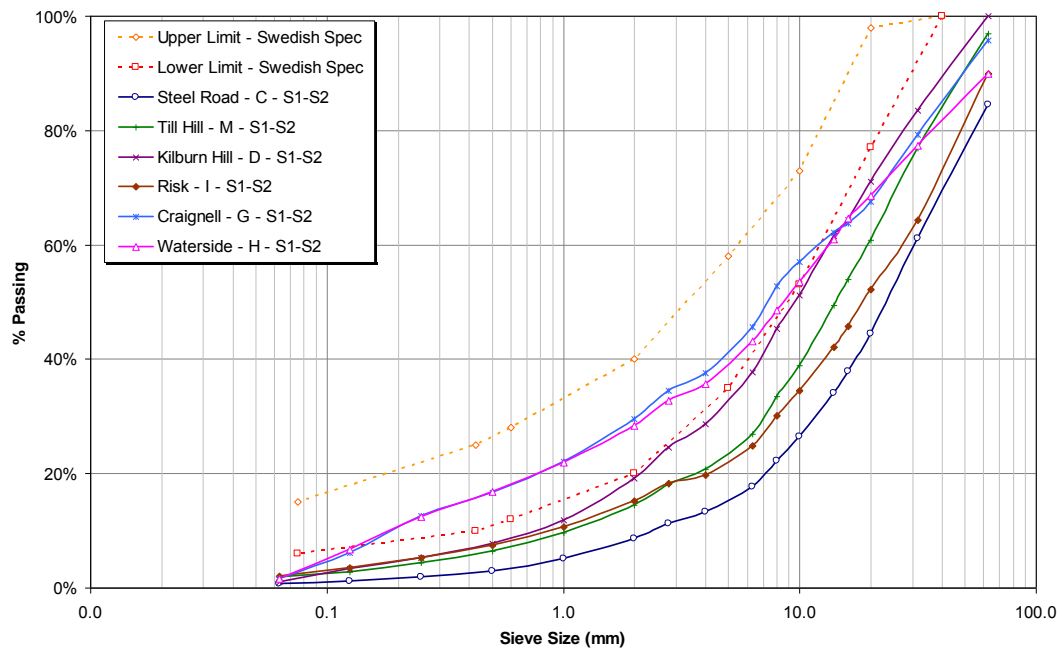


Figure 5.11 – Grading envelopes for surfacing layers on six monitoring sites

#### 5.1.5.2. Density and water absorption

The European standard EN 1097-6:2000 [BS 2000] was followed for density and water absorption testing. For all sites the fraction between 31.5mm to 4mm was tested. Only two of the sites, Kilburn Hill and Till Hill, had a finer fraction (4mm to 63µm) that was also tested for the purpose of benchmarking the differences. The relatively high water absorption results, typical of aggregates containing weaker stones, may be noted for the coarser fractions at Till Hill and Steel road. The following table show the results obtained.

Table 5.5 – Density and water absorption results

Site Name	Particle Size	Density on an oven dried basis (Mg/m <sup>3</sup> )	Density on a saturated and surface-dried basis (Mg/m <sup>3</sup> )	Apparent particle density (Mg/m <sup>3</sup> )	Water Absorption
Till Hill	31.5mm - 4mm	2.411	2.494	2.628	3.4%
Till Hill	4mm - 63µm	2.726	2.757	2.813	1.1%
Steel Road	31.5mm - 4mm	2.586	2.687	2.878	4.0%
Risk	31.5mm - 4mm	2.702	2.732	2.785	1.2%
Craignell	31.5mm - 4mm	2.717	2.731	2.756	0.6%
Waterside	31.5mm - 4mm	2.673	2.694	2.73	0.8%
Kilburn Hill	31.5mm - 4mm	2.609	2.659	2.746	1.9%
Kilburn Hill	4mm - 63µm	2.723	2.753	2.809	1.2%

#### 5.1.5.3. Ten Percent Fines

Ten percent fines (TFV) tests were carried out following the procedure of BS 812-111 [BS 1990c]. Although the standard recommends the use of the 10 to 14mm size fraction, this was not possible for most of the samples tested due to lack of material, priority having been to have sufficient of this size material for CBR tests, they being of high importance to the classification of the bearing capacity of the roads studied in the project. Only the fraction coarser than 22.4mm was available in quantity sufficient to perform the TFV test.

The BS 812-111 [BS 1990c] recommends that when not enough material at the recommended size fraction is available, either a smaller or larger size fraction than the standard should be used. In the specific case for the material collected, only larger than standard fraction was available in sufficient quantity. Although the recommended range for this size of particles was the material passing the 28mm sieve and retained on the 20mm sieve, this last one had to be changed for 22.4mm in order to allow the CBR to be performed in the recommended range by the standard.

To perform the test, a 300ton loading machine was used with manual loading control in order to meet the requirement of 2mm/min speed (Figure 5.12), as the aggregate tested was classified as normal crushed aggregate. After the total plunger penetration reached 20mm, the whole of the specimen was sieved on a 5mm sieve to separate the fines Figure 5.13. TFV determination was then calculated following the standard.

Table 5.6 summarizes the results obtained in this test. As an indicative value, BS 882 [BS 1992] "Specification for aggregates from natural sources for concrete" suggests that the aggregate used in pavement wearing surfaces should have a minimum TFV of 100kN, which has been achieved for all testing situations, even for that in soaked condition.



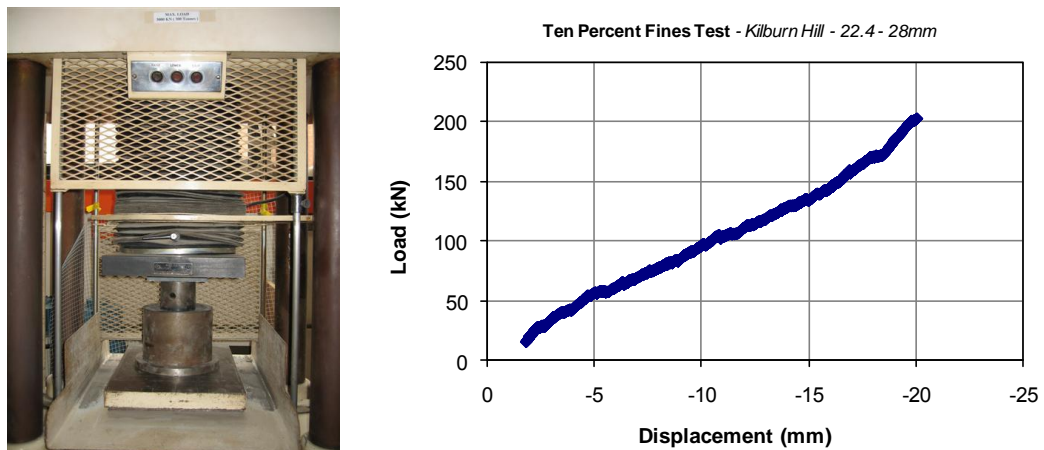


Figure 5.12 – TFB Loading Machine & Displacement results for Kilburn Hill Material



Figure 5.13 – Example of aggregate before and after TFB Test for Kilburn Hill material

Table 5.6 – Ten Percent Fines Results

Site Name	Particle Size	Condition	TFV (kN)
Kilburn Hill	22.4mm - 28mm	Dry	215
Kilburn Hill	10mm - 14mm	Dry	220
Kilburn Hill	10mm - 14mm	Soaked	135
Till Hill	22.4mm - 28mm	Dry	175
Risk	22.4mm - 28mm	Dry	210
Steel Road	22.4mm - 28mm	Dry	213
Waterside	22.4mm - 28mm	Dry	*
Craignell	22.4mm - 28mm	Dry	240

\* Not enough material of the needed fractions to carry out tests. CBR was given priority to TFV.

#### 5.1.5.4. California Bearing Ratio

California Bearing Ratio (CBR) tests were carried out in accordance to BS EN 13286-47 [BS 2004], with Proctor Mould B – 15cm in diameter and 12cm in height. The maximum particle size used was 22.4mm and the compaction was done by using a vibrating hammer. Figure 5.14 pictures the preparation procedure of a CBR sample and the loading apparatus.

As Proctor compaction tests could not be carried out due to the material particle size not meeting the requirements by the appropriate testing standard, no knowledge about optimum moisture content or maximum density was available. Therefore, it was chosen to vary the moisture content in a range of three values centred on an average value of 5% as reference. This value was chosen based on the typical moisture obtained in the construction of most of test sections in the Ringour Trials (see Section 5.2.3).



Figure 5.14 – Preparation and compaction of CBR samples & CBR Loading Apparatus



In case the workability of the material at 5% of moisture content was deemed to be low – i.e. the mixture was too dry, then this value was considered the lowest and higher moisture contents were then targeted for the other two tests based on the operator assessment. No situation on which 5% was deemed too wet was observed.

For each sample prepared, CBR was measured both on the top and bottom surface. Moisture content was also determined after the test was carried out using material from the centre of the sample. Because of the large number of tests to be accomplished, some samples had to be prepared on the day prior to test. Although care has been taken to ensure that moisture was kept constant, variation was still observed.

Figure 5.15 illustrates the CBR results as a function of the moisture content. For the purpose of the statistical analysis presented later in this thesis, the maximum values of CBR determined from the plotted curves were used.

Table 5.7 summarizes the results for all CBR tests as well as the wet and dry density measured for every sample.

Only the Steel Road & Waterside materials with the highest level of moisture, and the Craignell material with the two highest levels of moisture, yielded CBR values below 50%. Most of the other values were close to, or higher than, 100%.

Figure 5.15 illustrates the CBR results as a function of the moisture content. For the purpose of the statistical analysis presented later in this thesis, the maximum values of CBR determined from the plotted curves were used.

Table 5.7 – CBR Results

	Target moisture	Measured moisture	CBR		Wet Density (Mg/m <sup>3</sup> )	Dry Density (Mg/m <sup>3</sup> )
			Highest	Average		
Kilburn Hill	5.0%	4.70%	145%	129%	2.65	2.53
	6.0%	5.30%	150%	117%	2.66	2.53
	6.5%	5.09%	87%	79%	2.62	2.50
Steel Road	5.0%	4.80%	148%	115%	2.47	2.36
	6.0%	3.76%	205%	170%	2.57	2.48
	8.0%	6.11%	48%	30%	2.60	2.45
Risk	5.0%	4.55%	130%	92%	2.48	2.37
	5.5%	5.42%	118%	91%	2.64	2.50
	6.5%	5.55%	168%	94%	2.64	2.50
Till Hill	5.0%	4.50%	98%	84%	2.32	2.22
	6.0%	5.70%	108%	76%	2.45	2.32
	6.5%	5.18%	120%	95%	2.53	2.41
Waterside	5.0%	4.62%	111%	94%	2.52	2.40
	6.0%	5.82%	135%	99%	2.64	2.49
	7.0%	6.73%	26%	17%	2.58	2.42
Craignell	5.0%	4.46%	105%	74%	2.70	2.58
	6.0%	6.18%	28%	21%	2.68	2.53
	6.5%	6.02%	23%	14%	2.65	2.50

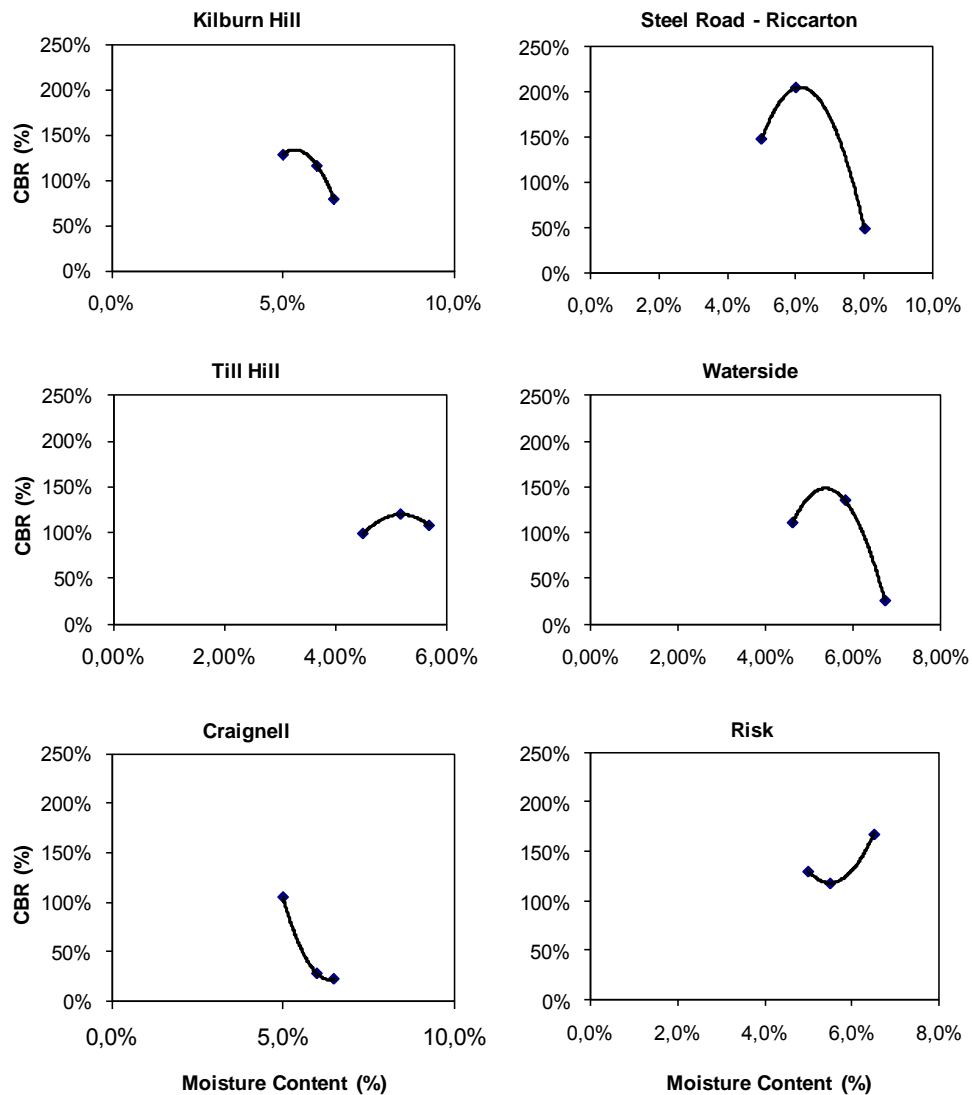


Figure 5.15 – CBR Results versus moisture

#### 5.1.5.5. Liquid Limit, Plastic Limit & Plasticity Index

The classification tests carried out on the materials were Liquid Limit and Plastic Limit following the procedure established by the standard BS 1377-2 [BS 1990a]. The maximum particle size used for both tests was 425 $\mu$ m, this fraction having been obtained from the trial pits specimens after sieving.

The liquid limit is the empirically established moisture content at which a soil passes from the liquid state to the plastic state. It provides a means of classifying a soil, especially when the plastic limit is also determined. The procedure employed uses a cone penetrometer (Figure 5.16a), thus, essentially, it is a static test depending on soil shear strength. The procedure adopted was a one-point test.

The plastic limit is the empirically established moisture content at which a soil becomes too dry to be plastic. The test basically consists in determining the minimum moisture at which it is possible to make thread of 3mm in diameter with the soil. Figure 5.16b exemplifies the procedure. Where a test could not be accomplished due to non-plastic behaviour, material has been identified.

Table 5.8 summarizes the Liquid Limit and Plastic Limit test results. Plasticity Index has also been derived from both results and recorded in the table.



Figure 5.16 – (a) Penetrometer for Liquid Limit determination & (b) Plastic Limit Test

Table 5.8 – Liquid Limit, Plastic Limit & Plasticity Index results

	Liquid Limit	Plastic Limit	Plasticity Index
Steel Road	32.5%	17.1%	15.5%
Kilburn Hill	26.4%	18.6%	7.8%
Craignell	27.2%	17.6%	9.6%
Waterside	23.7%	N/A	-
Risk	29.7%	N/A	-
Till Hill	25.6%	19.5%	6.2%

### 5.1.6. Statistical analysis

Two statistical models have been developed based on the data collected. The analysis was carried out as means to have readily available tools for the stakeholders of the RUTT project, providing a direct assessment tool of the monitored sites. The models are constructed on a statistical basis, not on a mechanistic approach as sought by this thesis; yet they are representative of the work carried out in the RUTT project and help the assessment of the results.

Ideally, all trafficking data should have been part of the database used to generate a model to forecast permanent deformation in the roads participating in the project. This was not possible for the reasons discussed earlier. Thus there were several restrictions requiring the data to be severely reduced, namely:

- Traffic data was based on timber volume rather than counting and classification of vehicles on site.
- Timber volume was only available for some sites monitored during the project.
- Linear distribution had to be used where data was not available on a monthly distribution in order to fill in the gaps between readings.
- Laboratory tests were only carried out for six materials. Some other sites only had CBR determined through empirical correlations with DCP carried out during trial pits.
- Sites on which the weather stations either failed to supply data, or those with incomplete details, had the rainfall predicted from the closest site possible.

Because of these restrictions, two different analyses were carried out. One analysis generated the so-called “Model 1”, that considered only data from the sites on which CBR laboratory tests have been carried. The second analysis generated the so-called “Model 2”, which took into account the data from all those sites with CBR values derived from DCP tests (carried out in trial pits) and where traffic data were available.

This procedure was adopted based on the fact that CBR values determined in the lab in comparison to those determined from DCP correlations presented a great difference in values and, therefore, justified the need of two different models.

Both models were calculated considering the permanent deformation as the dependent variable. The models are functions of the CBR of the surfacing material (designated as base), rainfall, traffic and of base & sub-base layers thicknesses – all being independent variables. Linear multiple variable correlation was the type of regression determined aided by the computational software Statsoft Statistica 7.

It is important to notice that the correlations suggested are restricted to the description of the permanent deformation for the sites and conditions established during the RUTT project. These models do not, in general, describe the mechanical behaviour of the materials employed in the project, nor do they represent an overall description of forest roads in a broader sense.

---

The input variables considered were:

- Vehicles – accumulated traffic in standard axle loads (ESAL) unit for the desired period of analysis. Attention must be given that, for the analysis carried out, ESAL was based on an articulated lorry fitted with super-single tyres.
- CBR of surfacing material (Base) – determined in the laboratory for use in Model 1, or derived from DCP for use with Model 2
- Rainfall – accumulated rainfall in mm for the desired period of analysis. When data was not available for the site, the information available for the closest weather station was used.
- Base thickness – thickness of the surfacing course in mm.
- Sub-base thickness – thickness of the layer immediate below surfacing in mm.

Figure 5.17 shows the predicted results obtained with Model 1 plotted against the observed values. From the 90 observations used to produce this model, 13 were deemed outliers and were therefore disregarded in order to improve the accuracy of the model. Figure 5.18 show the same type of graphic for Model 2. From the 194 observations used to produce the model, 9 outliers were disregarded. Outliners were considered when the observed value exceeded  $\pm 2$  standard deviations of the group.

The statistical details for Model 1 are summarized in Table 5.9 whereas for Model 2 details are in Table 5.1. It is evident that Model 1 has a much better coefficient of correlation ( $R^2=0.91$ ) than for model 2 ( $R^2=0.75$ ). This is possibly due to the CBR values determined in the laboratory (used in Model 1) supplying a much more realistic correlation to the permanent deformation developed on site, and certainly a strongly influence comes from the number of observation each model features. The higher the number of observations, the stronger the model is, although the coefficient of correlation may drop in value depending on their scatter.

The models are in the form of a linear polynomial regression in the form of the equation below. Table 5.11 summarizes the constant values ( $K_1 \dots K_5$ ) for the Equation 58 which establishes the relations between the variables and the parameters determined following the polynomial obtained in the analysis.

$$Rut(mm) = Var1 * K_1 + Var2 * K_2 + Var3 * K_3 + Var4 * K_4 + Var5 * K_5 + Intercept$$

Equation 58

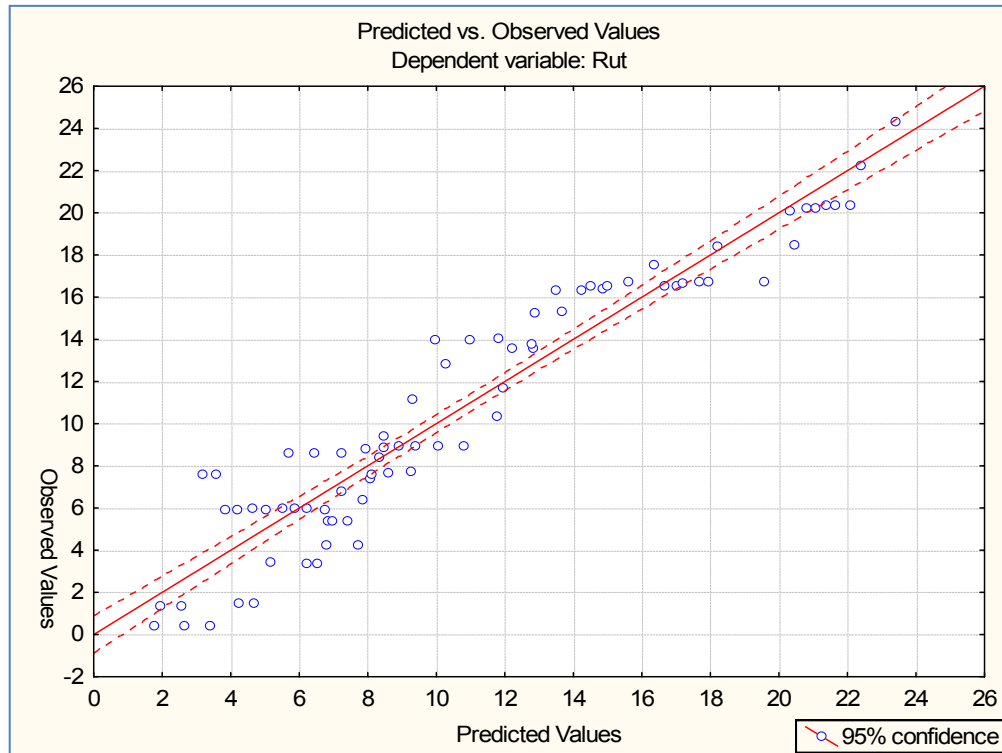


Figure 5.17– Predicted versus observed values for Model 1 (90 observations minus 13 outliers)

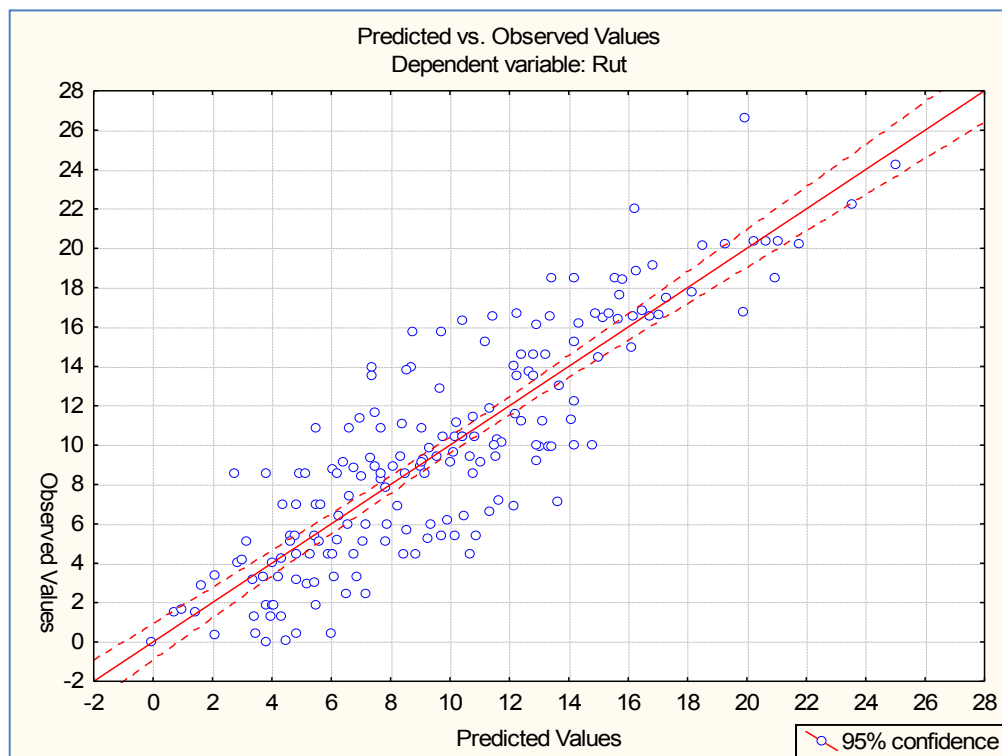


Figure 5.18 – Predicted versus observed values for Model 2 (194 observations minus 9 outliers)

Table 5.9 – Statistical results for Model 1

	Beta	Std. Error of Beta	B	Std. Error of B	t (220)	p-level
<b>Intercept</b>			-9.3030	2.1362	-4.3549	0.0000
<b>Traffic</b>	0.5153	0.0589	0.0014	0.0002	8.7562	0.0000
<b>CBR</b>	0.7954	0.1093	0.1431	0.0197	7.2750	0.0000
<b>Rainfall</b>	0.2684	0.0478	0.0039	0.0007	5.6090	0.0000
<b>Base</b>	-0.5533	0.1026	-0.0517	0.0096	-5.3953	0.0000
<b>Sub-base</b>	-0.1268	0.0394	-0.0059	0.0018	-3.2156	0.0020
<b>Multiple R</b>			0.9536			
<b>Multiple R<sup>2</sup></b>			<b>0.9094</b>			
<b>Adjusted R<sup>2</sup></b>			0.9030			
<b>F (5, 71)</b>			142.5777			
<b>p</b>			0.0000			
<b>Std.Err. Of Estimate</b>			1.9082			

Table 5.10 – Statistical results for Model 2

	Beta	Std. Error of Beta	B	Std. Error of B	t (220)	p-level
<b>Intercept</b>			2.0392	0.7201	2.8316	0.0052
<b>Traffic</b>	0.5433	0.0482	0.0016	0.0001	11.2721	0.0000
<b>CBR</b>	0.0582	0.0438	0.0060	0.0045	1.3284	0.1857
<b>Rainfall</b>	0.4108	0.0469	0.0064	0.0007	8.7589	0.0000
<b>Base</b>	0.2423	0.0422	0.0123	0.0021	5.7419	0.0000
<b>Sub-base</b>	-0.2473	0.0389	-0.0094	0.0015	-6.3537	0.0000
<b>Multiple R</b>			0.8643			
<b>Multiple R<sup>2</sup></b>			<b>0.7470</b>			
<b>Adjusted R<sup>2</sup></b>			0.7399			
<b>F (5, 62)</b>			105.7069			
<b>p</b>			0.0000			
<b>Std.Err. Of Estimate</b>			2.9134			

Where

*Var1* = Accumulated Traffic (ESALs)

*Var2* = CBR (%)

*Var3* = Accumulated Rainfall (mm)

*Var4* = Base thickness (mm)

*Var5* = Sub-base thickness (mm)

*K1 to K5 & Intercept* = Constants of the model summarized in Table 5.11.

It is important to note that although Model 1 features a better correlation coefficient, the number of observations on it is more limited. Furthermore, because DCP may be a readily available tool for forest engineers, unlike CBR tests that are more time consuming and require specific apparatus to be carried out, Model 2 may be more easily employed.

Table 5.11 - Models 1 &amp; 2 constants and details

	Model 1	Model 2
<b>N° of obs.</b>	77	185
<b>K1</b>	0.00135	0.00164
<b>K2</b>	0.14308	0.00596
<b>K3</b>	0.00393	0.00642
<b>K4</b>	-0.05169	0.01226
<b>K5</b>	-0.00592	-0.00939
<b>Intercept</b>	-9.30300	2.03917
<b>R<sup>2</sup></b>	0.91	0.75
<b>Data used</b>	Kilburn Hill, Steel Road, Risk, Till Hill, Waterside & Craignell	Gair, Steel Road, Kilburn Hill, Till Hill, Dryfehead, Bidhouse, Culreoch, Polmaddy, Craignell, Waterside, Risk, Brighton, Tallaminnock FD, Ferter

Figure 5.19 and Figure 5.20 illustrates the impact of each separate input variable on the total permanent deformation developed when changed from 0 to 100% in value. This shows the sensitivity of the models to each variable. It is emphasized that this should not be interpreted as a failure mechanism discussion, but as a statistical observation of the models.

It is possible to notice that, although CBR increase should influence negatively the permanent deformation development (higher CBR should decrease rutting), this was not observed either in Models 1 or 2, although in Model 1 this characteristic is a lot more evident. Conversely, CBR increase yields higher permanent deformation development. Although, certainly, this does not correspond to the mechanism of distress expected in a pavement, it is a statistical effect observed in this study. A possible explanation is that variables not controlled in this study may have influenced the way CBR correlated to permanent deformation development, such as drainage conditions. Even with higher CBR, a material in a soaked condition may behave worse than a lower CBR material in a dry condition. Also, it is conjectured that road owners may use better construction materials and/or practice where more destructive trafficking is anticipated.

Rainfall and traffic revealed the expected behaviour of increasing rutting with positive variation in their values. Likewise, sub-base and base decreased permanent deformation for an increase in thickness.

For Model 2 the rainfall was the input variable with the highest influence on the permanent deformation measured at the monitoring sites. Sub-base thickness was the variable which had the greatest influence on the inhibition of rutting.



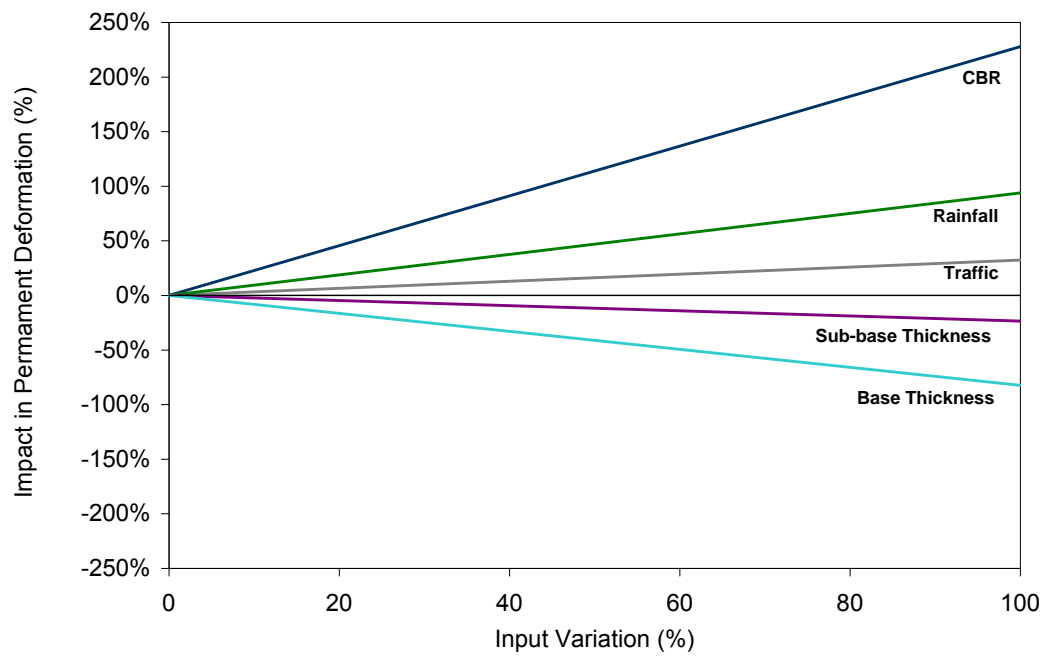


Figure 5.19 – Impact of input variation on permanent deformation according to Model 1

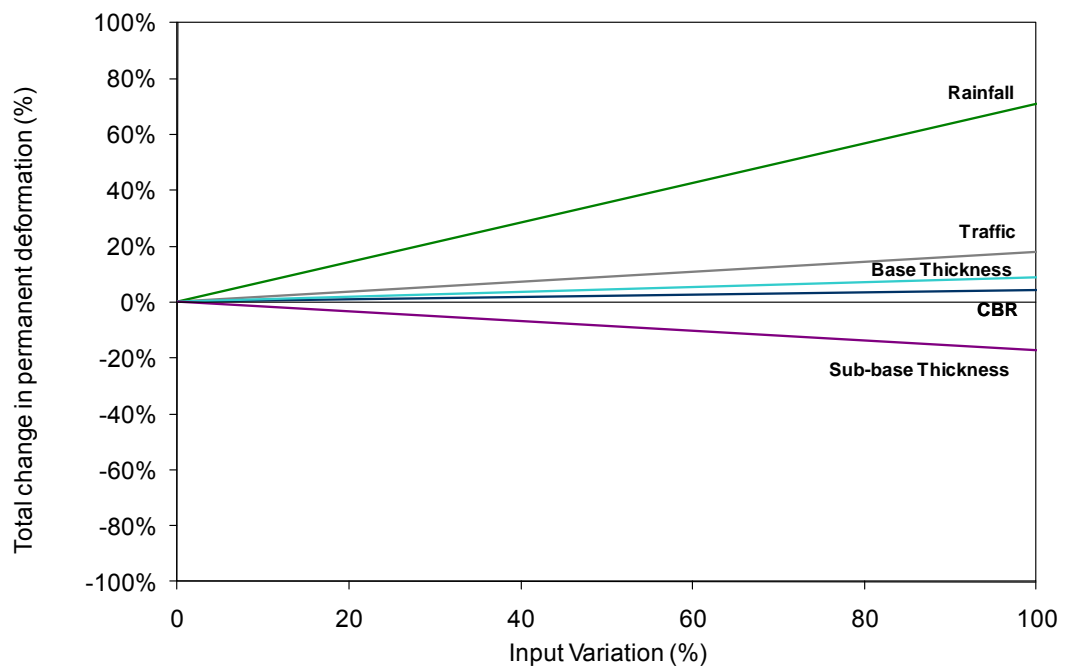


Figure 5.20 – Impact of input variation on permanent deformation according to Model 2

## 5.2. ACCELERATED PAVEMENT TRIALS

### 5.2.1. Test procedure

The procedure developed as the trials progressed. Initially, it was envisaged to run one vehicle at a time and by the time of the fourth trial two vehicles were run together. In this way two vehicles ran on the same pavement and their performance was compared directly. Thus the variability in preparation of surfaces encountered in the earlier trials at Risk [Tyrrell 2004b] was eliminated. The importance of tyre pressure became increasingly clear during the trials and more attention was paid to this in the later trials. Also, it was found that greater care needed to be taken to ensure that the vehicles kept on line while on the test surface.

The water tank was filled and the water level recorded. The test road was then heavily soaked prior and during the trial (Figure 5.21). The road was covered with a tarpaulin overnight for the seventh trial to maintain the test road in a soaked state. Watering took place after each run of 10 circuits so that there were pools of water on the surface. The supply tank was dipped at 0, 10, 20, 40, 70 & 100 passes to record the amount of water applied.



Figure 5.21 – Soaked surface during trial

The dimensions of the vehicles, wheel positions, tyre size and tread were measured and recorded (Appendix B). It was noted that the tread width varied on tyres of the same nominal size produced by different manufacturers. The tyre pressures were recorded from the third trial onwards. Not all the tyres were checked because valve extenders were missing from most of the inner tyres. It was learnt that the practice of not refitting tyre valve extenders had arisen because they tend to brake as mud is forced up from forest roads into the gap between the tyres. The result of a broken extender is a flat tyre and it is understandable that they are not, therefore, refitted. The disadvantage of this practice is, however, that the driver cannot undertake his responsibility to check tyre pressures. The gross weight of vehicles was obtained from weighbridges or by weight of vehicle plus amount of timber loaded. In addition, the front and back pairs of axles of the Foden were weighed.

Normally drivers vary the vehicle path on forest roads to spread any damage or rutting. To hasten rut formation, each driver was instructed to keep to the same wheel tracks for the duration of the test. Sets of two marker posts were aligned to the position of the drivers in their cabs to keep the vehicle along the same line each time, approximately one metre away from the wall edges. All the runs were conducted in the same direction. Vehicles ran round a circular route so that they were running down the slope. It took approximately 5 hours to complete the 100 vehicle passes and take measurements.



Figure 5.22 – Example of pictures taken in the wheel paths at the end of each round of passes

Photographs were taken at each instrumented section to record the ruts pictorially after each set of passes (Figure 5.22).

Samples of all aggregates were collected and sent for testing. This included moisture content and grading analyses. Also the moisture content was measured on site for some trials using a microwave for the “before” and “after” condition of the aggregate, more so with the later trials.

At the end of each trial, a record sheet was composed containing the following item:

- Lorry weight
- Lorry tyre pressure and axle configuration
- Amount of water sprinkled
- Moisture content of the layers before and after the tests
- Profiles at 10, 20, 40, 70 and 100 passes at two cross sections at chainages of 12 and 18m along the trial
- Rut measurements at every 1m along the right hand wheel path from 7.5 to 22.5m chainage
- DCP readings, where applicable
- Notes and remarks about the trial.

Trial 2 was run after Trial 1 with no resurfacing or regularization, as well as Trial 10, after Trial 9. For Trial 3, a shallow correction of the rutting caused by the previous trials was performed with material distributed over the wheel paths without compaction. From Trial 4 onwards the top 150mm was removed, remixed, replaced and recompactd.

The dynamic cone penetrometer (DCP) was used as means of providing information about the layer’s bearing capacity and also to help identify the pavement structure as-built.

The automatic layer analysis procedure first calculates the penetration rate at each test point and the average penetration rate for the entire test. For each test point it then calculates the value of the average rate minus the rate at that point. These values are then summed in turn starting at the first test to find the cumulative difference sum at each point. By the nature of the calculation, this sum will be zero at the final test point. At one point this sum will reach a maximum absolute value. The depth of the point at which the sum reaches this maximum value is defined as the first Test layer boundary. This procedure has a similar effect to drawing a straight line from the first point to the last point and finding the depth of the intermediate point which is furthest from this straight line. The

---

procedure is then repeated for the test points above this first boundary and for the points below it. In this way the second and third boundaries can be identified. The procedure is repeated until the points between any two boundaries do not exhibit sufficient fluctuation from a straight line to allow a further boundary to be identified with any degree of confidence [TRL 2006].

The results obtained for the four trials on which DCP testing was performed, are presented in Table 5.12.

Table 5.12 – Thicknesses and CBR value deduced from DCP testing

Trial #	Material	Condition	Chainage (m)	Offset (m)	Layers	Thickness (mm)	Penetration Rate	CBR (%)
1	<i>Morrington Type 1</i>	Dry	7	2.75	Base	277	13.8	19
					Sub-base	339	3.99	70
			15	2.75	Base	423	8.58	31
					Sub-base	180	3.6	78
			23	2.75	Base	264	13.27	20
					Sub-base	346	3.64	77
4	<i>Morrington Type 1</i>	Wet	12	1.85	Base	302	6.04	45
					Sub-base	323	3.59	78
			12	3.70	Base	303	5.5	50
					Sub-base	345	4.08	68
			18	1.85	Base	306	3.73	75
					Sub-base	359	3.8	74
			18	3.70	Base	382	5.46	50
					Sub-base	290	3.22	88
7	<i>Risk</i>	Wet	12	1.85	Base	251	5.02	55
				3.70	Base	301	5.02	55
11	<i>Craignell FC Type 1</i>	Wet	15	3.70	Base	245	15.31	17
					Sub-base	406	4.27	65

Mini-falling weight deflectometer tests were also carried out at Ringour to estimate the material stiffness and as a tool to control compaction level during the section construction. Figure 5.23 show the results for each of the materials used in the trials. These results show the value of stiffness deduced by the Keros Prima 100 software, from Dynatest, at the top of the assessed layer. Mini-fwd test results for Ringour trial section construction are in Appendix E.

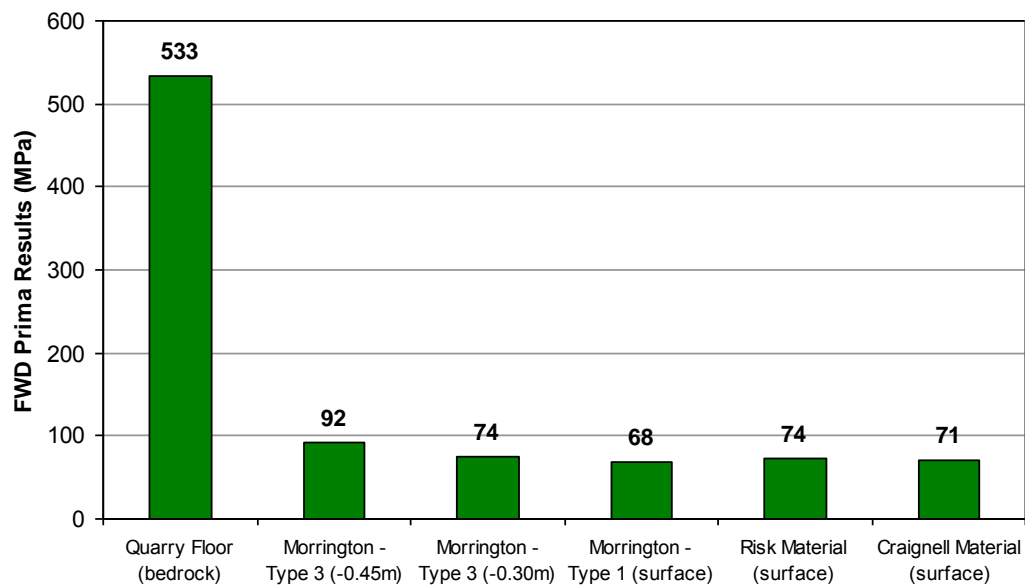


Figure 5.23 – FWD Results - summary of deduced stiffness values

The results show that while the DCP is useful in finding layer boundaries, its interpretation in terms of CBR needs to be treated with caution. While the Risk material featured lower than the Morrington material, as expected, the uppermost layer seems to be loosened by the driving action – especially when the aggregate is dry, thereby under-representing the results.

The mini FWD results (Appendix E) suggest that this device does not give results which are indicative of in-aggregate rutting potential. Despite clearly observable differences between the rutting of the different aggregate used, the stiffness values were sensibly constant for the 3 different aggregates assessed. This result is not altogether surprising as plastic and resilient behaviour are known not to be well correlated.

The existence of a solid quarry floor at the bottom of the trials' constructions will have prevented deep-seated rutting. Shallow, near-surface, rutting in the upper aggregate layer is almost always the distress mode that is most evident. This is in-line with the observations made in the earlier study [Forestry Enterprise 2004] which, by way of exhumed cross-sections of many pavements in the forests, showed that in-aggregate shear deformation was almost always the cause of rutting

### 5.2.2. Permanent deformation data

The rutting data collected in all the trials was analysed following the procedures described in Section 4.2.4. Although both VSD and rut depth procedures have been used to calculate the permanent deformation, only the data calculated using the rut depth

algorithm is presented, as it yielded best results. This is possibly due to the high rut shoulder heave observed throughout the trials.

The values for rut depth were calculated for all sections measured, usually two, and for both wheel paths. The results were then averaged to compose the final permanent deformation. For those trials on which two vehicles were run at the same time, only the outer wheel paths of each vehicle was used to determine the permanent deformation, as the centre of the test section was usually disturbed by both vehicles.

Figure 5.24 illustrates a comparison of the results obtained in the trials. In this picture, the rutting rate is plotted as a function of the total permanent deformation measured at the end of the trial divided by the total number of ESALs. The rate obtained is a constant value that approximates the speed that rutting occurs after the initial settlement. Trial 8B is highlighted as the fastest rutting rate among all trials, and Trial 9A as the slowest.

Figure 5.25 summarizes the rutting development in all trials as a function of the number of vehicle passes (independent of their ESAL). The trends are all power fits added to the experimental points, so as to minimize the dispersion of the results. Table 5.13 summarizes all results and each trial's characteristics. In Appendix F, all the measured cross sections are graphically represented.

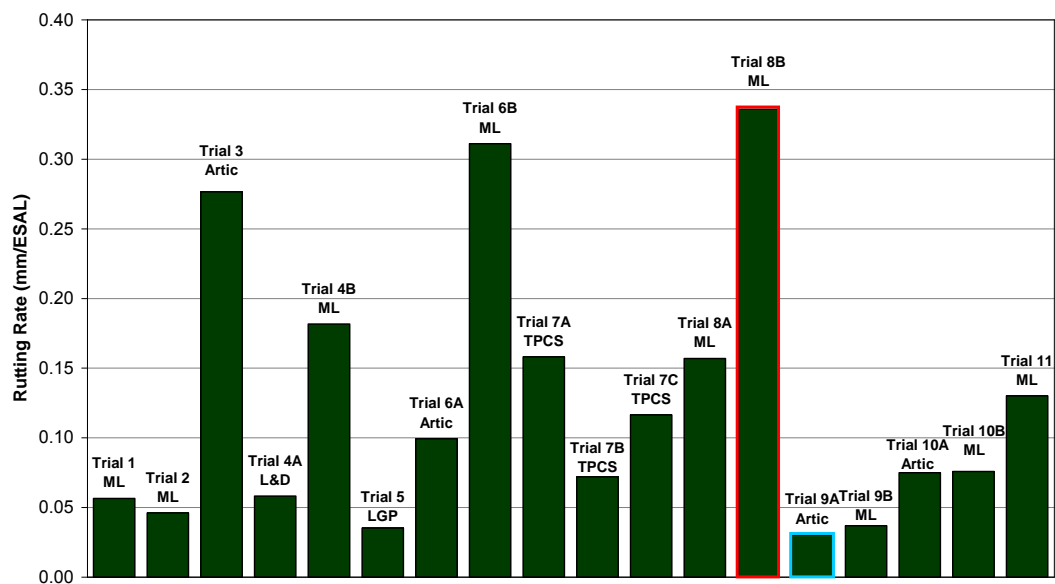


Figure 5.24 – Rutting rates observed according to number of ESALs



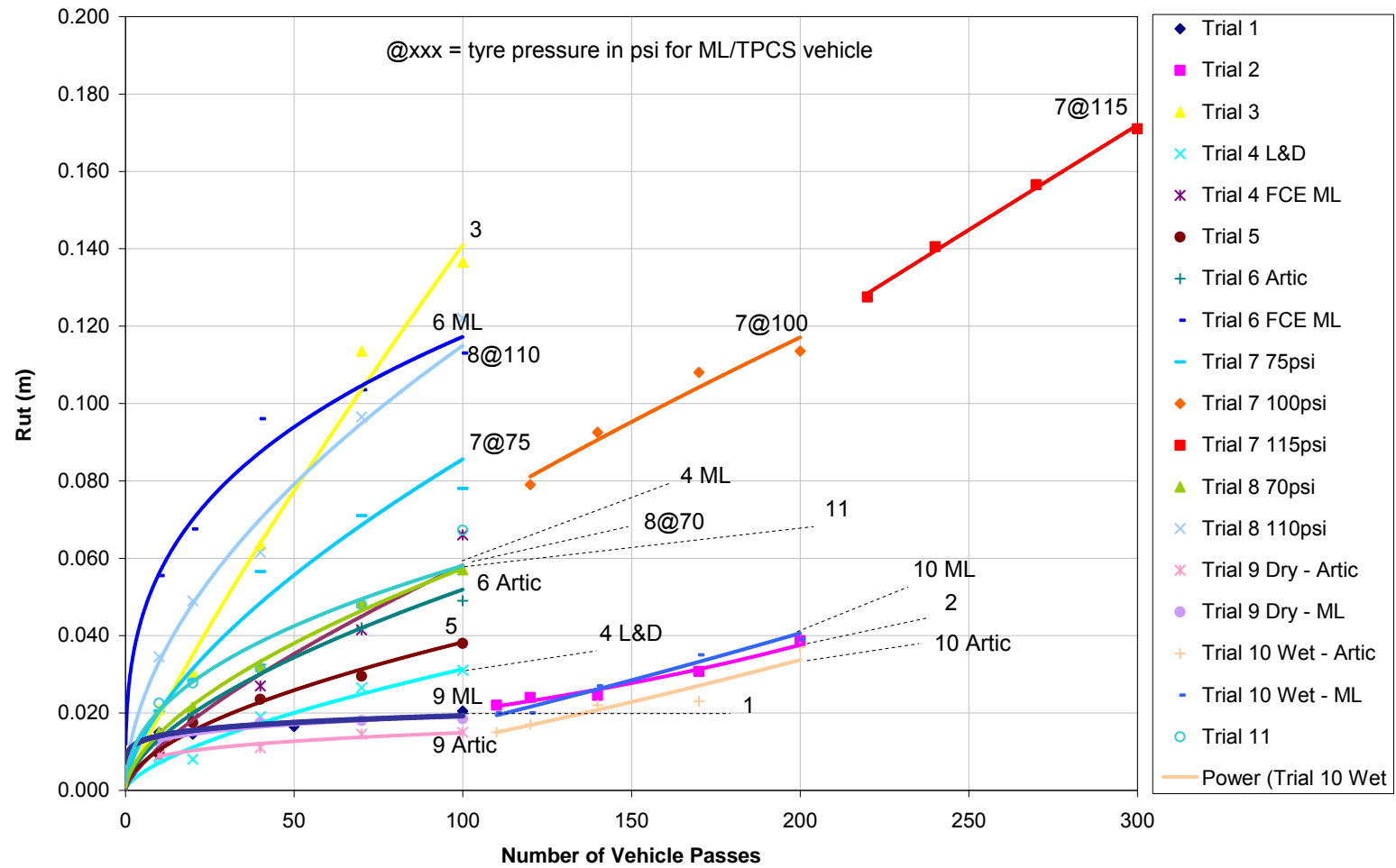


Figure 5.25 – Rutting observed in trials at Ringour



Table 5.13 – Ringour trials summary chart

	Vehicle	Vehicle ESAL	Tyre Fitment	Mean Tyre Pressure (psi)	Material tested	Moisture Condition	CBR (%)	Rutting (mm)	Number of ESALs	Rutting Rate (mm/ESAL)	Ranking*
Trial 1	Multi-Lift	3,63	Twin Tyres	+	Morring. T1	Dry	23	21	363	0,056	14
Trial 2	Multi-Lift	3,63	Twin Tyres	+	Morring. T1	Wet	55	17	363	0,046	15
Trial 3	Artic	4,94	Sup. Singles	114	Morring. T1	Wet	55	137	494	0,276	3
Trial 4A	Lorry & Drag	5,33	Twin Tyres	121	Morring. T1	Wet	55	31	533	0,058	13
Trial 4B	Multi-Lift	3,63	Twin Tyres	+	Morring. T1	Wet	55	66	363	0,182	4
Trial 5	LGP	10,80	Twin Tyres	74	Morring. T1	Wet	55	38	1080	0,035	17
Trial 6A	Artic	4,94	Sup. Singles	105	Risk NS	Wet	55	49	494	0,099	9
Trial 6B	Multi-Lift	3,63	Twin Tyres	113	Risk NS	Wet	55	113	363	0,311	2
Trial 7A	TPCS	4,94	Sup. Singles	75	Risk NS	Wet	55	78	494	0,158	5
Trial 7B	TPCS	4,94	Sup. Singles	100	Risk NS	Wet	55	35	494	0,072	12
Trial 7C	TPCS	4,94	Sup. Singles	115	Risk NS	Wet	55	58	494	0,116	8
Trial 8A	Multi-Lift	3,63	Twin Tyres	70	Morring. T1	Wet	55	57	363	0,157	6
Trial 8B	Multi-Lift	3,63	Twin Tyres	110	Morring. T1	Wet	55	122	363	0,336	1
Trial 9A	Artic	4,94	Sup. Singles	100	Craignell FC T1	Dry	++	15	494	0,030	18
Trial 9B	Multi-Lift	5,15	Twin Tyres	100	Craignell FC T1	Dry	++	19	515	0,037	16
Trial 10A	Artic	4,94	Sup. Singles	100	Craignell FC T1	Wet	++	37	494	0,075	11
Trial 10B	Multi-Lift	5,15	Twin Tyres	100	Craignell FC T1	Wet	17	39	515	0,076	10
Trial 11	Multi-Lift	5,15	Twin Tyres	110	Craignell FC T1	Wet	17	67	515	0,130	7

\* 1 being the worst result - more rutting

+ tyre pressures weren't measured

++ as DCP measurement weren't recorded, no CBR estimate was obtained

Figure 5.25 shows the development of rutting for the trials. For the pavements with low total rutting there is normally an initial high rate of rutting followed by a stabilising response (e.g. Trials 1, 9 & 10). This type of response is very common [Dawson 2008]. This is the response desired of the best pavements where traffic levels are to be highest and long-term performance must be assured.

Other pavements show an on-going development of rutting. In some cases this development is very large and rapid (e.g. Trial 3) but, for the most part, it is moderately fast. Such a response is appropriate for a less frequently trafficked pavement or one that only needs to provide service for a limited time.

Figure 5.25 also clearly shows the effect of tyre inflation pressure. Consider Trial 7 in which the tyre pressure was progressively increased. With the pressure at 520 and 690 kPa (75 and 100 lbs/in<sup>2</sup>) the rutting initially increased but then began to slow, yet the application of further trafficking at higher pressures caused the rutting to recommence and to accelerate. Similarly comparing the two Trial 8 tests the damage due to the 760 kPa (110 lbs/in<sup>2</sup>) tyres is much greater. Trial 4B – with the same vehicle, same aggregate and an intermediate mean tyre pressure, performs between the two cases of Trial 8. Trial 3 is amongst the worst behaviour of all trials (it has the highest total rutting, 137mm, see Table 8). The use of “super-single tyres” with a mean tyre pressure of 786kPa (114 lbs/in<sup>2</sup>) generates a condition for which such behaviour was to be expected.

Regarding the vehicle used, the much greater rutting that occurs under the FC’s Multi-Lift vehicle is apparent when compared with that occurring due to the articulated vehicle used on the same pavements (Trials 6, 9 & 10). This is despite the fact that the articulated lorry has “super-single” tyres which, it is known from other studies, are more damaging than the twin tyres which fitted to the Multi-Lift vehicle. The disparity, however, for the present could not be easily equated. For Trial 6 this might be explained due to tyre inflation problems. The rear axle did not have tyres at the same pressures and this almost certainly resulted in local overloading and accelerated damage. For the other trials, the reasoning is not so clear. It may relate to the more limited opportunity for load distribution along the length of a rigid-bodied lorry than along an articulated one. Table 5 does not indicate that the individual axles are very differently loaded, so a “rogue” axle loading does not seem to be the explanation in this case. A possible explanation is provided by the common perception that the crane on the vehicle causes undue loading on the front axles. The vehicle is known, from many observations before this project, to be more damaging than ordinary four axle tippers of otherwise similar characteristics.

---

The same explanation is almost certainly valid for the comparison of Trials 4A and 4B. Trial 4B caused approximately twice as much rutting as 4A, and a three times higher rutting rate, when related to number of ESALs. Nevertheless, a close study shows that the VSD levels were very similar for both vehicles (see Trial 4 – Appendix F); the heaving effect on the right hand side wheel path – trafficked by the FC's Multi-Lift – was responsible for increasing the rutting measurement, suggesting higher shear stresses near the surface. This may be explained by the later finding that the rear-most axle of the Multi-Lift was running virtually on two wheels – a factor that is likely to be responsible for a very high stress level between tyre and pavement, provoking higher shear stresses near the surface.

With the so-called “low ground pressure” vehicle, the novelty of spreading the load across the pavement through multiple wheels is negated by the heavily loaded axles of the rear of the tractor unit. Visibly, these appear to have been the chief cause of damage and the results in Figure 5.25 appear to confirm this although the lack of a direct comparison to the trafficking of the same pavement by another vehicle hinders interpretation.

Table 5.13 seeks to interpret the data in a somewhat different manner by looking only at the rate of rutting during the last 60 passes of each trial. The aim is to be able to separate-out any bedding-down effects. The results (last column) yield a consistent story regarding the (twin-tyred) Multi-Lift vehicle. Its rate of rutting is either similar or greater for the Multi-Lift than for the articulated vehicle (with “super-single” tyres on its trailer) – Trials 6, 9 & 10. This goes against received wisdom and also against the analytical results from the further described in Chapter 6. Super-single tyres impose more concentrated loading, therefore the near-surface response of the pavement materials should be more important for roads trafficked by such wheels, than the response of the middle layers which will have more influence on the road's response to twin-tyred vehicles. However, the trafficking studies at Ringour show that near-surface response is uniformly important (as shown by the localised heave exhibited in the rut profiles) and that the twin-tyred vehicles may even produce slightly more damage to the surface. On the earlier trials this can be explained by reference to the uneven tyre inflation pressures, but another explanation has to be found for the later trials. It is tentatively conjectured that the effect of the rigid body may be a contributory factor, but no direct evidence for this is available.

Nevertheless, a sole comparison between two trials of very similar conditions - Trials 3 and 4B-, apart from the first to be run with a vehicle fitted with super singles while the second with twin tyres, have presented a rating rate quite different. Trial 3 (Super Singles) have developed rutting 1.5 times faster than Trial 4B, suggesting the less damaging effect of the twin tyres.

---

Regarding the “low-ground pressure” vehicle, however, the story is somewhat different. Despite applying a very high number of equivalent standard axes compared to other vehicles, and showing some of the largest ruts, the continuing rate of rutting is very low. This suggests that the vehicle does not prevent rut initiation but limits ongoing damage due to an inherent “kneading” action occasioned by the multiple wheels over the road width. Nevertheless, this does lead to some looser aggregate on the pavement surface which can collect between the wheel tracks allowing higher than expected rutting, even when the VSD reading is low.

The observations of the progress of rutting under the LGP vehicle and other trucks suggests that major contributors can be the axles that are overlooked – i.e. the drive axles in the case of the tractor pulling the LGP trailer and the steering axles of many of the trucks. In each case there is a high stress localised under a relatively small footprint (with added drive shear in the case of a driving axle). In the longer term, it would be advantageous to consider reduction of stresses under these axles.

### 5.2.3. Water added

A summary of the water added and its effect on wetting the pavement is given in Figure 5.26. The water depth applied in the trial represents the equivalent in mm of rainfall. The soaking depth is the amount sparged prior to the trial start, and the water depth the amount during the trial. Whenever there was rain during the test, a rain gauge was used to log the amount of water and this amount was included in the results presented below.

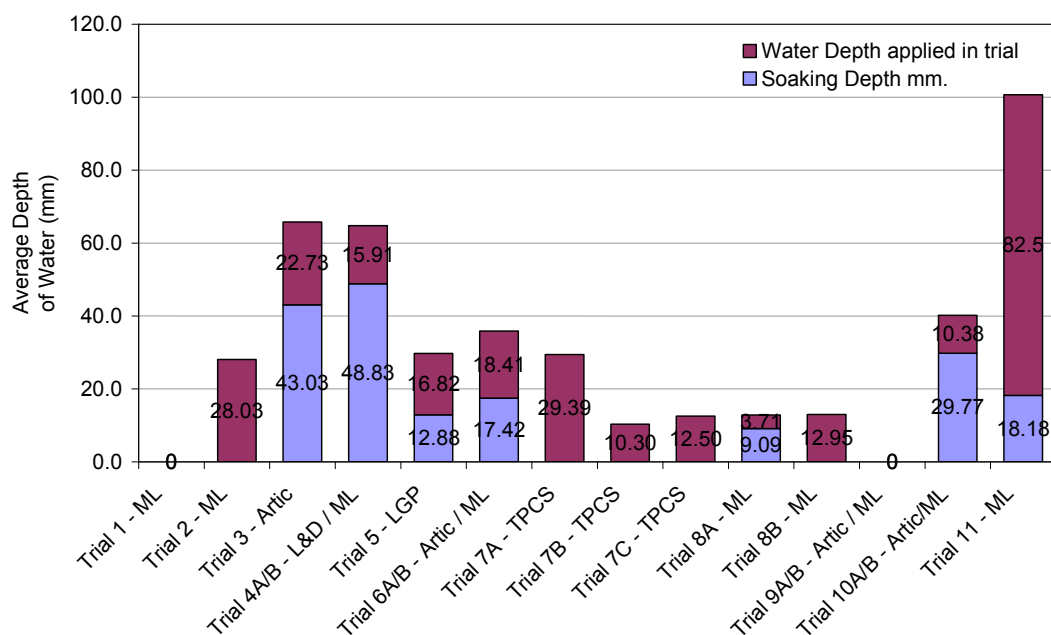


Figure 5.26 – Depth of water applied and achieved

Table 5.14 – Moisture contents of trial pavements

Trial	Material	Moisture Content	Remarks	Trial	Mat.	Moisture Content	Remarks
Trial 1	Type 1	N/A			Risk	5.50%	
Trial 2	Type 1	3.31%	Before the start of the Trial	Trial 7	Risk	5.00%	Right hand side wheel path
		4.02%	At the end of the trial		Risk	6.10%	Left hand side wheel path
Trial 3	Type 1	3.90%	Wheel Track - 0 to 7cm depth	Trial 8	Type 1	4.34%	
		5.70%	Rut bottom - Right hand wheel track		Type 1	5.17%	
Trial 4	Type 1	3.66%	Before the start of the Trial	Trial 9	Craignell	3.48%	
		4.14%	At the end of the trial	Trial 10	Craignell	5.26%	4.73% - at the end of the trial
Trial 5	Type 1	5.17%		Trial 11	Craignell	5.30%	at the end of test section construction
Trial 6	Risk	6.20%					

The moisture content of the pavement was also measured in most of the trials. Results for that are presented in Table 5.14. The results indicate a moisture content during wet trials ranging from 3.3 to 6.2%.

The combined analysis of Table 5.14 and Table 5.13 concerning the effect of moisture and materials points to some interesting results. There is a clear ranking of rutting from Risk (greatest) to Craignell (least). The relative moisture content has a lesser effect on rutting than the material chosen though some effect can be seen (e.g. compare Trials 9 & 10 where other parameters are constant).

Trial 2 (ranked 13<sup>th</sup> in Table 5.13) behaved somewhat better than Trial 1 (ranked 11<sup>th</sup>), had the same lorry and the same construction, but was “wet” instead of “dry”. One possible explanation is that, as the lorry trafficked the same wheel path during both trials, the initial movement that occurred in Trial 1 compacted the aggregate, limiting the opportunity for further deformation in Trial 2.

Furthermore, following the assessment of Figure 5.25, it is possible to notice that the majority of the rutting from Trial 1 came from the early passes, resulting in a rather stable behaviour after 20 passes of the vehicle. Trial 2, however, presents an increasing rate of rutting throughout the test, resembling incremental collapse behaviour of the material. The relatively small permanent deformation registered is a valid response to the very low moisture content for a “wet” trial (3.7% was sampled - lowest of all trials).

Considered this way, the wetter condition is, after all, associated with poorer performance. Because the behaviour in the first trial probably affected the performance in the second, more disturbance and reconstruction was included between subsequent trials.

#### 5.2.4. Instrumentation – $\epsilon$ mu coils

##### Trials 9 & 10

Trials 9 & 10 were instrumented with two sets of coils at the section T4. One monitored the rutting caused by an articulated lorry (“Artic”) fitted with super singles, and the other monitored the rutting in the Multi-Lift (ML) wheel path. At both sections, the instruments were installed at 75mm and 150mm depth. A “floating” coil also allowed monitoring the deformation in the near surface. Figure 5.27 summarizes the results from Trial 9 (dry condition), and Figure 5.28 the results from Trial 10 (wet condition).

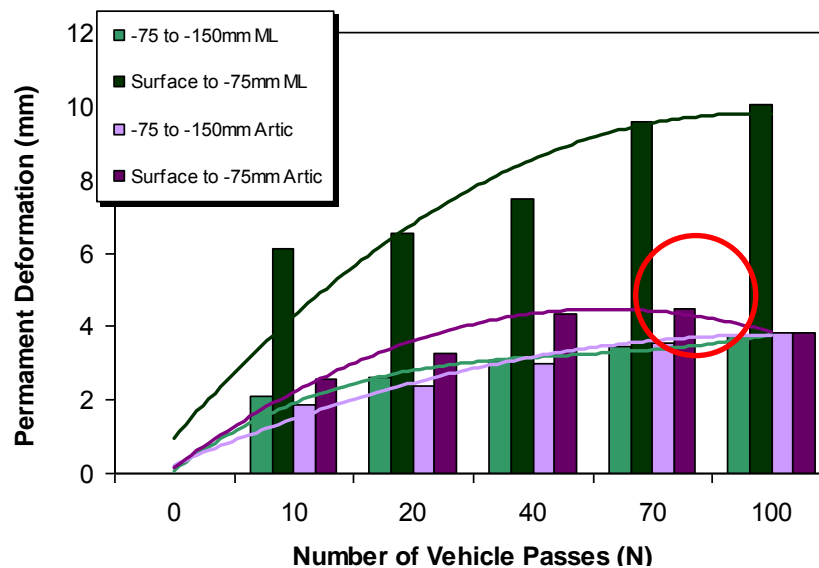


Figure 5.27 – Permanent deformation measured from instrumentation reading at Trial 9

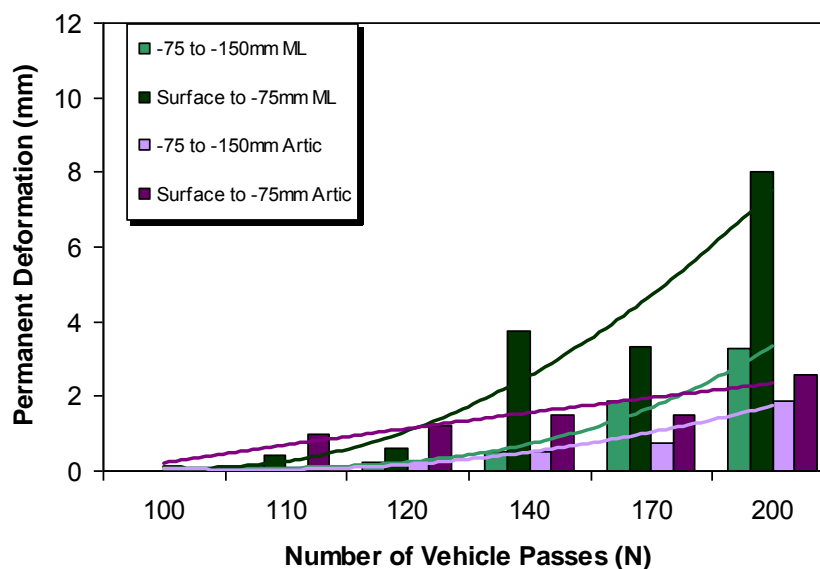


Figure 5.28 – Permanent deformation measured from instrumentation reading at Trial 10

The point highlighted with a circle in Figure 5.27 shows a decrease in the permanent deformation between the surface and a point 7.5mm deep at the wheel path on which the Artic vehicle was running. Whereas in the rut depth readings that could be interpreted as a possible reduction in the heave formed sideways to the wheel path, possibly due to lateral displacement of the driver in the test section or a running-off water erosion of the heaves, that could not be the reasoning while using coils. The most likely cause is the significant rotation of the uppermost coil due to the shear deformation within the aggregate of which the localised heave next to the wheel path is another symptom. This would reduce the signal transmitted between the coils that form an electromagnetic pair and would then be interpreted (in error) as an increase in spacing.

Figure 5.29 shows, in one single chart, the rutting development in Trials 9 and 10 according to the coil readings. It is evident that, with the addition of water in the interval between Trial 9 and Trial 10 (at 100 passes), the rutting rate starts to increase with no tendency to stop towards the end of the Trial, as occurred in Trial 9. It is also obvious that the Multi-Lift vehicle presents a higher rate of near-surface rutting, whereas the Artic tends to give a similar level of permanent deformation between the surface and mid-layer.

Table 5.15 summarizes the values found for the total permanent deformation including both the results from the instrumentation and the results from the profiling beam. To make the comparison, both values measured between the surface and 75mm depth and between 75mm to 150mm depth were summed. Differences in the results deduced from the two sources could be expected because the profiling beam measures the total permanent deformation of the pavement structure relative to a datum (concrete rails) whereas the coils measure relative difference between each other. Furthermore, the permanent deformation measured with the beam considers the heave effect (rut depth), whereas the coils effectively measure VSD. Figure 5.30 illustrates the great differences of both methods directly on a section profile from Trial 10.

The results suggest that most of the permanent deformations measured in Trials 9 & 10 (under the Multi-Lift trafficking) are within the top 150mm of the pavement (half the thickness of the surfacing layers). For the Artic results, the difference between the two methods of strain measurement is greater, therefore suggesting that a greater part of the deformation occurred below the level instrumented by the coils.

---

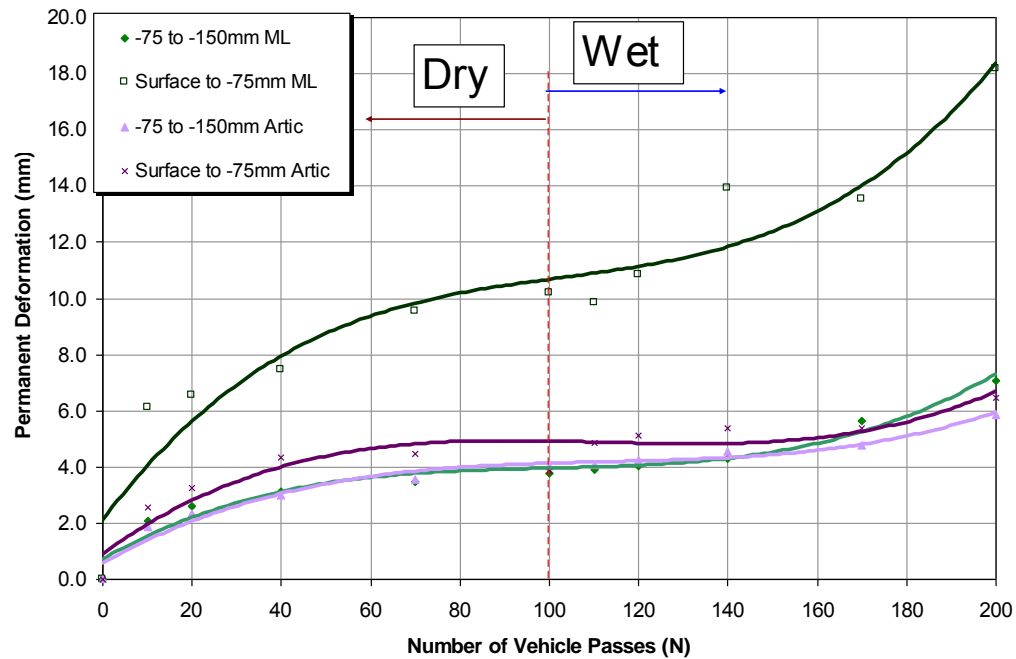
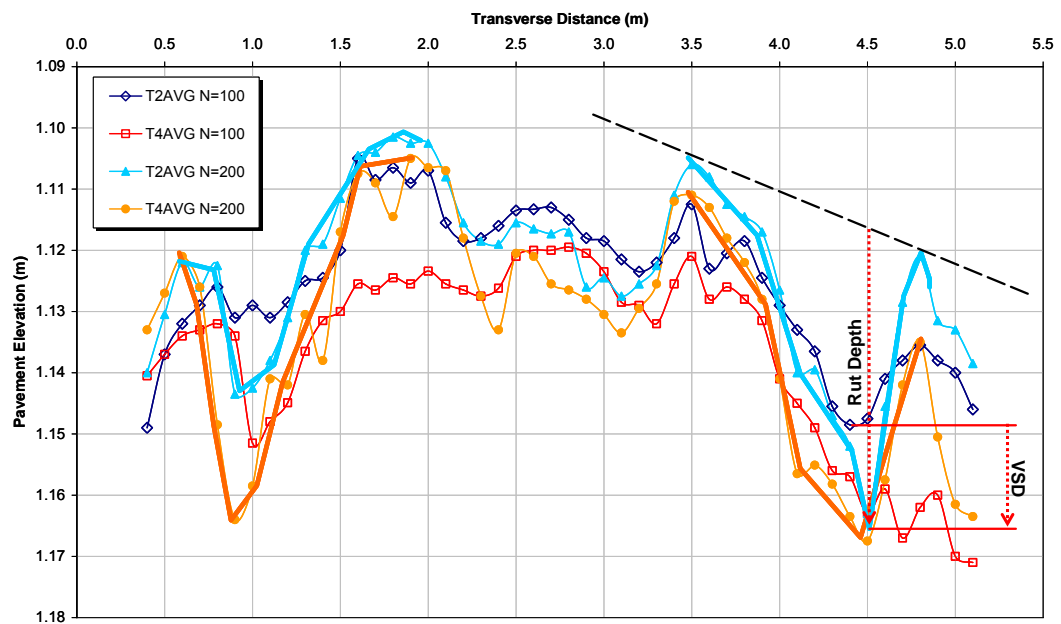
Figure 5.29–  $\epsilon$ mu coil reading at Trials 9 & 10

Figure 5.30 – Rut depth versus VSD measurement in Trial 10

Table 5.15 – Comparison between  $\epsilon$ mu coils and profiling beam for Trials 9 & 10

	Coil Reading				Profiling Beam			
	ML	Artic	ML	Artic	ML	Artic	ML	Artic
	Surface - 75mm		75 - 150mm		Total		Total	
<b>Trial 9 (Dry)</b>	10.1	3.8	3.7	3.8	<b>13.8</b>	<b>7.6</b>	<b>19.0</b>	<b>15.0</b>
<b>Trial 10 (Wet)</b>	8.0	2.6	3.3	1.9	<b>11.3</b>	<b>4.4</b>	<b>39.0</b>	<b>37.0</b>



Trial 11

Although three sets of coils were installed in Trial 11, only two sets provided reliable information. It was found that the method of installation, despite providing a more homogenous substrate to the coils ( $\epsilon$ mu coils were installed during the construction of the test section at appropriate depths), may have led to some rocking of the instruments during compaction. This may have caused some coils to lose their alignment and, therefore, to give biased readings.

Figure 5.31 shows the results for Trial 11. Sensors in both sets show higher readings for the coils positioned nearer the surface, although diverging somewhat in the results. Figure 5.32 helps to explain the differences in the readings from the profiling beam records. It is possible to notice that on section T4, where the first set of coils (CC1) was installed, less rutting occurred in the near-surface in comparison to section T2.

The total permanent deformation registered in Table 5.13 for Trial 11 is 67mm, whereas the coil instruments read a total permanent deformation of less than 15mm. As already discussed in the results for Trial 9 & 10, the main difference relies on the methods of analysis employed, that is, one uses rut depth while the other, VSD.

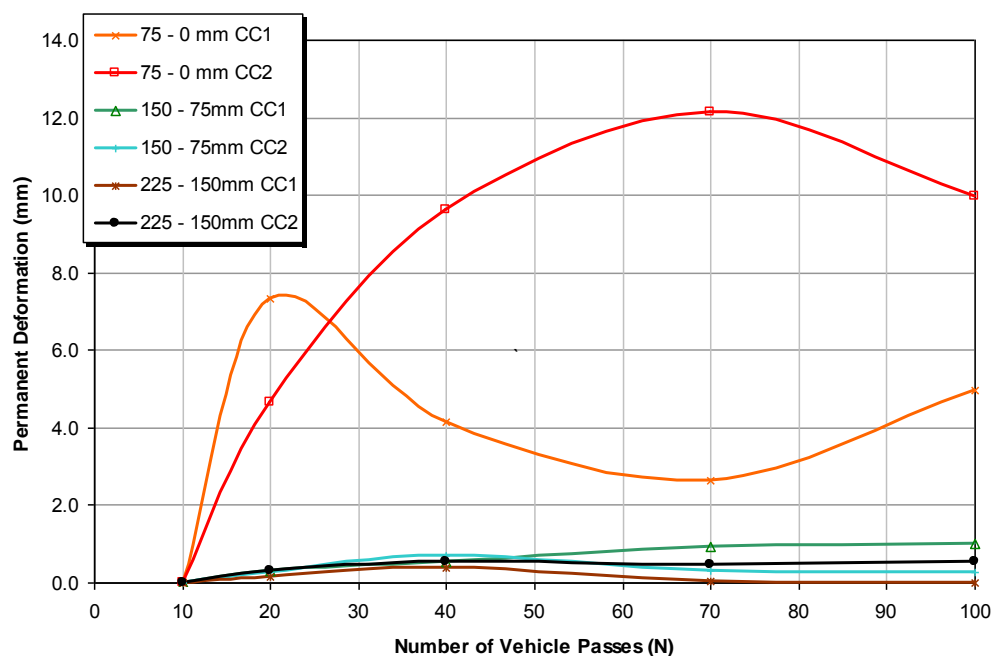


Figure 5.31 –  $\epsilon$ mu coil result for Trial 11

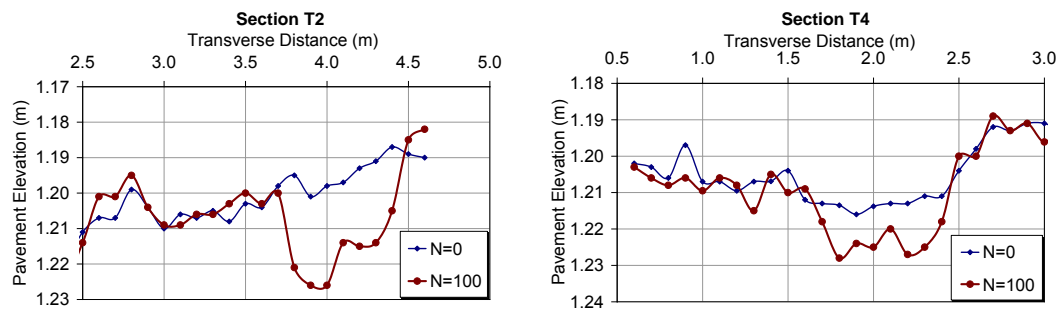


Figure 5.32 – Cross section reading using profiling beam at Trial 11

### 5.3. KEY FINDINGS

Despite the challenges encountered, many of which are unavoidable in a research study of the magnitude of the RUTT project that deals with in-service roads, many important conclusions may be drawn:

- It appears that most of the rutting occurring in the sites surveyed came shortly after their construction/resurfacing, leading to the assumption that workmanship may be a highly important variable. Lack of compaction of the layer could be one of the likely reasons for the high initial rutting rates.
- This assumption is reassured by the results obtained in the Reference Sections. Those which were properly compacted following the protocol established for the project - Linfer, Polmaddy and Waterside developed a lower rutting rate in contrast to Kilburn Hill and Till Hill for which a roller compactor wasn't available.
- Most of the reference sections behaved as expected, rutting less where the wedge of added aggregate was thickest, most of them presented a final level of permanent deformation close to that observed in the monitoring sections which had not been overlayed. Partly this is thought to be due to the difficulties of timely compaction. Such an observation reinforces the importance of compaction for good trafficking performance – a major finding from the previous trials at Risk [Forestry Enterprise 2004].
- From the observation that ruts are generally less in the reference sections where there is a greater thickness of aggregate over the old pavement, it may be concluded that the use of aggregate to the so-called “Swedish” specification is beneficial as, otherwise, greater rutting would be expected in the thicker aggregate overlay if the overlay aggregate was not fit for its purpose. This had often been the case in former

forest road construction [Forestry Enterprise 2004] where rutting had been observed to be greater in surface aggregate when the foundation was of a reasonable quality.

- The method proposed for determining the permanent deformation development due to wandering traffic on a non-level pavement, by the use of wheel path areas, seems to be a way forward in the analysis of rutting in unsealed roads.
- DCP readings supplied a good source of information for the determination of layers thickness but not as good a source from which to derive CBR, especially for surfacing layers. It seems that for the case of forest roads, because surfaces tend to be about 100 to 150mm thick, the DCP yields artificially low CBR values, possibly due to the disturbing effect of/on the cone tip in the first few centimetres of penetration.
- Although the material quality of the forest roads are sometimes judged to be of poor quality, those samples collected from the trial pits and tested in the laboratory presented characteristics of material close to standard quality, in many respects, for road construction. Gradings could be improved somewhat to provide more stable and less permeable materials.
- Use of the correlation relationships (Models 1 and 2) allow the conclusions that:
  - statistical models are not functionally related to any particular distress mechanism. Instead, they simply and numerically correlate rutting observations to input variables. Therefore, their validity beyond the sites surveyed during this project is, necessarily, somewhat conjectural.
  - for Model 1, permanent deformation has a high, yet, direct dependency on CBR (whereas an inverse relationship is logically required). This may indicate, simply, that better materials are utilised where higher traffic is anticipated by road owners.
  - for Model 2, with a far greater number of observations included, rainfall is seen to have the most significant influence on rutting.
- The protocol proposed for weather monitoring on site was successful and provided reliable data for the analysis.
- The portable aluminium beam used for cross section profiling proved to be an excellent tool for permanent deformation monitoring. The laser measuring device, although of high quality results, has a low reading speed which can lead to incorrect readings, in some cases due to user fatigue.

As far as the accelerated pavement trials went, the conclusions drawn from the work done in the Ringour Trials are:

---

- 
- The means of loading and the type of aggregate used have a bigger influence on rutting performance than the relative moisture level of the aggregate (over the range of moisture conditions considered).
  - Reducing overloading of trucks and controlling tyre pressures may be a more economic means of managing pavement deterioration than by using higher quality aggregates (the other meaningful option). This suggests that some kind of policing or QA (Quality Acceptance) system for truck operators might be worth considering.
  - The DCP, once again, proved its value for assessing pavement layer thickness and, except near the surface, aggregate quality. The mini-FWD, on the other hand, has arguably less applicability in determining likelihood of rutting.
  - As far as rutting is concerned the type of vehicle appears to make some difference, but it has not been clearly established which factors of the different types of vehicles are most important in controlling propensity to rut. This aspect could usefully be investigated further, especially given the variety of options available and the need to have vehicles that can easily manoeuvre in the forest environment.
  - The rigid-based dual tyre (Multi-Lift) vehicle produced similar or slightly greater rutting than vehicles equipped with super-single tyres. This observation is rather at variance with other studies and also with analytical computations of the different loading arrangements on damage generation. Possibly, this is a function of the rigid chassis arrangements of the dual-tyred vehicle employed resulting in uneven loading due to lack of flexibility, but this explanation has not been verified.
  - Rutting damage is not only generated by the rear or trailer tyres. Indeed, given the attention that has been paid to these by researchers and vehicle designers, there may be more damage generated by steer and/or drive axles.
  - For the LGP vehicle, principal rutting damage seems to be caused by the tractor unit that pulls it. However, after an initially high rate of rutting damage, the rate slows very significantly, probably because of a 'kneading' action caused by the offset LGP trailer tyres pressing heave back.
  - Taking the previous two points together, consideration could usefully be given to the optimum design of forest timber haulage vehicles so as to extend pavement life.
  - Near-surface rutting is the pre-eminent mode of rutting. This was, to some degree, inevitable given the solid quarry floor at the base of the trials, but the observation matches that made in an earlier study on forest roads in the same region.
  - Although all precautions were taken in order to avoid wander in the trafficking during the trials, some still existed. Furthermore, it seems that the superficial water that was
-

added during the trials facilitate the heaves at the edge of the wheel paths created throughout the trial to fade. Hence, it is noticeable during the analysis made for permanent deformation that the rut depths may not represent properly the amount of rutting occurred. As a suggestion, the procedure later developed to analyse the monthly monitoring section readings - Section 4.6 -, using the area developed under the wheel path, may lead to a better representation of the process.

The trials provided a strong source of results for wide use in future researches. Finally, although some of the objectives of this project have not been achieved to the extent that was initially hoped for, the overall study has enabled the effects of material and condition to be evaluated and the study also provide a reliable basis for future researches.

## 6. MECHANISTIC ANALYSIS

### 6.1. INTRODUCTION

For the purpose of Low Volume Road (LVR) pavement design, computations of the stress strain-state in granular layers, when performed, are often simplified so that only linear elastic conditions are assumed. The stress distribution allows for calculation of the resilient behaviour, but does not assist with calculation of the plastic deformation that classically takes place in the form of rutting. The purpose of the calculations performed now, is that by looking into the stress state of the pavement and using non-linear elastic modelling, associated to the shakedown concept, a pragmatic analysis of plastic deformation is possible.

In addition, with changing loading conditions on these roads – e.g. as a consequence of the introduction of Tyre Pressure Control Systems (TPCS) and super single tyres, as discussed in the previous chapters – more detailed analysis of such stress states is required, so that their effect can be analytically assessed.

This chapter aims to describe, mechanistically, the behaviour of a low volume road with a traditional pavement solution leading to the development of a design procedure. To accomplish that, mechanistic analyses using a conventional layered pavement structure are carried out in order to provide a better understanding of the elasto-plastic mechanisms at work in the constituent unbound granular material.

Typically LVR are largely constructed of a granular layer(s) which is(are) responsible for distributing the load onto the subgrade. The existing pavement design guides look into limiting the resilient strain at the top of the subgrade as a means of preventing its collapse due to excessive rutting.

From Section 2.4.1, there are basically four modes of rutting: a vertical depression only, which is self-stabilizing after traffic compaction takes place (Mode 0), rutting due to shear stresses in the aggregate layer(s) only (Mode 1), shear in the subgrade only (Mode 2) and a vertical depression due to particle wear and loss (Mode 3).

As Mode 0 failure is self-stopping once adequate compaction has taken place and Mode 3 can be addressed by particle strength requirements, independent of the stress analysis, both of these mechanisms can be discounted for the purpose of the analysis covered in

---

this chapter. Hence, mechanisms of rutting such as Modes 1 & 2 will be further discussed in Chapter 7, based on the findings presented next.

## 6.2. ANALYSIS PERFORMED

For the analysis of the proposed study, five key parameters were considered - Figure 6.1. Load arrangements were studied in terms of the use of dual tyres or super singles. Not only do they represent typical loading conditions, but from an analytical point of view a considerably different stress condition applied to the pavement. A dual tyred axle will spread the same load over the same total area - assuming equal tyre pressures; nonetheless, instead of having the load concentrated into two spots (super singles), it will distribute more evenly into four spots in a dual tyre arrangement.

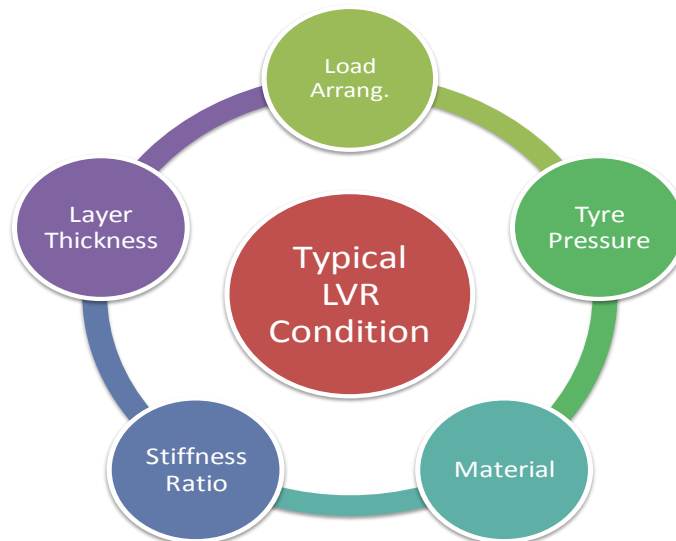


Figure 6.1 – Parameters considered for the analysis carried out

The variation in effect due to two different tyre pressure levels was included so as to look at the possibility of using TPCS as an option to reduce rutting in Low Volume Roads. Hence, typical tyre pressures of 800kPa (116psi) and 400kPa (58psi), available in commercial TPCS systems were used (Table 3.3).

A two layered pavement structure was analysed composed of an unbound granular layer used as the trafficking layer and a semi-infinite subgrade. Three different granular materials ranging from poor to good quality specifications were chosen to represent the base layer.

In accordance with convention, rutting will be assessed in the subgrade in terms of an allowable vertical stress on its top. As the variation in the stress level will be most

dependant on the stiffness ratio between the moduli ( $E$ ) in the base layer and in the subgrade ( $E_{bas}/E_{sub}$ ), it is a sound assumption that by varying the ratios  $E_{bas}/E_{sub}$ , not only can three different UGM ranges be assessed but also a range of subgrade qualities.

Finally, in order study the aggregate layer thickness, a ratio between the thickness of the aggregate layer (UGL) and the load radius (AggThick/LoadRadius) were used. Like the stiffness ratio, all the values were normalized so that the response of every structure could be easily interpolated from the results.

Three different materials were selected from the University of Nottingham database (see Section 6.4.2). A total of 180 different combinations of load arrangement, tyre pressure, unbound granular material, stiffness ratio between base & subgrade and the ratio between base thickness & loaded radius - which is a function of the tyre pressure - were computed. Below are the input parameters and their ranges:

- Loading: dual tyres, super singles
- Tyre pressure: 400kPa, 800kPa
- Materials: NIP, NIG, CAF
- Ratio between stiffness of base and sub-base ( $E_{bas}/E_{sub}$ ): 2, 4 & 8
- Ratio between aggregate layer (UGL) and loading radius ( $r$ ): 1.0, 1.3, 1.7, 2.5 & 3.5

As usual in LVRs, the UGL was taken to be the trafficked layer. The thickness of the UGL was between 9.5 and 66.5cm (Figure 6.3) and the subgrade resilient modulus ranged from 45-350MPa. All problems were analyzed and their primary input values are summarized in Appendix G.

All problems were numbered according to the material code first, followed by a sequential number - [material code]xx - with the following logic:

- Analysis were grouped into batches of 5 runs - as enabled by the Kenlayer software, with a Run ID. The IDs from 1 to 3 represented analysis with Dual Tyres at 400kPa of tyre inflation. IDs from 4 to 6, Dual tyres at 800kPa; IDs 7 to 9, Super Singles at 400kPa and, IDs 10 to 12 were those with Super Singles at 800kPa of tyre inflation.
- Each Run ID, composed of 5 problems, had a specific stiffness ratio ( $E_{bas}/E_{sub}$ ). Each problem had, then, a specific UGL thickness as defined by the ratios 1.0 to 3.5.

The complete 'experimental' matrix is illustrated by Figure 6.2.



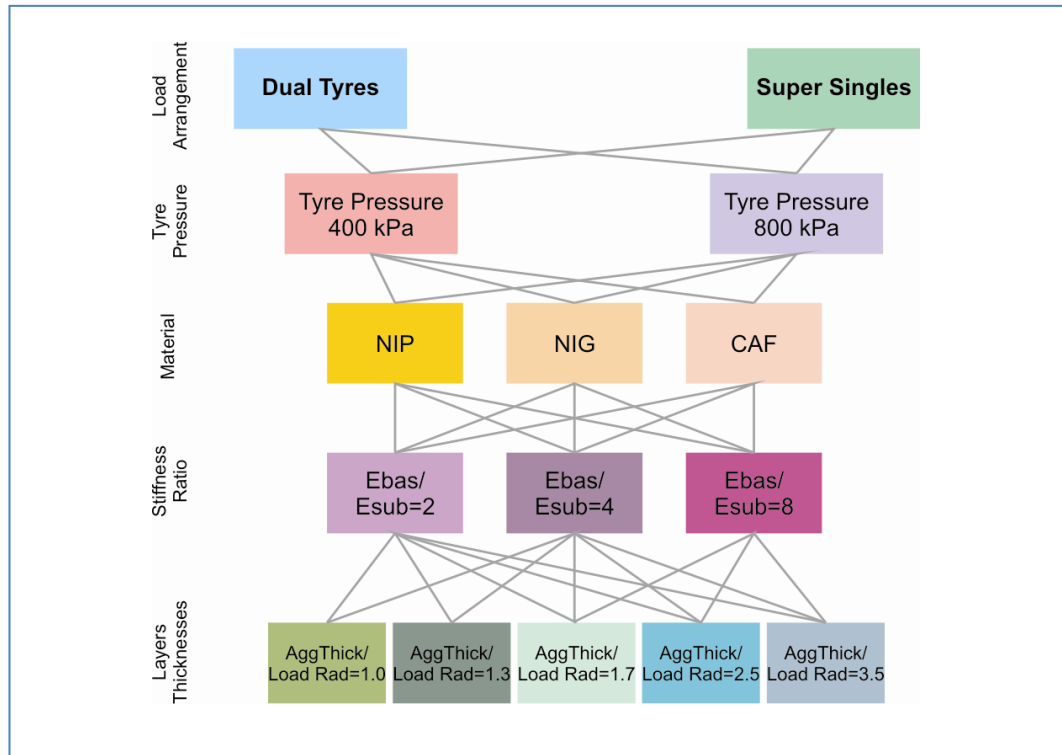


Figure 6.2 – Experiment matrix – total of 180 analyses

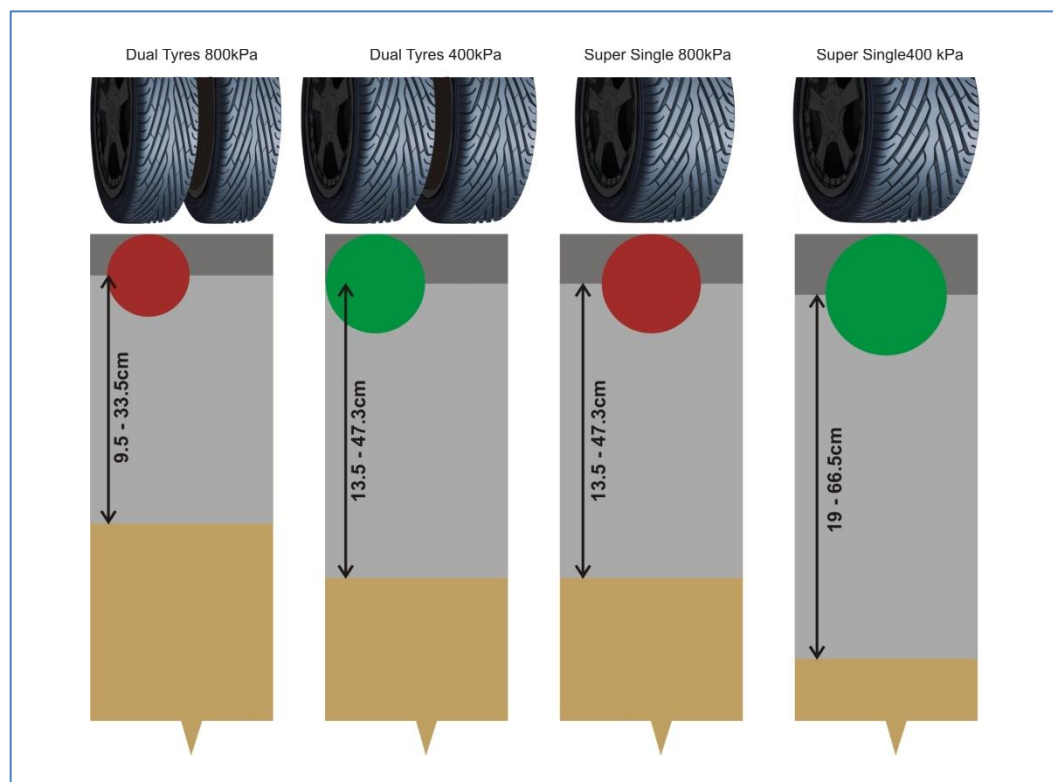


Figure 6.3 – Granular layer thickness evaluated varying as a function of load arrangement and tyre pressure

The computer program used was the Kenlayer, from the Kenpave package. The software was developed by Huang [2003]. One advantage of the Kenlayer program is its greater capability of treating UGM as a non-linear elastic material. It achieves this by repeatedly using the  $k$ - $\theta$  model (Equation 8) to estimate layer stiffness. This allows the computation of the elastic modulus of the layer according to the stress state it is subject to (due to external loading and geostatic forces). However, this non-linearity is only partial as each layer will have the same value of resilient modulus across its complete width, even though the stresses will vary across that width.

Despite this benefit, the computational framework does not prevent the computation of tensile stresses which may lead to erroneous values at certain stress points. Kenlayer doesn't provide a cut off limit to deal with the tensile stress computed in the granular layers. Hence, tensions may be recorded, for example, at the base of stiffer layers laying on top of softer subgrade.

Nonetheless, the stress-dependent stiffness provided by the  $k$ - $\theta$  model results in the material's stiffness dropping where tension is computed, thereby allowing strain and some consequent re-distribution of the tensile stress to take place. In addition, the distortions caused by the computations of the tensile stress is minimized by the correction Kenlayer performs with the so-called "Method 3", on which the negative or small horizontal stresses are modified according to the Mohr-Coulomb theory of failure, so that the strength of the material is not to be exceeded. This "method" is selected when PHI ( $\phi$ ) value is greater than zero and smaller than  $90^\circ$  [Huang 2003].

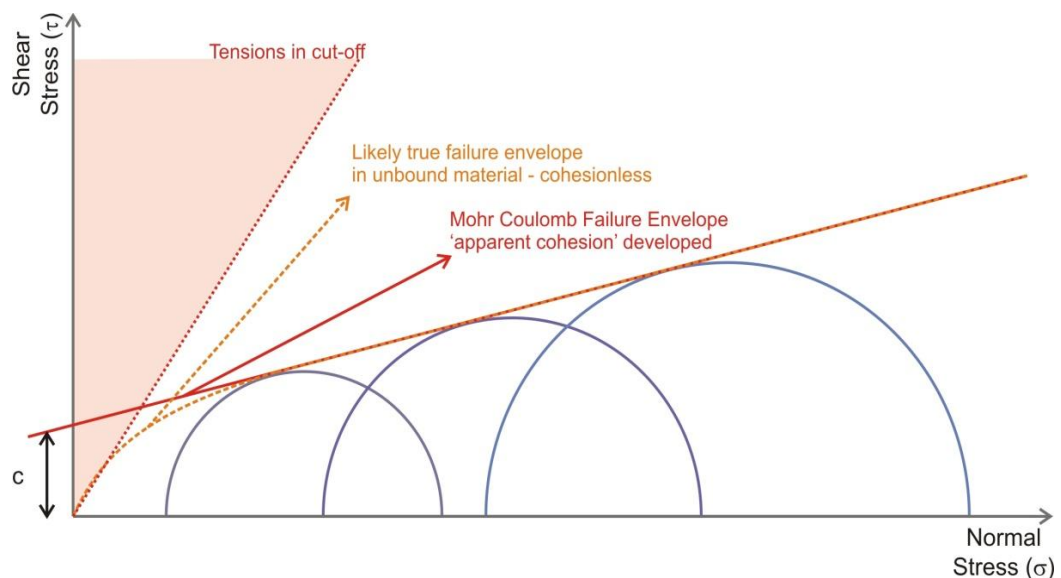


Figure 6.4 – Mohr Coulomb cohesion intercept

Notwithstanding this feature, unreasonable negative stresses may be permitted by the Mohr-Coulomb failure envelope as it includes an apparent cohesion intercept in granular materials that may not be realistic at low stress levels. A likely failure envelope in a shear stress x normal stress space is pictured in Figure 6.4. Because of the linearity of the envelope proposed by Mohr-Coulomb, a false cohesion is determined, allowing the material to undergo stress within the tensile cut-off limit. Consequently, the Mohr-Coulomb model tends to predict a larger tensile strength than that observed experimentally for granular materials when  $c > 0$ , mainly at lower stress levels.

### 6.3. METHODOLOGY

All calculations performed in order to achieve all of the 180 analysis indicated in the experimental matrix (Figure 6.2) were guided by a sequential line of actions, which can be summarized as follows:

#### Input parameters

- i. The stress dependant non-linear model considered for the granular materials was the  $k-\theta$  model; parameters used were those in Table 6.5. The subgrade was modelled as linear elastic.
  - ii. All materials were assumed to have the same behaviour throughout the year, not developing any seasonal variation (one period).
  - iii. A total number of cycles of 80 were adopted for numerical integration with a convergence tolerance of 0.1% being set.
  - iv. Layers were considered to be fully bonded.
  - v. For the output of the stress and strain values, analysis was requested at a total of 180 points of analysis (15 variable depth points x 12 lateral Y displacement points)
  - vi. Poisson Ratios of the granular layers were considered to be 0.35 and a value of 0.45 was adopted for subgrades. The bulk unit weight used was  $19\text{kN/m}^3$  for all materials.
  - vii. Contact pressure and radius are as discussed in Section 6.4.1.
  - viii. A maximum number of 15 iterations was requested for the nonlinear analysis. Typically convergence for the problems run were achieved after 5 to 10 iterations. A tolerance of 1% was set as the default for convergence.
  - ix. The depth considered for computing the elastic modulus of the granular layer was set to be at the mid-depth, as recommended by the software. Although any point
-

in a nonlinear granular layer can be used for computing the elastic modulus, Huang [2003] suggests that the  $z$  coordinate at the mid-depth of each layer be used for Methods 1 and 3, in order to minimize the tensile stress development. Likewise, the  $Y$  coordinate to equate the modulus was considered to be at an equal distance as the mid-depth.

- x. Finally,  $\phi$  was attributed as per the Mohr-Coulomb failure parameter in Table 6.5. A  $\phi$  greater than 0 and smaller than  $90^\circ$  will trigger Method 3 in the program to attempt for tensile correction in the granular layer.

All input parameters are exemplified in Figure 6.5 as shown in the heading of a result text file from the program.

#### pxq plots calculations

The output results were computed, in terms of the stress invariants  $p$  and  $q$ , from the principal stresses obtained in the calculations.  $p$  values were calculated as per Equation 1 while  $q$  values from Equation 2 & Equation 3. In addition, some filtering, as follows, was required in order to make further adjustments to the tensile stress calculated.

- i. Normal stresses were used to equate  $p$  &  $q$  values for every point of analysis, as represented in Table 6.1;  $p/q$  ratio was then equated as per Table 6.2.
- ii. If  $q/p > 3$  or  $q/p < 0$ , the values were disregarded. For the first condition ( $q/p > 3$ ) this implies that a tensile stress was being reported. The second condition ( $q/p < 0$ ) also indicates a negative stress being computed, what is likely to be a miscalculation derived from tensile stress developed and not redistributed. Table 6.3 shows an example of  $p$  and  $q$  values considered following removal of impermissible values. These may be compared with those initially reported in Table 6.1.
- iii. For each problem,  $p$  and  $q$  results were fitted into a polynomial of 6th order by the least squares method built-in in Microsoft® Excel. Coefficients were annotated.
- iv. Using a numerical secant method aided by an Excel macro spreadsheet, the intersection between polynomial with a line crossing the  $pxq$  space from (250,0) to (0,250)<sup>5</sup> was determined.
- v. the Drucker-Prager yield surface was then added to the plot and the proximity of the stress state to it was assessed by means of a variable, here called “ $S$ ” and described further in the next Section.

---

<sup>5</sup> a discussion for the (250,0) to (0,250) line is included in Chapter 7.

A typical p x q plot after all steps carried out is shown in Figure 6.6. Appendix includes the plots obtained for the whole experimental matrix.

Figure 6.5 – Example of Kenlayer output file with input parameters - NIG1 - Problem 1

```

TITLE -NIG1

MATL = 2 FOR NONLINEAR ELASTIC LAYERED SYSTEM
NDAMA = 0, SO DAMAGE ANALYSIS WILL NOT BE PERFORMED
NUMBER OF PERIODS PER YEAR (NPY) = 1
NUMBER OF LOAD GROUPS (NLG) = 1
TOLERANCE FOR INTEGRATION (DEL) -- = 0.001
NUMBER OF LAYERS (NL)----- = 2
NUMBER OF Z COORDINATES (NZ)----- = 15
LIMIT OF INTEGRATION CYCLES (ICL)- = 80
COMPUTING CODE (NSTD)----- = 9
SYSTEM OF UNITS (NUNIT)----- = 1

Length and displacement in cm, stress and modulus in kPa, unit weight in kN/m^3, and temperature in C

THICKNESSES OF LAYERS (TH) ARE : 13.5
POISSON'S RATIOS OF LAYERS (PR) ARE : 0.35 0.45
VERTICAL COORDINATES OF POINTS (ZC) ARE: 0 1 3 5 8 13.5 17 23 30 34 47 60 80 150 200
ALL INTERFACES ARE FULLY BONDED

FOR PERIOD NO. 1 LAYER NO. AND MODULUS ARE : 1 7.151E+04 2 2.200E+05

LOAD GROUP NO. 1 HAS 2 CONTACT AREAS
CONTACT RADIUS (CR)----- = 13.5
CONTACT PRESSURE (CP)----- = 400
NO. OF POINTS AT WHICH RESULTS ARE DESIRED (NPT)-- = 12
WHEEL SPACING ALONG X-AXIS (XW)----- = 0
WHEEL SPACING ALONG Y-AXIS (YW)----- = 34.5

RESPONSE PT. NO. AND (XPT, YPT) ARE:
1 0.000 0.000
2 0.000 9.500
3 0.000 13.500
4 0.000 17.250
5 0.000 19.000
6 0.000 30.000
7 0.000 50.000
8 0.000 80.000
9 0.000 100.000
10 0.000 120.000
11 0.000 150.000
12 0.000 200.000

NUMBER OF NONLINEAR LAYERS (NOLAY)----- = 1
MAXIMUM NUMBER OF ITERATIONS FOR NONLINEAR ANALYSIS (ITENOL) = 15

LAYER NUMBER (LAYNO) AND SOIL TYPE (NCLAY) ARE: 1 0

Z COORDINATES (ZCNOL) FOR COMPUTING ELASTIC MODULUS ARE: 6.75
R COORDINATE (RCNOL) FOR COMPUTING ELASTIC MODULUS ----- = 0
X COORDINATE (XPTNOL) FOR COMPUTING ELASTIC MODULUS ----- = 0
Y COORDINATE (YPTNOL) FOR COMPUTING ELASTIC MODULUS ----- = 6.75
SLOPE OF LOAD DISTRIBUTION (SLD) ----- = 0
TOLERANCE (DELNOL) FOR NONLINEAR ANALYSIS ----- = 0.01
RELAXATION FACTORS (RELAX) FOR NONLINEAR ANALYSIS OF EACH PERIOD ARE: 0.5

UNIT WEIGHT OF LAYERS (GAM) ARE: 19 19

LAYER NO. = 1 NCLAY = 0 K2 = 0.29 K0 = 0.54

LAYER NUMBER AND GEOSTATIC STRESS (GEOS) ARE: 1 1.28250

FOR PERIOD 1 LAYER NO. = 1 NCLAY = 0 PHI = 46 KI = 71510

FOR LOAD GROUP 1 LAYER NO. AND X COORDINATE FOR COMPUTING MODULUS ARE: 1 0
FOR LOAD GROUP 1 LAYER NO. AND Y COORDINATE FOR COMPUTING MODULUS ARE: 1 6.75
PERIOD NO. 1 LOAD GROUP NO. 1

AT ITERATION 1 LAYER NO. AND MODULUS ARE : 1 7.151E+04
AT ITERATION 2 LAYER NO. AND MODULUS ARE : 1 2.606E+05
AT ITERATION 3 LAYER NO. AND MODULUS ARE : 1 3.529E+05
AT ITERATION 4 LAYER NO. AND MODULUS ARE : 1 3.980E+05
AT ITERATION 5 LAYER NO. AND MODULUS ARE : 1 4.201E+05
AT ITERATION 6 LAYER NO. AND MODULUS ARE : 1 4.309E+05
AT ITERATION 7 LAYER NO. AND MODULUS ARE : 1 4.362E+05
AT ITERATION 8 LAYER NO. AND MODULUS ARE : 1 4.388E+05

LAYER NUMBER AND THREE NORMAL STRESSES INCLUDING GEOSTATIC STRESSES
1 326.508 94.799 110.619
LAYER NUMBER AND ADJUSTED THREE NORMAL STRESSES INCLUDING GEOSTATIC
STRESSES FOR COMPUTING ELASTIC MODULUS ARE:
1 326.508 94.799 110.619

```

Table 6.1 – P&amp;Q Values as obtained equated from the principal stresses output

	P											
	Y=0	Y=9.5	Y=13.5	Y=17.25	Y=19	Y=30	Y=50	Y=80	Y=100	Y=120	Y=150	Y=200
Z=0	339	317	178	21	115	415	117	-6	-3	0	-1	1
Z=1	375	352	196	63	77	372	54	-3	-1	0	0	0
Z=3	305	266	168	102	116	300	82	-1	-1	0	0	0
Z=5	240	202	144	111	119	235	80	1	0	0	0	0
Z=8	154	133	109	97	100	151	64	4	1	1	0	0
Z=13.5	18	35	45	50	49	24	28	9	3	1	1	0
Z=17	94	94	91	90	90	96	55	7	2	1	0	0
Z=23	66	69	68	68	68	68	42	8	3	1	1	0
Z=30	46	50	50	50	50	49	32	9	4	2	1	0
Z=34	39	42	43	43	43	41	28	9	4	2	1	0
Z=47	24	26	26	26	26	25	19	8	5	3	1	0
Z=60	16	17	18	18	18	17	14	7	4	3	1	1
Z=80	10	10	10	10	10	10	9	6	4	3	2	1
Z=150	3	3	3	3	3	3	3	2	2	2	1	1
Z=200	2	2	2	2	2	2	2	2	1	1	1	1

	Q											
	Y=0	Y=9.5	Y=13.5	Y=17.25	Y=19	Y=30	Y=50	Y=80	Y=100	Y=120	Y=150	Y=200
Z=0	43	98	135	185	153	31	82	24	10	5	2	1
Z=1	44	93	228	118	126	55	91	19	8	4	2	1
Z=3	129	182	199	105	134	138	164	12	6	3	2	1
Z=5	196	222	180	92	121	202	193	5	3	2	1	1
Z=8	254	237	176	116	134	252	198	6	2	1	1	0
Z=13.5	324	265	227	213	216	310	165	24	8	3	1	0
Z=17	154	131	116	110	111	148	111	17	6	3	1	0
Z=23	125	115	110	108	108	122	94	22	9	4	2	1
Z=30	99	98	96	96	96	99	77	24	11	5	2	1
Z=34	87	88	88	88	88	88	69	25	12	6	3	1
Z=47	60	63	64	64	64	62	50	24	13	7	4	1
Z=60	44	46	46	46	46	45	37	21	13	8	4	2
Z=80	28	29	30	30	30	29	25	17	12	8	5	2
Z=150	9	10	10	10	10	9	9	8	7	6	4	2
Z=200	5	5	5	6	6	5	5	5	4	4	3	2

Table 6.2 – P/Q Ratio calculated in RAD (Red cells - ratio&gt;1.249 ; blue cells - ratio &lt;0)

	Y=0	Y=9.5	Y=13.5	Y=17.25	Y=19	Y=30	Y=50	Y=80	Y=100	Y=120	Y=150	Y=200
Z=0	0.13	0.30	0.65	1.46	0.92	0.07	0.61	-1.33	-1.31	1.49	-1.27	0.70
Z=1	0.12	0.26	0.86	1.08	1.02	0.15	1.04	-1.40	-1.42	-1.49	-1.49	-1.16
Z=3	0.40	0.60	0.87	0.80	0.86	0.43	1.11	-1.47	-1.46	-1.51	-1.55	-1.43
Z=5	0.68	0.83	0.90	0.69	0.79	0.71	1.18	1.42	1.54	1.53	1.50	1.55
Z=8	1.03	1.06	1.02	0.88	0.93	1.03	1.26	1.05	1.03	1.06	1.20	1.35
Z=13.5	1.51	1.44	1.37	1.34	1.35	1.49	1.40	1.23	1.22	1.18	1.09	0.99
Z=17	1.02	0.95	0.91	0.89	0.89	1.00	1.11	1.18	1.20	1.18	1.13	1.05
Z=23	1.09	1.03	1.01	1.01	1.01	1.06	1.15	1.20	1.22	1.21	1.18	1.13
Z=30	1.13	1.10	1.09	1.09	1.09	1.12	1.17	1.22	1.23	1.23	1.21	1.17
Z=34	1.15	1.13	1.12	1.12	1.12	1.14	1.18	1.22	1.23	1.23	1.22	1.19
Z=47	1.19	1.18	1.18	1.18	1.18	1.19	1.21	1.23	1.24	1.24	1.23	1.22
Z=60	1.21	1.21	1.21	1.21	1.21	1.21	1.22	1.24	1.24	1.25	1.24	1.23
Z=80	1.23	1.23	1.23	1.23	1.23	1.23	1.24	1.25	1.25	1.25	1.25	1.24
Z=150	1.25	1.25	1.25	1.25	1.25	1.25	1.26	1.26	1.26	1.26	1.26	1.25
Z=200	1.26	1.26	1.26	1.26	1.26	1.26	1.26	1.26	1.26	1.26	1.26	1.26

Red cells represent the p/q ratios greater than 1:3 ( $72^\circ \approx 1.249$  RAD) and the blue cells represent p/q ratios smaller than zero.

Table 6.3 – Values considered for p x q plot after filtering

	P											
	Y=0	Y=9.5	Y=13.5	Y=17.25	Y=19	Y=30	Y=50	Y=80	Y=100	Y=120	Y=150	Y=200
Z=0	339	317	178	0	115	415	117	0	0	0	0	1
Z=1	375	352	196	63	77	372	54	0	0	0	0	0
Z=3	305	266	168	102	116	300	82	0	0	0	0	0
Z=5	240	202	144	111	119	235	80	0	0	0	0	0
Z=8	154	133	109	97	100	151	0	4	1	1	0	0
Z=13.5	0	0	0	0	0	0	0	9	3	1	1	0
Z=17	94	94	91	90	90	96	55	7	2	1	0	0
Z=23	66	69	68	68	68	68	42	8	3	1	1	0
Z=30	46	50	50	50	50	49	32	9	4	2	1	0
Z=34	39	42	43	43	43	41	28	9	4	2	1	0
Z=47	24	26	26	26	26	25	19	8	5	3	1	0
Z=60	16	17	18	18	18	17	14	7	4	3	1	1
Z=80	10	10	10	10	10	10	9	6	4	0	2	1
Z=150	0	0	0	0	0	0	0	0	0	0	0	0
Z=200	0	0	0	0	0	0	0	0	0	0	0	0

	Q											
	Y=0	Y=9.5	Y=13.5	Y=17.25	Y=19	Y=30	Y=50	Y=80	Y=100	Y=120	Y=150	Y=200
Z=0	43	98	135	0	153	31	82	0	0	0	0	1
Z=1	44	93	228	118	126	55	91	0	0	0	0	0
Z=3	129	182	199	105	134	138	164	0	0	0	0	0
Z=5	196	222	180	92	121	202	193	0	0	0	0	0
Z=8	254	237	176	116	134	252	0	6	2	1	1	0
Z=13.5	0	0	0	0	0	0	0	24	8	3	1	0
Z=17	154	131	116	110	111	148	111	17	6	3	1	0
Z=23	125	115	110	108	108	122	94	22	9	4	2	1
Z=30	99	98	96	96	96	99	77	24	11	5	2	1
Z=34	87	88	88	88	88	88	69	25	12	6	3	1
Z=47	60	63	64	64	64	62	50	24	13	7	4	1
Z=60	44	46	46	46	46	45	37	21	13	8	4	2
Z=80	28	29	30	30	30	29	25	17	12	0	5	2
Z=150	0	0	0	0	0	0	0	0	0	0	0	0
Z=200	0	0	0	0	0	0	0	0	0	0	0	0

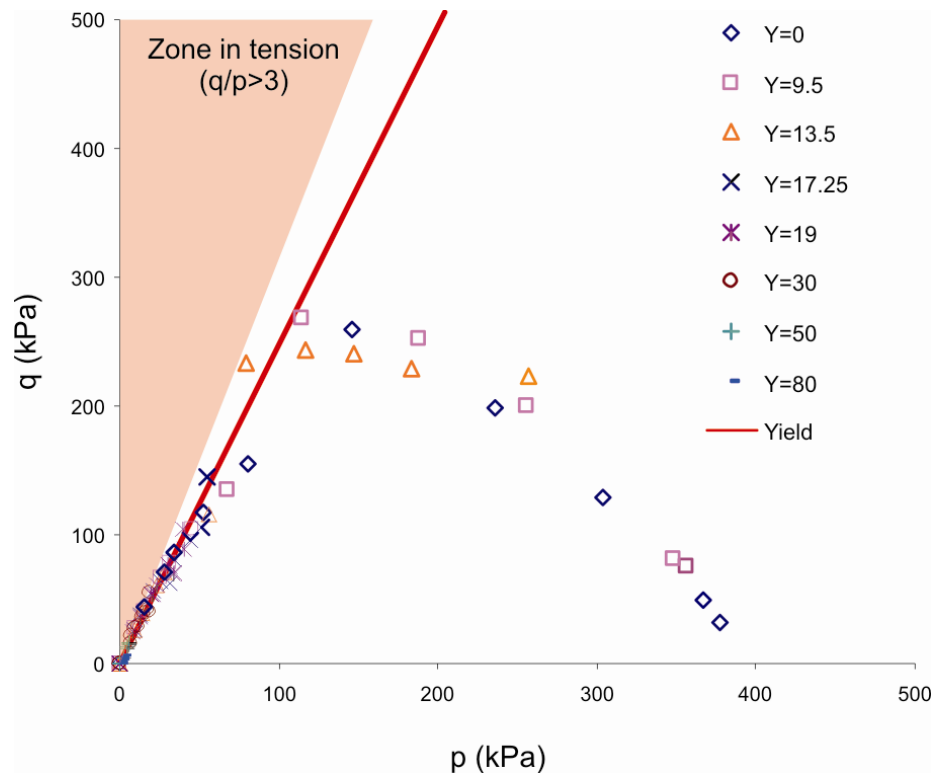


Figure 6.6 – Typical plot of computed stresses in the pavement

## 6.4. PARAMETER INPUTS

### 6.4.1. Loading arrangements

The loading arrangements used were those representative of typical trucks on LVRs in the United Kingdom. Equivalent radii were obtained by distributing 45kN wheel loads over circular areas at the tyre pressure, circular loads being the Kenlayer input mode. The distances used between tyres were based on measurements made in pavement trials in Scotland described in Section 4.3.2. Dual tyres are based on a typical tyre designation 295/80R22.5 and the “super singles” on 385/65R22.5 tyres. Figure 6.7 illustrates the radii and load position for all loading arrangements studied.

Arguably, the tyre pressure distribution may not be uniform [COST 334 Addis 2000] nor circular. Huang [2003] suggest that a more approximate tyre print would be best described by a two semi-circles connected by a rectangular area. Despite the common sense in the argument of non-uniform tyre pressure distribution in non-perfect circular shape, these considerations are too complex to be readily modelled. Possibly, an advanced Finite Element Analysis (FEA) tool such as Ansys® or Abaqus® could achieve this. The use of such tools, however, can be rather complex and time-consuming and the required input variables not simple to determine.

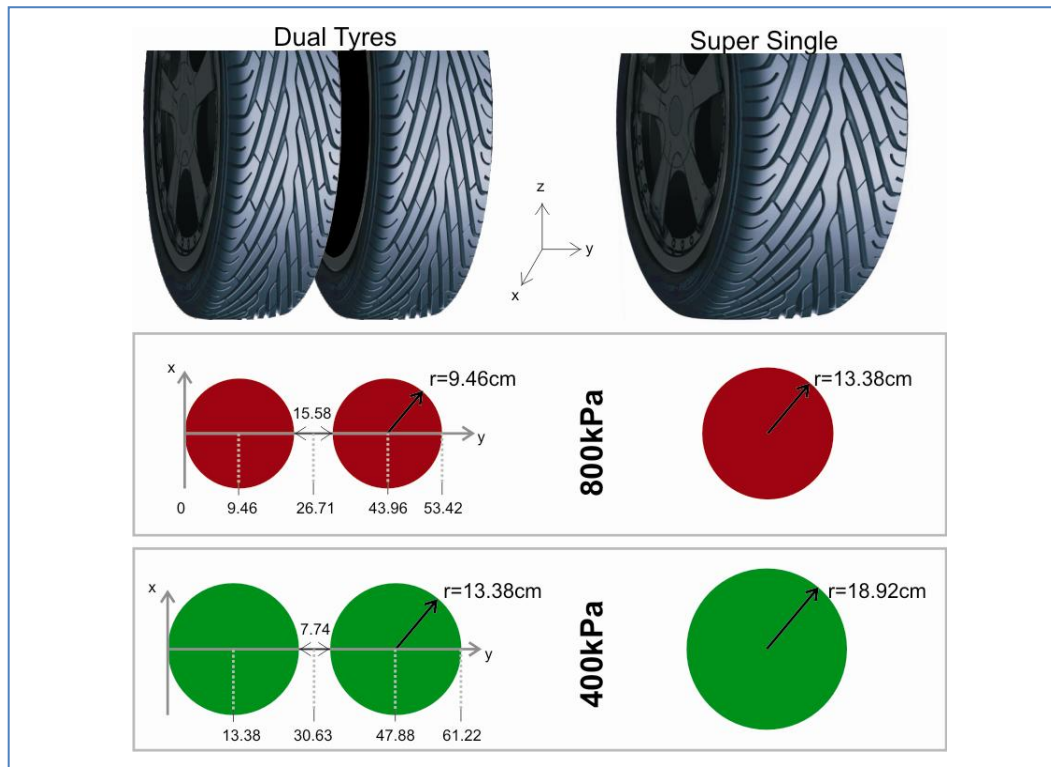


Figure 6.7 – Equivalent, circular loaded wheel areas



In regard to the pressures chosen, although lorries fitted with TPCS may run with tyre pressures as low as 200kPa and as high as 900kPa, pressures of 400kPa and 800kPa were deemed to be closer to the operational values. These values are supported by the trials run at Ringour in Scotland and by the operational presets given in Table 3.3.

#### 6.4.2. Materials

As it was not possible to test the materials used in the full scale trials in Scotland for repeated load characteristics in order to determine the resilient modulus and the other necessary parameters for this analysis, materials were selected from the University of Nottingham database [Arnold 2004]. This also enabled a wider range of material behaviour to be considered.

Arnold [2004] studied the rutting of granular pavements by examining the permanent deformation behaviour of granular and subgrade materials used in a Northern Ireland, United Kingdom pavement field trial and in accelerated pavement tests at CAPTIF (Transit New Zealand's test track) located in Christchurch New Zealand.

The parameters needed for the analysis were available and provided a comprehensive source of information. Six materials were assessed for a choice of three. Table 6.4 summarizes the materials considered along with a brief description.

Characterization of the materials by Arnold [2004] and others included particle size distribution, monotonic shear failure triaxial tests and repeated load triaxial test. The Drucker-Prager failure surface had been determined as well as the shakedown boundaries and the non-linear parameters for the  $k-\theta$  model.

Figure 6.8 shows the resilient behaviour of the tentative materials considered for analysis from Arnold's database over a range of sum of stresses,  $\theta$ , between 0 to 900kPa. Figure 6.9 shows the shakedown ranges boundaries for the same materials; for comparison, the yield envelope is also shown along with the shakedown limits.

The linear functions indicating the stress boundaries between shakedown Ranges A, B and C are summarised in Table 6.5 in terms of intercept ( $d$ ) and slope ( $\beta$ ) along with the Mohr-Coloumb parameters,  $c$  and  $\phi$ . Range A, B & C are fields of stress in which permanent deformation under repeated loading is stabilising, incrementally increasing or de-stabilising, respectively (see Section 2.5). The range boundaries are defined in terms of pseudo-Drucker-Prager surface values in  $p$ - $q$  space.

---

Table 6.4 – Materials tested in the Repeat Load Triaxial apparatus [Arnold 2004]

Material Name	Description
NI Good	Premium quality crushed rock - graded aggregate with a maximum particle size of 40mm from Banbridge, Northern Ireland, UK.
NI Poor	Low quality crushed quarry waste rock - graded aggregate (red in colour) with a maximum particle size of 40mm from Banbridge, Northern Ireland, UK.
CAPTIF 1	Premium quality crushed rock – graded aggregate with a maximum particle size of 40mm from Christchurch, New Zealand.
CAPTIF 2	Same as CAPTIF 1 but contaminated with 10% by mass of silty clay fines.
CAPTIF 3	Australian class 2 premium crushed rock – graded aggregate with a maximum particle size of 20mm from Montrose, Victoria, Australia.
CAPTIF 4	Premium quality crushed rock – graded aggregate with a maximum particle size of 20mm from Christchurch, New Zealand.

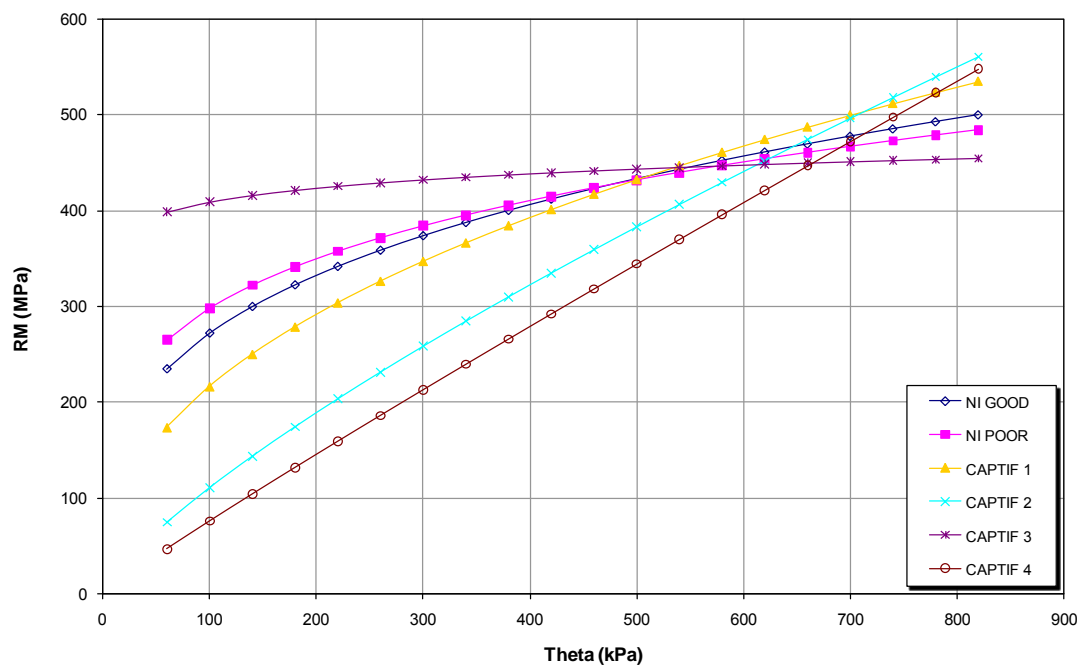


Figure 6.8 – Resilient Modulus curves for Arnold's materials [2004]

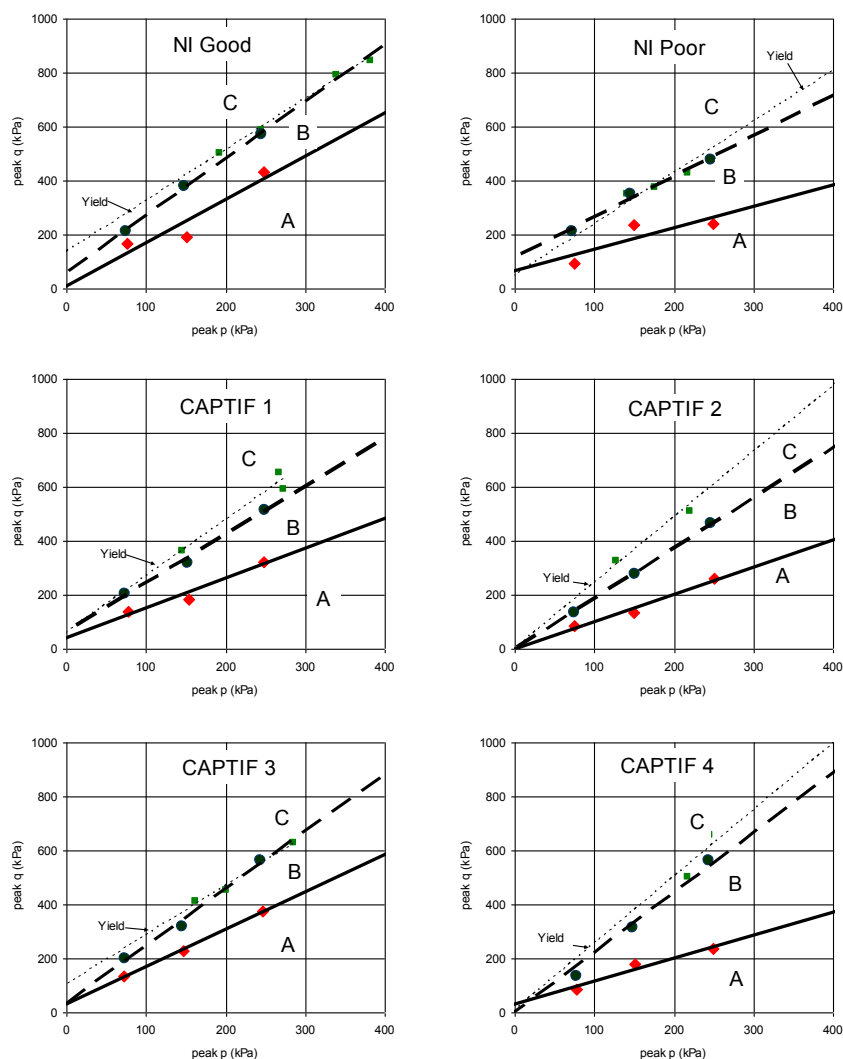


Figure 6.9 – Shakedown range boundaries for Arnold's materials [2004]

Table 6.5 – Properties of Materials Analysed

Name	Bulk Unit Weight	Mohr-Coulomb Failure parameters		Drucker-Prager (p-q stress space)		Shakedown range boundary A-B		Shakedown range boundary B-C		K-Θ Constants	
	$\rho_b$ (kN/m <sup>3</sup> )	c (kPa)	$\phi$ (°)	d (kPa)	$\beta$ (°)	d (kPa)	$\beta$ (°)	d (kPa)	$\beta$ (°)	$k_1$ (kPa)	$k_2$
NI Good (NIP)	19	74	46	135	62	10	58	59	65	71510	0.29
NI Poor (NIP)	21	27	46	49	62	65	39	114	56	103460	0.23
CAPTIF 2 (CAF)	22.8	0	61	0	68	0	45	0	62	3200	0.77

The materials for the mechanistic analysis were selected on the basis of a good diversity of materials with behaviours expected to reproduce typical granular materials used in low volume road pavements. The three materials chosen were: Northern Ireland Good (NIG), Northern Ireland Poor (NIP) and CAPTIF 2 (CAF). The latter was chosen due to its well balanced behaviour. The resilient modulus has a good linearity with a coefficient  $k_2$  of 0.77. The shakedown ranges are well distributed, as the granular material coarse fraction is balanced with added fines.

NI Poor is known to be of a poor quality. Its relatively low cohesion ( $c$ ) and poor angle of friction ( $\phi$ ) translated into a moderate stiffness characteristics but a fairly pronounced non-linearity with  $k_2$  of 0.23, the lowest of the three chosen materials. The resilient modulus does not increase much in highly stressed areas. NI Good is a granular material of a similar stiffness of NIP. Despite the similar stiffness, its strength is higher than that of the NIP material and its "Range A" shakedown stress envelope is substantially wider.

The higher stiffness CAF beyond  $\theta=600\text{kPa}$  - obtainable immediate under the wheel load, ought to provide a better stress distribution in the granular layer than the other materials. As a result, pavements designed with CAF may perform better as far as rutting is concerned, therefore leading to a thinner design. In the case of the NIG, a similar thickness to the NIP may be expected due to the similar stiffness, but the in-layer rutting is likely to be lower.

The three materials selected for the analysis have their characteristics summarized in Table 6.5 and are further detailed elsewhere [Arnold 2004].

#### Subgrade stiffness

As discussed earlier in Section 6.2, the subgrade was only referenced by its stiffness. A range of  $E_{\text{bas}}/E_{\text{sub}}$  between 2 and 8 is expected to cover a good range of usual stiffness ratio resembling typical LVR structures. Hence, the subgrade variation was mainly driven by the stiffness considered in the base layer.

### **6.5. VALIDATION OF THE ANALYSIS**

Three different available software were approached for use in this analysis. Ideally a finite element analysis ought to be used for better results. The framework of finite element analysis allow for a full 3D analysis and can certainly provide more accurate results; not to mention that the flexibility it provides for the geometry modelling, material characterization, non-linearity both vertically and laterally, load distribution, etc.

---

Ahlborn [1972] developed Elsym in the University of California at Berkeley. It is a widely recognized and traditional software used in mechanist analysis. In its latest version it is known as Elsym5. Despite its limitations on the material constitutive modelling, Elsym5 allows for a realistic representation of the field load since it accepts more than one loaded area.

Many other softwares were based in the same principles used in Elsym, such as Bisar and Everstress, among others. Its limitations however are the limited number of layers that can be used (up to five layers) and the fixed resilient modulus and Poisson's ratio for the linear elastic analysis it can perform.

Given the complexity of the boundary conditions, specific constitutive models of pavement materials as well as the improvement of computational methods, other modern tools such as Finite Element Analysis packages have been used to simulate pavement response. Researchers such as Duncan *et al.* [1968] started using the Finite Element Method (FEM) for pavement structural analyses. FEM has some advantages over layered elastic solutions because it provides greater flexibility in modelling the nonlinear response characteristics of all the materials that make up the pavement section [Monismith 1992].

Almeida [1993] developed at the University of Nottingham the finite element program known as Fenlap. The program is an axi-symmetric finite element routine which uses 8-node rectangular-elements using a linear elastic Hooke's model for the asphalt layer and the subgrade, and for the UGL a non-linear elastic  $k-\theta$  model.

Dresden has enhanced the Fenlap code, by updating some of the code but largely making additions to the number of material constitutive models available. This latest version includes, in addition to a linear elastic model, Brown's, Loach's, Pappin's, Boyce's, Mayhew's, Dresden and Linear elastic anisotropic models. The version also incorporates horizontal load or pressure and the upper and lower depth of that pressure, what corresponds to the inner and outer radius of the vertical pressure. Accordingly the program calculates horizontal Resilient Modulus and horizontal Poisson's ratio if requested.

Fenlap was the preferred solution to be use for the mechanistic analysis proposed. However, in a preliminary use of the program it was found to be difficult to obtain convergence. The program solves each problem iteratively, as the stiffness of each element has to be recalculated after the initial calculation of stress in the element. This is repeated until a harmonious set of stiffnesses and stress is obtained. As in Fenlap the loading is not put on in one increment at every step, but in a series of sub-loading steps, a more accurate estimate of resilient strains to be obtained. Nonetheless, the initial

---

computations performed, convergence to a harmonious set of stresses and stiffnesses was not achieved.

This may have been a result in consequence to a high stiffness gradient at the surface for unsealed or chip-sealed pavements. However, the causes were not investigated in any detail and it was decided to use the Kenlayer code which, despite the limitations previously mentioned has the capability to perform the calculations intended.

Kenlayer, however, is broadly similar to Elsym, with the advantage of being able to consider the vertical non-linearity of unbound granular materials. This enables the software to correct the stiffness of the layer, somewhat, according to stresses applied. Kenlayer make the use of  $k-\theta$  model.

As a form to guide the results, some preliminary tests were carried out. They provided the reference for the analysis, assuring proper use of the tool. They are described ahead.

→ Kenlayer versus Elsym 5

A very simple verification was to compare Kenlayer and Elsym5 results running with the same input values. A simple pavement structure with a thin bituminous surfacing was added. The comparison in Table 6.6 show very little difference between Kenlayer and Elsym.

Table 6.6 – Comparison for Kenlayer and Elsym5 results in a linear elastic analysis

	Depth (cm)	Kenlayer				Elsym5			
		p = 500kPa		p = 900kPa		p = 500kPa		p = 900kPa	
		$\sigma_v$ (kPa)	$\sigma_R$ (kPa)	$\sigma_v$ (kPa)	$\sigma_R$ (kPa)	$\sigma_v$ (kPa)	$\sigma_R$ (kPa)	$\sigma_v$ (kPa)	$\sigma_R$ (kPa)
Bituminous Surfacing (E=3.0GPa)	0	500	2250	900	3083	-500	-1927	-900	-3444
	2	493	596	840	791	-493	-608	-840	-796
	4	472	-691	744	-1791	-471	691	-743	1797
Granular Material (E=230MPa)	12	333	44	450	35	-331	-42	-448	-34
	50	29	-63	31	-66	-28	91	-29	94
Subgrade (E=40MPa)	100	10	0	10	0	-10	0	-10	-1
	150	5	0	5	0	-5	0	-6	-1

Tension (-)

Compression (+)

Tension (+)

Compression (0)

→ Non-linearity effect

In a second analysis, it was desired to have a benchmark value obtained from Kenlayer to assess the effect of its non-linear model calculations. Fenlap was chosen as a good reference because previous published works had already used its code and provided reliable information [Almeida 1993, Werkmeister 2003, Dawson & Kolisoja 2004].

Both codes were used to simulate a simple pavement structure (Figure 6.10) using two different granular materials from Vesilahti/Finland - data obtained from collaborators from the University of Nottingham [Kolisoja 2007]. One was called a "milled mixture" -  $k_1=51,377\text{kPa}$   $k_2=0,33$ ; it was composed by recycling a granular base layer with old bituminous surfacing mixed; the other one a crushed stone with  $k_1=48,076\text{kPa}$   $k_2=0,38^6$ . Table 6.7 summarizes the tests carried out: 1 problem solved for each materials, using first a  $k$ - $\theta$  model, and later a linear elastic value for the Resilient Modulus for each layer.

Table 6.8 summarizes the results. The greater variation registered in the results are the tensile stresses developed at the bottom of the base course. Fenlap demonstrates better ability at tension redistribution with its tension cut-off mechanism, as expected. This agrees with the results later found as presented in Table 6.2. Zeroing the tensile stress measured in the  $p \times q$  space as the chosen correction mechanism seems to provide a fair approximation, although introducing an error to some extent. This error, however, is attenuated as most of the stress loci expected to cause the permanent deformation are located from the mid-height upwards, where the shear stresses are higher.

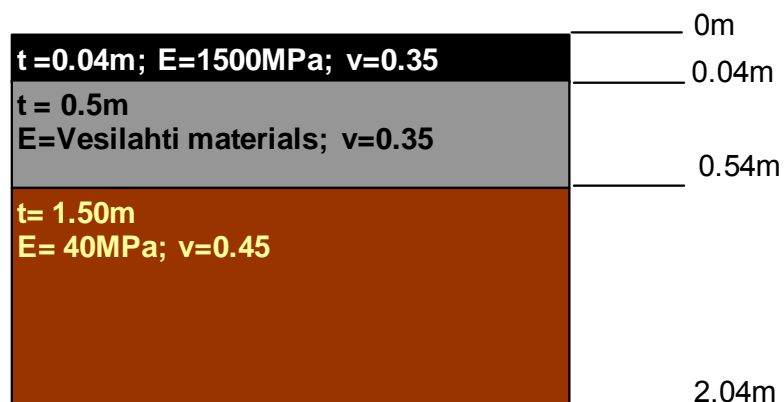


Figure 6.10 – Structure used for the non-linearity effect comparison between Kenlayer and Fenlap

<sup>6</sup> Note that  $k_1$  &  $k_2$  referenced are not normalized against  $p_a$  or  $\theta_0$ . The constants are for use in the simple model  $MR=k_1\theta^{k_2}$ .

Table 6.7 – Comparison for Kenlayer and Fenlap results in a non-linear elastic analysis

Problem 1	Non-linear elastic analysis using k-theta parameters for Mix Milled Material
Problem 2	Linear Elastic using the RM for Mix Milled Material
Problem 3	Linear Elastic using the RM for Crushed Stone
Problem 4	Non-linear elastic analysis using k-theta parameters for Crushed Stone

Table 6.8 – Comparison between Kenlayer and Fenlap with a linear elastic and a non-linear elastic models.

KENLAYER	Depth Z (cm)	Problem 1		Problem 2		Problem 4		Problem 3	
		Mix Milled - Non linear		Mix Milled - Linear		Crushed Stone Non Linear		Crushed Stone Linear	
		Szz	Srr	Szz	Srr	Szz	Srr	Szz	Srr
	0	550	1435	550	3774	550	1027	550	3919
	2	552	610	517	503	552	604	514	495
	4	541	84	469	-2316	541	179	464	-2476
	29	142	-18	143	-4	143	-18	143	-4
	54	25	-104	52	-16	22	-115	53	-14
	129	7	0	11	0	7	1	11	0
	204	4	0	5	0	4	0	5	0

FENLAP	Depth Z (cm)	Mix Milled - Non linear		Mix Milled - Linear		Crushed Stone Non Linear		Crushed Stone Linear	
		Szz	Srr	Szz	Srr	Szz	Srr	Szz	Srr
		Szz	Srr	Szz	Srr	Szz	Srr	Szz	Srr
	0	580	1190	605	2940	579	1090	607	3040
	2	422	631	264	216	431	644	254	189
	4	154	-240	-82	-1760	168	-138	-97	-1830
	4	527	100	447	136	533	98	441	135
	29	93	-9	149	-12	89	-7	151	-12
	54	69	-9	68	4	70	-10	69	5
	54	47	23	62	24	45	23	63	24
	129	34	32	32	31	34	32	32	31
	204	19	20	19	20	19	20	18	20

COMPARISON	Depth Z (cm)	Mix Milled - Non linear		Mix Milled - Linear		Crushed Stone Non Linear		Crushed Stone Linear	
		Szz	Srr	Szz	Srr	Szz	Srr	Szz	Srr
		Szz	Srr	Szz	Srr	Szz	Srr	Szz	Srr
	0	105%	121%	110%	128%	105%	106%	110%	129%
	2	131%	103%	196%	233%	128%	107%	202%	262%
	4	351%	-35%	-17%	132%	322%	-77%	-21%	135%
	4								
	29	154%	187%	104%	282%	160%	241%	106%	322%
	54	279%	1118%	131%	-22%	313%	1161%	129%	-39%
	54								
	129	461%		285%		489%		280%	
	204	506%		388%		521%		382%	

\* Greater percentage indicated



→ *Geostatic forces sensitivity in Kenlayer*

One issue which arose during the first analysis was the little sensitivity Kenlayer seemed to be demonstrating to the geostatic forces. Little or none sensibility could be noticed while different weights were attributed to the layers.

For this evaluation, three levels of gamma values were attributed in a two layered analysis in which none of the other parameters were changed. A two layer structure was modelled, loaded by a single load of 400kPa contact pressure, using a linear elastic modulus for both layers. This allowed the computations to show the effect based solely in the variation in the self weights of the materials.

Three levels of gamma values were input: a zero value, completely disregarding the effect of self weight in both layers; a set of typical values expected for a granular material as the granular layer a for a soil subgrade of 21 and 19 kN/m<sup>3</sup> respectively; and finally an extreme value of 2000 kN/m<sup>3</sup> completely out of range of a reasonable value so that a clear impression could be noted if at all considered in the calculations.

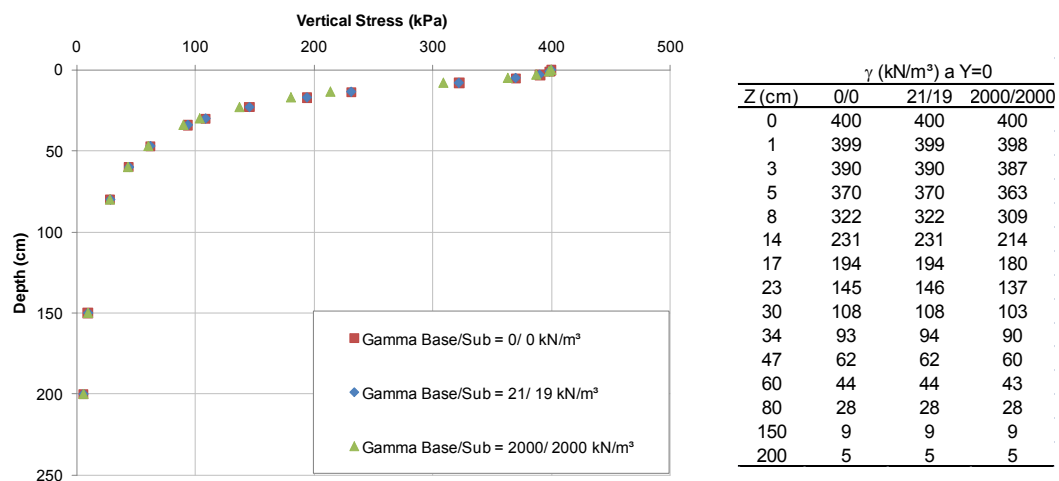


Figure 6.11 – Kenlayer sensitivity measurement to variation in material self weight values

The results in Figure 6.11 demonstrate that no, or very little, sensitivity can be expected from Kenlayer in regard to self weight values. The calculations for null and for a standard range of values (~20 kN/m<sup>3</sup>) yielded the same results. Very little difference was noticed for a unit weight value of 2000kN/m<sup>3</sup> either, demonstrating that geostatic forces do not make a noticeable difference.

For the purpose of the analysis carried out, one of the main issues concerns the development of tensile stresses; mainly due to negative radial stresses developing in the analysed space. Areas with low stresses easily show tension due to the fact that no

overburden stress can be felt in-layer. This effect can be seen in Table 6.2, where the cell highlighted in blue shows negative values of  $p$  and  $q$ . This would possibly have been avoided if the software had made an appropriate consideration of the geostatic forces.

## 6.6. RESULTS

All results from the experiment matrix produced a  $p \times q$  plot, totalling 180 graphs. They were all analysed following the procedure as described in Section 6.3. There is a slight change in formulation for calculating  $p$  and  $q$  when super singles are used, as Kenlayer assumes a radial analysis with only one load applied, as opposed to a Cartesian when twin tyres were used; this, however, is transparent for the analysis carried out.

A typical set of plots obtained for the NIG1 analysis is Figure 6.12. There a Northern Ireland Good material was analysed under a dual tyre loading arrangement with tyre pressures considered at 400kPa. The granular layer thickness varied from one loading radius to 3.5, assuming thickness equivalent to 13.5cm in Problem 1, 17cm in Problem 2 and 23cm, 33.8cm, 47.3cm in Problems 3 to 5 respectively. The subgrade was assumed to have a Resilient Modulus equal to half of the Resilient Modulus measured at the mid-depth of the UGL, 220,000kPa. The remainder of the results are summarized in Appendix .

The main goal of the exercise is to promote a more qualitative study of the likelihood of the UGM developing permanent deformation; it is expected that the proximity of a certain stress state in a UGM to its yield failure envelope will provide a basis for the assessment of the rutting likelihood of rutting of the structure due to plastic deformation in the UGM.

From previous studies [Dawson & Kolisoja 2004] and from the Shakedown approach (see Section 2.5) it is known that, if the stress states in the pavement are kept a long way from failure then no rutting in the granular layers will occur, but that if the stresses approach the static failure envelope, then the speed of development of rutting in the granular layer increases.

In addition, after a careful study of the results, the computed stresses were found to be largely independent of granular material type, indicating that these stiffness non-linearities lead to very similar computed stiffnesses for the same loading and layer sequence.

Figure 6.13 shows a combined plot of the results for two of the extreme conditions assessed - under dual tyred loading with contact pressure of 400kPa and under a super single loading with contact pressure of 800kPa - and the locus studied by Mundy [2002].

---

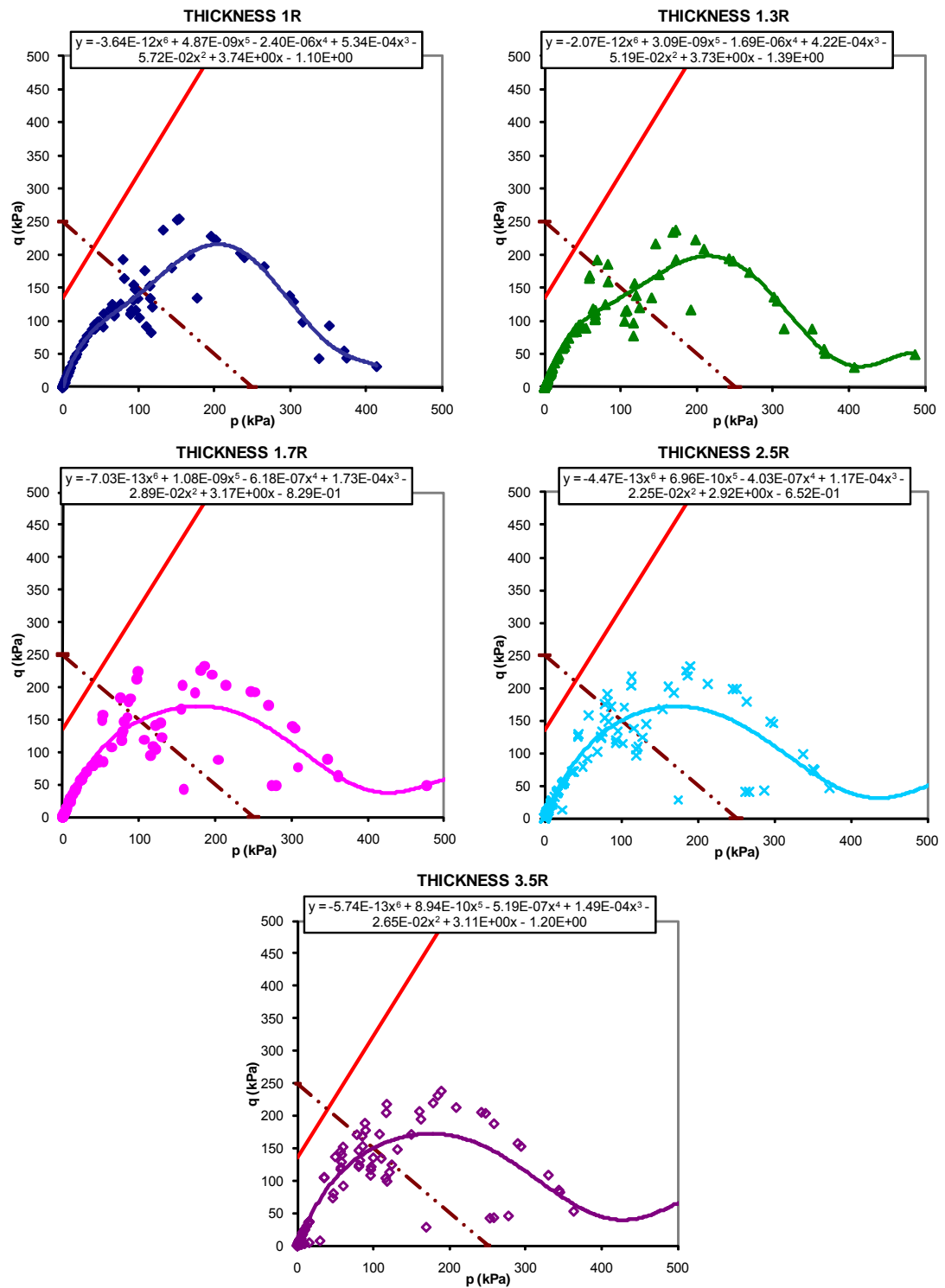


Figure 6.12 – Set of results obtained for all five problems run for NIG1

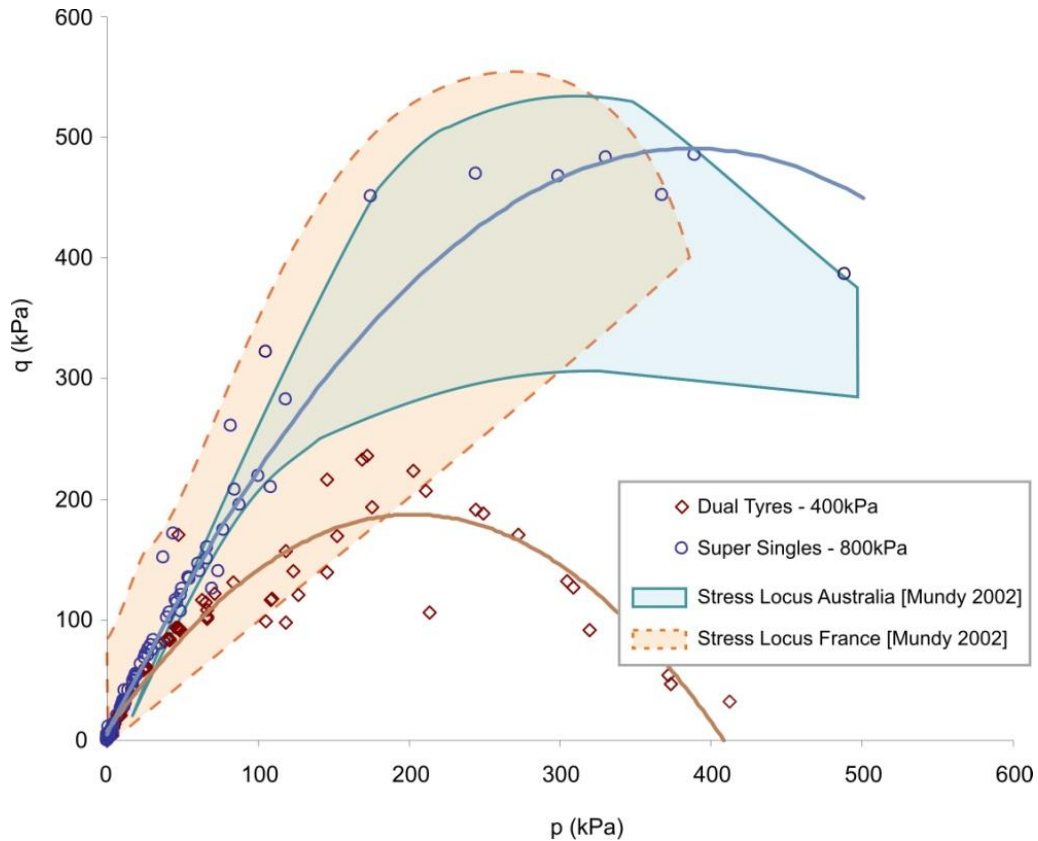


Figure 6.13 – Resulting stress loci example compared to Australia and France loci according to Mundy [2002]

Both the French pavement locus and the Australian pavement locus seem to anticipate, to some extent, the results found. The stress state for the twin tyre with contact pressure of 400kPa is lower than both loci identified by Mundy. This could possibly be explained by the lower tyre inflation used in this analysis.

The super singles at 800kPa on the other hand seem to be quite at the top of the Australian envelope; a reasonable result as very heavy vehicles in that country are in current use. The range of stresses determined here seem to be, therefore, within an expected range. Clearly, it seems to be a well defined locus where the stresses in the pavement tend to approach its failure envelope. If the proximity is to be evaluated, then the likelihood of the pavement developing permanent strains can be assessed.

In order to perform this assessment, a stress line (S) can be plotted in a ratio -1:1 to provide a reference (see further discussion in Section 0). Figure 6.14 illustrates the proximity to failure when, for the same structure, the loading arrangement changes from a less damaging dual tyred axle with tyre pressures at 400kPa to super singles at 800kPa.

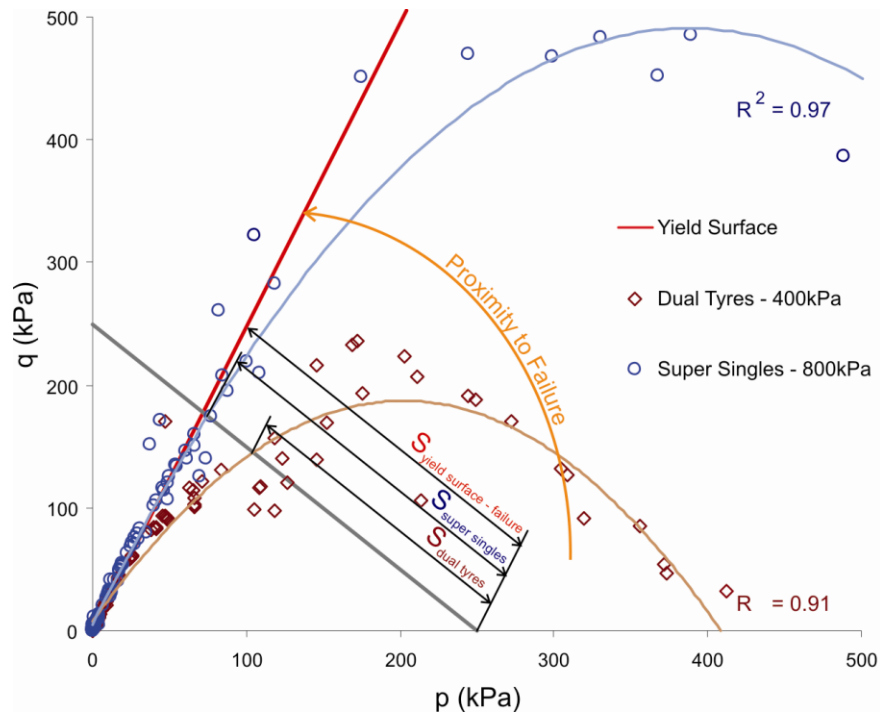


Figure 6.14 – Example of two  $p, q$  plots.  $S_{\text{yield surface-failure}}$  represents the Drucker Prager yield surface.

These measurements were performed for every analysis and are pictured in Appendix . The  $S$  values calculated are summarized in Appendix G. Figure 6.15 provides a contour plot of the  $S$  values grouped per material. The  $S$  values for the failure are also plotted in order to allow the assessment of proximity.

A careful analysis of the plots shows that, despite the materials properties, the stress loci appear to have quite a similar behaviour for all materials. The computed stresses were found to be largely independent of granular material type, indicating that these stiffness non-linearities lead to very similar computed stiffnesses for the same loading and layer sequence.

The stress distribution is more dependent on the loading and layer thickness, expressing a rather strong effect when towards the lower limit of the Loading Radius/Aggregate Thickness that was used.

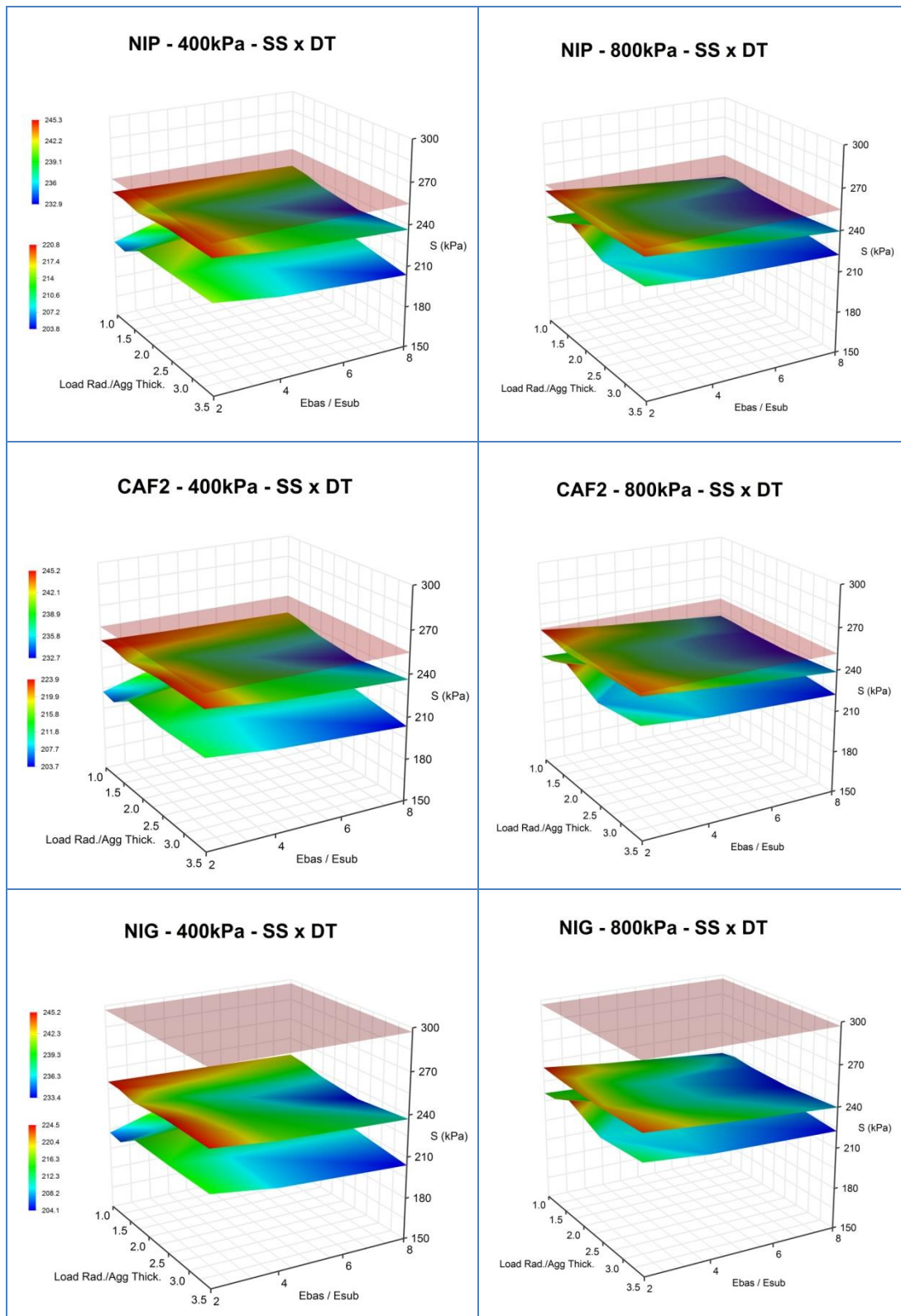


Figure 6.15 – S results for the experiment matrix. (from top to bottom: failure,  $S_{SS}$  &  $S_{DT}$  surfaces)

## 6.7. KEY FINDINGS

The analysis described in this chapter is the first step for the proposal of a simplified pavement design procedure. It aimed to look into the rationale involved in the stress distribution from a permanent deformation perspective. A pavement layer which has a stress condition that brings the granular base material near to its failure envelope is likely to develop permanent strains. From the shakedown concept it is possible to say that the closer to the failure line it is, the higher will be the likelihood of failure.

The study has helped to improve the understanding of the effect of tyre pressure and contact area in regard to permanent deformation. To achieve this, several scenarios were modelled using the Kenlayer software varying aggregate material, thickness, stiffness, tyre pressure & arrangement. The findings can be summarized as follows:

- The available finite element tools may have an advantage over traditional tools such as the Kenlayer software. However, the analyses carried out with all protocols yielded consistent results.
  - The preliminary analysis revealed Kenlayer to be a good substitute for simpler tools as Elsym5, but still finds difficulty in overcoming tensile stresses in the analysis. Fenlap produced a more consistent set of stresses in the granular layer, but was found more difficult to achieve convergence, therefore, making the use of Kenlayer a more practical option.
  - Despite use of the so-called Method 3 to prevent tension from developing in the granular layer, tensile stresses were still measured. A 'work-around' was put in place by zeroing the p/q ratios greater than 3 and smaller than zero. This helped resolved part of the problem. Nevertheless, as the values were simply disregarded, a new stress arrangement didn't come in place, thereby allowing small errors to be incurred.
  - The geostatic forces do not seem to have any effect in the calculations. This certainly allows the development of undesirable tension.
  - The stress loci reported in the calculations performed demonstrate a good correlation with those available in the literature that were originated in other different ways. This permits the conclusion that the procedures used in the calculations are valid and that the results can be used further.
  - The introduction of the assessment of different loading arrangements and different tyre pressures enables up-to-date vehicle arrangements to profit from the analyses performed.
-

- The results usually show a fairly well defined locus of maximum stresses. By comparing this stress envelope with the failure envelope, conclusions can be established about the more damaging effect of super singles over twin tyres and, likewise, the greater damage inflicted by high tyre pressures compared to that incurred by lower tyre pressures.
- All stress surfaces evidenced a closer proximity to failure when both types of tyre arrangements are at higher pressures, suggesting that the benefit of lower pressures is less pronounced for super single tyred systems. In addition, super singles always produced higher levels of stress and are, therefore, more likely to develop permanent deformation, or stresses that will allow rutting to develop faster.
- Regarding the influence of aggregate, it is apparent that, except for the softest aggregates, greater aggregate thickness reduces the maximum stress experienced in the aggregate. However, this is not a very strong effect, and a change in tyre pressures or wheel arrangements is more likely to deliver a significant change in stress experienced and, hence, the likelihood of rutting or its magnitude). The effect of changing aggregate stiffness, alone, or stress condition (and, thus, rutting) is mixed. No strong trend shows up and, in any event, the effect is rather insignificant.
- The results show that there are some points (stress states) well beyond static failure, perhaps even in tensile stress state. Clearly these are impossible, and as previously discussed, possibly a consequence of the use of the layered elastic method that is provided by Kenlayer. It is known from other work that finite element computations with appropriate tension cut-off models can result in few or no stresses in this zone. The remaining stress points are scattered over the  $p$ - $q$  space, but there is usually a fairly well defined locus of maximum stresses through.

A more reliable analysis would be expected to be the benefit of better non-linear elastic models and, most importantly, a more rigorous cut-off limit for the tensile stress. Nevertheless, overall, the procedure developed for the analysis provided a good and consistent result and may be used as a reference for the next Chapter to propose a simplified design method.

---



## 7. METHODOLOGY PROPOSAL AND VALIDATION

### 7.1. INTRODUCTION

Literature review from Chapter 3 has shown that, until now, there are two main streams in designing unsealed or thinly sealed low volume roads: from empirical correlations and linear elastic mechanistic methods. The Available empirical-mechanistic design guides for LVRs, of both types, address the task solely by protecting the subgrade from permanent deformation.

Studies from Douglas [1997], Arnold [2004], Dawson & Kolisoja [2004], Tyrrel [2004b], El Abd [2006], Korkiala-Tanttu [2008], among others, have observed that most rutting in LVR pavements originates in the granular layers. Recognizing such a problem, some studies [Werkmeister 2003, Arnold 2004, Korkiala-Tanttu 2008] have already presented procedures for permanent deformation assessment in granular layers although their approaches are not sufficiently simplified for routine application to LVRs.

This research has founded most of its studies on this previous work and attempts now to propose a methodology that is

- capable of designing a pavement constructed of granular layers, either unsealed or thinly sealed,
- simple to perform so will be an attractive proposition for routine LVR design,
- mechanistically based, so that it can be used with loadings and materials outside of routine experience with some confidence.

Thus, the purpose of this chapter is to pack the results from Chapter 6 into a design method.

Rutting can occur for a number of reasons. Dawson & Kolisoja [2004] observed four main mechanisms of rutting which have been discussed in Section 2.4.1. Mode 0 is a self-stopping occurrence once adequate compaction has taken place, and can, therefore, be tackled by using adequate compaction protocols. Mode 1 will be more evident with canalised trafficking where wheel wander is limited. Mode 2 is expected to be more evident under wandering traffic. Mode 3 can be addressed by particle strength requirements, independent of the stress analysis - an aspect not considered further in this thesis.

---

Section 7.3 will address Mode 1 type of rutting; the aggregate in-layer permanent deformation. Section 7.4 will address Mode 2 rutting, primarily as a function of subgrade strain. This will later be packed into a two-stage design procedure (see Section 7.5).

Several important observations could be made on the basis of the stress analysis carried out in the previous Chapter. One of them, in agreement with observations made in previous studies, is about the existence of a stress locus in the pavement, which varies according to the type of structure used, being a function, primarily, of layer thickness, material stiffness properties, strength and loading condition.

As far as a design guide is concerned, in addition to these parameters, another two seem to attract some attention. They are the number of load repetitions and climate effects.

For the assessment of permanent deformation of granular materials due to the number of loads, there seems no better approach than the Shakedown theory. It has already been shown by Werkmeister [2003] and Arnold [2004] that applying the Shakedown theory to UGM allows the determination of a range of stresses in which the permanent deformation behaviour assumes a predictable deformation regime. When consideration is given to

- the low volume of traffic on a LVR – a number of load cycles that can assume figures of hundreds only,
- the difficulty of predicting that traffic - and measuring it for that matter, as seen in the RUTT project,
- the complication of modelling the granular behaviour,

it seems much fairer to use a range of permissible stresses as the basis of pavement design, rather than to make an exact computation that would be likely to give a false sense of accuracy to users.

In regards to climate effects, these are mostly translated into moisture variation. Neither granular materials nor soils, for the level of precision - or imprecision - here discussed, need to be considered as affected by temperature. Nonetheless, freezing and thawing, do bring quite a considerable change in rutting behaviour and they need therefore, to be addressed to some extent. This is briefly discussed later in Section 7.3.

## **7.2. PAVEMENT STRESS LOCUS**

Chapter 6 provided the analysis of what could be considered as the primary design parameters. The determination of a pavement stress locus for a given scenario seems to effectively give precise information on which to base design, as proximity to failure gives

---

a good indication on the likelihood of rutting propensity. Thus, by developing a tool which allows the prediction of the proximity to the material's failure, the determination of the required layer thickness can be achieved, thereby limiting the likelihood of failure by excessive rutting. Figure 6.14 has already introduced this analysis.

The first attempt to measure this proximity was to manually assess the stress curves, by calculating the distance from the stress locus, plotted in  $p$ - $q$  space, to the yield surface by using a tentative line running from  $p=250\text{kPa}$   $q=0\text{kPa}$ , crossing both the stress surface and the static failure envelope, up to a point at  $p=0\text{kPa}$   $q=250\text{kPa}$ . The difference in the 'S' value (measured from the  $q=0$  axis upto the stress envelope) from the 'S' value (measured from the  $q=0$  axis upto the yield envelope) gauges the proximity of the loaded structure to failure by rutting.

Results of 'S' values could then be manually calculated and recorded. The downside of such manual measurements would be the difficulty in reproducing the results, should future work be carried out. This would not only be because of operator dependency, but also due to the number of analysis, which is somewhat cumbersome. For this reason it was decided to use an Excel regression line to define the stress locus.

As can be observed from Figure 7.1, the polynomial fits may present some inconsistencies towards the higher values of mean normal stresses. Use of the 6th order polynomial best fit is capable of preserving the initial  $p$ - $q$  ramp intact even if awkward 'tails' may develop for high mean normal stresses at a low deviatoric stress range. This mismatch is most associated with higher stiffness granular layers.

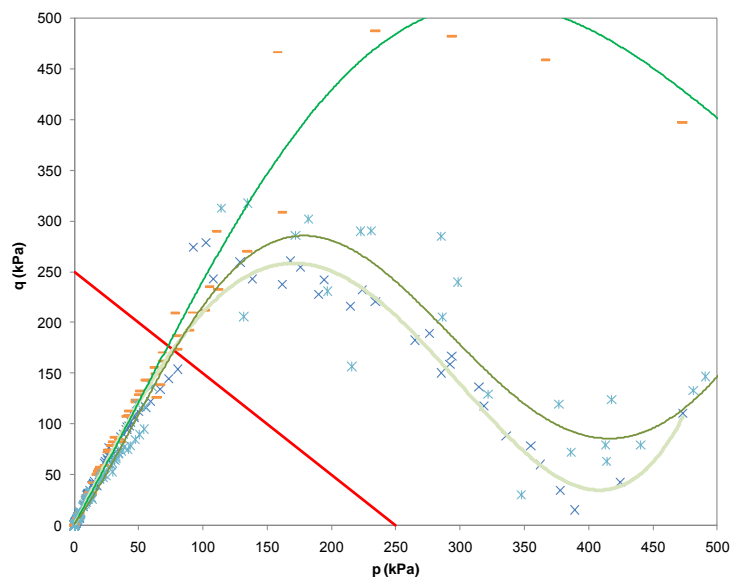


Figure 7.1 – Stress envelopes for NIG7, NIG8 & NIG9 - Problems 1 connected by a 6th order polynomial line of regression

The difference resulting from a manual analysis, as compared to the computational method using the best fit regressions, needed to be assessed for consistency. All 60 'S' values for the Northern Ireland 'Good' aggregate, measured in both manners, are compared in a line of equality in Figure 7.2. There is a very good match between the values calculated by both approaches, with a tendency for the values calculated using the best fit approach to result in higher values. The analysis proves that using a computational method is consistent and can be considered, therefore, as the final result.

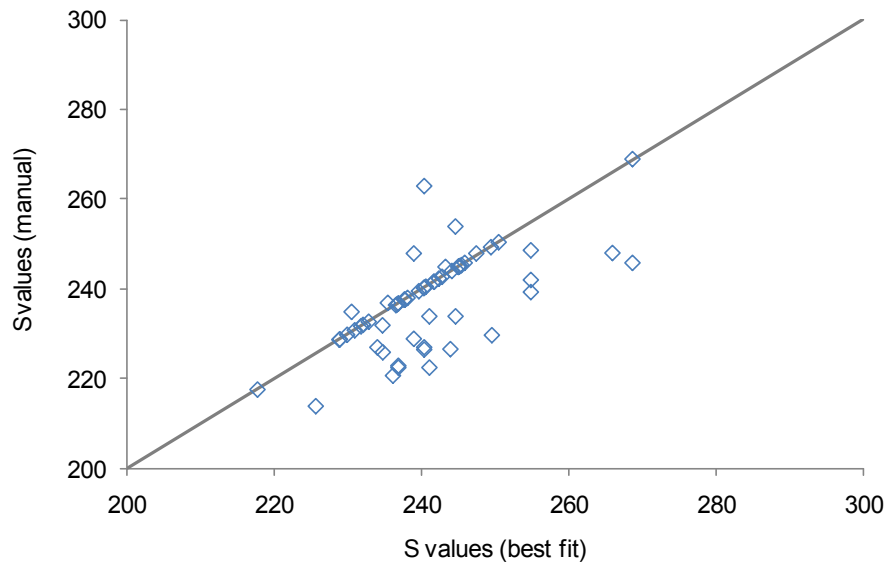


Figure 7.2 – Comparison of the S values resulting from a manual and a computational measurement using a polynomial line of regression

Now the choice of line selected for the 'S' value determination, the (250,0)(0,250) S line, must be defended. Arguably, different lines could have been selected, but the one suggested has proved reasonably reliable for the purpose of assessing proximity to failure as observed in the results from Chapter 6. From the results, there was an indication that this S line crossed the loci and the yield surface where the two came closest together. Thus, the difference between the two values of 'S' measured along this line is the most critical difference and so is where the assessment needs to take place.

To further evaluate this, all results for the Northern Ireland Good material were drawn on a single plot (Figure 7.3). The red circle points to the a large concentration of stress pairs in the p,q space. It becomes evident that the (250,0)(0,250) S line crosses the stress loci at a point that is close to the best possible. The distance along this line from  $q=0$  until the failure envelope is reached has been labelled ' $S_f$ ', as an abbreviation of "Stress to failure". The ' $S_f$ ' values for all 180 calculations are summarized in Appendix .

Another important observation from Figure 6.15, already established in Section 6.6, was that the stress loci appear to have a similar behaviour for all materials. The computed stresses were found to be largely independent of granular material type, indicating that these stiffness non-linearities lead to very similar computed stiffnesses for the same loading and layer sequence.

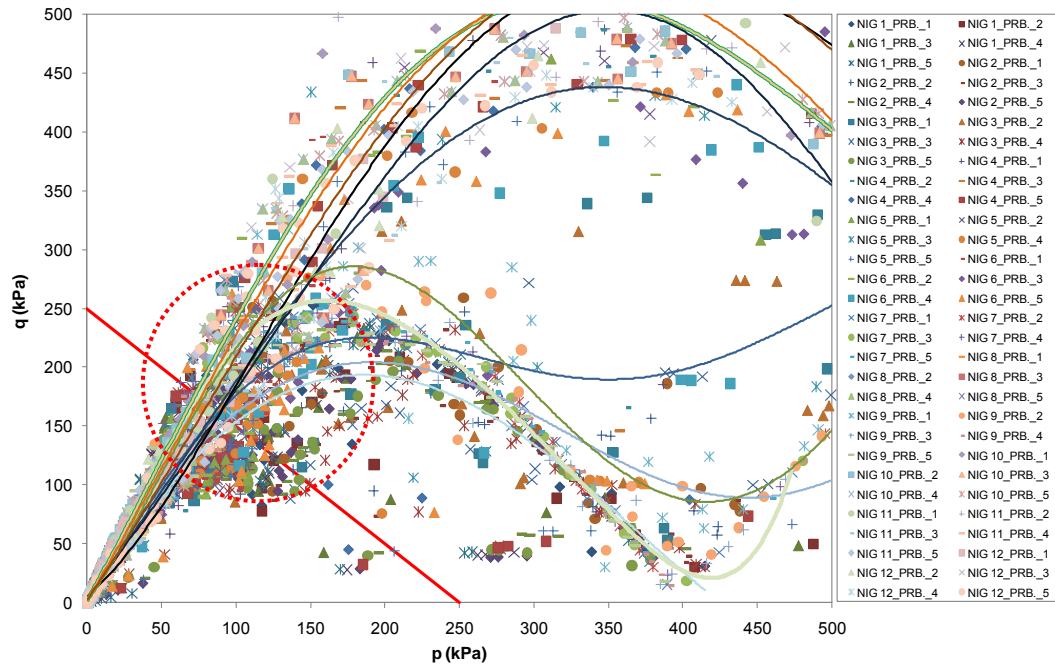


Figure 7.3 – Loci of stress concentration - compiled result for the NIG

Hence, a reasonable conclusion is that the values of 'S' are also very similar for pavements with granular layers made from any of the materials. Therefore, the effective number of values of 'S' can be reduced to 60 for the pavement stress assessment for the purpose of a design procedure.

### 7.3. THICKNESS DESIGN

In order to make simpler interpolations of the results for all 60 cases so as to provide the means of determining the stress locus in the aggregate layer under assessment, design charts (Figure 7.4) were produced to help a more immediate evaluation of the 'S' values that had been compiled in the table of results summarized in Appendix G. They are grouped into four charts; one for each loading condition: dual tyre loading at 400 and 800kPa and, likewise, for super single tyres.

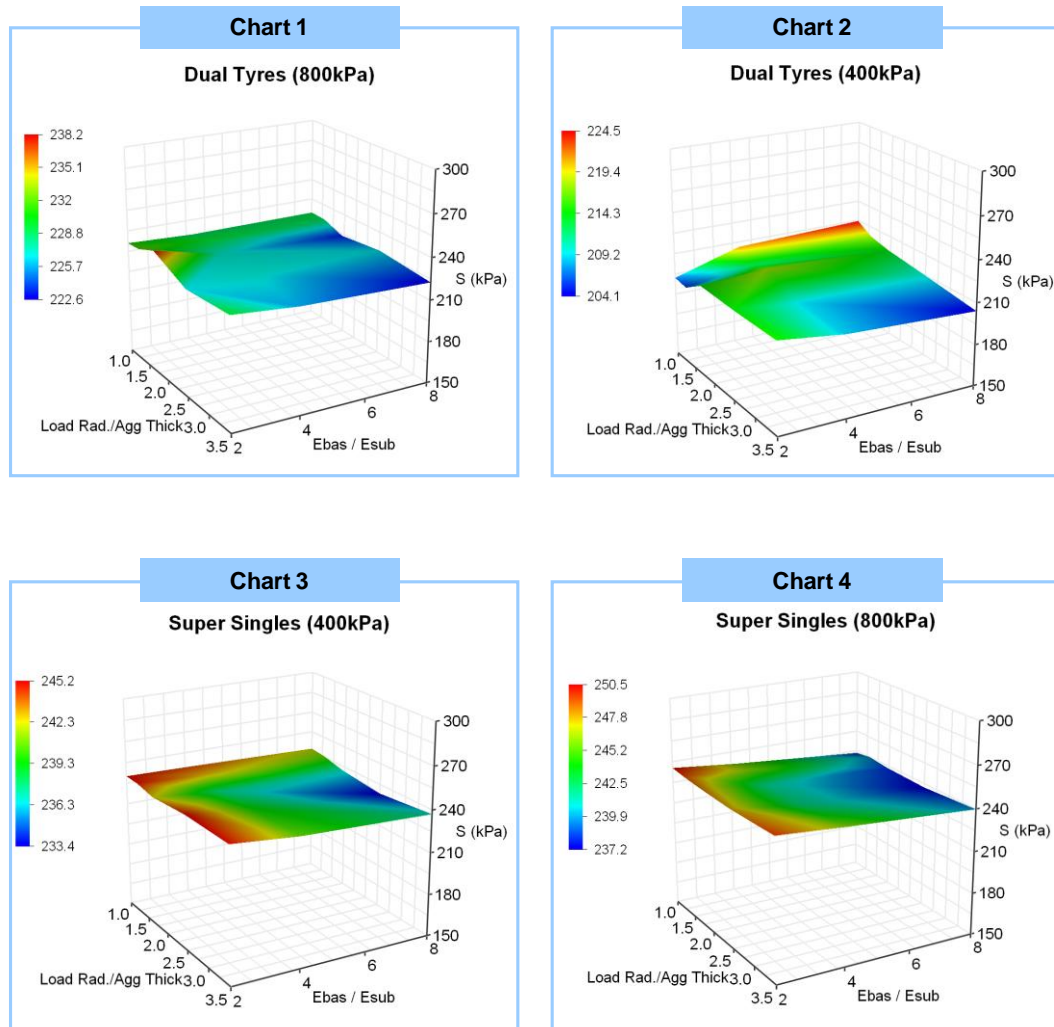


Figure 7.4 – Design charts for the determinations of the S parameters in the aggregate layer

With the design charts expressing the stress locus in the granular layer as a function of the layer thickness to the load radius ratio, and of the nominal aggregate stiffness (expressed as a multiplication of the subgrade stiffness), it is then possible to determine the required pavement thickness. This is achieved by limiting the 'S' value to a certain amount of the stress to failure, ' $S_f$ '.

Thus, knowing the tyre arrangements and pressures allows the appropriate plot to be selected and knowing the aggregate thickness and the layer stiffnesses allows the value of 'S' to be obtained. This may then be compared with ' $S_f$ ' which can be computed directly from a knowledge of the failure characteristics of the granular material being considered. It can be either assessed from experience or if the friction and cohesion characteristics of the granular layer are known ( $\phi'$  and  $c'$ ), then the value of ' $S_f$ ' can be calculated using Equation 59 to Equation 61.

$$S_f = \sqrt{2} \frac{a' - 250M}{1 + M} \quad \text{Equation 59}$$

$$\text{Where } M = \frac{6 \sin \phi'}{3 - \sin \phi'} \quad \text{Equation 60}$$

$$\text{and } a' = c' \cos \phi' \quad \text{Equation 61}$$

Dawson & Kolisoja [2004] have studied the allowable level of stresses in the pavement to prevent rutting. This was found to be a level of  $q/q_f$  equal 0.70, i.e. the deviatoric (or shear) stress applied,  $q$ , is limited to 70% of that needed to induce static failure,  $q_f$ . It was suggested, however, that for the materials studied in their research, this level could be set at 50-55% of failure depending on whether the conditions being considered were a) “normal” or b) very wet or thawing.

Because the method of computing stresses is rather different - a non-linear analysis was used as opposed to a Boussinesq stress considerations - and because of the use of a ‘S’ line running through the most critical stress locus already, using the ‘S’ line (with a gradient of -0.5, whereas the  $q/q_f$  ratio is defined on a line with a gradient of +3), it is possible to estimate that, the following permissible stress limits could be set as follows:

- $S \leq 0.9 \times S_f$  to prevent rutting in the granular layer in normal conditions, and
- $S \leq 0.75 \times S_f$  to prevent rutting in the granular layer in wet or thawing conditions.

If the stress level is greater than the permissible percentage the aggregate must either be replaced or treated, e.g. by adding a covering layer of higher quality material, and the new stress distribution reassessed. Alternatively, the loading condition can be changed. Section 0 presents a design flow chart which helps to visualize the suggested process.

#### 7.4. SUBGRADE VERIFICATION

The previous sections approaches the design for the required granular layer thickness to prevent permanent deformation from happening in the aggregate layer. This is an usual observation as discussed.

However, it is also necessary to verify that the added aggregate will provide a competent enough layer to distribute the traffic loading onto the subgrade without allowing permanent deformation to develop in the pavement foundation. Dawson & Kolisoja [Dawson & Kolisoja 2004] also show that the deviatoric stress on the top of the subgrade should not exceed a stress level of four times the undrained strength of the subgrade.

This limit provided an acceptable level of stress without causing permanent deformation to be observed in layer.

If that consideration can be accepted then the stress computations made for the same number of scenarios studied, only needs to be compared to the subgrade's material undrained strength. Figure 7.5 and Figure 7.6 allow determination of the expected vertical stress level on top of the subgrade for each scenarios. The first graph outputs the results for all the dual tyre computations while the second graph provides the results for the super singles.

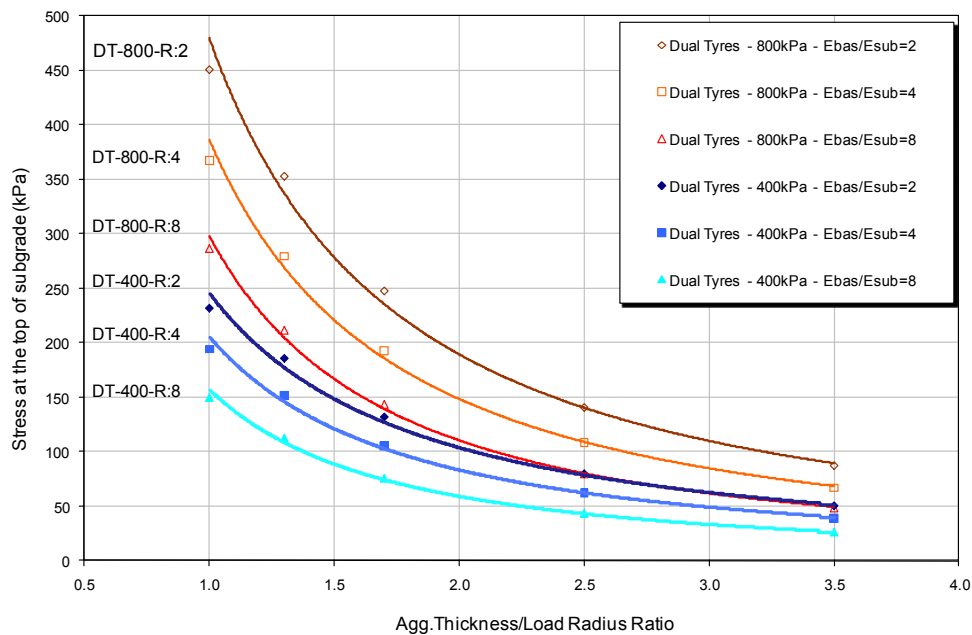


Figure 7.5 – Vertical stress at the top of the subgrade as a function of loading and aggregate in Dual Tyre loading arrangements



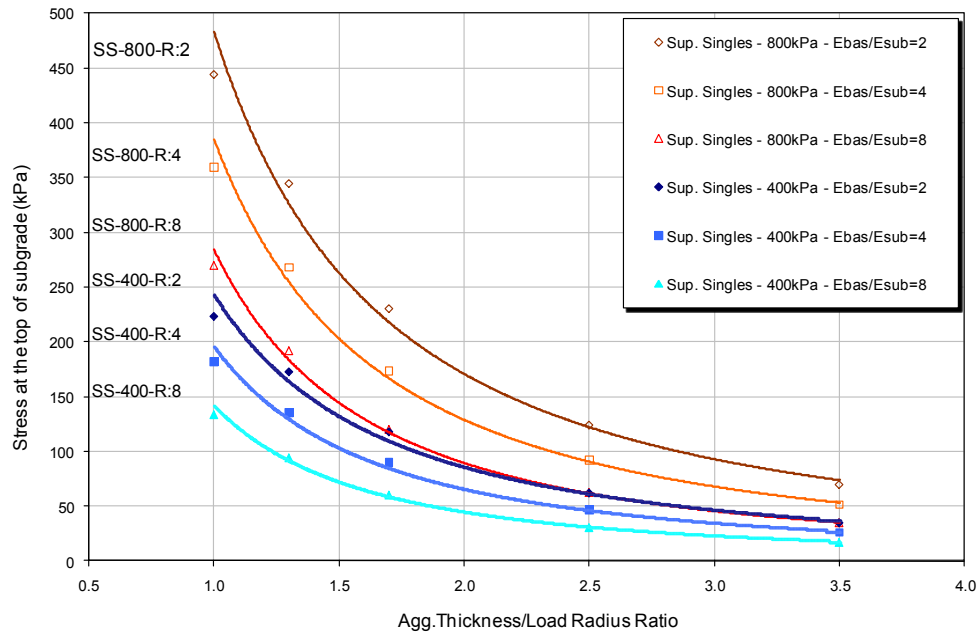


Figure 7.6 – Vertical stress at the top of the subgrade as a function of loading and aggregate in Single Tyre loading arrangements

The vertical stresses found to be imposed on top of the subgrade must then be compared to the failure strength of the subgrade. In the case where strength is inadequate, the thickness of the granular base layer is increased until the stress is sufficiently less than that which would be sufficient to cause static failure.

## 7.5. METHODOLOGY RATIONALE

The methodology which is proposed in this Chapter is largely based on other studies as the author collaborated with many experienced researchers in the field of Low Volume Roads. There are several studies which have advanced the LVR design methods and the aim of the proposed method is to package the existing knowledge into a design guide.

The rationale behind the proposed method is that the thickness of the granular base layer is increased until the stress is acceptably less than that which would be sufficient to cause static failure. This approach was adopted on the basis that, in most of the pavements observed, rutting is not due to subgrade over-stressing, so an advanced design approach is not warranted.

Provided the imposed  $q/q_f$  ratio was less than 70% (55% in very wet conditions or where trafficking in spring-thaw conditions is required) then the onset of significant rutting should be avoided. This has been converted to  $S/S_f$  ratios of less than 90% and 75% respectively

As Mode 0 failure is self-stopping once adequate compaction has taken place and Mode 3 can be addressed by particle strength requirements, independent of the stress analysis, both these mechanisms have been discounted for this analysis.

Section 7.3 addressed Mode 1 rutting; designing the pavement to prevent aggregate in-layer permanent deformation. Section 7.4 addressed Mode 2 rutting, limiting the allowable stress on top of subgrade.

Flowcharts of the suggested procedure are given in Figure 7.7 and Figure 7.8. The former guides through the selection of the aggregate whereas the latter allows determination of the required thickness of aggregate to assure no rutting in the subgrade.

The Stage 1 chart leads the user to compute the thickness of aggregate required to ensure no rutting in the subgrade and the Stage 2 chart allows the user to select an aggregate. In order to compute the stresses in Stage 1 it is necessary to estimate the design thickness, so Stage 2, in which the thickness is designed, may undermine this assumption made in computing Stage 1. Hence it is necessary to use the two stages repeatedly until the results and the assumptions broadly match. In fact, one recursion is probably all that is necessary to achieve a workable solution.

A simple worked example can be found in Appendix I. A fully detailed example of the method applied can be found elsewhere [Dawson *et al.* 2008].

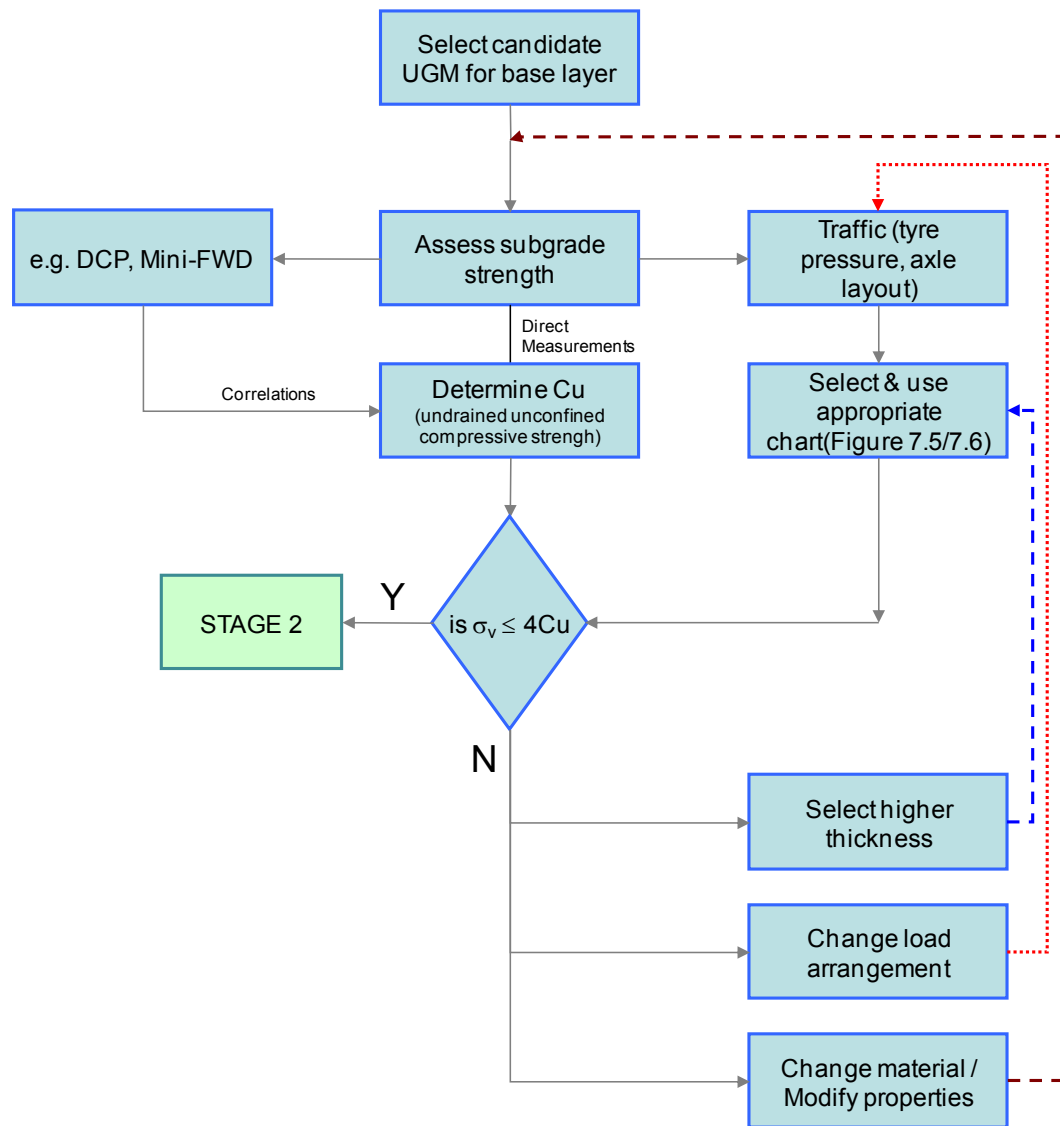
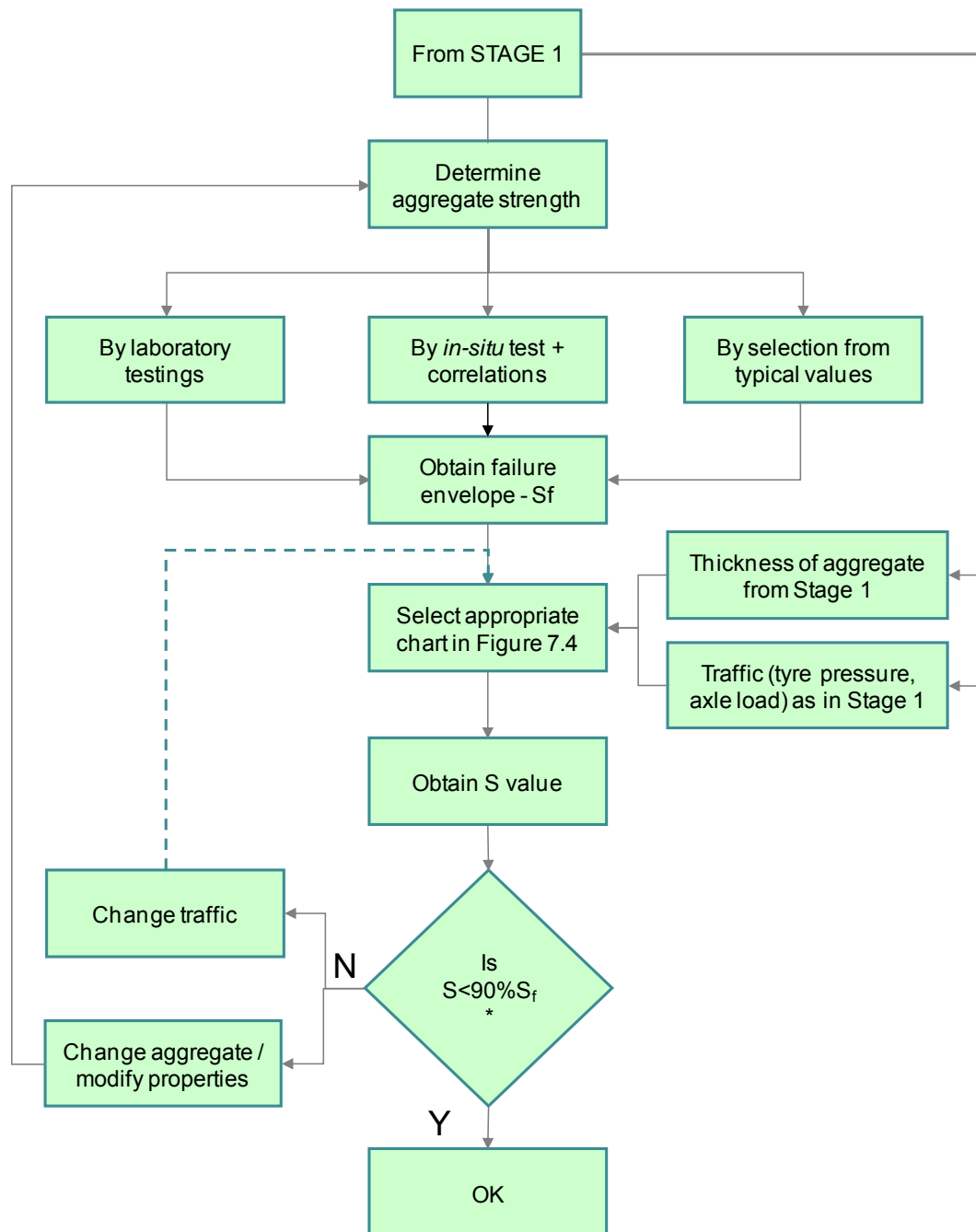


Figure 7.7 – Flow chart for Stage 1 design



\* or  $S < 75\%S_f$  for wet/thawed conditions

Figure 7.8 – Flow chart for Stage 2 design

## 7.6. METHOD LIMITATIONS

Permanent deformation could be accounted through a rational modelling of the plastic deformation generated by each vehicle pass throughout the pavement's life or, in a more qualitative fashion, that would predict the likelihood of a specific structure to rut. This last rationale has been the option used in this study, as a means of promoting a readily accessible tool for engineers looking after LVRs. The proposed methodology still treats the pavement analytically, but permits a more fundamental description of UGL behaviour than in simple linear elastic analysis but that simplifies elasto-plastic analysis for routine use, thereby reducing demands of material characterization and computational skills.

The framework of the proposed method contributes to LVR pavement design procedures mainly due to its simplicity. There are quite a few assumptions that were made, based on the work done by other researchers. Despite its simplicity, it is nonetheless possible to account for permanent deformation development in the pavement layers.

Nevertheless, some limitations are evident. They are:

- The  $p, q$  stresses calculated at individual points in the pavement sometimes give values that are not credible. This was mainly due to the lack of a calculation method which applied a full tension cut-off.
  - The insensitivity to geostatic forces by Kenlayer has possibly helped in the scattered observations and in the development of tension in the granular material. The proposed filtering provided a good work-around but didn't redistribute the calculated stress to account for those which were discounted.
  - Although the calculations performed seem to be consistent and give a consistent picture when compared to other methods, it is believed that a finite element analysis would contribute to stress locus determinations of a higher validity, possibly with less scattered  $p, q$  plots.
  - A pavement structure of two layers was considered. Despite its simplicity it does provide a representative condition found in the vast majority of Low Volume Roads. In addition, a thin surface layer is assumed not to influence the pavement stress distribution, but only to reduce water penetration in the pavement and to improve surface riding quality, such as reduced potholing and roughness conditions. A fuller analysis could, possibly, address this limitation.
  - The use of the undrained strength (for both the aggregate and the subgrade) as a limiting threshold is observational. There is, therefore, a degree of empiricism input in the method. Simplifying the complexities of the permanent deformation development
-

in aggregate material cannot be achieved without concessions. Those used in the approach introduced in this thesis attempt to be as clear as possible and allow future work to replace them with improved solutions.

## 7.7. VALIDATION

Despite the RUTT project providing in-situ results for an immediate validation, such was not straightforward. The problems faced with traffic counting yielded a considerable amount of uncertainty to some of the results. It would need considerable more work on the data in order to attempt to make it available for validation of the method proposed, and yet, it would have to allow some assumptions.

For this reason, the author's work was validated by collaborators in Finland, using the design approach presented in this thesis in the analysis of some Heavy Vehicle Simulator (HVS) test results. The validation work was performed out by Prof. Pauli Kolisoja and is reported elsewhere [Brito *et al.* 2009]. The work concluded that the verification example gives at least qualitative support to the suggested design approach. It must, however, be recognised that the verification is based on a very limited amount data, because well-documented experimental results from rutting tests performed with low volume road types of structure are extremely scarce.

---

## **8. CONCLUSIONS**

### **8.1. SUMMARY OF MAIN CONCLUSIONS**

#### **8.1.1. Unbound granular materials and road layers - Chapter 2**

Most methods currently used for LVR design neglect permanent deformation in the granular layers and design the pavement layers as means to protect the subgrade from permanent deformation.

The stress level analysis in Australian and French pavements [Mundy 2002] suggests the existence of a stress loci for a combination of road structure and pavement materials. The existence of these loci depends on the material quality and provides a basis for use in design methods. It should be, therefore, considered as a potential analysis tool.

Permanent deformation development in Low Volume Roads occurs in the form of ruts and represent the main distress modes in these pavements. This is broadly a consequence of the deformability in the granular layers, as they are typically the competent material, responsible for the stress distribution. Modelling the deformability is vital for the concept of a mechanistic design approach.

#### **8.1.2. Low Volume Road design and operation - Chapter 3**

The empirical-mechanistic approaches are of growing use as computer programs are more readily available. Permanent deformation assessment, however, remains out of scope of the main pavement design guides (PDG) for Low Volume Roads design. The available empirical-mechanistic PDG for low volume roads use the concept of protecting the subgrade from permanent deformation by varying the required base layer. This is done by limiting the calculated vertical strain on top of the subgrade - which assumes a correlation between elastic and plastic behaviour that cannot be defended mechanically (even if there may be some empirical support for such a relationship).

Despite studies having advanced in the understanding of permanent deformation in granular layers, design guides have failed to introduce this on a routine basis. All of the guides researched neglect the failure mechanism of rutting in the granular material, whereas observations by others and by the author (as reported in other chapters) show rutting of the upper granular material to be the main distress seen in practice.

---

Simple tools as the Dynamic Cone Penetrometer, Clegg Hammer and Mini-FWD are being more actively employed as tools to aid in-situ evaluation. Well used, they may represent a great advantage for Low Volume Roads design procedures which lack readily available tools for material strength assessment.

In addition, new types of loading arrangements such as Low Ground Pressure Vehicles are being explored as means of producing less damaging vehicles. The Tyre Pressure Control Systems introduced in some countries are also being adapted more widely as a manner to make a vehicle flexible for both highway and low volume road traffic. The adjustment in tyre pressure inflation allegedly allows a different pavement contact pressure thereby allowing heavy loaded vehicles to run in weaker roads, but cannot be readily accounted by current PDGs.

### **8.1.3. Full Scale Trials in Scotland - Chapters 4 & 5**

This chapter reported a range of trial LVR pavements. Overall the investigation protocol produced good results. Problems, however, with traffic counting represented a major drawback in the project. Traffic counting on forest roads, are to be installed on a paved area or over a bridge to facilitate collection of better readings. It is also suggested that more scattered sites with monitoring areas concentrated on a lower number of locations should be employed as means of more concise information gathering and analysis.

It appears that most of the rutting occurring in the sites surveyed came shortly after their construction/resurfacing, leading to the conclusion that workmanship may be a highly important variable. Lack of compaction of the layer could be one of the likely reasons for the high initial rutting rates. Establishing the effect of weather on rutting further to the existing knowledge was, however, difficult to achieve; this was mainly due to the difficulties faced in monitoring traffic conditions. A newly developed method was needed to assess permanent deformation development due to wandering traffic on a non-level pavement; this was achieved by the use of wheel path areas, and seemed to be a way forward in the analysis of rutting in unsealed roads.

DCP readings supplied a good source of information for the determination of layer thickness but not as good a source from which to derive CBR, especially for surfacing layers. It seems that for the case of forest roads, because surfaces tend to be about 100 to 150mm thick, the DCP yields artificially low CBR values, possibly due to the disturbing effect of/on the cone tip in the first few centimetres of penetration.

Although the material of the forest roads are sometimes judged to be of poor quality, those samples collected from the trial pits and tested in the laboratory presented

---



characteristics of material close to standard quality, in many respects, for road construction. Gradings could be improved somewhat to provide more stable and less permeable materials.

Reducing overloading of trucks and controlling tyre pressures may be a more economic means of managing pavement deterioration than by using higher quality aggregates (the other meaningful option). This suggests that some kind of policing or QA (Quality Acceptance) system for truck operators might be worth considering.

Rutting damage is not only generated by the rear or trailer tyres. Indeed, given the attention that has been paid to these by researchers and vehicle designers, there may be more damage generated by steer and/or drive axles.

Finally, near-surface rutting is the pre-eminent mode of rutting. This was, to some degree, inevitable given the solid quarry floor at the Ringour site, but the observation matches that made in an earlier study on forest roads in the same region and on the sites surveyed in Chapter 4.

#### **8.1.4. Mechanistic Analysis - Chapter 6**

Despite the ability to take into account non-linear behaviour of the granular materials, Kenlayer has presented a basic limitation in regard to geostatic forces. The code does not seem to take into account the bulk stresses in the calculations. This allows the development of undesirable tension in granular material that required filtering in the analysis. The so-called Method 3 which aids redistribution of calculated tensile stresses that go beyond the Mohr-Coulomb failure parameters may represent some help - this was not investigated - but won't prevent tension from developing in unbound materials.

The stress loci reported in the calculations demonstrate a good correlation with those available in the literature that were originated in other ways. This allows the conclusion that the procedures used in the calculations are valid and that the results could be used further.

The results usually show a fairly well defined locus of maximum stress. By comparing this stress envelope with the failure envelope, conclusions can be established about the more damaging effect of super singles over twin tyres and, likewise, the greater damage inflicted by high tyre pressures compared to that incurred by lower tyre pressures.

All stress surfaces evidenced a closer proximity to failure when both types of tyre arrangements are at higher pressures, suggesting that the benefit of lower pressures is less pronounced for super single tyred systems. In addition, super singles always

---

produced higher levels of stress and are, therefore, more likely to develop permanent deformation, or stresses that will allow rutting to develop faster.

Regarding the influence of aggregate, it is apparent that, except for the softest aggregates, greater aggregate thickness reduces the maximum stress experienced in the aggregate. However, this is not a very strong effect, and a change in tyre pressures or wheel arrangements is more likely to deliver a significant change in stress experienced and, hence, the likelihood of rutting or its magnitude). The effect of changing aggregate stiffness, alone, or stress condition (and, thus, rutting) is mixed. No strong trend shows up and, in any event, the effect is rather insignificant.

#### **8.1.5. Methodology Proposal and Validation - Chapter 7**

The proposed methodology is largely based in other studies which the author had access and of which the supervisor of this thesis had participated. Several studies which have advanced the LVR design methods were the basis for the proposed method, which could pack the existing knowledge into a design guide.

A characteristic stress line (from  $p=250\text{kPa}$  to  $q=250\text{kPa}$ ) provided a good reference for scaling the proximity of the stress envelope modelled in the pavement to the failure surface. This enabled the determination of a safety reference to be developed so as to maintain the working range within a limit to which the pavement would not develop permanent deformation leading to an incremental collapse. In a parallel to the Shakedown theory, this means keeping the pavement in Range B.

A pavement experiencing a stress state envelope which has a Stress variable ( $S$ ) up to 90% of the stress value to failure ( $S_f$ ) - for non-freezing climate and good drainage conditions - is considered to be working under acceptable levels of permanent deformation. Should the condition of material be in an undrained situation or experience freeze-thawing cycles, then a limit of 75% of  $S_f$  is recommended.

The proposed approach was validated by collaborators in Finland [Brito *et al.* 2009]. It is recognized that further work is necessary. Although data collected did provide in situ results for an immediate validation, this was not a straightforward task. Hence some more work is required in this area (see Section 8.2).

### **8.2. RECOMMENDATIONS FOR FUTURE WORK**

Some recommendations from the work developed are here summarized to improve the results obtained and also to make advances in Low Volume Road design procedures.

---

- 
- There is a lack for simple in situ assessment tools that can provide road engineers with better guidance at low cost and time constraints. Where possible, it is suggested that the design guide be completed with guidelines for DCP, Clegg hammer or mini-FWD as tools to help assess material's stiffness.
  - Incorporation of a material 'library' to the design guide will provide important guidelines. It is likely that this will need to be done regionally.
  - The calculation procedure should be automated required in order to produce a simple tool readily available for road engineers.
  - Mechanistic tools should be employed to provide a better tensile cut-off limit, by redistributing the stresses until a solution is obtained without unrealistic tensile stresses in the unbound material. A finite element analysis ought to provide a better analysis tool than the one used. It is recommended that the UMAT code developed by Steven [2005] for use with Abaqus be considered. Preliminary analysis carried out by the author demonstrates an excellent potential for improved S values.
  - The flow charts of the proposed design method can possibly undergo more improvements if connected to an example which provides the user with a good starting point. Some of this has already been done by Dawson *et al.* [2008].
  - Calculations should be carried out to refine the S values. They must include the geostatic forces in order to improve stress evaluation. The calculations performed could certainly have achieved more consistency, requiring less filtering, if bulk stresses had been considered.
-

---

## REFERENCES

- AASHTO [1986] *Guide for design of pavement structures*, American Association of State Highway & Transportation Officials. Washington, DC.
- AASHTO [1992] *T 294-92 I - Interim method of test for resilient modulus of unbound granular base/subbase materials and subgrade soils*, SHRP Protocol P46. American Association of State Highway & Transportation Officials. Washington, DC.
- AASHTO [1993] *AASHTO Guide for design of pavement structures*, American Association of State Highway and Transportation Officials. Washington, DC.
- AASHTO [2000] AASHTO PP 38-00. *Standard practice for determining maximum rut depth in asphalt pavement*, Washington, DC.
- AASHTO [2004] *Development of the 2002 Guide for Design of New and Rehabilitated Pavement Structures: Phase II*, NCHRP Project 1-37A. Washington, DC.
- Abu-Farsakh, M. Y., Nazzal, M. D., Alshibli, K. & Seyman, E. [2005] 'Application of dynamic cone penetrometer in pavement construction control.' *Transportation Research Record*, 1913, 53-61.
- Addis, R. R. [2000] Effects of wide single tyres and dual tyres. *COST-334 Final Report - Executive Summary*.
- Ahlborn, G. [1972] ELSYM, computer program for determining stresses and deformations in five layer elastic systems. University of California.
- Ahlvin, R. G. [1959] Developing a set of CBR design curves. *Instruction Report No. 4*. US Army Engineer Waterways Experimental Station.
- Akou, Y., Heck, J. V., Kazai, A., Hornych, P., Odéon, H. & Piau, J. M. [1999] 'Modelling of flexible pavements using the finite element method and a simplified approach. Unbound granular materials - laboratory testing, in-situ testing and modelling.' *Proceedings of International Workshop on Modelling and Advanced Testing for Unbound Granular Materials*, Correia, A. G.
- Allen, J. [1973] *The effect of non-constant lateral pressures of the resilient response of granular materials*, Doctorate Thesis, University of Illinois at Urbana-Champaign.
- Allen, J. J. & Thompson, M. R. [1974] 'Resilient response of granular materials subjected to time dependent lateral stresses.' *Transportation Research Record*, 510, 1-13.
- Almeida, J. C. G. R. [1993] *Analytical techniques for the structural evaluation of pavements*, Doctorate Thesis, University of Nottingham.
- Andrei, D., Witczak, M., Schwartz, C. W. & Uzan, J. [2004] 'Harmonized resilient modulus test method for unbound pavement materials.' *Transportation Research Record*, 1874, 29-37.
-

- Arnold, G. [2004] *Rutting of granular pavements*, Doctorate Thesis, University of Nottingham.
- ASTM [2005] ASTM E1703 / E1703M. *Standard test method for measuring rut-depth of pavement surfaces using a straightedge*, Philadelphia, USA.
- ASTM [2009] ASTM D6951 / D6951M. *Standard test method for use of the dynamic cone penetrometer in shallow pavement applications*, Philadelphia, USA.
- Austrroads [1992] *Pavement design: a guide to the structural design of road pavements.*, Sydney.
- Austrroads [1995] *A guide to the structural design of road pavements*, Sydney.
- Austrroads [2004] *Austrroads pavement design guide*, Sydney.
- Austrroads [2008] AGPT02/08. *Guide to pavement technology - Part 2: Pavement Structural Design*, Sydney.
- Austrroads [2009] *Guide to pavement technology - Part 6: Unsealed pavements*, Sydney.
- Ayres, M. & Witczak, M. [1998] 'AYMA - A mechanistic probabilistic system to evaluate flexible pavement performance.' *Proceedings of Transportation Research Board, 77th Annual Meeting*, Washington, DC. Paper No.980738.
- Barksdale, R. D. [1972] 'Laboratory evaluation of rutting in base course materials.' *Proceedings of Third International Conference on Structural Design of Asphalt Pavements*, London, UK. 161-174.
- Belt, J., Ryyänen, T. & Ehrola, E. [1997] 'Mechanical properties of unbound base course.' *Proceedings of 8<sup>th</sup> International Conference on Asphalt Pavements*, vol. 1, Seattle. 771-781.
- Biarez, J. [1962] *Contribution à l'étude des propriétés mécaniques des sols et des matériaux pulvérulents*, Doctorate Thesis, Université de Grenoble. French
- Bonaquist, R. F. & Witczak, M. W. [1997] 'A comprehensive constitutive model for granular materials in flexible pavement structures.' *Proceedings of 8th International Conference on Asphalt Pavements*, vol. 1, 783-802.
- Boyce, J. R. [1980] 'A non-linear model for the elastic behaviour of granular materials under repeated loading.' *Proceedings of International Symposium on Soils under Cyclic and Transient Loading*, Swansea, UK. 285-294.
- Bradley, A. [2002] 'Evaluation of forest access road designs for use with CTI-equipped log haul trucks phase II: seasoned access roads.' *Advantage Report*, 3, 7, 20p.
- Brito, L. A. T., Dawson, A. & Kolisoja, P. [2009] 'Analytical evaluation of unbound granular layers in regard to permanent deformation.' *Proceedings of Bearing Capacity of Roads, Railway and Airfields (BCR<sup>2</sup> A'09)*, Tutumluer, E. and Al-Qadi, L. Taylor and Francis Group. London.
- Brito, L. A. T. & Dawson, A. R. [2008] Roads under timber traffic - monitoring study. *Final Research Project. NTEC Report No: 08023*.
- Brito, L. A. T., Dawson, A. R. & Tyrrell, R. W. [2008] Roads under timber transport - Ringour trials. *NTEC Report 08022*.
-

- Brown, S. F. [1996] '36<sup>th</sup> Rankine lecture: soil mechanics in pavement engineering.' *Geotechnique*, 46, 3, 383-426.
- Brown, S. F. & Hyde, A. F. L. [1975] 'Significance of cyclic confining stress in repeated-load triaxial testing of granular material.' *Transportation Research Record*, 537, 49-58.
- Brown, S. F. & Pell, P. S. [1967] 'An experimental investigation of the stresses, strains and deflections in a layered pavement structure subjected to dynamic loads.' *Proceedings of 2<sup>nd</sup> International Conference on Structural Design of Asphalt Pavements*, 487-504.
- BS [1990a] BS 1377-2:1990. *Methods of test for soils for civil engineering purposes. Classification tests*, London, UK.
- BS [1990b] BS 812-112:1990. *Testing aggregates. Method for determination of aggregate impact value (AIV)*, London, UK.
- BS [1990c] BS 812-111:1990. *Testing aggregates. Methods for determination of ten per cent fines value (TFV)*, London, UK.
- BS [1992] BS 882:1992. *Specification for aggregates from natural sources for concrete*, London, UK.
- BS [1997] BS EN 933-1:1997. *Tests for geometrical properties of aggregates. Determination of particle size distribution. Sieving method*, London, UK.
- BS [2000] BS EN 1097-6:2000. *Tests for mechanical and physical properties of aggregates. Determination of particle density and water absorption*, London, UK.
- BS [2004] BS EN 13286-47:2004. *Unbound and hydraulically bound mixtures. Test method for the determination of California bearing ratio, immediate bearing index and linear swelling*, London, UK.
- BS [2006] BS EN ISO 12236:2006. *Geosynthetics. Static puncture test (CBR test)*, London, UK.
- CEN [2004] EN 13286-7. *Repeated load triaxial test*, Comité Européen de Normalisation.
- Ceratti, J., Núñez, W., Gehling, W. & Oliveira, J. [2000] 'Rutting of Thin Pavements - Full-Scale Study.' *Transportation Research Record*, 1716, 7.
- Chan, F. W. K. [1990] *Permanent deformation resistance of granular material layers in pavements*, Doctorate Thesis, University of Nottingham.
- Chazallon, C. [2000] 'An elastoplastic model with kinematic hardening for unbound aggregates in roads.' *Proceedings of Aggregates in Road Construction UNBAR 5*, Balkema, Rotterdam. 265-270.
- Chazallon, C., Habiballah, T. & Hornych, P. [2002]. 'Elastoplasticity framework for incremental or simplified methods for unbound granular materials for roads'. *BCRA workshop on modelling of flexible pavements*. Lisbon.
- Chen, D. H., Zaman, M. M. & Laruros, J. G. [1994] 'Resilient moduli of aggregate materials: variability due to testing procedure and aggregate type.' *Transportation Research Record*, 1462, 57-64.
-

- Chen, W.-F. [1994] *Constitutive equations for engineering materials*, New York, Elsevier.
- Coghlan, G. T. [1999] Opportunities for low-volume roads. *TRB A5002*. Committee on Low Volume Roads. Unpublished.
- COURAGE [1999] Construction with unbound road aggregates in Europe. *4th Framework Programme, Contract No.: RO-97-SC.2056*.
- Dawson, A., Correia, A. G., Jouve, P., Paute, J.-L. & Galjaard, P. J. [1994] 'Modelling resilient and permanent deflections in granular and soil pavement layers.' *Proceedings of 4th Int. Conf. Bearing Capacity of Roads & Airfields*, vol. 2, Minneapolis. 847-861.
- Dawson, A. & Kolisoja, P. [2004] Permanent deformation. *Report on Task 2.1. Roadex II Project*.
- Dawson, A., Kolisoja, P. & Vuorimies, N. [2005] 'Permanent deformation behaviour of low volume roads in the northern periphery areas.' *Proceedings of 7th Int. Conf. Bearing Capacity of Roads, Railways and Airfields*, Trondheim.
- Dawson, A., Kolisoja, P., Vuorimies, N. & Saarenketo, T. [2007] 'Design of low-volume pavements against rutting - a simplified approach.' *Proceedings of Transportation Research Board Low Volume Roads Conference 2007*, Austin.
- Dawson, A. R. [2008] 'Rut accumulation in low-volume pavements due to mixed traffic.' *Transportation Research Record*, 2068, 78-86.
- Dawson, A. R., Kolisoja, P. & Vuorimies, N. [2008] Understanding low-volume pavement response to heavy traffic loading. *Roadex III Report on Task B-2*.
- Dawson, A. R. & Wellner, F. [1999] Plastic behaviour of granular materials. *Final Report ARC Project 933, Reference PRG990*. University of Nottingham, UK.
- Douglas, R. A. [1997] *Unbound roads trafficked by heavily loaded tyres with low inflation pressure*, London, ROYAUME-UNI, Institution of Civil Engineers. 0965-092x
- Douglas, R. A. & Valsangkar, A. J. [1992] 'Unpaved geosynthetic-built resource access roads: Stiffness rather than rut depth as the key design criterion.' *Journal of Geotextiles and Geomembranes*, 11, 1, 45-59.
- Douglas, R. A., Woodward, W. D. H. & Rogers, R. J. [2003] 'Contact pressures and energies beneath soft tires - modelling effects of central tire inflation-equipped heavy-truck traffic on road surfaces.' *Transportation Research Record*, 1819, 221-227.
- Duncan, J. M., Monismith, C. L. & Wilson, E. L. [1968] 'Finite element analysis of pavements.' *Highway Research Record*, 228, 18-33.
- Dunlap, W. A. [1963] A report on a mathematical model describing the deformation characteristics of granular materials. *Technical Report No. 1, Proj. 2-8-62-27*. Texas Transportation Institute, Texas A & M University, College Station.
- Edwards, J. P., Thom, N. H. & Fleming, P. R. [2004] 'Development of a simplified test for unbound aggregates and weak hydraulically bound materials utilising the NAT.' *Proceedings of 6<sup>th</sup> International Symposium on Unbound Materials in Roads*, Nottingham, UK.
-

- El-Basyouny, M. M. & Witczak, M. W. [2004] *Appendix GG-1: calibration of permanent deformation models for flexible pavements*, NCHRP 1-37A.
- El Abd, A. [2006] *Développement d'une méthode de prédiction des déformations de surface des chaussées à assises non traitées*, Doctorate Thesis, Université de Bordeaux 1. French
- El Abd, A., Hornych, P., Breysse, D., Denis, A. & Chazallon, C. [2004] 'A simplified method of prediction of permanent deformations of unbound pavement layers.' *Proceedings of 6th International Symposium on Pavements Unbound (UNBAR6)*, Nottingham, England.
- Elliot, R. P. & Lourdesnathan, D. [1989] 'Improved characterization model for granular bases.' *Transportation Research Record*, 1227, 128-133.
- FEG [2000] Forest traffic and public roads - solutions for the future. *Report of DTI/Institution of Agricultural Engineers*. Forest Engineering Group, Mission to Sweden.
- ForestryEnterprise [2004] *The forestry civil engineering handbook*,
- Gabr, M. A., Coonse, J. & Lambe, P. C. [2001] 'A potential model for compaction evaluation of piedmont soils using dynamic cone penetrometer (DCP).' *Geotechnical Testing Journal*, 24, 3, 308-313.
- Giroud, J. P. & Noiray, L. [1981] 'Geotextile reinforced unpaved road design.' *Proceedings of ASCE Journal, Geotechnical Engineering Division*, 1107, GT9, 1233-1254.
- Granlund, P., Eliasson, T. & Persson, B. [1999] Bra affär med CTI bilen. *Skogforst resultat Nr4 / 1999*. English abstract. Cited in Saarenketo and Aho 2005.
- Hall, K. D. & Bettis, J. B. [2000] Development of comprehensive low-volume pavement design procedures. *MBTC 1070, Final Report*.
- Hammit, G. M. [1970] Thickness requirements for unsurfaced roads & airfields bare base support. *Technical Report S-70-5*. US Army Engineer Waterways Experimental Station. Cited in Little 1992.
- Harison, J. A. [1987] 'Correlation between California Bearing Ratio and Dynamic Cone Penetrometer strength measurement of soils.' *Proceedings of the Institution of Civil Engineers (London)*, 83, 2, 833-844.
- Head, K. H. [2006] *Manual of soil laboratory testing*, 3 ed. Cobham, UK, Whittles Publishing.
- Hicher, P. Y., Daouadji, A. & Fedghouche, D. [1999]. 'Elastoplastic modelling of cyclic behaviour of granular materials'. *Unbound Granular Materials*. Lisbon. 161-168.
- Hicks, R. G. [1970] *Factors influencing the resilient properties of granular materials*, Doctorate Thesis, University of California.
- HighwaysAgency [2005] Series 800 Road Pavements - (11/04) Unbound, Cement And Other Hydraulically Bound Mixtures. *Manual Of Contract Documents For Highway Works - Volume 1. Specification For Highway Works*
-



- HighwaysAgency [2007] Series 800 Road Pavements - (11/04) Unbound, Cement And Other Hydraulically Bound Mixtures. *Manual of Contract Documents For Highway Works - Volume 2. Notes for Guidance On The Specification For Highway Works*,
- HMSO [1994] *Design manual for roads and bridges*, Vol 7, HD 25/94, Part 2, Foundations.
- Hoff, I., Baklokk, L. J. & Aurstad, J. [2004] 'Influence of laboratory compaction method on unbound granular materials.' *Proceedings of 6th International Symposium on Pavements Unbound UNBAR6*, Dawson, A. R. Rotterdam, Netherlands.
- Hornych, P., Kazai, A. & Piau, J. M. [1998] 'Study of the resilient behaviour of unbound granular materials.' *Proceedings of 5th Conference on Bearing Capacity of Roads and Airfields*, vol. 3, Trondheim, Norway. 1277-1287.
- Huang, Y. H. [2003] *Pavement analysis and design*, 2nd ed. Prentice Hall.
- Hujeux, J. C. [1985]. 'Une loi de comportement pour le chargement cyclique des sols'. *Génie parassismique, Presse des Ponts et Chaussées*. Paris. 316-331. French
- Janoo, V., Irwin, L., Knuth, K., Dawson, A. & Eaton, R. [1999] 'Use of inductive coils to measure dynamic and permanent pavement strains.' *Proceedings of Accelerated Pavement Testing International Conference*, Reno, USA.
- Janoo, V. C. & Bayer II, J. J. [2001] The effect of aggregate angularity on base course performance. *ERDC/CRREL TR-01-14*. US Army Corps of Engineers.
- Johnson, T. C., Berg, R. L. & Dimillio, A. [1986] 'Frost action predictive techniques: An overview of research results.' *Transportation Research Record*, 1089, 147-161.
- Jouve, P., Martinez, J., Paute, J. L. & Ragneau, E. [1987] 'Rational model for the flexible pavement deformations.' *Proceedings of 6th International Conference on Structural Design of Asphalt Pavements*, vol. 1, 50-64.
- Kaloush, K. E. & Witczak, M. W. [2000] Development of a permanent to elastic strain ratio model for asphalt mixtures. *NCHRP 1-37 A. Inter Team Technical Report*.
- Karasahin, M. [1993] *Resilient behaviour of granular materials for analysis of highway pavements*, Doctorate Thesis, University of Nottingham.
- Khedr, S. [1985] 'Deformation characteristics of granular base course in flexible pavement.' *Transportation Research Record*, 1043, 131-138.
- Khogali, W. E. I. & Mohamed, E. H. [2004] 'Novel approach for characterization of unbound materials.' *Transportation Research Record*, 1874, 38-46.
- Khogali, W. E. I. & Zeghal, M. [2000] 'On the resilient behaviour of unbound aggregates.' *Proceedings of 5<sup>th</sup> International Symposium on Unbound Aggregates in Road Construction*, Nottingham, UK.
- Kim, S.-H., Little, D. N., Masad, E. & Lytton, R. L. [2004] 'Prediction of anisotropic resilient responses for unbound granular layer considering aggregate physical properties and moving wheel load.' *Proceedings of Aggregates: Asphalt Concrete, Portland Cement Concrete, Bases, and Fines. Twelfth Annual Symposium*, Denver. 24p.
-

- Kolisoja, P. [1994] 'Simple automatic stress path control system for triaxial testing.' *Proceedings of 13<sup>th</sup> International Conference on Soil Mechanics and Foundation Engineering, Part 1*, New Delhi, India.
- Kolisoja, P. [1997] *Resilient deformation characteristics of granular materials*, Doctorate Thesis, Tampere University of Technology.
- Kolisoja, P. [2007] Vesilahti test site data. 10/10/2007. Tampere/FinalInd. *Personal Communication, e-mail*.
- Korkiala-Tanttu, L. [2008] *Calculation method for permanent deformation of unbound pavement materials*, Doctorate Thesis, Helsinki University of Technology.
- Korkiala-Tanttu, L. [2009] 'Verification of rutting calculation for unbound road materials.' *Proceedings of the Institution of Civil Engineers, Transport* 162, TR2, 107-114.
- Lashine, A. K., Brown, S. F. & Pell, P. S. [1971] Dynamic properties of soils. *Report No. 2 Submitted to Koninklijke/Shell Laboratorium*. University of Nottingham, UK.
- Leahy, R. B. [1989] *Permanent deformation characteristics of asphalt concrete*, Doctorate Thesis, University of Maryland.
- Lekarp, F. [1997] *Permanent deformation behaviour of unbound granular materials*, Doctorate Thesis, Kungl Tekniska Högskolan.
- Lekarp, F. & Dawson, A. [1998] 'Modelling permanent deformation behaviour of unbound granular materials.' *Construction and Building Materials*, 12, 1, 9-18.
- Lekarp, F. & Isacsson, U. [2000] 'Development of a large-scale triaxial apparatus for characterization of granular materials.' *International Journal on Road Materials and Pavement Design*, 1, 2, 165-196.
- Lekarp, F., Isacsson, U. & Dawson, A. [2000] 'State of the Art - II: Permanent strain response of unbound aggregates.' *Journal of Transportation Engineering*, 126, 1, 76-83.
- Lentz, R. W. & Baladi, G. Y. [1981] 'Constitutive equation for permanent strain of sand subjected to cyclic loading.' *Transportation Research Record*, 810, 50-54.
- Little, P. H. [1992] *The design of unsurfaced roads using geosynthetics*, Doctorate Thesis, University of Nottingham.
- Lytton, R., Uzan, J., Fernando, E. G., Roque, R., Hiltunen, D. & Stoffels, S. [1993] Development and validation of performance prediction models and specifications for asphalt binders and paving mixes. *Report No. SHRP-A-357*. The Strategic Highway Research Program
- MetOffice [2007] *Weather data*. [online] Available at: <<http://www.metoffice.gov.uk/>> [2007]
- Mohammad, L. N., Puppala, A. J. & Alavilli, P. [1994] 'Influence of testing procedure and LVDT location on resilient modulus of soils.' *Transportation Research Record*, 1462, 91-101.
- Monismith, C. L. [1992] 'Analytically based asphalt pavement desing and rehabilitation: theory to practice 1962-1992.' *Transportation Research Record*, 1354, 5-26.
-

- Monismith, C. L., Seed, H. B., Mitry, F. G. & Chan, C. K. [1967] 'Prediction of pavement deflections from laboratory tests.' *Proceedings of 2<sup>nd</sup> International Conference on Structural Design of Asphalt Pavements*, 109-140.
- Morgan, J. R. [1966] 'The response of granular materials to repeated loading.' *Proceedings of 3<sup>rd</sup> Conference ARRB*, 1178-1192.
- Mundy, M. [2002] *Unbound pavement materials and analytical design*, Doctorate Thesis, University of Nottingham.
- Munro, R. & MacCulloch, F. [2007] Tyre pressure control on timber haulage vehicles. *Roadex III Report on Task B-2*.
- Nataatmadja, A. & Parkin, A. K. [1989] 'Characterization of granular materials for pavements.' *Canadian Geotechnical Journal*, 26, 725-730.
- Nishi, M., Yoshida, N., Tsujimoto, T. & Ohashi, K. [1994] 'Prediction of rut depth in asphalt pavements.' *Proceedings of 4<sup>th</sup> International Conference on the Bearing Capacity of Roads and Airfields*, Minneapolis, USA. 1007-1019.
- Núñez, W., Ceratti, J., Gehling, W. & Oliveira, J. [2008] 'Twelve years of Accelerated Pavement Testing in Southern Brazil; Challenges, Achievements and Lessons Learned. Plenary Session.' *Proceedings of 3rd International Conference on Accelerated Pavement Testing - APT'08*, Transportation Research Board. Madrid, Spain.
- Pappin, J. W. [1979] *Characteristics of granular material for pavement analysis*, Doctorate Thesis, University of Nottingham.
- Paute, J. L., Horny, P. & Benaben, J. P. [1996] 'Repeated load triaxial testing of granular materials in the French network of Laboratories des Ponts et Chaussées.' *Proceedings of European Symposium Euroflex 1993*, Correia, A. G. Balkema. 53-64.
- Paute, J. L., Jouve, P., Martinez, J. & Ragneau, E. [1988]. 'Mode`le de calcul pour le dimensionnement des chaussées souples'. *Bull. de Liaison des Laboratoires des Ponts et Chaussées*. 21-36, Cited in Lekarp et al. 2000. French
- Pezo, R. F. [1993]. 'A general method of reporting resilient modulus tests of soils-A pavement engineer's point of view'. *72<sup>nd</sup> Annual Meeting of the TRB*.
- Piouslin, S. & Done, S. [2005] DCP analysis and design of low volume roads by new TRL software UK DCP. *Seminar: Sustainable Access and Local Resource Solutions, PIARC - RGC, Siem Reap, TRL*.
- Powell, M. J., Potter, J. F., Mathew, H. C. & Nunn, T. [1984] The structural design of bituminous roads. *Laboratory report 1132* Transport and Research Laboratory.
- Raad, L. & Figueroa, J. L. [1980] 'Load response of transportation support systems.' *Transportation Engineering Journal, ASCE*, 106, 1, 111-128.
- Raad, L., Minassian, G. & Gartin, S. [1992] 'Characterization of saturated granular bases under repeated loads.' *Transportation Research Record*, 1369, 73-82.
- Rada, G. & Witczak, M. W. [1981] 'Comprehensive evaluation of laboratory resilient moduli results for granular material.' *Transportation Research Record*, 810, 23-33.
-

- Richardson, I. R. [1999] *The stress-strain behaviour of dry granular material subjected to repeated loading in a hollow cylinder apparatus*, Doctorate Thesis, University of Nottingham.
- Saarenketo, T. [1995a] 'The use of dielectric and electrical conductivity measurement and ground penetrating radar for frost susceptibility evaluations of subgrade soils.' *Proceedings of Application of Geophysics to Engineering and Environmental Problems*, Bell, R. S. Florida, USA. 73-85.
- Saarenketo, T. [1995b] 'Using electrical methods to classify the strength properties of Texas and Finnish base course aggregates.' *Proceedings of 3<sup>rd</sup> Annual Symposium Proceedings, Center for Aggregates Research*, Austin, USA. 19p.
- Saarenketo, T. [2001] 'GPR based road analysis - a cost effective tool for road rehabilitation - case history from Highway 21, Finland.' *Proceedings of 20<sup>th</sup> ARRB Conference*, Melbourne, Australia. 19p.
- Saarenketo, T. [2006] *Electrical properties of road materials and subgrade soils and the use of ground penetrating radar in traffic infrastructure surveys*, Doctorate Thesis, University of Oulu.
- Saarenketo, T. [2008] Percostations in forest road applications in Scotland. *Summary Report 2006 - 2008. RUTT Project Report*. Roadscanners/ Finland.
- Saarenketo, T. & Aho, S. [2005] Managing spring thaw weakening on low volume roads. *Report on Task 2.3. Roadex II Project*.
- Saarenketo, T., Kolisoja, P., Luiro, K., Majjala, P. & Vuorimies, N. [2002] 'Percostation for real-time monitoring of moisture variations, frost depth and spring thaw weakening.' *Proceedings of Transportation Research Board Meeting*
- Saarenketo, T. & Scullion, T. [1996] 'Laboratory and GPR tests to evaluate electrical and mechanical properties of Texas and Finnish base course aggregates.' *Proceedings of Sixth International Conference on Ground Penetrating Radar*, Sendai, Japan. 477-482.
- Saarenketo, T., Scullion, T. & Kolisoja, P. [1998] 'Moisture susceptibility and electrical properties of base course aggregates.' *Proceedings of BCRA'98*, vol. 3, Trondheim, Norway. 1401-1410.
- Saba, R. G., Huvstig, A., Sund, E., Hildebrand, G., Elsander, J., Evensen, R. & Sigursteinsson, H. [2006] Performance prediction models for flexible pavements: a state-of-the-art report. *NordFoU Project: Pavement Performance Models*.
- Seed, H. B., Mitry, F. G., Monismith, C. L. & Chan, C. K. [1967] Prediction of flexible pavement deflections from laboratory repeated load tests. *NCHRP Report No. 35*. National Cooperative Highway Research Program.
- Semmelink, C. J. & de Beer, M. [1995] 'Rapid determination of elastic and shear properties of road building materials with the K-mould.' *Proceedings of UNBAR4 Symposium*, University of Nottingham, U. Nottingham.
- Seyhan, U. & Tutumluer, E. [1999] 'Characterization of unbound aggregates using the new fastCell.' *Proceedings of 1999 Federal Aviation Administration Technology Transfer Conference*, Atlantic City, USA.
-

























- Sharp, K. G. [2004] 'Full scale accelerated pavement testing: a southern hemisphere and asian perspective.' *Proceedings of 2<sup>nd</sup> International Conference on Accelerated Pavement Testing*, Minneapolis.
- Sharp, R. W. [1983] *Shakedown-analyses and the design of pavement under moving surface load*, Doctorate Thesis, University of Sydney.
- Shaw, P. S. [1980] *Stress-strain relationships for granular materials under repeated loading*, Doctorate Thesis, The University of Nottingham.
- Shell [1985] Addendum to the "Shell pavement design manual". Shell International Petroleum Company.
- Simpson, A. L. [2001] Characterization of transverse profiles. *FHWA Report N° FHWA-RS-01-024*.
- StandardsAustralia [1995] Australian Standard 1289.6.8.1. *Method of testing soils for engineering purposes - Soil strength and consolidation tasks - Determination of the resilient modulus and permanent deformation of granular unbound pavement materials*, Sydney, Australia.
- Steven, B. D. [2005] *The development and verification of a pavement response and performance model for unbound granular pavements*, Doctorate Thesis, University of Canterbury.
- Sweere, G. T. H. [1989] 'Design philosophy.' *Proceedings of International Symposium on Unbound Aggregates in Roads (UNBAR 3)*, University of Nottingham. Keynote paper, 239-252.
- Sweere, G. T. H. [1990] *Unbound granular bases for roads*, Doctorate Thesis, University of Delft.
- Tam, W. A. & Brown, S. F. [1988] 'Use of the falling weight deflectometer for in situ evaluation of granular materials in pavements.' *Proceedings of 14<sup>th</sup> ARRB*, vol. 14, part 5, 155-163.
- Taylor, K. L. [1971] *Finite element analysis of layered road pavements*, Doctorate Thesis, University of Nottingham.
- Taylor, M. [2008] Application of HDM 4 to forestry haulage costs. *Final Report*.
- Theyse, H. L. [2000] 'The development of mechanistic-empirical permanent deformation design models for unbound pavement materials from laboratory and accelerated pavement test data.' *Proceedings of UNBAR 5*, Nottingham. 285-293.
- Theyse, H. L. [2002] Stiffness, strength, and performance of unbound aggregate material: application of South African HVS and laboratory results to California flexible pavements. University of California Pavement Research Center.
- Thom, N. H. [1988] *Design of road foundations*, Doctorate Thesis, University of Nottingham.
- Thom, N. H. & Brown, S. F. [1987] 'Effect of moisture on the structural performance of a crushed-limestone road base.' *Transportation Research Record*, 1121, 50-56.
-

- Thom, N. H. & Brown, S. F. [1988] 'The effect of grading and density on the mechanical properties of a crushed dolomitic limestone.' *Proceedings of 14<sup>th</sup> ARRB Conference, Part 7*, 94-100.
- Thom, N. H. & Brown, S. F. [1989] 'The mechanical properties of unbound aggregates from various sources.' *Proceedings of UNBAR 3*, Nottingham. 130-142.
- Thom, N. H. & Dawson, A. R. [1993] 'The permanent deformation of a granular material modelled using hollow cylinder testing.' *Proceedings of European Symposium on Flexible pavements Euroflex 1993*, Lisbon. 97-128.
- Thom, N. H., Edwards, J. P. & Dawson, A. R. [2005] 'A practical test for the laboratory characterization of pavement foundation materials.' *Proceedings of ICAR Symposium*, Austin.
- Thompson, M. R. & Robnett, Q. L. [1979] 'Resilient properties of subgrade soils.' *Journal of Transportation Engineering*, ASCE, 105, 1, 71-89.
- Tian, P., Zaman, M. M. & Laguros, J. G. [1998] 'Gradation effects on resilient moduli of aggregate bases.' *Transportation Research Record*, 1619, 75-84.
- TransitNewZealand [2007] *New Zealand supplement to the document, Pavement Design - a guide to the structural design of road pavements (Austroads, 2004)*,
- TRL [1993] *A guide to the structural design of bitumen-surfaced roads in tropical and sub-tropical countries*, Overseas Road Note 31. London.
- TRL [2006] Measuring road pavement strength and designing low volume sealed roads using the dynamic cone penetrometer. *User Manual, UK DCP 3.1, Unpublished Project Report. UPR/IE/76/06. Project Record No R7783*.
- Tseng, K. & Lytton, R. [1989]. 'Prediction of permanent deformation in flexible pavement materials'. *Implication of Aggregates in the Design, Construction, and Performance of Flexible Pavements*, ASTM STP 1016. ASTM. 154-172.
- Tutumluer, E., Seyhan, U. & Garg, N. [1998] 'Characterization of anisotropic aggregate behavior under variable confinement conditions.' *Geotechnical Special Publication, Application of Geotechnical Principles in Pavement Engineering*, ASCE Annual Convention, 85, 1-12.
- Tyrrell, R. W. [2004a] Surfacing specification for principal forest roads. Forestry Civil Engineering, Forestry Commission.
- Tyrrell, W. [2004b] 'Pavement trials at Risk Quarry, Kirroughtree.' *Proceedings of 6th International Symposium on Unbound Materials - Unbar 6*, Nottingham.
- Uzan, J. [1985] 'Characterisation of granular material.' *Transportation Research Record*, 1022, 52-59.
- Veverka, V. [1979] 'Raming van de spoordiepte bij wegen met een bitumineuze verharding.' *De Wegentechniek*, 24, 3, cited in Lekarp et al. [2000]. Dutch
- Visser, A. T. [2007] 'Procedure for evaluating stabilization of road materials with nontraditional stabilizers.' *Transportation Research Record*, 2, 1989, 21-26.
- Visser, A. T. & Hall, S. [2003] 'Innovative and cost-effective solutions for roads in rural areas and difficult terrain.' *Transportation Research Record*, 1819, 169-173.
-

- 
- Webster, S. L. & Alford, S. J. [1978] Investigation of construction concepts for pavements across soft ground. *Report TR-S-78-6*. US Army Waterways Experiment Station.
- Webster, S. L. & Watkins, J. E. [1977] Investigation of construction techniques for tactical bridge approach roads across soft ground. *Report TR-S-77-1*. US Army Waterways Experiment Station.
- Wenzel, J. [1998] 'Die erfassung des tragverhaltens ungebundener schichten in straßenkonstruktionen - bearing capacity of unbound granular layers in pavements.' *Wissenschaftliche Zeitschrift der Hochschule für Architektur und Bauwesen Weimar*, B, 5, German
- Werkmeister, S. [2003] *Permanent deformation behaviour of unbound materials in pavement constructions*, Doctorate Thesis, Dresden University of Technology.
- Werkmeister, S., Dawson, A. R. & Wellner, F. [2001] 'Permanent deformation behaviour of unbound granular materials and the shakedown-theory.' *Transportation Research Record*, 1757, 75-81.
- Witczak, M. W. [2004] *Harmonized test methods for laboratory determination of resilient modulus for flexible pavement design*, NCHRP 01-28A.
- Witczak, M. W. & Uzan, J. [1988] The universal airport pavement design system: granular material characterization. University of Maryland, Department of Civil Engineering, MD.
- Witczak, M. W., Zapata, C. E. & Mirza, M. W. [2004] Appendix CC-1: correlation of CBR values with soil index properties. *NCHRP 1-27A*.
- Wolff, H. & Visser, A. T. [1994] 'Incorporating elasto-plasticity in granular layer pavement design.' *Institution of Civil Engineers Transportation*, 105, 259-272.
- Yau, A. & Von Quintus, H. L. [2002] Study of LTPP laboratory resilient modulus test data and response characteristics. *Final Report, FHWA-RD-02-051*. U.S. Department of Transportation Federal Highway Administration Research, Development, and Technology.
-

## APPENDIXES

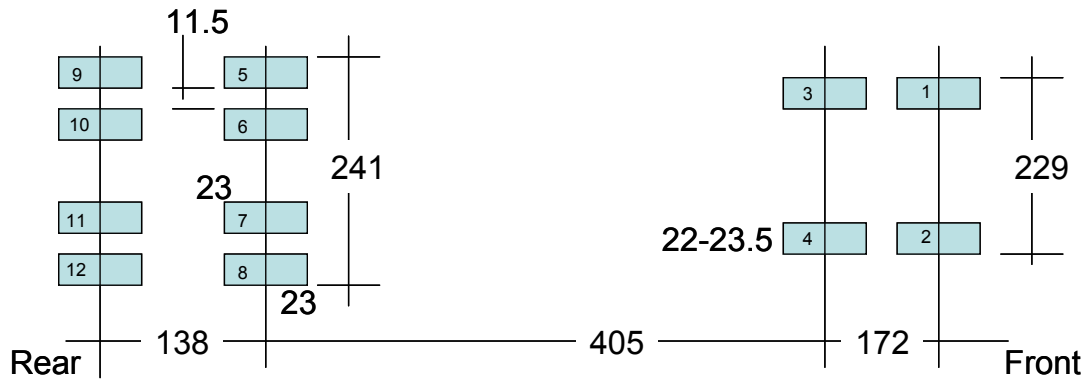
The list below describes the Appendixes to this thesis. Some of them were included *in-print* as they were deemed essential by the author for a thorough understanding of the analysis presented herein. The other relevant appendixes that may represent a cumbersome amount of data but may be used in future work in addition to a further understanding of the work carried out were only included in the CD. A summary list is presented below with

	Description	Copy format	File type (if in digital format)
<b>Appendix A</b>	Accelerated Pavement Facility Layout at Ringour		
<b>Appendix B</b>	Dimension of Vehicles Used in the APT at Ringour		
<b>Appendix C</b>	Weather station results from Monitoring Sections in RUTT		 
<b>Appendix D</b>	Permanent deformation data for the monitoring sections in RUTT		 
<b>Appendix E</b>	Mini-FWD Results from test section at Ringour		 
<b>Appendix F</b>	Permanent deformation data from APT at Ringour		 
<b>Appendix G</b>	Experiment Matrix for Mechanistic Analysis and S results	 	 
<b>Appendix H</b>	"p q" Plots for the all problems solved for the experiment matrix		 
<b>Appendix I</b>	Proposed Design methods - Worked Example	 	





**FC Foden Multilift Truck type345, Registration SN51 ONW**  
all 12 tyres are 295/80R22.5 – **Trial 1,2,4,6,8,9**



Tyre pressures not recorded for Trials 1,2 & 4

All tyres with 70 lb/in<sup>2</sup> for Trial 8A, and 110 lb/in<sup>2</sup> for Trial 8B

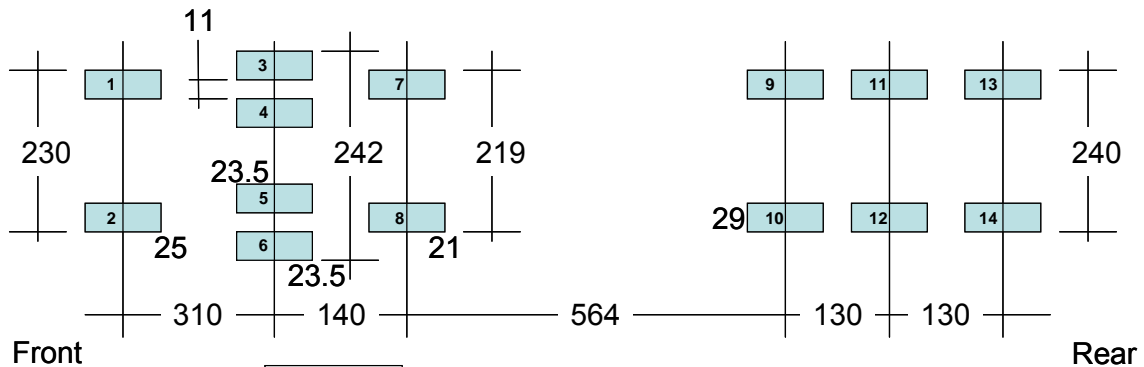
All tyres with 100 lb/in<sup>2</sup> for Trial 9

n.b. 1 lb/in<sup>2</sup> = 6.895 kPa

Trial 6		Prior to Trial 8	
1 – p=111 lb/in <sup>2</sup>	7 – p=?	1 – p=118 lb/in <sup>2</sup>	7 – p=117 lb/in <sup>2</sup>
2 – p=117 lb/in <sup>2</sup>	8 – p=118 lb/in <sup>2</sup>	2 – p=115 lb/in <sup>2</sup>	8 – p=108 lb/in <sup>2</sup>
3 – p=116 lb/in <sup>2</sup>	9 – p=99 lb/in <sup>2</sup>	3 – p=125 lb/in <sup>2</sup>	9 – p=98 lb/in <sup>2</sup>
4 – p=114 lb/in <sup>2</sup>	10 – p=?	4 – p=109 lb/in <sup>2</sup>	10 – p=40 lb/in <sup>2</sup>
5 – p=116 lb/in <sup>2</sup>	11 – p=?	5 – p=107 lb/in <sup>2</sup>	11 – p=10 lb/in <sup>2</sup>
6 – p=?	12 – p=110 lb/in <sup>2</sup>	6 – p=110 lb/in <sup>2</sup>	12 – p=108 lb/in <sup>2</sup>

**John Miller Ltd, Articulated DAF Truck Type 95-530, Registration SJ55 GXA**  
**with Dennison Trailer chassis 17003**

front 8 tyres are 295/80R22.5, rear 6 tyres are 385/65R22.5 – **Trial 3, 8, 9**

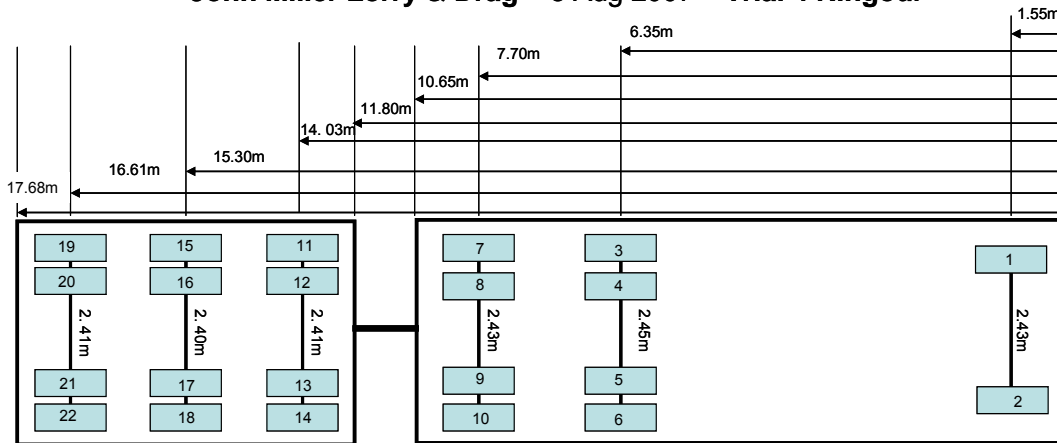


Trial 3	
1 – p=114 lb/in <sup>2</sup>	8 – p=105 lb/in <sup>2</sup>
2 – p=120 lb/in <sup>2</sup>	9 – p=124 lb/in <sup>2</sup>
3 – p=107 lb/in <sup>2</sup>	10 – p=116 lb/in <sup>2</sup>
4 – p=? lb/in <sup>2</sup>	11 – p=102 lb/in <sup>2</sup>
5 – p=? lb/in <sup>2</sup>	12 – p=125 lb/in <sup>2</sup>
6 – p=98 lb/in <sup>2</sup>	13 – p=126 lb/in <sup>2</sup>
7 – p=108 lb/in <sup>2</sup>	14 – p=125 lb/in <sup>2</sup>

All tyres with 100 lb/in<sup>2</sup> for Trial 9

n.b. 1 lb/in<sup>2</sup> = 6.895 kPa

## John Miller Lorry & Drag – 8 Aug 2007 – Trial 4 Ringour

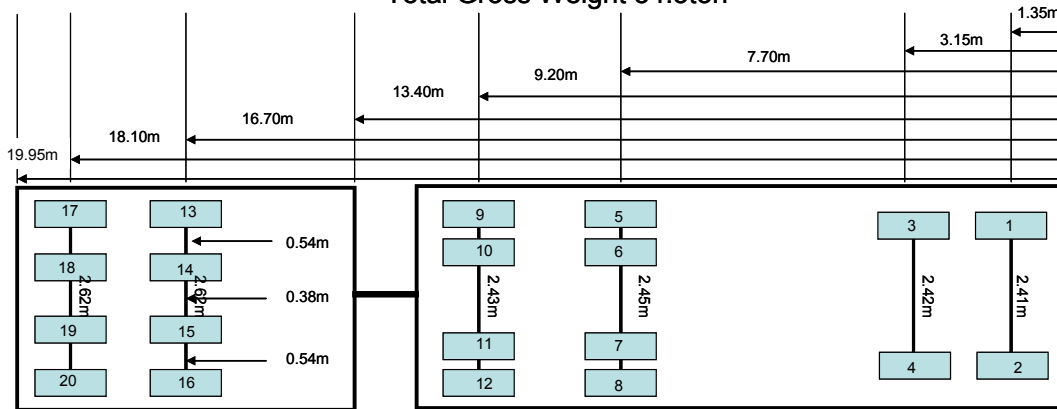


- |                                     |                                     |
|-------------------------------------|-------------------------------------|
| 1 – 300mm p=117 lb/in <sup>2</sup>  | 12 – 240mm p=128 lb/in <sup>2</sup> |
| 2 – 300mm p=132 lb/in <sup>2</sup>  | 13 – 240mm p=126 lb/in <sup>2</sup> |
| 3 – 265mm p=116 lb/in <sup>2</sup>  | 14 – 240mm p=126 lb/in <sup>2</sup> |
| 4 – 265mm p=117 lb/in <sup>2</sup>  | 15 – 235mm p=128 lb/in <sup>2</sup> |
| 5 – 265mm p=120 lb/in <sup>2</sup>  | 16 – 215mm p=116 lb/in <sup>2</sup> |
| 6 – 265mm p=117 lb/in <sup>2</sup>  | 17 – 245mm p=?                      |
| 7 – 265mm p=118 lb/in <sup>2</sup>  | 18 – 210mm p=96 lb/in <sup>2</sup>  |
| 8 – 260mm p=118 lb/in <sup>2</sup>  | 19 – 240mm p=128 lb/in <sup>2</sup> |
| 9 – 250mm p=110 lb/in <sup>2</sup>  | 20 – 240mm p=130 lb/in <sup>2</sup> |
| 10 – 265mm p=115 lb/in <sup>2</sup> | 21 – 240mm p=?                      |
| 11 – 240mm p=129 lb/in <sup>2</sup> | 22 – 240mm p=126 lb/in <sup>2</sup> |

n.b. 1 lb/in<sup>2</sup> = 6.895 kPa

## “Low Ground Pressure” Vehicle – 18 Aug 2007 – Trial 5 Ringour

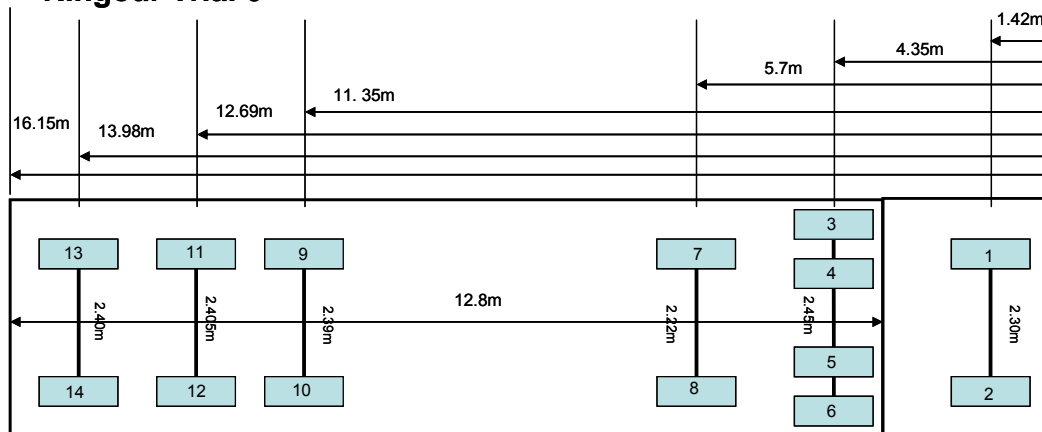
Total Gross Weight 54.5ton



- |                                    |                                     |
|------------------------------------|-------------------------------------|
| 1 – 300mm p=109 lb/in <sup>2</sup> | 11 – 250mm p=?                      |
| 2 – 300mm p=109 lb/in <sup>2</sup> | 12 – 250mm p=65 lb/in <sup>2</sup>  |
| 3 – 300mm p=103 lb/in <sup>2</sup> | 13 – 290mm p=69 lb/in <sup>2</sup>  |
| 4 – 300mm p=76 lb/in <sup>2</sup>  | 14 – 290mm p=68 lb/in <sup>2</sup>  |
| 5 – 230mm p=56 lb/in <sup>2</sup>  | 15 – 290mm p=108 lb/in <sup>2</sup> |
| 6 – 250mm p=?                      | 16 – 290mm p=57 lb/in <sup>2</sup>  |
| 7 – 230mm p=?                      | 17 – 290mm p=61 lb/in <sup>2</sup>  |
| 8 – 250mm p=63 lb/in <sup>2</sup>  | 18 – 290mm p=56 lb/in <sup>2</sup>  |
| 9 – 230mm p=65 lb/in <sup>2</sup>  | 19 – 290mm p=58 lb/in <sup>2</sup>  |
| 10 – 230mm p=?                     | 20 – 290mm p=56 lb/in <sup>2</sup>  |

n.b. 1 lb/in<sup>2</sup> = 6.895 kPa

## John Miller Ltd, Articulated – with Tag Axle – Registration SF05 CVM Ringour Trial 6



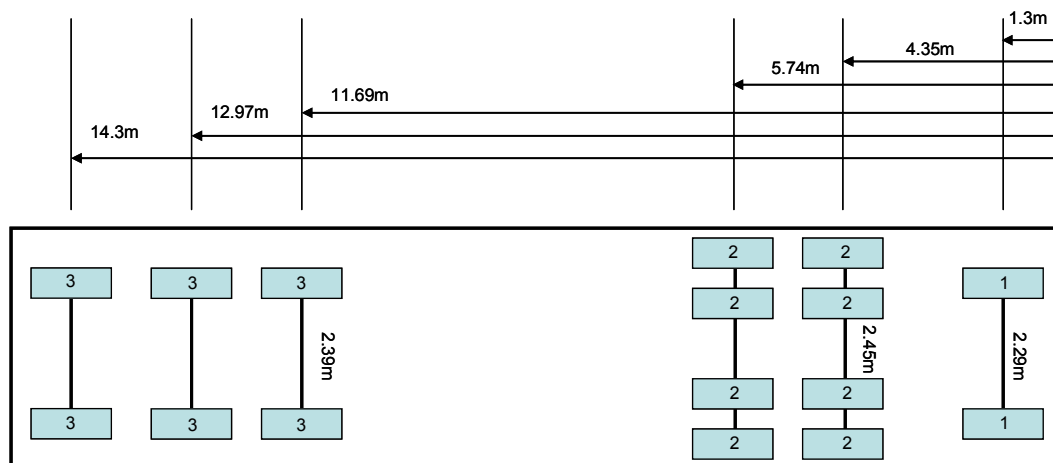
1 – 295 x 80 235mm p=110 lb/in<sup>2</sup>  
 2 – 295 x 80 235mm p=107 lb/in<sup>2</sup>  
 3 – 295 x 80 255mm p=100 lb/in<sup>2</sup>  
 4 – 295 x 80 250mm p=? lb/in<sup>2</sup>  
 5 – 295 x 80 220mm p=? lb/in<sup>2</sup>  
 6 – 295 x 80 255mm p=100 lb/in<sup>2</sup>  
 7 – 295 x 80 225mm p=110 lb/in<sup>2</sup>  
 8 – 295 x 80 230mm p=103 lb/in<sup>2</sup>  
 9 – 385 x 65 285mm p=110 lb/in<sup>2</sup>  
 10 – 385 x 65 300mm p=100 lb/in<sup>2</sup>

11 – 385 x 65 300mm p= 97 lb/in<sup>2</sup>  
 12 – 385 x 65 285mm p=108 lb/in<sup>2</sup>  
 13 – 385 x 65 285mm p=110 lb/in<sup>2</sup>  
 14 – 385 x 65 285mm p=110 lb/in<sup>2</sup>

Loaded length 11.7m

n.b. 1 lb/in<sup>2</sup> = 6.895 kPa

## TCPS Vehicle – 19 Sep 2007 – Trial 7 Ringour James Jones



7400kg 7400kg 7400kg

1 – 295/80 22.5 – 240  
 2 – 295/80 22.5 – 250  
 3 – 385/65 22.5 – 290

6500kg

9500kg

6000kg

Tyre pressures set from cab

Run ID	Problem #	Material ID	Agg Thick / Radius Ratio	Agg. Thick. (cm)	Stiff. Ratio (Ebas/Esub)	Subgrade Stiff. (kPa)	Tyre Pres. (kPa)	Radius (cm)	Tyre Arrang.	Svalue for Material (kPa)	S to Load Condition (kPa)	% of S mobilized	Depth of subgrade (cm)	$\sigma_v$ @ top subgrade (kPa)
NIP1	Problem 1	Norther Ireland Poor	1.0	13.5	2	215000	400	13.5	Dual Tyres	254.9	207.3	81.3%	13.5	231.8
	Problem 2	Norther Ireland Poor	1.3	17.0	2	215000	400	13.5	Dual Tyres	254.9	205.9	80.8%	17.0	185.7
	Problem 3	Norther Ireland Poor	1.7	23.0	2	215000	400	13.5	Dual Tyres	254.9	214.0	84.0%	23.0	131.9
	Problem 4	Norther Ireland Poor	2.5	33.8	2	215000	400	13.5	Dual Tyres	254.9	214.4	84.1%	33.8	79.7
	Problem 5	Norther Ireland Poor	3.5	47.3	2	215000	400	13.5	Dual Tyres	254.9	215.0	84.4%	47.3	50.4
NIP2	Problem 1	Norther Ireland Poor	1.0	13.5	4	110000	400	13.5	Dual Tyres	254.9	220.8	86.6%	13.5	194.2
	Problem 2	Norther Ireland Poor	1.3	17.0	4	110000	400	13.5	Dual Tyres	254.9	212.3	83.3%	17.0	151.7
	Problem 3	Norther Ireland Poor	1.7	23.0	4	110000	400	13.5	Dual Tyres	254.9	217.7	85.4%	23.0	105.4
	Problem 4	Norther Ireland Poor	2.5	33.8	4	110000	400	13.5	Dual Tyres	254.9	209.2	82.1%	33.8	62.3
	Problem 5	Norther Ireland Poor	3.5	47.3	4	110000	400	13.5	Dual Tyres	254.9	208.8	81.9%	47.3	38.6
NIP3	Problem 1	Norther Ireland Poor	1.0	13.5	8	50000	400	13.5	Dual Tyres	254.9	217.8	85.5%	13.5	150.1
	Problem 2	Norther Ireland Poor	1.3	17.0	8	50000	400	13.5	Dual Tyres	254.9	217.8	85.4%	17.0	112.9
	Problem 3	Norther Ireland Poor	1.7	23.0	8	50000	400	13.5	Dual Tyres	254.9	214.5	84.2%	23.0	75.8
	Problem 4	Norther Ireland Poor	2.5	33.8	8	50000	400	13.5	Dual Tyres	254.9	210.1	82.5%	33.8	43.4
	Problem 5	Norther Ireland Poor	3.5	47.3	8	50000	400	13.5	Dual Tyres	254.9	203.8	80.0%	47.3	26.2
NIP4	Problem 1	Norther Ireland Poor	1.0	9.5	2	252000	800	9.5	Dual Tyres	254.9	231.0	90.6%	9.5	450.4
	Problem 2	Norther Ireland Poor	1.3	12.0	2	252000	800	9.5	Dual Tyres	254.9	232.1	91.1%	12.0	352.5
	Problem 3	Norther Ireland Poor	1.7	16.0	2	252000	800	9.5	Dual Tyres	254.9	238.2	93.4%	16.0	247.2
	Problem 4	Norther Ireland Poor	2.5	24.0	2	252000	800	9.5	Dual Tyres	254.9	226.7	89.0%	24.0	140.2
	Problem 5	Norther Ireland Poor	3.5	33.5	2	252000	800	9.5	Dual Tyres	254.9	229.9	90.2%	33.5	86.8
NIP5	Problem 1	Norther Ireland Poor	1.0	9.5	4	126000	800	9.5	Dual Tyres	254.9	229.0	89.8%	9.5	367.3
	Problem 2	Norther Ireland Poor	1.3	12.0	4	126000	800	9.5	Dual Tyres	254.9	230.0	90.2%	12.0	279.4
	Problem 3	Norther Ireland Poor	1.7	16.0	4	126000	800	9.5	Dual Tyres	254.9	227.1	89.1%	16.0	192.9
	Problem 4	Norther Ireland Poor	2.5	24.0	4	126000	800	9.5	Dual Tyres	254.9	227.1	89.1%	24.0	108.7
	Problem 5	Norther Ireland Poor	3.5	33.5	4	126000	800	9.5	Dual Tyres	254.9	225.6	88.5%	33.5	66.9
NIP6	Problem 1	Norther Ireland Poor	1.0	9.5	8	63000	800	9.5	Dual Tyres	254.9	231.8	91.0%	9.5	286.1
	Problem 2	Norther Ireland Poor	1.3	12.0	8	63000	800	9.5	Dual Tyres	254.9	228.9	89.8%	12.0	211.3
	Problem 3	Norther Ireland Poor	1.7	16.0	8	63000	800	9.5	Dual Tyres	254.9	222.6	87.3%	16.0	143.4
	Problem 4	Norther Ireland Poor	2.5	24.0	8	63000	800	9.5	Dual Tyres	254.9	226.6	88.9%	24.0	79.9
	Problem 5	Norther Ireland Poor	3.5	33.5	8	63000	800	9.5	Dual Tyres	254.9	222.6	87.3%	33.5	48.6

Run ID	Problem #	Material ID	Agg Thick / Radius Ratio	Agg. Thick. (cm)	Stiff. Ratio (Ebas/Esub)	Subgrade Stiff. (kPa)	Tyre Pres. (kPa)	Radius (cm)	Tyre Arrang.	Svalue for Material (kPa)	S to Load Condition (kPa)	% of S mobilized	Depth of subgrade (cm)	$\sigma_v$ @ top subgrade (kPa)
NIP7	Problem 1	Norther Ireland Poor	1.0	19.0	2	215000	400	19	Super Singles	254.9	245.3	96.2%	19.0	222.8
	Problem 2	Norther Ireland Poor	1.3	24.0	2	215000	400	19	Super Singles	254.9	245.1	96.1%	24.0	172.3
	Problem 3	Norther Ireland Poor	1.7	32.0	2	215000	400	19	Super Singles	254.9	242.4	95.1%	32.0	117.6
	Problem 4	Norther Ireland Poor	2.5	48.0	2	215000	400	19	Super Singles	254.9	245.2	96.2%	48.0	62.0
	Problem 5	Norther Ireland Poor	3.5	66.5	2	215000	400	19	Super Singles	254.9	245.1	96.2%	66.5	34.8
NIP8	Problem 1	Norther Ireland Poor	1.0	19.0	4	110000	400	19	Super Singles	254.9	244.2	95.8%	19.0	181.6
	Problem 2	Norther Ireland Poor	1.3	24.0	4	110000	400	19	Super Singles	254.9	242.8	95.3%	24.0	135.1
	Problem 3	Norther Ireland Poor	1.7	32.0	4	110000	400	19	Super Singles	254.9	237.8	93.3%	32.0	89.5
	Problem 4	Norther Ireland Poor	2.5	48.0	4	110000	400	19	Super Singles	254.9	239.7	94.0%	48.0	46.2
	Problem 5	Norther Ireland Poor	3.5	66.5	4	110000	400	19	Super Singles	254.9	240.6	94.4%	66.5	25.7
NIP9	Problem 1	Norther Ireland Poor	1.0	19.0	8	50000	400	19	Super Singles	254.9	241.7	94.8%	19.0	133.9
	Problem 2	Norther Ireland Poor	1.3	24.0	8	50000	400	19	Super Singles	254.9	240.4	94.3%	24.0	94.3
	Problem 3	Norther Ireland Poor	1.7	32.0	8	50000	400	19	Super Singles	254.9	236.8	92.9%	32.0	60.2
	Problem 4	Norther Ireland Poor	2.5	48.0	8	50000	400	19	Super Singles	254.9	232.9	91.4%	48.0	30.3
	Problem 5	Norther Ireland Poor	3.5	66.5	8	50000	400	19	Super Singles	254.9	236.6	92.8%	66.5	16.7
NIP10	Problem 1	Norther Ireland Poor	1.0	13.5	2	250000	800	13.5	Super Singles	254.9	250.5	98.3%	13.5	444.7
	Problem 2	Norther Ireland Poor	1.3	17.0	2	250000	800	13.5	Super Singles	254.9	249.5	97.9%	17.0	345.0
	Problem 3	Norther Ireland Poor	1.7	23.0	2	250000	800	13.5	Super Singles	254.9	248.7	97.6%	23.0	230.7
	Problem 4	Norther Ireland Poor	2.5	33.8	2	250000	800	13.5	Super Singles	254.9	248.1	97.4%	33.8	124.3
	Problem 5	Norther Ireland Poor	3.5	47.3	2	250000	800	13.5	Super Singles	254.9	249.7	98.0%	47.3	70.0
NIP11	Problem 1	Norther Ireland Poor	1.0	13.5	4	125000	800	13.5	Super Singles	254.9	245.5	96.3%	13.5	359.5
	Problem 2	Norther Ireland Poor	1.3	17.0	4	125000	800	13.5	Super Singles	254.9	245.9	96.5%	17.0	268.1
	Problem 3	Norther Ireland Poor	1.7	23.0	4	125000	800	13.5	Super Singles	254.9	241.8	94.9%	23.0	173.5
	Problem 4	Norther Ireland Poor	2.5	33.8	4	125000	800	13.5	Super Singles	254.9	242.2	95.0%	33.8	91.7
	Problem 5	Norther Ireland Poor	3.5	47.3	4	125000	800	13.5	Super Singles	254.9	245.9	96.5%	47.3	51.1
NIP12	Problem 1	Norther Ireland Poor	1.0	13.5	8	60000	800	13.5	Super Singles	254.9	237.7	93.3%	13.5	270.0
	Problem 2	Norther Ireland Poor	1.3	17.0	8	60000	800	13.5	Super Singles	254.9	240.4	94.3%	17.0	191.8
	Problem 3	Norther Ireland Poor	1.7	23.0	8	60000	800	13.5	Super Singles	254.9	237.8	93.3%	23.0	119.7
	Problem 4	Norther Ireland Poor	2.5	33.8	8	60000	800	13.5	Super Singles	254.9	236.9	93.0%	33.8	61.9
	Problem 5	Norther Ireland Poor	3.5	47.3	8	60000	800	13.5	Super Singles	254.9	239.5	94.0%	47.3	34.2

Run ID	Problem #	Material ID	Agg Thick / Radius Ratio	Agg. Thick. (cm)	Stiff. Ratio (Ebas/Esub)	Subgrade Stiff. (kPa)	Tyre Pres. (kPa)	Radius (cm)	Tyre Arrang.	Svalue for Material (kPa)	S to Load Condition (kPa)	% of S mobilized	Depth of subgrade (cm)	$\sigma_v$ @ top subgrade (kPa)
CAF1	Problem 1	CAPTIF 2	1.0	13.5	2	195000	400	13.5	Dual Tyres	251.8	207.5	82.4%	13.5	231.2
	Problem 2	CAPTIF 2	1.3	17.0	2	195000	400	13.5	Dual Tyres	251.8	205.7	81.7%	17.0	183.4
	Problem 3	CAPTIF 2	1.7	23.0	2	195000	400	13.5	Dual Tyres	251.8	214.2	85.0%	23.0	129.0
	Problem 4	CAPTIF 2	2.5	33.8	2	195000	400	13.5	Dual Tyres	251.8	212.2	84.3%	33.8	77.6
	Problem 5	CAPTIF 2	3.5	47.3	2	195000	400	13.5	Dual Tyres	251.8	213.3	84.7%	47.3	49.1
CAF2	Problem 1	CAPTIF 2	1.0	13.5	4	100000	400	13.5	Dual Tyres	251.8	220.5	87.6%	13.5	195.3
	Problem 2	CAPTIF 2	1.3	17.0	4	100000	400	13.5	Dual Tyres	251.8	212.6	84.4%	17.0	148.7
	Problem 3	CAPTIF 2	1.7	23.0	4	100000	400	13.5	Dual Tyres	251.8	219.2	87.1%	23.0	101.0
	Problem 4	CAPTIF 2	2.5	33.8	4	100000	400	13.5	Dual Tyres	251.8	209.1	83.0%	33.8	59.4
	Problem 5	CAPTIF 2	3.5	47.3	4	100000	400	13.5	Dual Tyres	251.8	208.3	82.7%	47.3	36.9
CAF3	Problem 1	CAPTIF 2	1.0	13.5	8	45000	400	13.5	Dual Tyres	251.8	223.9	88.9%	13.5	158.5
	Problem 2	CAPTIF 2	1.3	17.0	8	45000	400	13.5	Dual Tyres	251.8	217.8	86.5%	17.0	113.3
	Problem 3	CAPTIF 2	1.7	23.0	8	45000	400	13.5	Dual Tyres	251.8	215.0	85.4%	23.0	73.5
	Problem 4	CAPTIF 2	2.5	33.8	8	45000	400	13.5	Dual Tyres	251.8	210.5	83.6%	33.8	42.0
	Problem 5	CAPTIF 2	3.5	47.3	8	45000	400	13.5	Dual Tyres	251.8	203.7	80.9%	47.3	25.7
CAF4	Problem 1	CAPTIF 2	1.0	9.5	2	325000	800	9.5	Dual Tyres	251.8	231.0	91.7%	9.5	450.2
	Problem 2	CAPTIF 2	1.3	12.0	2	325000	800	9.5	Dual Tyres	251.8	232.8	92.5%	12.0	348.7
	Problem 3	CAPTIF 2	1.7	16.0	2	325000	800	9.5	Dual Tyres	251.8	238.0	94.5%	16.0	242.2
	Problem 4	CAPTIF 2	2.5	24.0	2	325000	800	9.5	Dual Tyres	251.8	225.3	89.5%	24.0	137.0
	Problem 5	CAPTIF 2	3.5	33.5	2	325000	800	9.5	Dual Tyres	251.8	229.9	91.3%	33.5	87.1
CAF5	Problem 1	CAPTIF 2	1.0	9.5	4	162000	800	9.5	Dual Tyres	251.8	229.0	90.9%	9.5	370.7
	Problem 2	CAPTIF 2	1.3	12.0	4	162000	800	9.5	Dual Tyres	251.8	229.6	91.2%	12.0	274.2
	Problem 3	CAPTIF 2	1.7	16.0	4	162000	800	9.5	Dual Tyres	251.8	226.4	89.9%	16.0	185.4
	Problem 4	CAPTIF 2	2.5	24.0	4	162000	800	9.5	Dual Tyres	251.8	227.0	90.2%	24.0	104.0
	Problem 5	CAPTIF 2	3.5	33.5	4	162000	800	9.5	Dual Tyres	251.8	225.6	89.6%	33.5	66.3
CAF6	Problem 1	CAPTIF 2	1.0	9.5	8	80000	800	9.5	Dual Tyres	251.8	229.3	91.1%	9.5	292.6
	Problem 2	CAPTIF 2	1.3	12.0	8	80000	800	9.5	Dual Tyres	251.8	225.5	89.6%	12.0	203.4
	Problem 3	CAPTIF 2	1.7	16.0	8	80000	800	9.5	Dual Tyres	251.8	223.3	88.7%	16.0	133.4
	Problem 4	CAPTIF 2	2.5	24.0	8	80000	800	9.5	Dual Tyres	251.8	226.3	89.9%	24.0	73.7
	Problem 5	CAPTIF 2	3.5	33.5	8	80000	800	9.5	Dual Tyres	251.8	222.4	88.3%	33.5	46.9

Run ID	Problem #	Material ID	Agg Thick / Radius Ratio	Agg. Thick. (cm)	Stiff. Ratio (Ebas/Esub)	Subgrade Stiff. (kPa)	Tyre Pres. (kPa)	Radius (cm)	Tyre Arrang.	Svalue for Material (kPa)	S to Load Condition (kPa)	% of S mobilized	Depth of subgrade (cm)	$\sigma_v$ @ top subgrade (kPa)
CAF7	Problem 1	CAPTIF 2	1.0	19.0	2	205000	400	19	Super Singles	251.8	245.1	97.3%	19.0	223.9
	Problem 2	CAPTIF 2	1.3	24.0	2	205000	400	19	Super Singles	251.8	245.2	97.4%	24.0	171.3
	Problem 3	CAPTIF 2	1.7	32.0	2	205000	400	19	Super Singles	251.8	242.4	96.3%	32.0	116.0
	Problem 4	CAPTIF 2	2.5	48.0	2	205000	400	19	Super Singles	251.8	245.0	97.3%	48.0	61.0
	Problem 5	CAPTIF 2	3.5	66.5	2	205000	400	19	Super Singles	251.8	244.9	97.3%	66.5	34.3
CAF8	Problem 1	CAPTIF 2	1.0	19.0	4	102000	400	19	Super Singles	251.8	243.8	96.8%	19.0	183.9
	Problem 2	CAPTIF 2	1.3	24.0	4	102000	400	19	Super Singles	251.8	243.1	96.5%	24.0	132.3
	Problem 3	CAPTIF 2	1.7	32.0	4	102000	400	19	Super Singles	251.8	237.6	94.4%	32.0	85.6
	Problem 4	CAPTIF 2	2.5	48.0	4	102000	400	19	Super Singles	251.8	239.1	94.9%	48.0	44.0
	Problem 5	CAPTIF 2	3.5	66.5	4	102000	400	19	Super Singles	251.8	240.3	95.4%	66.5	24.7
CAF9	Problem 1	CAPTIF 2	1.0	19.0	8	51000	400	19	Super Singles	251.8	242.2	96.2%	19.0	144.1
	Problem 2	CAPTIF 2	1.3	24.0	8	51000	400	19	Super Singles	251.8	240.5	95.5%	24.0	95.9
	Problem 3	CAPTIF 2	1.7	32.0	8	51000	400	19	Super Singles	251.8	236.5	93.9%	32.0	59.2
	Problem 4	CAPTIF 2	2.5	48.0	8	51000	400	19	Super Singles	251.8	232.7	92.4%	48.0	29.8
	Problem 5	CAPTIF 2	3.5	66.5	8	51000	400	19	Super Singles	251.8	236.5	93.9%	66.5	16.7
CAF10	Problem 1	CAPTIF 2	1.0	13.5	2	350000	800	13.5	Super Singles	251.8	250.8	99.6%	13.5	448.4
	Problem 2	CAPTIF 2	1.3	17.0	2	350000	800	13.5	Super Singles	251.8	249.5	99.1%	17.0	344.4
	Problem 3	CAPTIF 2	1.7	23.0	2	350000	800	13.5	Super Singles	251.8	246.5	97.9%	23.0	228.1
	Problem 4	CAPTIF 2	2.5	33.8	2	350000	800	13.5	Super Singles	251.8	248.1	98.5%	33.8	122.9
	Problem 5	CAPTIF 2	3.5	47.3	2	350000	800	13.5	Super Singles	251.8	249.6	99.1%	47.3	69.3
CAF11	Problem 1	CAPTIF 2	1.0	13.5	4	170000	800	13.5	Super Singles	251.8	245.9	97.6%	13.5	365.6
	Problem 2	CAPTIF 2	1.3	17.0	4	170000	800	13.5	Super Singles	251.8	245.8	97.6%	17.0	263.7
	Problem 3	CAPTIF 2	1.7	23.0	4	170000	800	13.5	Super Singles	251.8	241.6	95.9%	23.0	166.6
	Problem 4	CAPTIF 2	2.5	33.8	4	170000	800	13.5	Super Singles	251.8	241.8	96.0%	33.8	87.8
	Problem 5	CAPTIF 2	3.5	47.3	4	170000	800	13.5	Super Singles	251.8	245.6	97.5%	47.3	49.3
CAF12	Problem 1	CAPTIF 2	1.0	13.5	8	80000	800	13.5	Super Singles	251.8	238.1	94.5%	13.5	279.5
	Problem 2	CAPTIF 2	1.3	17.0	8	80000	800	13.5	Super Singles	251.8	237.9	94.5%	17.0	185.1
	Problem 3	CAPTIF 2	1.7	23.0	8	80000	800	13.5	Super Singles	251.8	236.7	94.0%	23.0	110.8
	Problem 4	CAPTIF 2	2.5	33.8	8	80000	800	13.5	Super Singles	251.8	236.2	93.8%	33.8	57.3
	Problem 5	CAPTIF 2	3.5	47.3	8	80000	800	13.5	Super Singles	251.8	238.8	94.8%	47.3	32.0



Run ID	Problem #	Material ID	Agg Thick / Radius Ratio	Agg. Thick. (cm)	Stiff. Ratio (Ebas/Esub)	Subgrade Stiff. (kPa)	Tyre Pres. (kPa)	Radius (cm)	Tyre Arrang.	Svalue for Material (kPa)	S to Load Condition (kPa)	% of S mobilized	Depth of subgrade (cm)	$\sigma_v$ @ top subgrade (kPa)
NIG1	Problem 1	Norther Ireland Good	1.0	13.5	2	220000	400	13.5	Dual Tyres	297.1	207.1	69.7%	13.5	232.6
	Problem 2	Norther Ireland Good	1.3	17.0	2	220000	400	13.5	Dual Tyres	297.1	205.7	69.2%	17.0	186.3
	Problem 3	Norther Ireland Good	1.7	23.0	2	220000	400	13.5	Dual Tyres	297.1	214.9	72.3%	23.0	132.3
	Problem 4	Norther Ireland Good	2.5	33.8	2	220000	400	13.5	Dual Tyres	297.1	214.5	72.2%	33.8	80.0
	Problem 5	Norther Ireland Good	3.5	47.3	2	220000	400	13.5	Dual Tyres	297.1	215.1	72.4%	47.3	50.6
NIG2	Problem 1	Norther Ireland Good	1.0	13.5	4	110000	400	13.5	Dual Tyres	297.1	221.3	74.5%	13.5	194.0
	Problem 2	Norther Ireland Good	1.3	17.0	4	110000	400	13.5	Dual Tyres	297.1	212.3	71.5%	17.0	151.1
	Problem 3	Norther Ireland Good	1.7	23.0	4	110000	400	13.5	Dual Tyres	297.1	217.9	73.3%	23.0	104.7
	Problem 4	Norther Ireland Good	2.5	33.8	4	110000	400	13.5	Dual Tyres	297.1	214.5	72.2%	33.8	61.9
	Problem 5	Norther Ireland Good	3.5	47.3	4	110000	400	13.5	Dual Tyres	297.1	208.7	70.2%	47.3	38.4
NIG3	Problem 1	Norther Ireland Good	1.0	13.5	8	55000	400	13.5	Dual Tyres	297.1	224.5	75.6%	13.5	155.3
	Problem 2	Norther Ireland Good	1.3	17.0	8	55000	400	13.5	Dual Tyres	297.1	217.7	73.3%	17.0	116.7
	Problem 3	Norther Ireland Good	1.7	23.0	8	55000	400	13.5	Dual Tyres	297.1	214.0	72.0%	23.0	78.4
	Problem 4	Norther Ireland Good	2.5	33.8	8	55000	400	13.5	Dual Tyres	297.1	209.8	70.6%	33.8	45.0
	Problem 5	Norther Ireland Good	3.5	47.3	8	55000	400	13.5	Dual Tyres	297.1	204.1	68.7%	47.3	27.3
NIG4	Problem 1	Norther Ireland Good	1.0	9.5	2	265000	800	9.5	Dual Tyres	297.1	231.0	77.7%	9.5	451.0
	Problem 2	Norther Ireland Good	1.3	12.0	2	265000	800	9.5	Dual Tyres	297.1	232.1	78.1%	12.0	352.7
	Problem 3	Norther Ireland Good	1.7	16.0	2	265000	800	9.5	Dual Tyres	297.1	238.2	80.2%	16.0	247.2
	Problem 4	Norther Ireland Good	2.5	24.0	2	265000	800	9.5	Dual Tyres	297.1	226.7	76.3%	24.0	140.1
	Problem 5	Norther Ireland Good	3.5	33.5	2	265000	800	9.5	Dual Tyres	297.1	229.9	77.4%	33.5	87.0
NIG5	Problem 1	Norther Ireland Good	1.0	9.5	4	132000	800	9.5	Dual Tyres	297.1	229.0	77.1%	9.5	368.0
	Problem 2	Norther Ireland Good	1.3	12.0	4	132000	800	9.5	Dual Tyres	297.1	229.9	77.4%	12.0	279.1
	Problem 3	Norther Ireland Good	1.7	16.0	4	132000	800	9.5	Dual Tyres	297.1	227.2	76.5%	16.0	192.3
	Problem 4	Norther Ireland Good	2.5	24.0	4	132000	800	9.5	Dual Tyres	297.1	227.1	76.5%	24.0	108.4
	Problem 5	Norther Ireland Good	3.5	33.5	4	132000	800	9.5	Dual Tyres	297.1	225.6	75.9%	33.5	67.0
NIG6	Problem 1	Norther Ireland Good	1.0	9.5	8	66000	800	9.5	Dual Tyres	297.1	229.4	77.2%	9.5	287.2
	Problem 2	Norther Ireland Good	1.3	12.0	8	66000	800	9.5	Dual Tyres	297.1	228.9	77.0%	12.0	210.8
	Problem 3	Norther Ireland Good	1.7	16.0	8	66000	800	9.5	Dual Tyres	297.1	223.3	75.1%	16.0	142.6
	Problem 4	Norther Ireland Good	2.5	24.0	8	66000	800	9.5	Dual Tyres	297.1	226.6	76.3%	24.0	79.4
	Problem 5	Norther Ireland Good	3.5	33.5	8	66000	800	9.5	Dual Tyres	297.1	222.6	74.9%	33.5	48.6

Run ID	Problem #	Material ID	Agg Thick / Radius Ratio	Agg. Thick. (cm)	Stiff. Ratio (Ebas/Esub)	Subgrade Stiff. (kPa)	Tyre Pres. (kPa)	Radius (cm)	Tyre Arrang.	Svalue for Material (kPa)	S to Load Condition (kPa)	% of S mobilized	Depth of subgrade (cm)	$\sigma_v$ @ top subgrade (kPa)
NIG7	Problem 1	Norther Ireland Good	1.0	19.0	2	220000	400	19	Super Singles	297.1	245.1	82.5%	19.0	223.6
	Problem 2	Norther Ireland Good	1.3	24.0	2	220000	400	19	Super Singles	297.1	245.0	82.5%	24.0	172.8
	Problem 3	Norther Ireland Good	1.7	32.0	2	220000	400	19	Super Singles	297.1	242.4	81.6%	32.0	117.9
	Problem 4	Norther Ireland Good	2.5	48.0	2	220000	400	19	Super Singles	297.1	245.2	82.5%	48.0	62.1
	Problem 5	Norther Ireland Good	3.5	66.5	2	220000	400	19	Super Singles	297.1	245.1	82.5%	66.5	34.9
NIG8	Problem 1	Norther Ireland Good	1.0	19.0	4	110000	400	19	Super Singles	297.1	244.2	82.2%	19.0	181.4
	Problem 2	Norther Ireland Good	1.3	24.0	4	110000	400	19	Super Singles	297.1	242.9	81.8%	24.0	134.4
	Problem 3	Norther Ireland Good	1.7	32.0	4	110000	400	19	Super Singles	297.1	237.7	80.0%	32.0	88.8
	Problem 4	Norther Ireland Good	2.5	48.0	4	110000	400	19	Super Singles	297.1	239.6	80.6%	48.0	45.8
	Problem 5	Norther Ireland Good	3.5	66.5	4	110000	400	19	Super Singles	297.1	240.7	81.0%	66.5	25.5
NIG9	Problem 1	Norther Ireland Good	1.0	19.0	8	55000	400	19	Super Singles	297.1	242.0	81.5%	19.0	139.2
	Problem 2	Norther Ireland Good	1.3	24.0	8	55000	400	19	Super Singles	297.1	240.6	81.0%	24.0	98.2
	Problem 3	Norther Ireland Good	1.7	32.0	8	55000	400	19	Super Singles	297.1	236.9	79.7%	32.0	62.7
	Problem 4	Norther Ireland Good	2.5	48.0	8	55000	400	19	Super Singles	297.1	233.4	78.6%	48.0	31.6
	Problem 5	Norther Ireland Good	3.5	66.5	8	55000	400	19	Super Singles	297.1	237.1	79.8%	66.5	17.5
NIG10	Problem 1	Norther Ireland Good	1.0	13.5	2	270000	800	13.5	Super Singles	297.1	250.5	84.3%	13.5	447.8
	Problem 2	Norther Ireland Good	1.3	17.0	2	270000	800	13.5	Super Singles	297.1	249.5	84.0%	17.0	347.5
	Problem 3	Norther Ireland Good	1.7	23.0	2	270000	800	13.5	Super Singles	297.1	248.7	83.7%	23.0	232.4
	Problem 4	Norther Ireland Good	2.5	33.8	2	270000	800	13.5	Super Singles	297.1	248.1	83.5%	33.8	125.3
	Problem 5	Norther Ireland Good	3.5	47.3	2	270000	800	13.5	Super Singles	297.1	249.8	84.1%	47.3	70.5
NIG11	Problem 1	Norther Ireland Good	1.0	13.5	4	135000	800	13.5	Super Singles	297.1	245.7	82.7%	13.5	363.4
	Problem 2	Norther Ireland Good	1.3	17.0	4	135000	800	13.5	Super Singles	297.1	246.0	82.8%	17.0	270.5
	Problem 3	Norther Ireland Good	1.7	23.0	4	135000	800	13.5	Super Singles	297.1	241.8	81.4%	23.0	174.9
	Problem 4	Norther Ireland Good	2.5	33.8	4	135000	800	13.5	Super Singles	297.1	242.2	81.5%	33.8	92.5
	Problem 5	Norther Ireland Good	3.5	47.3	4	135000	800	13.5	Super Singles	297.1	246.1	82.8%	47.3	51.6
NIG12	Problem 1	Norther Ireland Good	1.0	13.5	8	68000	800	13.5	Super Singles	297.1	238.1	80.1%	13.5	280.0
	Problem 2	Norther Ireland Good	1.3	17.0	8	68000	800	13.5	Super Singles	297.1	239.8	80.7%	17.0	198.5
	Problem 3	Norther Ireland Good	1.7	23.0	8	68000	800	13.5	Super Singles	297.1	238.2	80.2%	23.0	123.9
	Problem 4	Norther Ireland Good	2.5	33.8	8	68000	800	13.5	Super Singles	297.1	237.2	79.8%	33.8	64.2
	Problem 5	Norther Ireland Good	3.5	47.3	8	68000	800	13.5	Super Singles	297.1	239.8	80.7%	47.3	35.5

## Worked Example

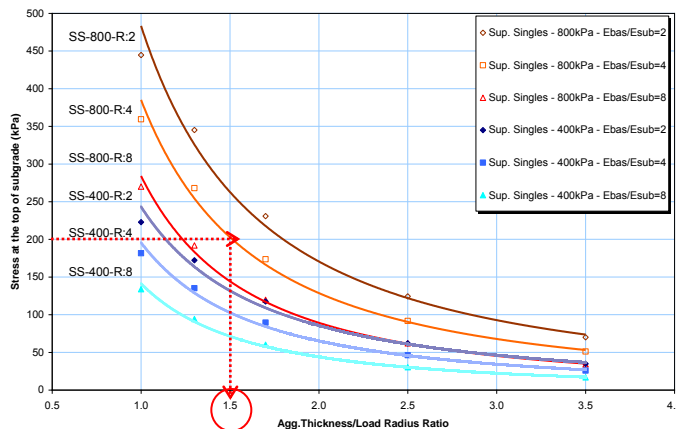
*Subgrade* – Dry silt

*Base course* – Crushed gravel (candidate material)

*Traffic* – Lorries with super singles fitted ; 800kPa tyre inflation (116psi)

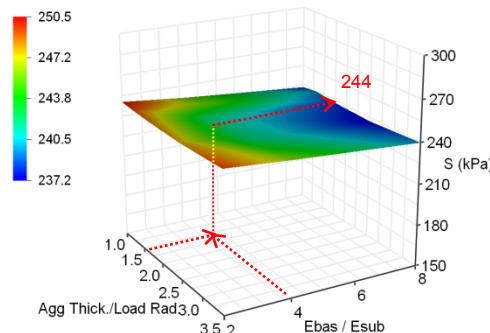
- i. Assessment of the subgrade indicates  $C_u = 50\text{kPa}$ ;  $M_r = 40\text{MPa}$
- ii. Assessment of base course – crushed gravel  $\rightarrow$  DCP = 15mm/blow (From Figure 44 of the Roadex Report Task 2.1), equivalent to CBR =15% ( $M_r$  approximately 150MPa)
- iii. 800kPa of tyre pressure on a super single tyre  $\rightarrow$  Radius =13.5
- iv. Chart B selected  $\rightarrow$  Super Singles  $\rightarrow E_{bas}/E_{sub} \cong 4$
- v. Subgrade allowable stress =  $4C_u = 200\text{kPa}$  on Chart from Figure 7.5 (SS-800-R4 line)

Pavement will require 1.5 Agg. Thick/ Load Rad. Ratio (20cm of base)



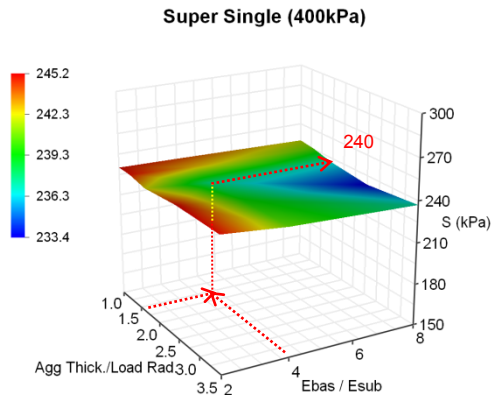
- v. Failure envelope – Consider material as NIP ( $S_f = 255\text{ kPa}$ )
- vi. Select Chart 4 (Figure 7.4)  $\rightarrow$  Super Singles  $\rightarrow E_{bas}/E_{sub} \cong 4 \rightarrow$  Agg. Thick/Load Rad. = 1.5
- vii.  $S = 244\text{kPa}$ ;  $S/S_f = 96\%$   $\rightarrow$  Failed to prevent rutting in the base layer (90% is limit)

Super Singles (800kPa)

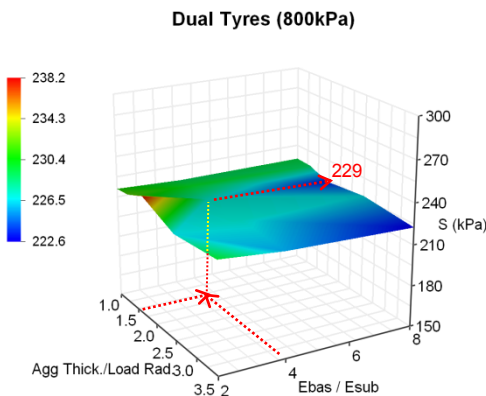


## Worked Example - Continued

- ix. Alternative 1 – Change Traffic – Super Singles with 400kPa (58psi)
- x. Select Chart 3 → Super Singles → Ebas/Esub  $\cong$  4 → Agg. Thick/ Load Rad. = 1.5
- xi.  $S = 240\text{kPa}$ ;  $S/S_f = 94\%$  → Failed to prevent rutting in the base layer



- xii. Alternative 2 – Change Traffic – Twin Tyres with 800kPa (116psi)
- xiii.  $S = 229\text{kPa}$ ;  $S/S_f = 89\%$  → OK (now  $<90\%$ )



- xiv. {Another alternative would have been to change the material to make it stronger}.
- xv. FINALLY – return to stage 1 with new traffic (radius of tyre now 9.5cm) and use Chart from Figure 7.6 with the SS-800-R4 line to obtain 1.65 Agg. Thick/ Load Rad. ratio, i.e. base thickness should be  $1.65 \times 9.5 = 16\text{cm}$  thick. As thickness difference is small, 20cm is selected as the new base layer.
- xvi. If 16cm had been selected, stage 2 would need reassessment.

*Remark: As the Chart 1 to 4 may not be sufficiently precise for graphical interpolation, data from Appendix G can be used for improved results.*